CARBON AND NITROGEN PARTITIONING IN CANOLA

(*Brassica napus* L.)

A thesis submitted for the degree of Doctor of Philosophy

of The Australian National University

by

Steven Paul King

The research presented in this thesis was conducted in the laboratories

of CSIRO Plant Industry, Canberra.

CERTIFICATE OF ORIGINALITY

This thesis contains original research data that has not been included in any other theses and has not been published by other researchers. References are appropriately made in the text to ideas, concepts and data that are not the candidate's own. As well, the assistance that the candidate received while conducting this research is duly acknowledged.

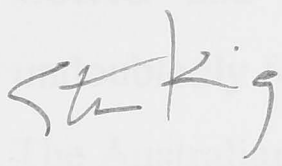

Steven Paul King

29 August 1997

ACKNOWLEDGEMENTS

As I type these words, there are only a few finishing touches to be put on this thesis and I have time to reflect. Even after 3.5 years, I am still amazed at my good fortune. The Australian government's scheme to bring foreign students to Australia, through an Overseas Postgraduate Research Scholarship (OPRS), an Australian National University Ph.D. scholarship, and a Cooperative Research Centre for Plant Science Graduate Assistantship opened the door to a whole new life. This opportunity to live in another country has changed me in ways that I probably don't fully appreciate yet. Exposure to the incredible quality and depth of plant science in CSIRO and the ANU and the cooperative atmosphere between researchers, undoubtedly fostered by the CRC for Plant Science, constitutes only one component. The Australian lifestyle was equally important and was extremely refreshing.

It is not an exaggeration for me to thank everyone in Subprogram YA of CSIRO Plant Industry because almost everyone lent assistance at some point. Bob Furbank, my cosupervisor, has both a brilliant mind and an enthusiastic personality consequently he was receptive to looking beyond the leaf and was the source of many experimental ideas. John Lunn, a postdoctoral fellow, unselfishly trained me in biochemistry and patiently endured many basic questions and hours in the cold room. Murray Badger, my cosupervisor in the Molecular Plant Physiology group of the ANU's Research School of Biological Sciences, was extremely supportive. Hart Schroeder (CSIRO) and Chris Jones (John Innes Centre, Norwich, UK) were instrumental in troubleshooting the initially unresponsive canola transformation system. Stuart Craig and Celia Miller (CSIRO Plant Industry, Electron Microscopy Unit) and Graham Scofield (CSIRO) did most of the seed microscopy work reported in Figure 2.4 and Graham realized the potential significance of the floral mutant and took the photographs used in Figure 5.11. Peter Eastmond and Steve Rawsthorne (John Innes Centre) shared their seed photosynthesis data prior to publication.

I am extremely pleased with the last 3.5 years and it would not have been possible without the professional help, the available resources and the personal support from many friends and colleagues. Simply inspirational!

TABLE OF CONTENTS

ABBREVIATIONS

The symbols and abbreviations that are listed in *Plant Physiology*'s Instructions to Contributors have been adopted and are used without definition. The abbreviations not included in this list are listed below:

AS	asparagine synthetase
BA	6-benzylaminopurine
DAA	days after anthesis
DAFF	days after first flower
IBA	indole-3-butyric acid
NOS	nopaline synthase
NPTII	neomycin phosphotransferase
OCS	octopine synthase
PEPC	phospho*enol*pyruvate carboxylase
SPS	sucrose-phosphate synthase
SSC (1 x)	150 mM NaCl, 15 mM sodium citrate, pH 7.0
SuSy	sucrose synthase
TDZ	thidiazuron
TE	10 mM Tris, 1 mM EDTA, pH 8.0

NOMENCLATURE

DNA sequences originating from microbes are presented as lowercase italics (eg. *nptII*) and those from plants are presented as normal text and the first letter is capitalized if the gene is nuclear-encoded (eg. RbcS). Gene products are presented in uppercase (eg. NPTII). Shoots regenerating from tissue culture were numbered sequentially and were given a SK-prefix (eg. SK43). Regenerants from the same callus had the same identification number and were followed by a letter and may or may not be independent transformation events (eg. SK96A, SK96B).

ABSTRACT

Sources of assimilates required for the growth and development of canola (*Brassica napus* L.) change during its life cycle. Leaves senesce before rapid seed filling within 35 d after first flower, therefore assimilates needed for seed storage-product synthesis must be derived from silique wall (pod wall), seed or stem photosynthesis and remobilization of stored reserves. Silique wall photosynthetic capacity was greater than leaf on a chlorophyll basis but not on an area basis due to a 75 to 80 % lower chlorophyll content per unit area. Total extractable ribulose-1,5-bisphosphate carboxylase / oxygenase (Rubisco) activity in silique wall tissue was higher than leaf (23 vs. 13 μmol mg chlorophyll^{-1} min^{-1}). In contrast to leaves, the silique wall preferentially partitioned $^{14}CO_2$ into sucrose rather than starch. The predominant accumulated carbohydrates were hexoses, however, and correspondingly high soluble acid invertase activities suggest vacuolar localization of cleaved sucrose as hexose. Hexose contents rapidly declined in parallel with rapid seed growth and were presumably remobilized. Seed starch and hexose were localized to the seed coat or liquid endosperm and were depleted on the transition to rapid embryo growth. Sucrose imported into seeds during storage-product synthesis appears to be cleaved by sucrose synthase (20 nmol min^{-1} seed^{-1}) rather than soluble acid or alkaline invertases (1.5, 6.6 nmol min^{-1} seed^{-1}) and sucrose-phosphate synthase (SPS)-mediated sucrose resynthesis may modulate carbon allocation to glycolysis.

In addition to the silique wall, developing seeds had significant CO_2 fixation capacity and the major component of this capacity was embryo Rubisco. Total Rubisco activity was 14.3 nmol min^{-1} embryo^{-1} (3.8 μmol min^{-1} mg chlorophyll^{-1}) at 28 days after anthesis (DAA) with smaller contributions from seed coat and embryo PEPC. Rubisco activities were probably maximal *in vivo* because of high silique cavity CO_2 concentrations (0.8 to 2.5 %). Seed chlorophyll content rapidly increased over 10-fold from 20 to 30 DAA and with 20 % of incident light transmitted through the silique wall, embryos demonstrated appreciable photosynthetic electron transport rates. Seeds were estimated to have a 1.2 to 2.5-fold higher CO_2 refixation capacity than silique wall endocarp during oil filling.

Transgenic plants were produced to perturb normal source to sink relations. Transformation vectors were constructed containing cDNA clones encoding for SPS and asparagine synthetase (AS), key enzymes for the biosynthesis of carbon and nitrogen transport compounds. These genes were cloned in the sense direction under the control of either constitutive or tissue-specific promoters. Before successful transformation with *Agrobacterium*, plant regeneration frequencies had to be increased by identifying and modifying the most critical tissue culture factors of explant age and water source. Incorporation of the transgenes was confirmed in regenerated shoots by Southern blot analysis and transgene expression or activities of its product was assayed in T_1 progeny. SPS activities in the leaves, silique wall and seed of T_1 progeny ranged from 92 % reductions to 8.6-fold increases compared to untransformed plants and were correlated with profound effects on plant growth and development.

This thesis has provided baseline knowledge on source to sink carbohydrate metabolism during seed filling. These data allow the identification of suitable targets for the genetic manipulation of seed assimilate partitioning and preliminary assessment of transgenic plants with perturbed source metabolism suggested that these changes can indeed affect seed sinks.

CHAPTER 1: INTRODUCTION

GENERAL ASPECTS

Brassica napus L. and *B. rapa* L. (formerly *B. campestris* L.) are two species of rapeseed. *B. rapa* is a diploid species while *B. napus* is an amphidiploid derived from *B. rapa* and *B. oleracea* (U, 1935). Cultivars of both species can be of canola-quality, indicating that the anti-nutritional compounds erucic acid and glucosinolates are present in minimal amounts, and are simply known as canola or oilseed rape. In recent years, canola has been increasingly grown in many parts of the world as a high value crop (for review, see Kimber and McGregor, 1995). The harvestable product is the seeds which typically contain 40 percent oil and this oil is high in unsaturated fats with excellent nutritional properties (for review, see McDonald, 1995). After oil extraction, seed meal can be used as a high protein feed (for review, see Bell, 1995). Non-canola-quality rapeseed oil has a number of industrial applications (for reviews, see Korbitz, 1995; Sonntag, 1995).

Canola is a C_3 dicotyledon with an indeterminate growth habit. At the onset of flowering, the main raceme bolts upwards and produces flowers (Fig. 1.1A). Secondary branching also occurs from the main raceme. A pollinated carpel extends to form a silique (i.e. pod) within which seeds develop (Fig. 1.1B) and silique development is from the base of the raceme upwards. Individual seeds follow the growth and development patterns typical of other dicotyledonous crops (Fig. 1.1C). Double fertilization produces both a diploid embryo and a triploid liquid endosperm while the surrounding seed coat is maternal.

Developing seeds receive assimilates through the phloem from photosynthetic source tissues (Fig. 1.2). In these source tissues, photosynthesis produces the energy needed to fix atmospheric CO_2 into organic carbon. Some of this carbon is then exported as sucrose to young leaves and roots during vegetative growth and to seeds during reproductive growth. Once in sink tissues, sucrose is cleaved into its constituent hexoses and either stored as starch or utilized by the respiratory pathways to produce energy or substrates for fatty acids, protein and other compounds. Nitrogen is taken up from the soil as nitrate or ammonium and is

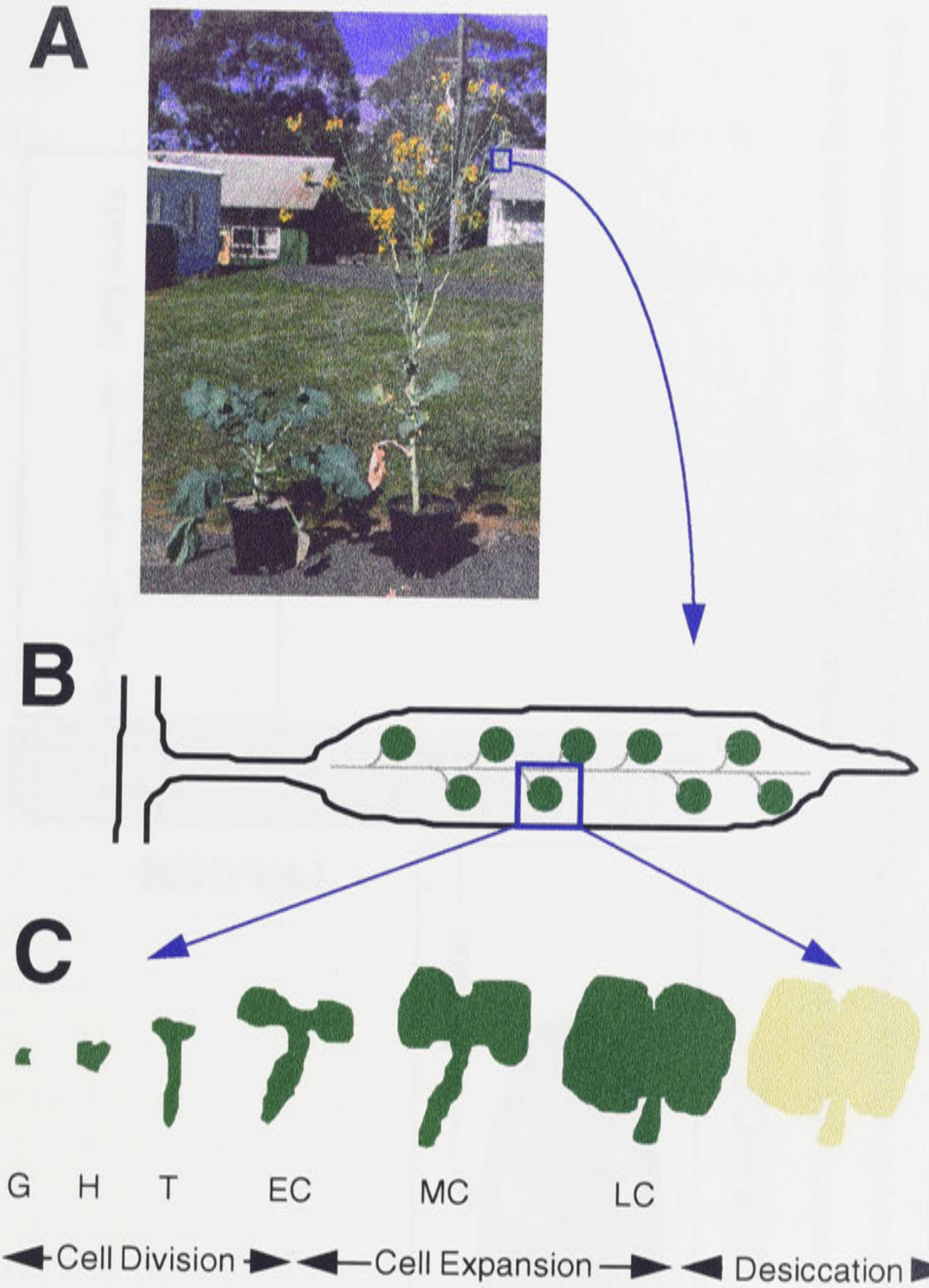

Figure 1.1. Growth and development in canola. A: At the initiation of flowering the main stem bolts and produces many flower-bearing branches. Pollinated flowers extend to form siliques (box). B: Developing seeds within the silique cavity are attached to the rest of the plant by a central septum. C: Dicotyledonous embryos develop through globular (G), heart (H), torpedo (T), early-cotyledonary (EC), mid-cotyledonary (MC), late-cotyledonary (LC), and desiccation phases.

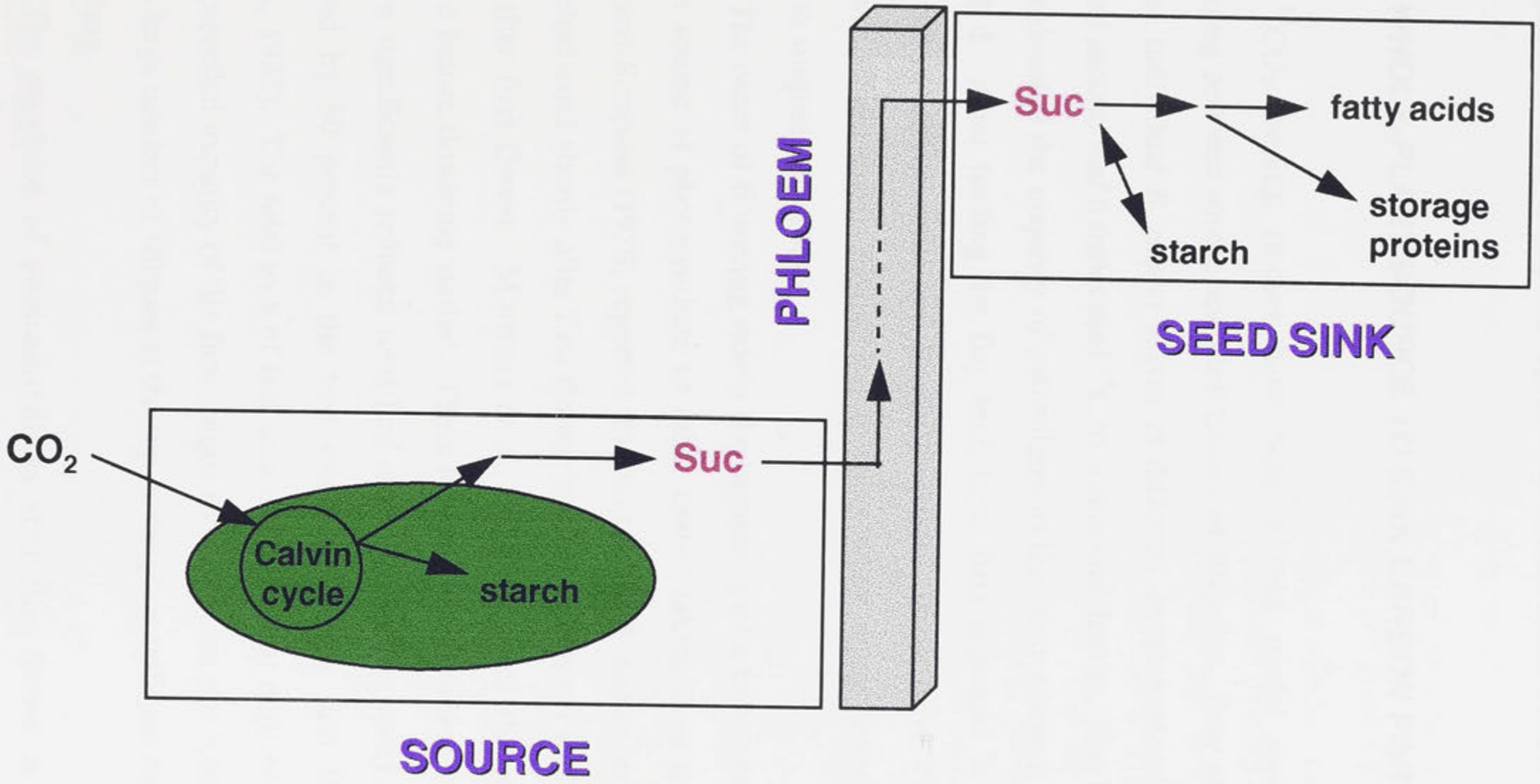

Figure 1.2. A simplified scheme of source to sink carbon provision. Photosynthetically-fixed CO_2 is used to synthesize Suc and starch. Suc is transported in the phloem to developing seeds where it is utilized to form a transient starch reserve and the fatty acid and protein storage products. Suc, Sucrose.

reduced to organic forms either in the roots or in the leaves (Andrews, 1986). The form of organic nitrogen transported to sink tissues, for use in the synthesis of protein and other compounds, varies with species but is typically glutamine and asparagine or ureides in tropical legumes (Lea and Miflin, 1980).

WHOLE-PLANT SOURCE TO SINK CARBON PARTITIONING

$^{14}CO_2$ feeding studies have been a very useful tool to track carbon partitioning between source and sink tissues of *Brassica*. Brar and Thies (1977) fed $^{14}CO_2$ to individual *B. napus* leaves at different developmental stages. The fully expanded second leaf translocated ^{14}C to young sink leaves. The fully expanded fifth leaf translocated the majority of assimilates to the stem where it was retained for at least 28 d. After feeding the flag leaf, label first appeared in the stem and then transferred to silique walls and finally to seeds. Major et al. (1978) demonstrated that lower leaves export assimilates to roots while upper leaves and stems export carbon to siliques and seeds.

The onset of flowering marks the beginning of a transition from leaves being the sole source of photosynthate to other tissues taking over assimilate provision. Clarke and Simpson (1978) reported that maximum *B. napus* leaf area indices were not reached until shortly after first flower but leaf area was rapidly declining by two weeks after first flower. Morrison et al. (1992) showed that the first two leaves senesced before flowering started. These leaves were, however, quite small and may not have significantly reduced total leaf area. In another study, total leaf area had decreased by 80 percent in the two weeks following first flower (Pechan and Morgan, 1985). The total loss of leaf area did not occur until 46 d after first flower which preceded maturity of the first silique by 8 d (Kasa and Kondra, 1986). At this stage, a large number of siliques at the top of the plant will just be commencing rapid seed filling.

The provision of photoassimilates after first flower is critical. Over 50 percent of final above-ground biomass in *B. napus* was assimilated after flowering (Thurling, 1974; Lewis and Thurling, 1994). Of this total, approximately 40 percent

ended up in the seeds (Lewis and Thurling, 1994). Vegetative yield (all above-ground biomass except seeds) over the life of the plant shows a strong correlation (r = 0.93 - 0.96) to final seed yield (Campbell and Kondra, 1978). The number of siliques per plant is also very important (Campbell and Kondra, 1978; Tayo and Morgan, 1979). Silique area indices are, however, poorly correlated with seed yield (Clarke and Simpson, 1978). Leaf shading or removal around first flower caused reductions in the numbers of open flowers, siliques per plant and plant height (Tayo and Morgan, 1979). The number of seeds per individual silique and weight per seed were unaffected which indicates that the reduced number of siliques were responsible for the lower seed yield per plant. In a separate study, the removal of all leaves at late flowering caused a 35 percent reduction in final seed yield (Freyman et al., 1973). Leaves are obviously important components of yield but the effect could be either direct or indirect. Direct provision of assimilates to seeds is straightforward. Alternatively, carbon could be translocated to growing raceme meristems thereby feeding the development of additional autotrophic siliques.

Rood et al. (1984b) have nicely demonstrated the developmental transition of assimilate sources in *B. rapa* using whole plant $^{14}CO_2$ labelling. At first flower, stems and leaves were the major incorporation sites. This label then translocated to roots and seeds. When the lower siliques were filling, the major incorporation sites were stems and silique walls. These labelled assimilates were translocated predominantly to the seeds. During seed ripening, silique walls and stems incorporated $^{14}CO_2$. Again, most label was transferred to seeds and this preferential partitioning progressively increased with development.

The high proportion of apparent stem incorporation in the work of Rood et al. (1984b) is somewhat surprising. A long pulse length (1 h) could potentially overestimate incorporation if some of the stem label was fixed in another tissue and be en route to sink tissues. Addo-Quaye et al. (1986), however, found a significant proportion of stem label after a shorter 15 minute pulse period of *B. napus*. Canola stems contain chlorophyll and have stomata (Major, 1975; Brar and Thies, 1977) so it is possible that they are photosynthetically active but their vertical orientation would presumably make it difficult to intercept light efficiently.

Several weeks after first flower, leaf area is severely diminished at a time when there is a great sink demand for assimilates. The older siliques at the base of the raceme are actively synthesizing oil and protein storage products while new siliques are emerging at the top of the plant. At these later stages, the sources of carbon are unclear. Major et al. (1978) claimed that autotrophic *B. napus* siliques do not export carbon but solely supply their own seeds, however no data was presented to substantiate this claim. This claim is questionable because at the time of greatest seed sink demand, the photosynthetic capacity of the silique wall is declining. *B. rapa* silique photosynthetic rates peak at 20 to 30 d after anthesis (Singal et al., 1987; Dua et al., 1994) which is when the storage oil synthesis is beginning and storage protein synthesis has not yet begun in *B. napus* (Murphy and Cummins, 1989). Starch transiently stored in seeds in the first few weeks of development would be inadequate to entirely meet oil and protein synthesis requirements (Norton and Harris, 1975). Remobilization from silique wall reserves is a possible source because silique wall dry weight decreases during seed filling (Norton and Harris, 1975; Rood et al., 1984a). Constant stem and root dry weights argue against significant remobilization from these tissues in *B. rapa* (Rood et al., 1984a).

Sheoran et al. (1991) examined the effect of covering *B. rapa* siliques on seed yield. Covering siliques from 7 d after anthesis resulted in a 48 percent decrease in silique wall dry matter and a 73 percent decrease in seed dry matter. Coverage starting at 20 d after anthesis produced 59 percent less seed while only a 14 percent decrease occurred when siliques were covered from 40 d after anthesis. The simple explanation for these results is that silique primary CO_2 fixation is critical to seed filling. The absence of light could, however, also arrest light-dependent refixation of seed-respired CO_2 and light-dependent production of energy within developing embryos.

Instead of covering siliques, Rood and Major (1984) removed *B. napus* and *B. rapa* siliques at emergence. Four weeks after removal, dry weights of other plant parts were greater than an undefoliated control suggesting that siliques need to import assimilates. In a study by Khanna-Chopra and Sinha (1976), *B. rapa* seeds gained 68 mg dry matter during the phase of rapid dry weight accumulation. During this same period, the enclosing silique wall lost 40 mg dry matter. If it is assumed

that all of the 40 mg loss went to the seeds then the source of the extra 28 mg of seed dry matter is unknown. Almost half of the plant's leaf area had senesced at the start of the sampling period consequently leaves could likely only contribute dry matter by remobilization. Other possible sources are stem photosynthesis and/or remobilization, export from other siliques or seed photosynthesis.

Canola source-sink relations are complicated by its indeterminate nature. Provision of carbon to seed sinks can be from a number of sources at any one time. These sources and the relative contribution of each likely changes over whole-plant development. The possibilities of significant stem primary CO_2 fixation, seed fixation and the transfer of photoassimilates between siliques have not been adequately explored in the literature.

PHOTOSYNTHESIS AND CARBOHYDRATE METABOLISM

METABOLIC PATHWAYS

The photosynthetic light harvesting reactions occur in the thylakoid membranes of chloroplasts and through the photosynthetic electron transport chain produce oxygen, NADPH and ATP (Fig. 1.3) (for review, see Edwards and Walker, 1983). In theory, this energy can be used in any plastidial metabolic reaction, however photosynthetic electron transport in C_3 plants is normally coupled to Rubisco-dependent CO_2 fixation. The Calvin cycle (also known as the photosynthetic carbon reduction cycle or reductive pentose phosphate cycle) is localized to the chloroplast stroma and can be broadly divided into three components (Fig. 1.4). First, Rubisco catalyzes the carboxylation of ribulose-1,5-bisphosphate (RuBP) and CO_2 into the three-carbon compound 3-phosphoglycerate (3-PGA). Second, 3-PGA is reduced to triose-P using the photosynthetically-produced ATP and NADPH. Third, a portion of the produced triose-P is recycled to regenerate RuBP.

The remaining triose-P is further metabolized into sucrose and starch, regarded as the primary end products of photosynthesis (Fig. 1.5). In leaves, starch synthesis occurs in the chloroplast (for review, see Smith and Martin, 1993). For sucrose, triose-P is transferred to the cytosol in exchange for P_i by a specific

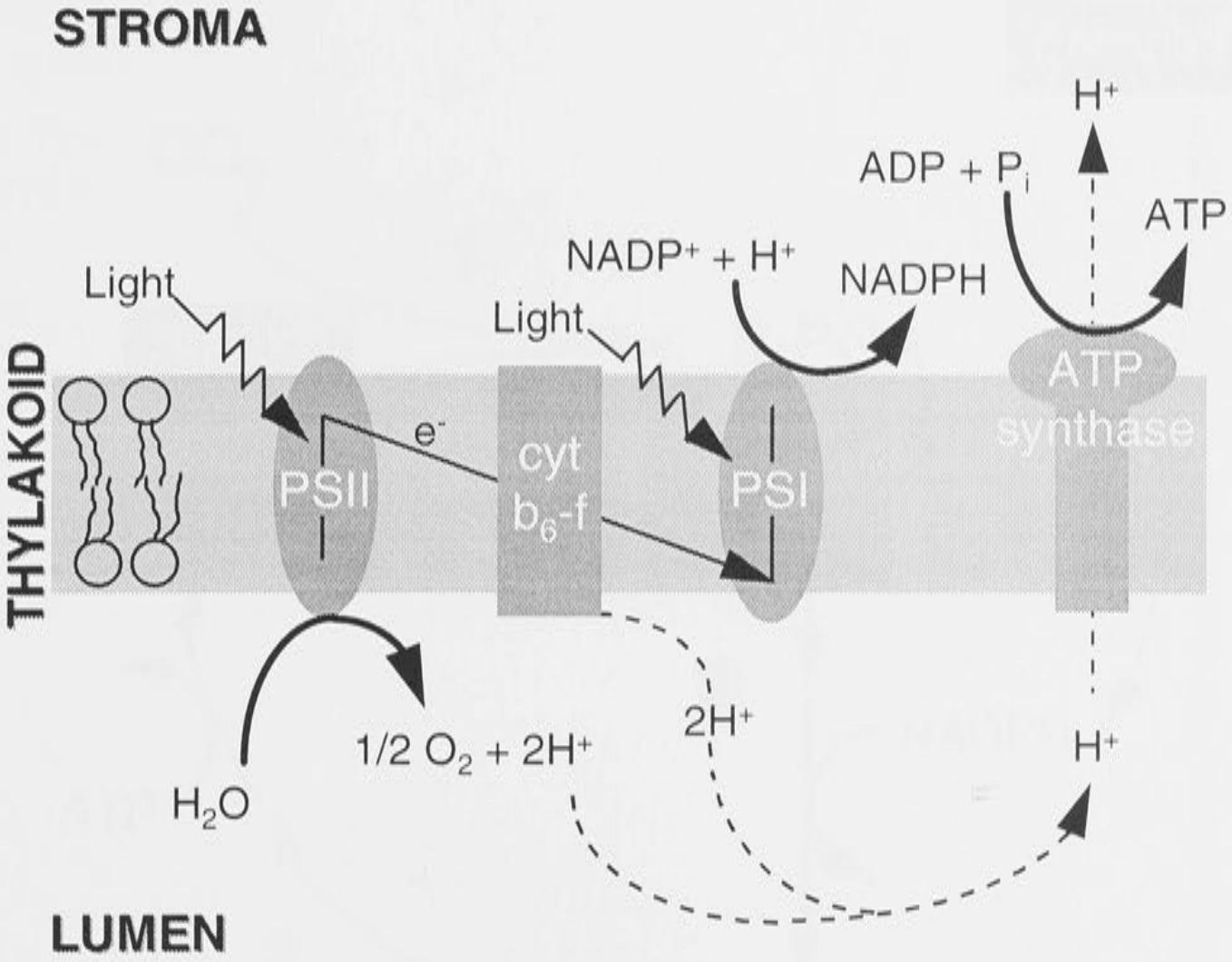

Figure 1.3. Photosynthetic electron transport. Light excites chlorophyll within the photosystem protein complexes (PSII, PSI) of the chloroplast thylakoid membranes. The excited electrons are sequentially transferred to adjacent pigments and reduce $NADP^+$ to NADPH on the stromal side. The oxidation of water on the lumen side produces oxygen and protons. These protons and those evolved by the cytochrome b_6-f complex acidify the lumen and drive the ATP synthase-mediated production of ATP.

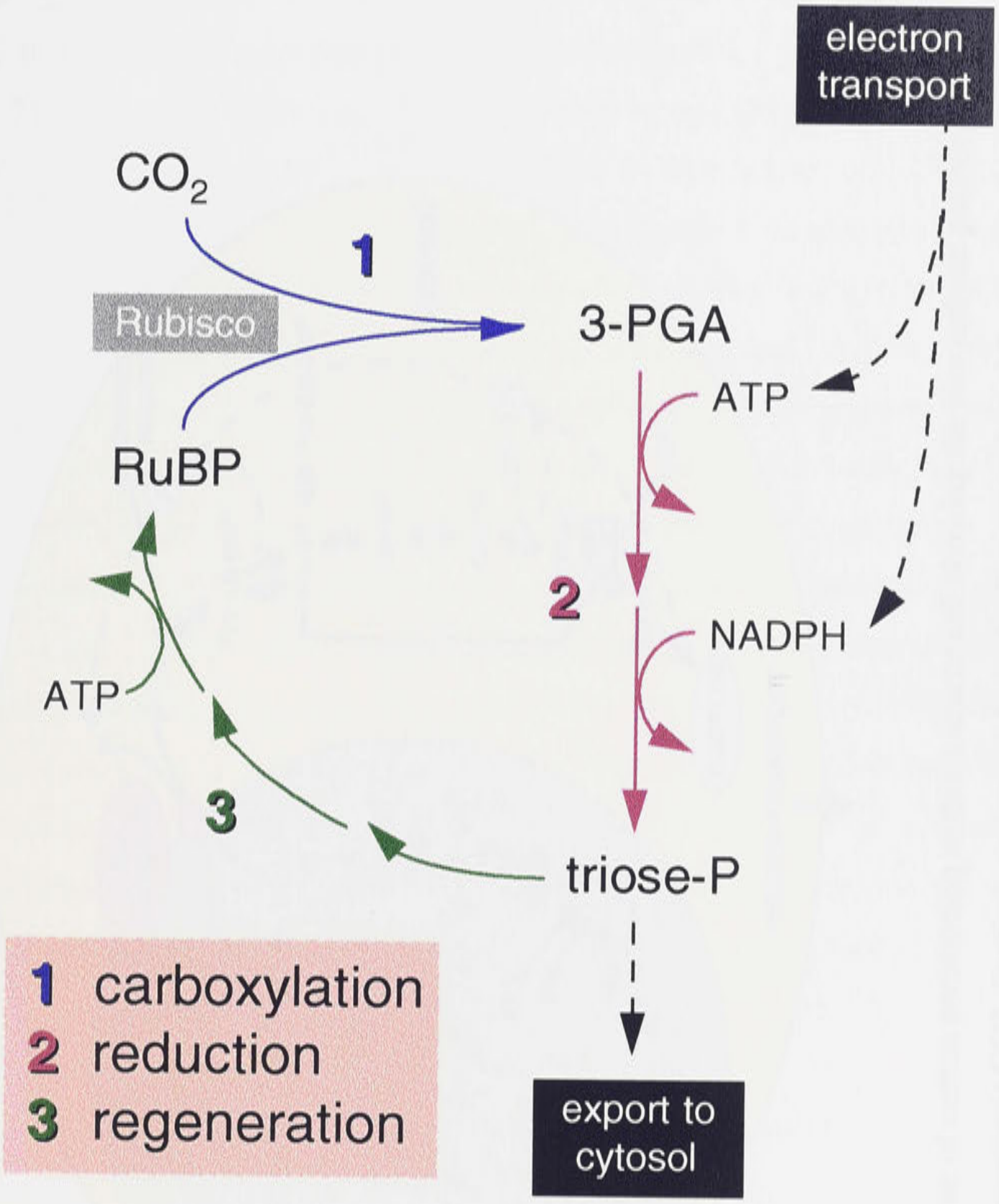

Figure 1.4. A simplified Calvin cycle scheme. CO_2 is fixed into organic carbon in the chloroplast stroma by the Rubisco-catylyzed carboxylation of RuBP. The 3-PGA produced is reduced to triose-P using energy produced from photosynthetic electron transport. Some of the triose-P is used to regenerate RuBP while the rest is used in other metabolic reactions.

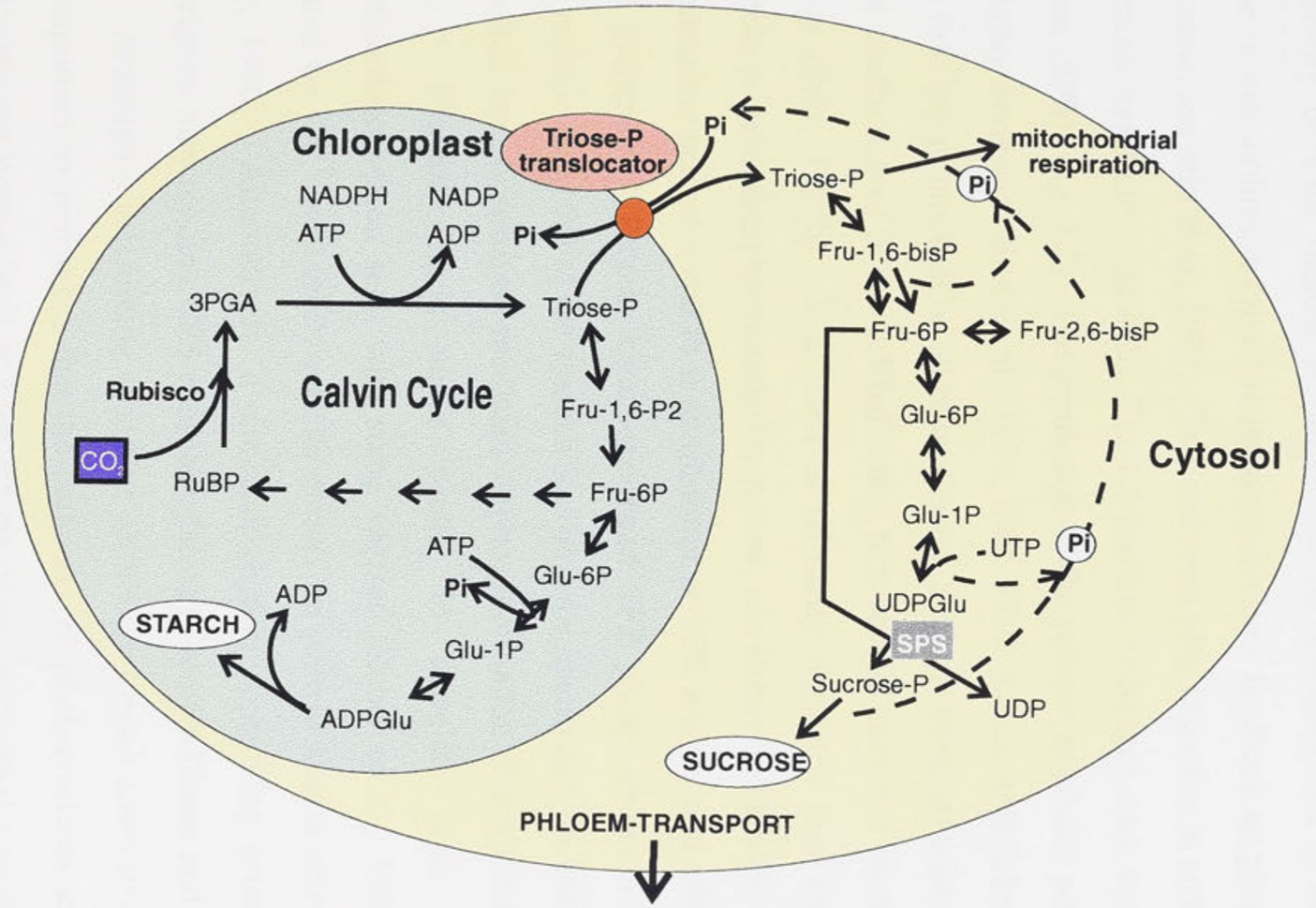

Figure 1.5. A simplified scheme of carbon partitioning within a source cell showing the biosynthetic pathways of the primary end products of photosynthetic CO2 fixation, sucrose and starch. Diagram adapted from original by M.R. Badger.

translocator where it is first converted to hexose-P then to sucrose (for review, see Stitt et al., 1987). In leaves of C_3 dicotyledonous species, photosynthetic carbon fixation typically leads to an accumulation of starch during the photoperiod which is remobilized to sink tissues during the subsequent dark period.

The proportion of photosynthate partitioned toward sucrose is important for productivity because sucrose is the principal carbon form transported to sink tissues in most species and sucrose or metabolites involved in its synthesis may feedback on photosynthetic rate (for review, see Stitt et al., 1987). Two enzymes play key roles in controlling the rate of sucrose synthesis; cytosolic Fru-1,6-bisPase (FBPase) and sucrose-phosphate synthase (SPS) (Fig. 1.5). The regulation of the sucrose synthesis pathway has been thoroughly reviewed (Stitt et al., 1987; Stitt, 1993; Quick and Schaffer, 1996) and only a few key points will be addressed here. SPS has been estimated to have a flux control coefficient of 0.3 to 0.5 indicating that several enzymes share control in this pathway (Stitt, 1995b). SPS itself is primarily regulated post-translationally by reversible protein phosphorylation (for review, see Huber and Huber, 1996). Glc-6-P is an allosteric activator and Pi is an inhibitor of SPS activity and affect the affinities for its substrates. Protein kinase-mediated SPS phosphorylation at a conserved serine residue (Ser158) of the spinach leaf enzyme inactivates the enzyme and can be reactivated by phosphatase-mediated dephosphorylation (McMichael et al., 1993, 1995). Phosphorylation status seems to correlate with the light/dark activation/deactivation seen with some species (Huber et al., 1989) and may be regulated by Ca^{+2} availability and its effects on protein kinase activity (Huber and Huber, 1996). Alternatively, a circadian rhythm controlling protein phosphatase transcription may regulate SPS phosphorylation in tomato (Jones and Ort, 1997).

Although it is tempting to reduce cellular processes down to individual steps, it is important to remember that the pathways of photosynthesis and carbohydrate partitioning are inter-related and the effects of environmental signals and molecular manipulation will be complex. These subcellular interactions ultimately affect whole-plant growth and development. Pathway identification is only the first step and much research is needed to determine the factors controlling metabolic flux from source to sink tissues.

LEAF PHOTOSYNTHESIS

Although there is little detailed published data on canola leaf photosynthesis and carbohydrate metabolism, it is unlikely to be much different from other C_3 species (for reviews, see Stitt et al., 1987; Wardlaw, 1990; Smith and Martin, 1993; Geiger and Servaites, 1994; Foyer and Galtier, 1996; Quick and Schaffer, 1996). Dekker and Sharkey (1992) and Sundby et al. (1993) have examined leaf photosynthetic regulation in two *B. napus* cultivars, one of which had a mutation in the D1 protein of the photosynthetic electron transport chain. Cold temperature effects on leaf carbohydrate metabolism have been examined in the short-term by Paul et al. (1990) and in the long-term by Hurry et al. (1995).

SILIQUE PHOTOSYNTHESIS

Although canola leaf photosynthesis is typical of many C_3 species, the provision of significant photoassimilates by siliques is somewhat unique although reproductive organs of other species are capable of photosynthesis; eg. wheat (Kriedemann, 1966; Singal et al., 1986a), pea (Lovell and Lovell, 1970; Sinha and Sane, 1976; Flinn et al., 1977), bean (Crookston et al., 1974), soybean (Quebedeaux and Chollet, 1975), chickpea (Singal et al., 1986b), and cotton (Wullshleger and Oosterhuis, 1990). In contrast to other species, the relative contribution in canola is very high because senescence quickly lowers functional leaf area before the completion of seed filling (Pechan and Morgan, 1985).

The bulk of research on silique photosynthetic capacity has been done in the toria ecotype of *B. rapa*. Silique wall total chlorophyll contents on a fresh weight basis are greatest early in development and then decline linearly with aging (Singal et al., 1987; Dua et al., 1994). These contents are less than in a leaf (Hozyo et al., 1972; Khanna-Chopra and Sinha, 1976; Singal et al., 1987) although expression of data on a fresh weight basis is deceptive because silique walls are thicker and will be heavier per unit area. In *B. napus*, stomata are less abundant than in leaves; 20 to 60 percent of that of the lower side of a leaf (Major, 1975; Brar and Thies, 1977).

Silique photosynthetic rates peak at 20 to 30 d after anthesis (Singal et al., 1987; Dua et al., 1994). At an irradiance of 1000 µmol quanta m^{-2} s^{-1}, intact siliques had a peak photosynthetic rate of 16 µmol CO_2 m^{-2} s^{-1} (Dua et al., 1994). Stomatal

conductance also peaked at this stage (742 mmol m^{-2} s^{-1}) while transpiration rate (13-18 mmol m^{-2} s^{-1}) and intercellular CO_2 concentration (280-288 µL L^{-1}) did not change until later developmental stages. Using isolated chloroplasts from silique walls, whole chain electron transport, PSI and PSII activities all followed the same trend as net photosynthesis over development (Dua et al., 1994). Activities of measured Calvin Cycle enzymes (Rubisco, NADP-GAP dehydrogenase, Ru-5-P kinase) decreased linearly with development (Singal et al., 1987). On a chlorophyll basis, Rubisco activities in silique walls were 3.5-fold greater than in leaves (Khanna-Chopra and Sinha, 1976). Enzymes and metabolites of carbon metabolism correlated with changes in photosynthetic rates (Singal et al., 1992). For example, sucrose phosphate synthase activity reached a maximum of 66 µmol kg^{-1} (protein) s^{-1} when the photosynthetic rate peaked at 21 d after anthesis. Exceptions to the trend were Fru-2,6-bisP and Fru-6-P-2-kinase which didn't peak until 42 d after anthesis.

A number of papers have been published on *Brassica* silique photosynthesis, although almost entirely from the toria ecotype of *B. rapa*, which each provide some insight, however a definitive study of canola photosynthesis and subsequent carbohydrate production has not been conducted.

CO_2 REFIXATION

SILIQUE WALL

In addition to the primary fixation of CO_2, it has been speculated that the interior silique wall minimizes carbon loss by refixing some of the vast amount of respired seed CO_2 (Mendham and Salisbury, 1995). Pod wall cross-sectioning revealed that there are two structural zones in pea (Fig. 1.6) (Atkins et al., 1977; Price and Hedley, 1988). The inner endocarp is separated from the mesocarp by a sclerenchyma layer and separate analysis of the inner and outer layers demonstrated that endocarp chlorophyll content (Price et al., 1988; Donkin and Price, 1990) and PEP carboxylase activities (Atkins et al., 1977; Price and Hedley, 1980; Price and Hedley, 1988) were considerably higher than the outer layers. On a fresh weight basis, Rubisco activities were the same or greater in the endocarp (Atkins et al.,

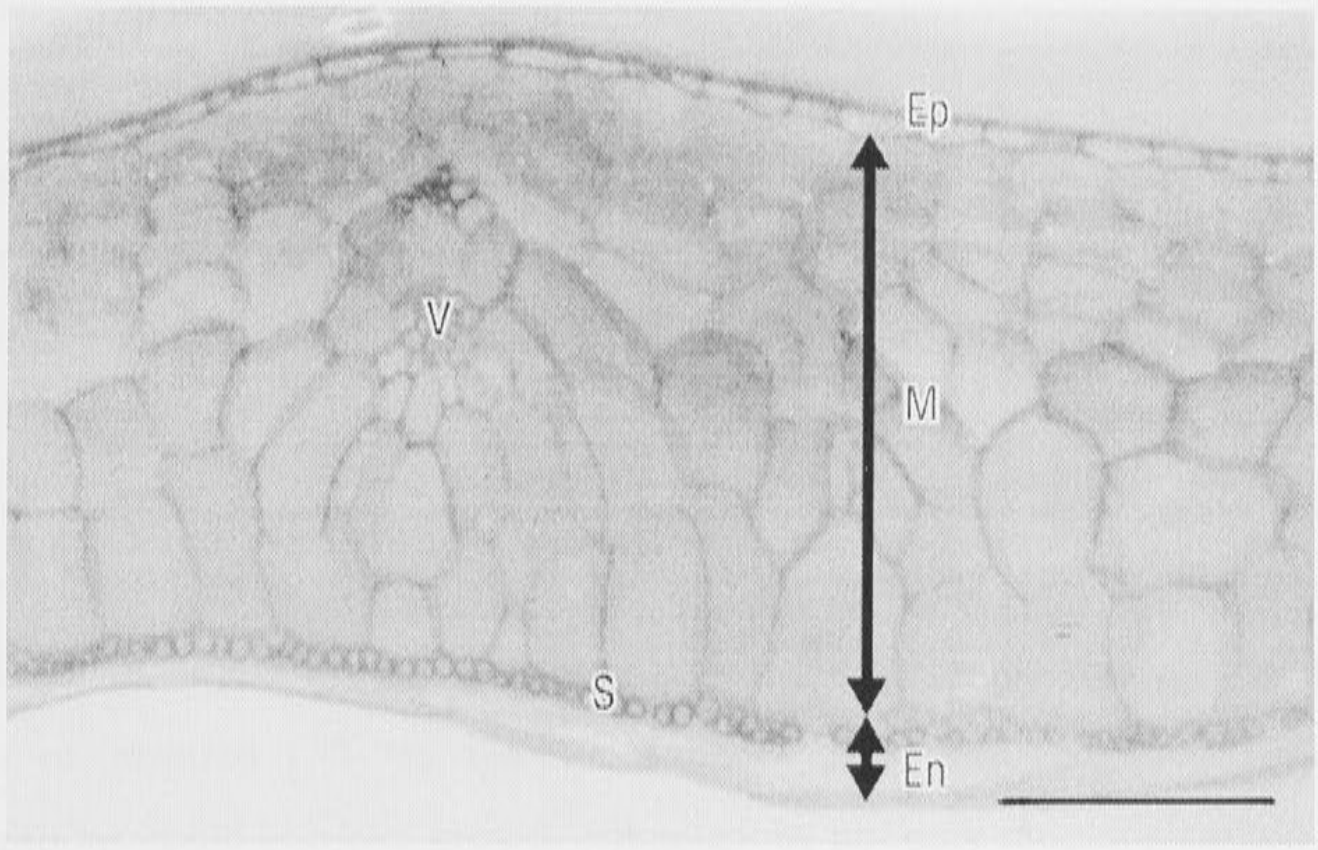

Figure 1.6. Transverse pod wall anatomy. The epidermis (Ep) is on the outer surface of the pod and much of the pod wall is composed of parenchyma cells in the interior mesocarp (M). A sclerenchyma layer (S) and parenchyma cells on the inner surface of the pod wall compose the endocarp (En). V, Vascular bundle. Bar, 300 μm.

1977; Price and Hedley, 1980; Price and Hedley, 1988) and importantly the endocarp received over 20 percent of incident light (Atkins et al., 1977; Price et al., 1988; Donkin and Price, 1990). In intact pea pods, photosynthetic carbon fixation was only greater than respiratory CO_2 evolution early in development when seed respiration rates were low (Harvey et al., 1976; Price and Hedley, 1988). Later in development, pod cavity CO_2 concentration reached a remarkable 4.3 percent at one stage (Harvey et al., 1976).

After injecting $^{14}CO_2$ into pea pod cavities, 45 percent of incorporated ethanol-soluble label was found in the endocarp while the remaining 55 percent was fixed by the outer layers (Atkins et al., 1977). By increasing the incident light to 2200 µmol quanta m^{-2} s^{-1} from 850 µmol quanta m^{-2} s^{-1} this ratio shifted to 66:34 percent (Atkins et al., 1977) and increasing irradiances lowered cavity CO_2 concentrations (Flinn et al., 1977). This light-dependence strongly suggests that photosynthetic electron transport and Rubisco are involved in CO_2 refixation. The pod wall sclerenchyma layer presumably acts as a diffusion barrier and would slow the loss of respired CO_2 to the atmosphere. The resulting high cavity CO_2 concentrations could improve growth efficiency by not only reducing carbon loss but also by the operation of Rubisco close to its V_{max} for the carboxylase reaction.

Although no reports have directly studied canola silique wall refixation, it is doubtful that PEP carboxylase is involved. Singal et al. (1987) reported that *B. rapa* leaf and silique wall activities were very similar. In addition, the ratio of Rubisco and PEP carboxylase activities for *B. rapa* leaf and silique wall tissues were comparable (7:1, 5:1) (Khanna-Chopra and Sinha, 1976). In contrast, pea enzyme ratios were 5:1 for leaf and only 0.7:1 for pod wall (Khanna-Chopra and Sinha, 1976). Pod cavity CO_2 concentrations were extremely high in pea (Harvey et al., 1976) while *B. rapa* concentrations peaked at a lower 0.63 percent (Sheoran et al., 1991).

It is unarguable that developing *Brassica* seeds must have high respiration rates to support growth and storage product synthesis consequently large amounts of CO_2 will be evolved. The fate of this CO_2 is open to a number of possibilities. First, seed-respired carbon may easily diffuse through the silique wall and escape to the atmosphere. Second, respired carbon may be efficiently refixed in the silique

wall inner layers. Third, developing canola embryos contain chlorophyll (Eastmond et al., 1996), therefore respired CO_2 might be refixed by the embryo itself.

SEED

Seed CO_2 fixation would be an intriguing mechanism for seeds to contribute to their own carbon economy by recycling respiratory CO_2. This recycling could theoretically be mediated by Rubisco and PEPC. *Brassica* seed PEPC activities have been shown to be three times greater than silique walls (Singal et al., 1987) and seemed to peak during the oil accumulation phase (Singal et al., 1995; Tittonel et al., 1995). This observation correlates with increasing respiration rates from 10 to 40 d after anthesis (Eastmond et al., 1996). One possible role for PEPC-mediated CO_2 fixation is the replenishment of TCA cycle intermediates. Although fatty acids are the predominant storage product in *Brassica* seeds, a significant amount of storage protein and chlorophyll are being synthesized during this time (Rakow and McGregor, 1975; Crouch and Sussex, 1981; Murphy and Cummins, 1989) and require α-ketoglutarate and oxaloacetate to be drawn from the TCA cycle (Fig. 1.7). PEPC-mediated provision of oxaloacetate may partially waive the need for the cycle to regenerate oxaloacetate. Isocitrate dehydrogenase, a TCA cycle enzyme, and PEPC activities were correlated in pea pod walls and seed coats but not in cotyledons (Hedley et al., 1975).

An alternative PEPC function in developing seeds could be the provision of acetyl-CoA, the precursor for fatty acid synthesis. After conversion of PEP and CO_2 into oxaloacetate, malate can be formed by cytosolic malate dehydrogenase (Fig. 1.7) (Sangwan et al., 1992; Singal et al., 1995). This malate can be decarboxylated to pyruvate by NAD(P) malic enzyme and then converted to acetyl-CoA through the pyruvate dehydrogenase complex. Activities of the required enzymes followed the same trends as PEPC during chickpea seed development (Singal et al., 1986b). If malate is taken up by fatty acid-synthesizing plastids before decarboxylation to pyruvate then the produced NADPH could be used in the energy-intensive fatty acid pathways (Dennis and Blakeley, 1993). This energy production may be the key difference between PEPC-dependent acetyl-CoA provision and the more direct

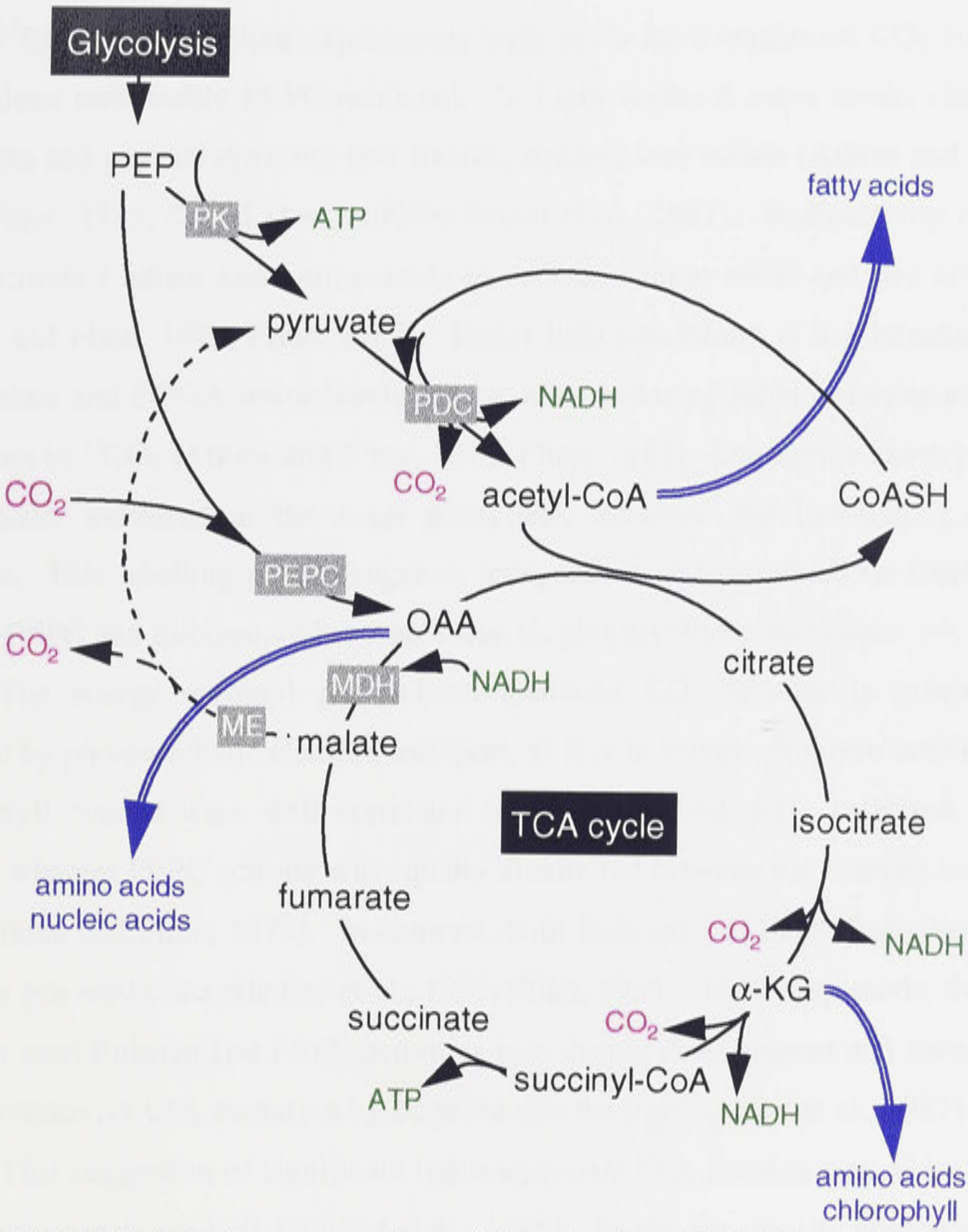

Figure 1.7. Respiratory reactions of the mitochondrial TCA cycle. Carbon enters the cycle as either acetyl-CoA or OAA after conversion from PEP produced in glycolysis. Cycle intermediates are withdrawn to be used for the synthesis of other compounds (blue) and the energy produced in the cycle (green) is used for mitochondrial electron transport. Note that the cycle evolves net CO_2 (red). PK, pyruvate kinase; PDC, pyruvate dehydrogenase complex; PEPC, phosphoenol-pyruvate carboxylase; MDH, malate dehydrogenase; ME, malic enzyme; OAA, oxaloacetate; α-KG, α-ketoglutarate.

conversion of PEP to acetyl-CoA through pyruvate by pyruvate kinase and the pyruvate dehydrogenase complex (Fig. 1.7).

$^{14}CO_2$ pulse-labelling experiments with seeds have confirmed CO_2 fixation into malate, presumably PEPC-mediated. In lupin seeds, *B. rapa* seeds, chickpea seed coats and pea embryos, the first fixation product was malate (Atkins and Flinn, 1978; Flinn, 1985; Singal et al., 1986b; Singal et al., 1987). Radioactivity chased into isocitrate / citrate and amino acids in darkened lupin seeds and pea embryos (Atkins and Flinn, 1978; Flinn, 1985). Under light conditions, it is interesting that both malate and 3-PGA immediately appear after exposing lupin embryos and pea seed coats to $^{14}CO_2$ (Atkins and Flinn, 1978; Flinn, 1985). During the chase period, radioactivity increased in the sugar phosphate, aspartate and isocitrate / citrate fractions. This labelling pattern suggests independent and simultaneous fixation of CO_2 by PEPC and Rubisco, rather than a true C_4 photosynthetic pathway.

The energy required for Rubisco-mediated CO_2 fixation is presumably supplied by photosynthetic electron transport, as it is in leaves. Rubisco activity and chlorophyll content were well correlated in lupin and both were localized to the embryo whereas PEPC activity was equally distributed between the embryo and seed coat (Atkins and Flinn, 1978). In contrast, both Rubisco and PEPC activities were found in pea seed coats (Hedley et al., 1975; Flinn, 1985). In *B. rapa* seeds, the ratio between seed Rubisco and PEPC activities rose during development and seeds were able to reduce net CO_2 evolution by 20 percent in the light (Singal et al., 1987).

This suggestion of significant light-dependent CO_2 fixation was addressed in developing canola seeds (Eastmond et al., 1996). Seeds, specifically embryos, were able to evolve O_2 in a light-dependent manner indicative of photosynthetic electron transport. Embryos had maximum net O_2 evolution rates of 3.1 nmol min^{-1} $embyro^{-1}$ around 40 d after anthesis which translated into an estimated gross evolution rate of 5.8 nmol min^{-1} $embyro^{-1}$ after adding the dark O_2 consumption (respiration) rate. Although O_2 evolution rates and chlorophyll content are only indicative of photosynthetic electron transport and not CO_2 fixation, Rubisco content and NADP-GAPDH activity (another Calvin Cycle enzyme) followed the same trend over development. Embryo chloroplasts, however, had a 2.5-fold higher uncoupled electron transport rate compared to leaf chloroplasts possibly suggesting that

reductant is being supplied to fatty acid synthesis rather than CO_2 fixation. In $^{14}CO_2$ pulse-labelling experiments of *B. rapa* seeds, insignificant levels of label were detected in 3-PGA apparently indicating the absence of Rubisco fixation capacity (Singal et al., 1987). This result is difficult to interpret because seeds were labelled at low CO_2 concentrations (500 µL L^{-1}) and photoinhibitory light levels (1000 µmol quanta m^{-2} s^{-1}) which are not representative of *in vivo* conditions (Sheoran et al., 1991; Eastmond et al., 1996)

In summary, the significance of developing *Brassica* seed CO_2 fixation has not been conclusively determined. Although embryos are capable of photosynthetic electron transport and contain Rubisco, CO_2 fixation has not been experimentally determined. As well, the purpose of high PEPC activities during storage product synthesis and the fate of the fixed carbon has not been established. The localization of these enzymes within seeds and their developmental profiles also needs to be determined in canola.

SEED CARBON UTILIZATION

SUCROSE CLEAVAGE AND CARBOHYDRATE POOLS

Seeds are an important sink tissue in many species, including canola. To be utilized in metabolism, imported sucrose has to be cleaved by either invertase or sucrose synthase (SuSy). Invertase isoforms are localized to different cellular compartments which affects their properties and metabolic role (for review, see Quick and Schaffer, 1996). Alkaline invertase has an optimum pH of 7 to 8 and is localized to the cytosol, soluble acid invertase has an optimum pH of 4 to 5.5 and is localized to the vacuole, and insoluble acid invertase is membrane-bound outside of the cell (apoplastic). Invertase cleavage of sucrose produces free fructose and glucose. In contrast, SuSy cleavage produces free fructose and UDP-Glc. SuSy generally occurs in the cytosol although a cell wall-bound form is associated with cellulose synthesis in cotton (Amor et al., 1995). Unlike invertase, SuSy can catalyze both the cleavage and also the synthesis of sucrose (for review, see Quick and Schaffer, 1996). The net direction of flux *in vivo* is unresolved and

controversial, however cellular pH (Morell and Copeland, 1985), substrate affinities and availability (for review, see Quick and Schaffer, 1996), and phosphorylation status (Huber et al., 1996) will all be influential.

In starch-storing species, SuSy activity has been positively correlated with starch storage (Chourey and Nelson, 1976; Edwards and ap Rees, 1986; Doehlert, 1990; Heim et al., 1993; Weber et al., 1995; Zrenner et al., 1995; Ross et al., 1996; Dejardin et al., 1997). In oil-storing species, starch and hexose accumulate transiently at the early stages of seed development (Norton and Harris, 1975; Hendrix, 1990; Munshi and Kochhar, 1994; Kuang et al., 1996; Kuo et al., 1997) and either invertases (Kuo et al., 1997) or SuSy (Hendrix, 1990) have been reported to have the highest sucrolytic enzyme activities. In cotton, these carbohydrate reserves are localized to the seed coat and most hexose is destined for epidermal hair growth (ie. cellulose fibres) (Hendrix, 1990). Similarly in cruciferous species, seed coat starch disappears during development as an epidermal mucilage layer is formed (Van Caeseele et al., 1981; Kuang et al., 1996).

Developmental profiles of sucrose metabolic enzymes in developing canola seeds have not been reported. The further localization of these enzymes and carbohydrate pools within seed constituents would help to postulate the roles of each. This knowledge is needed to identify suitable targets for the molecular manipulation of carbohydrate metabolism.

SUGAR DELIVERY

The bulk of seed-imported sugar in most dicotyledonous species is destined for the cotyledons of the developing embryo and the timing and pathways of this delivery are the subjects of continuing research (for reviews, see Thorne, 1985; Ho, 1988; Wolswinkel, 1992; Patrick and Offler, 1995; Patrick, 1997; Weber et al., 1997b). In dicotyledons, assimilates are delivered to the developing seed coat by a continuous vascular system and then move symplastically through the coat tissues (for reviews, see Patrick and Offler, 1995; Patrick, 1997). The subsequent transfer to the embryo must be apoplastic because the maternal seed coat is physically separate from the filial embryo. During early developmental stages, a cell wall-bound acid invertase seems to be involved in apoplastic transfer (Weber et al., 1995; Cheng et

al., 1996) and expression in faba bean has been localized to the thin-wall parenchyma cells of the inner seed coat (Weber et al., 1995). Invertase-mediated sucrose cleavage could explain the high hexose pools found during early developmental stages (Norton and Harris, 1975; Heim et al., 1993; Munshi and Kochhar, 1994).

Once the cotyledons have grown large enough to be in close contact with the seed coat, transfer cells develop on the faba bean cotyledonary epidermal surface and sucrose may pass intact from the seed coat. These cells are highly invaginated to expose more cotyledon surface area to the apoplastic space. Sucrose influx into faba bean cotyledons has a large energy-dependent component (Harrington et al., 1997b) and subsequent transfer to the cotyledon's storage parenchyma cells is likely symplastic (for reviews, see Patrick and Offler, 1995; Patrick, 1997). The expression of a sucrose transporter gene and the presence of H^+/ATPase and sucrose binding proteins in epidermal cells corresponded to the appearance of wall ingrowths (Harrington et al., 1997b). In addition, the H^+/ATPase and sucrose binding proteins were localized to the thin-walled parenchyma cells of the faba bean seed coat (Harrington et al., 1997a). Expression of a sucrose transporter gene has been localized to cotyledonary epidermal cells covering storage parenchyma cells while expression of a hexose transporter gene peaked earlier in development and was localized in epidermal cells covering dividing parenchyma cells (Weber et al., 1997a). These molecular biology results confirm the conclusions from physiological experiments that sucrose transfer from seed coats to cotyledons is active at later stages of development (for reviews, see Patrick and Offler, 1995; Patrick, 1997), however the existence of analogous mechanisms in oilseeds is presently unexplored.

RESPIRATION

Once sugar reaches cells synthesizing storage products, hexoses formed after sucrose cleavage have to be phosphorylated by hexokinases before further utilization (Fig. 1.8). For example, Glc-6-P is imported into pea embryo amyloplasts to synthesize starch (Smith and Denyer, 1992). For oil, protein and energy synthesis, hexose phosphate enters glycolysis, the first reaction series of respiration (Fig. 1.8) (for review, see Plaxton, 1996). These reactions take place in the cytosol (although the complete pathway can be duplicated in plastids; Dennis and Miernyk, 1982) and

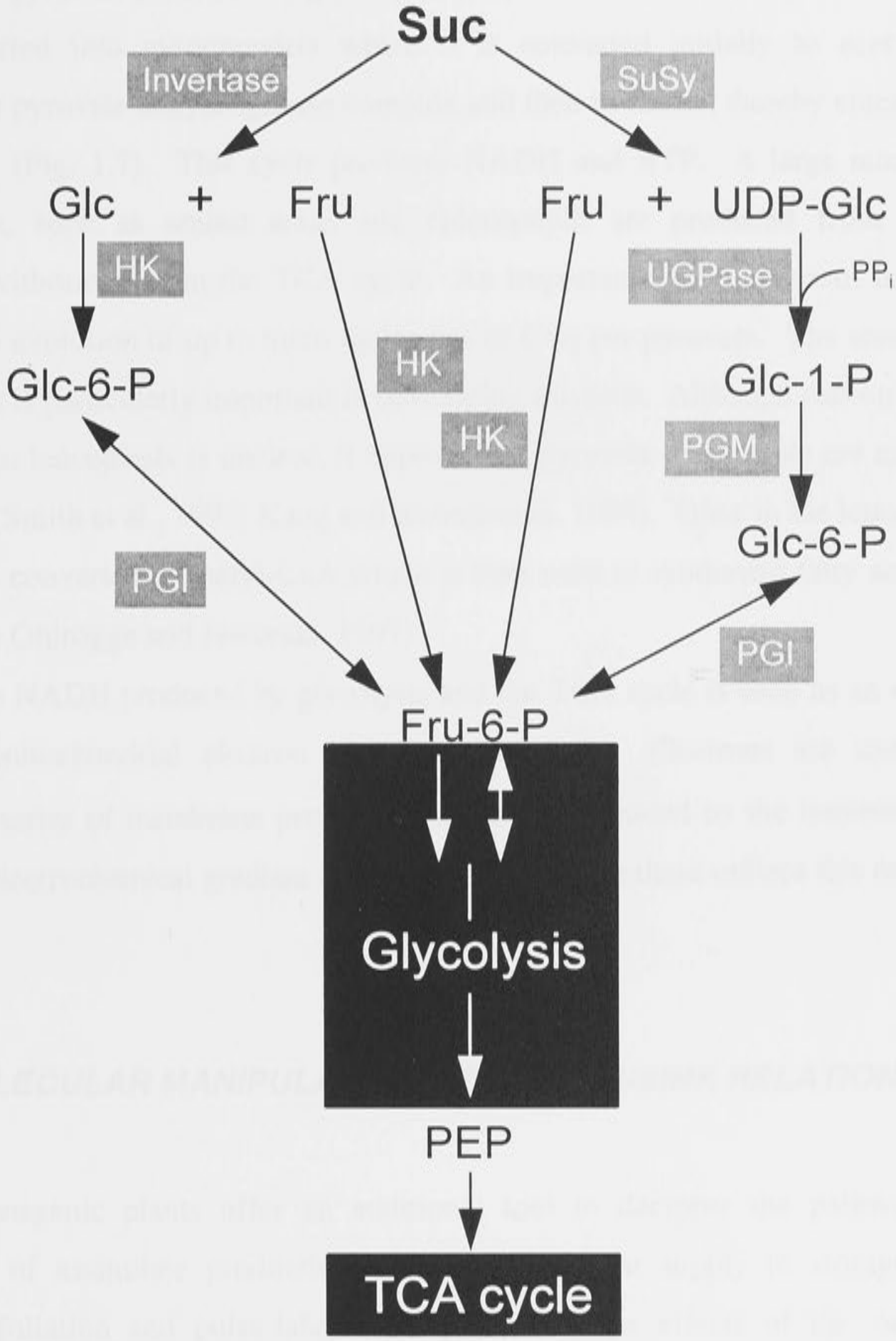

Figure 1.8. Carbon provision to glycolysis. Sucrose is cleaved by either invertases or sucrose synthase (SuSy) and the resulting hexoses are phosphorylated and converted to Fru-6-P. HK, hexokinase; UGPase, UDP-Glc pyrophosphorylase; PGM, phosphoglucomutase; PGI, phosphoglucoisomerase; PP_i, pyrophosphate.

yield pyruvate, NADH and ATP. Glycolytic intermediates can be removed to produce other compounds, such as the glycerol needed for storage oil formation.

The pyruvate produced by glycolysis can be utilized in two ways. First, it can be transported into mitochondria where it is converted initially to acetyl-CoA through the pyruvate dehydrogenase complex and then to citrate, thereby entering the TCA cycle (Fig. 1.7). This cycle produces NADH and ATP. A large number of compounds, such as amino acids and chlorophyll, are produced from carbon skeletons withdrawn from the TCA cycle. An important consequence of the TCA cycle is the evolution of up to three molecules of CO_2 per pyruvate. The second use of pyruvate is particularly important in developing oilseeds. Although carbon's point of entry into leucoplasts is unclear, it appears that pyruvate and malate are excellent substrates (Smith et al., 1992; Kang and Rawsthorne, 1994). Once in the leucoplasts, pyruvate is converted to acetyl-CoA which is then used to synthesize fatty acids (for review, see Ohlrogge and Jaworski, 1997).

The NADH produced by glycolysis and the TCA cycle is used as an electron donor in mitochondrial electron transport (Fig. 1.9). Electrons are transferred through a series of membrane proteins, protons are extruded to the intermembrane space, an electrochemical gradient is formed, and ATP synthase utilizes this energy to form ATP.

MOLECULAR MANIPULATION OF SOURCE-SINK RELATIONS

Transgenic plants offer an additional tool to decipher the pathways and regulation of assimilate production and the subsequent supply to storage sinks. Unlike defoliation and pulse-labelling experiments, the effects of up- or down-regulation of a single enzyme can be precisely monitored under normal growth conditions without confounding side effects. This approach has been used successfully for many enzymes involved in source-to-sink carbon metabolism (Table 1.1) and has been reviewed extensively (Blakeley and Dennis, 1993; Frommer and Sonnewald, 1995; Furbank and Taylor, 1995; Stitt, 1995a,b; Stitt and Sonnewald, 1995; Koßmann et al., 1996).

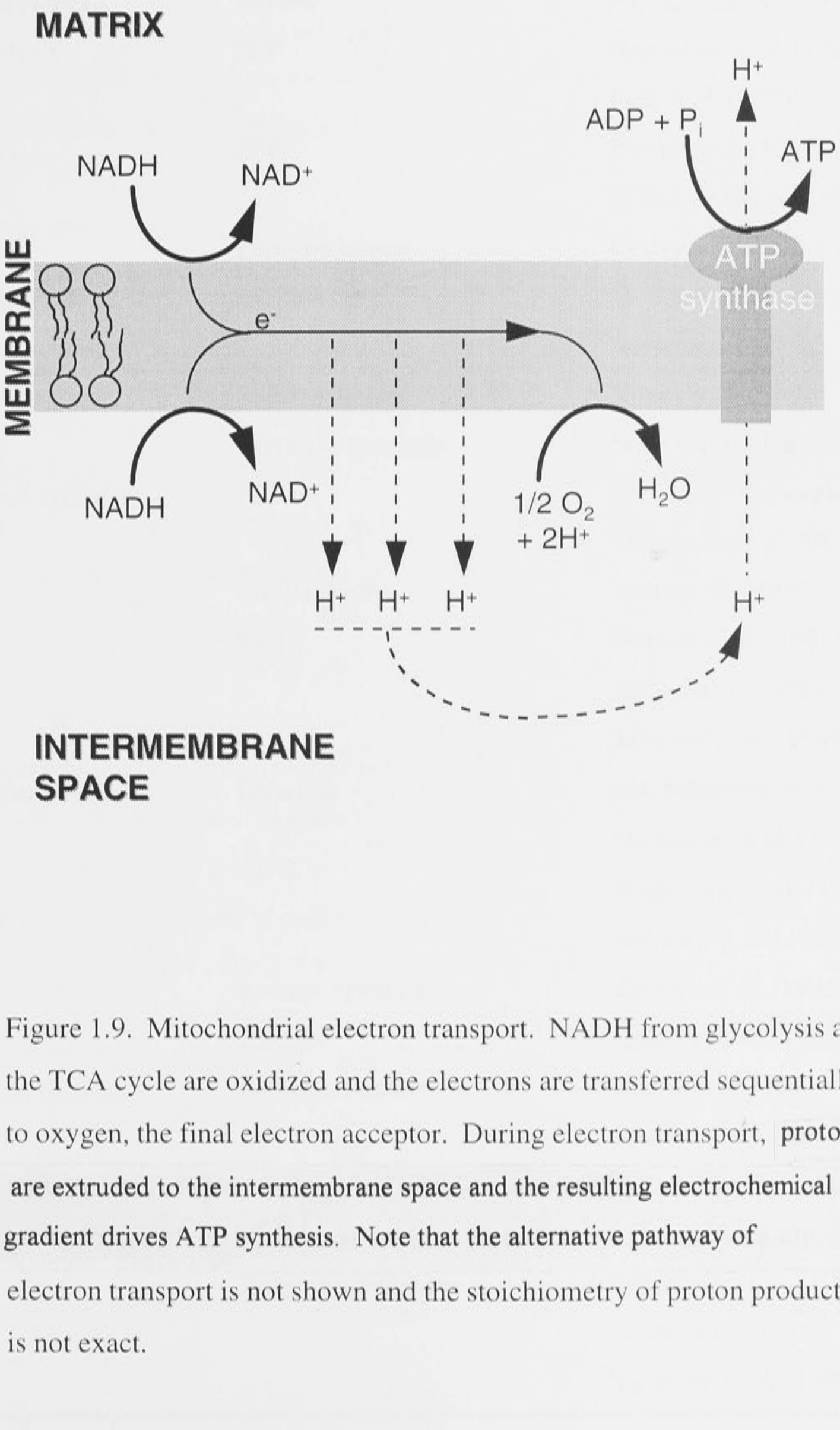

Figure 1.9. Mitochondrial electron transport. NADH from glycolysis and the TCA cycle are oxidized and the electrons are transferred sequentially to oxygen, the final electron acceptor. During electron transport, protons are extruded to the intermembrane space and the resulting electrochemical gradient drives ATP synthesis. Note that the alternative pathway of electron transport is not shown and the stoichiometry of proton production is not exact.

Table 1.1: Molecular manipulation of carbon metabolism in transgenic plants.

PROCESS	TARGET	REFERENCE
Photosynthesis	Review	Furbank and Taylor (1995)
Glycolysis	PFP	Hajirezaei et al. (1994)
		Paul et al. (1995)
	PFK	Burrel et al. (1994)
		Scott and Kruger (1995)
	Pyruvate kinase	Gottlob-McHugh et al. (1992)
Starch synthesis	AGPase	Müller-Röber et al. (1992)
		Stark et al. (1992)
	Starch synthase	Visser et al. (1991)
	Glycogen synthase	Shewmaker et al. (1994)
Sucrose synthesis	FBPase	Juan and Vasconcelos (1994)
		Zrenner et al. (1996)
	Fru-2,6-bisP	Scott et al. (1995)
	SPS	Worrell et al. (1991)
		Galtier et al. (1993, 1995)
		Micallef et al. (1995)
Sucrose cleavage	Invertase	von Schaewen et al. (1990)
		Dickinson et al. (1991)
		Sonnewald et al. (1991)
		Heineke et al. (1992)
	Sucrose synthase	Zrenner et al. (1995)
	UGPase	Zrenner et al. (1993)
Phloem transport	Pyrophosphatase	Jelitto et al. (1992)
		Sonnewald (1992)
		Lerchl et al. (1995)
		Geigenberger et al. (1996)
	Sucrose transporter	Riesmeier et al. (1994)
		Kühn et al. (1996)
		Lemoine et al. (1996)

Metabolic engineering involves either the reduction in the level of an endogenous enzyme (gene suppression), the increase of an endogenous enzyme's activity by the introduction of extra gene copies (overexpression), or the introduction of genes coding for novel enzymes. The results of these molecular manipulations have not always been predictable and have raised a number of important issues; multiple enzymes share regulatory control of metabolic fluxes through pathways, post-translational modification and alternative pathways can compensate for the suppression of one enzyme, enzymes catalyzing irreversible reactions can have low flux control, enzymes catalyzing reversible reactions are not always present in excess, and enzymes within and between pathways interact (Stitt and Sonnewald, 1995). Downregulation of enzyme activity, through antisense RNA, is relatively straightforward compared to attempts to increase the activity of endogenous enzymes. In fact, plant transformation with overexpression gene constructs can reduce the targeted endogenous enzyme's activity and this phenomenon is termed cosupression or gene silencing (for reviews, see Baulcombe, 1996; Stam et al., 1997). For successful overexpression, the choice of divergent gene sequences can avoid a plant's natural regulatory mechanisms. Bacterial genes are obviously divergent, although codon usage may pose a problem, and monocotyledonous sequences show low nucleotide identity to dicotyledonous sequences. Another issue to be considered is the targeted enzyme's subcellular location and isoform (Blakeley and Dennis, 1993) which requires the correct temporal and spatial expression of transgenes. This level of precision is limited by few promoter choices rather than the availability of coding sequences, largely because of the invaluable *Arabidopsis* and rice expressed sequence tag (EST) databases.

One example of metabolic engineering is the alteration of sucrose synthesis capacity. In source tissues, sucrose is the interface between CO_2 fixation and carbohydrate transport to sink tissues. SPS is believed to have significant control of the sucrose biosynthetic pathway and would therefore appear to be a good target for modification. A maize cDNA encoding SPS has been transformed into tomato under the control of a *rbcS* promoter. SPS activities in a transgenic line were up to six-fold higher than wild-type, sucrose contents were two-fold higher, and starch content

decreased by 50 % (Worell et al., 1991). Higher photosynthetic rates were detectable in transformed plants at saturating conditions (Galtier et al., 1993; Micallef et al., 1995; Galtier et al., 1995), sugar-to-starch CO_2 partitioning increased (Micallef et al., 1995; Galtier et al., 1995), a significant decrease in root dry weight increased the shoot-to-root ratio (Galtier et al., 1993), and these plants flowered earlier producing increased numbers of inflorescences and fruit (Micallef et al., 1995). Clearly, dramatic whole-plant effects were demonstrated through the introduction of a single gene into these tomato plants. Attempts to repeat these effects in potato and tobacco led to increased SPS protein but enzyme activity was unaffected because post-translational modification kept the excess protein inactivated (Sonnewald et al., 1994). It is therefore not clear whether dramatic effects on the whole plant level, such as those seen in tomato, can be reproduced in other species.

NITROGEN METABOLISM

In contrast to carbohydrate metabolism, the biochemistry of nitrogen metabolism in non-nodulating species has not been extensively studied. Nitrogen is nevertheless a major assimilate that is used to synthesize protein, nucleic acids and other compounds. Non-nodulated plants acquire inorganic nitrogen from the soil as either NO_3^- or NH_4^+. NO_3^- is reduced either in the roots or leaves (for review, see Andrews, 1986) by nitrate reductase and nitrite reductase to NO_2^- and then NH_4^+, respectively (Fig. 1.10). Due to the toxicity of ammonium, it must be quickly converted with glutamate to glutamine by glutamine synthetase. Glutamine can also be converted to the other amide, asparagine, by asparagine synthetase. These amides can then serve as nitrogen donors for the synthesis of other amino acids by aminotransferases.

Glutamine, glutamate, asparagine and aspartate are the predominant forms of nitrogen that are phloem-transported to sink tissues and the relative contents of each vary between species. In canola and *Arabidopsis*, glutamine and glutamate are the most abundant phloem amino acids but serine, aspartate and asparagine are also significant (Weibull and Melin, 1990; Lohaus, 1995; Lam et al., 1995). Asparagine

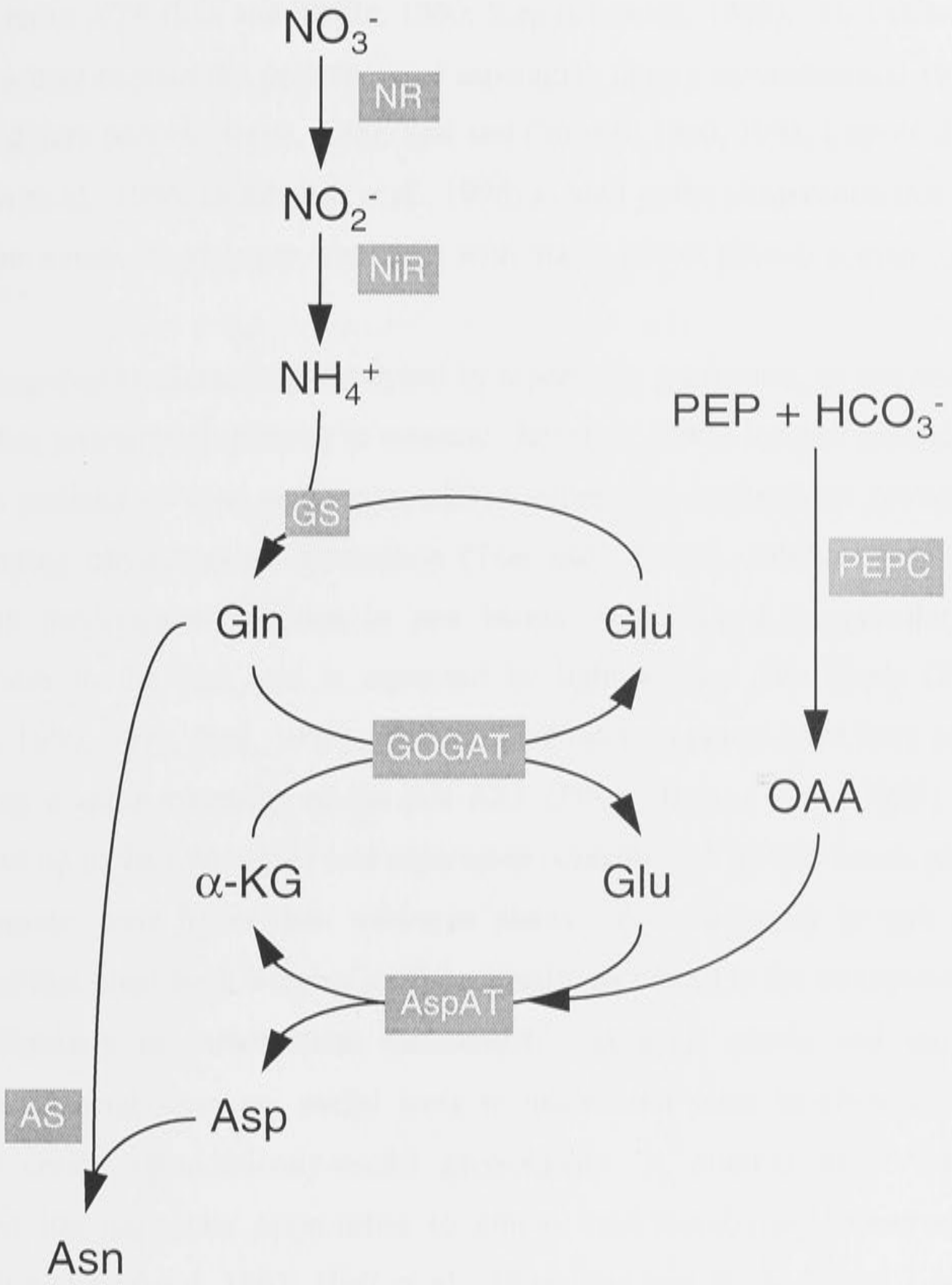

Figure 1.10. Nitrogen assimilation pathways. Soil-derived inorganic nitrogen is reduced to glutamine (Gln) by nitrate reductase (NR), nitrite reductase (NiR), and Gln synthetase (GS). Gln is further metabolized to other amino acids including asparagine (Asn), glutamate (Glu) and aspartate (Asp). GOGAT, glutamate synthase; AspAT, Asp aminotransferase; PEP, phosphoenolpyruvate; PEPC, PEP carboxylase; OAA, oxaloacetate; α-KG, α-ketoglutarate.

conserves carbon more efficiently and is more stable than glutamine but its synthesis requires extra ATP (Lea and Miflin, 1980; Siegiechowicz, 1988). This efficient use of carbon may explain the prevalence of asparagine during environmental stress and prolonged dark periods (Rabe, 1990; Tsai and Coruzzi, 1990, 1991; Lam et al., 1995; Chevalier et al., 1996; Dembinski et al., 1996) as well as the observation that phloem asparagine content is strongly correlated with maize kernel protein content (Lohaus, 1995).

Asparagine synthesis is catalyzed by asparagine synthetase, an enzyme whose activity has proven very difficult to measure (Joy et al., 1983; Joy and Ireland, 1990). With the isolation of gene sequences, mRNA expression studies have proven useful in generating physiological information (Tsai and Coruzzi, 1990). Expression of AS1, the predominant isoform in pea leaves, is localized to vascular tissue, accumulates in the dark and is repressed by light at very low levels (Tsai and Coruzzi, 1990, 1991; Tsai, 1991). Transformed tobacco plants have been produced containing a sense construct of the pea AS1 cDNA (Brears et al., 1993). These plants had up to 40-fold higher leaf asparagine contents and its substrates, glutamine and aspartate, were lower than wild-type plants. A rudimentary growth analysis suggested that plant fresh weights were marginally increased in the transgenic plants.

Similarly to carbohydrate metabolism, transgenic plants and mutants of amino acid metabolism are useful tools to understand plant biochemistry and to possibly create agronomically-useful germplasm. A number of reviews have examined the molecular approaches to amino acid metabolism (Coruzzi, 1991; McGrath and Coruzzi, 1991; Hoff et al., 1994; Lea and Forde, 1994; Lam et al., 1995, 1996; Oliveira et al, 1997). These approaches provide a unique tool to elucidate the relationships between source tissue amino acid content and seed amino acid and protein composition in an analogous way to the approach used in carbohydrate metabolism.

THESIS OBJECTIVES

The general objective of this thesis was to understand the biochemical and physiological factors determining seed yield in canola (*Brassica napus* L.). Obvious deficiencies existed in the literature, consequently it was hoped that a clearer picture of the factors involved in assimilate partitioning to seeds could be later exploited to design effective genetic engineering strategies for crop improvement.

First, the key elements of source-sink carbohydrate metabolism during seed filling were examined. Photosynthetic capacities, carbon partitioning, carbohydrate reserves and sucrose metabolic enzyme activities were determined while seeds were synthesizing storage products. Second, the CO_2 fixation capacities of developing seeds and silique wall were assessed and related to *in vivo* conditions. Third, DNA vectors designed to perturb normal assimilate partitioning were constructed and transformed into cotyledonary explants via *Agrobacterium*. Fourth, T_1 plants were screened for transgene expression levels, enzyme activities, and phenotypic changes.

CHAPTER 2: CARBOHYDRATE CONTENT AND ENZYME METABOLISM IN DEVELOPING SILIQUES

INTRODUCTION

The sources of assimilate for developing canola seeds have not been clearly elucidated. During the life of a plant there is a clear sequence of developmental phases proceeding from leaf to stem to silique (pod) to seed (Mendham and Salisbury, 1995). Leaf photosynthesis provides assimilate for the growth of shoot and root meristems. At the initiation of reproductive growth, there is a rapid increase in flower-bearing branches from the shoot apical meristem. Photosynthetic leaf area then quickly declines due to senescence (Pechan and Morgan, 1985) thereby removing one source of assimilate at a time when seeds have a great import demand. At this time, only the oldest seeds at the base of a plant would have begun storage product synthesis. In the absence of leaves, silique wall photosynthesis is the main source of assimilates during this growth phase and may contribute up to 50-60 percent of final plant dry matter (Lewis and Thurling, 1994).

Like most other dicotyledonous plants, canola produces seed storage products in the embryo (Murphy and Cummins, 1989). Early in development, the embryo is very small and the main seed constituents are the seed coat and liquid endosperm (Fowler and Downey, 1970). During these initial stages embryo cells are rapidly dividing. At the early- to mid-cotyledon stage, embryo cells begin to rapidly expand (Fig. 1.1 and Pomeroy et al., 1991) and the resulting growth consumes the liquid endosperm and the embryo fills the seed's internal space (Fowler and Downey, 1970). Coincident with rapid embryo growth, storage oil accumulates and peaks at maximum fresh weight (Rakow and McGregor, 1975; Murphy and Cummins, 1989; Hocking and Mason, 1993). There is a delay after oil accumulation initiation before storage protein accumulates (Crouch and Sussex, 1981; Murphy and Cummins, 1989).

Starch and sucrose are the major end products of photosynthetic carbon fixation and sucrose is the preferred form of carbon which is exported via the phloem

to sink tissue (see Chapter 1). The products of sucrose cleavage are converted to hexose phosphates and can enter the respiratory pathways via glycolysis to provide substrates and energy for growth and storage product synthesis.

This study has focussed on the growth and development of source silique wall and its developing seed sinks during the oil filling period. Photosynthetic carbon partitioning, carbohydrate content and sucrose metabolic enzymes have been measured and compared at the beginning, middle and end of this period. The objective was to identify key elements of source-sink carbohydrate metabolism in canola siliques.

MATERIALS AND METHODS

MATERIALS

Plants of *Brassica napus* L. cvs Westar, Hyola 42 were grown in a mixture of compost and perlite (1:1, v/v) supplemented with Osmocote slow-release fertilizer (Scotts, Nedlands, Australia). Plants were grown in a naturally-illuminated glasshouse with temperatures set at 23/18 ^{o}C day/night. At floral initiation emerging flowers were tagged three times weekly in the early morning. Only siliques from the main raceme and the first two branches were used for experiments. All plants were well-spaced to maximize light interception and to minimize canopy effects.

All biochemicals and enzymes were supplied by Boehringer Mannheim Australia (Sydney, NSW) or Sigma Chemical Co. (St. Louis, MO). Barium [^{14}C] carbonate was obtained from Amersham Australia (Sydney, NSW). All other reagents were of analytical grade.

LEAF AREA MEASUREMENTS

At weekly intervals following the opening of the first flower, leaf area was individually measured for all leaves from each of four plants. Each leaf outline was traced onto paper, cut out and weighed on an electronic balance. Paper weights were converted to leaf area using a standard curve. Each leaf was also visually scored for

its colour. Only leaves that had lost all green pigmentation were counted as being senescent.

PHOTOSYNTHETIC RATES

Net CO_2 consumption rates of intact fully-expanded leaves and 28 DAA siliques were measured using ADC LCA2 (ADC, Hoddenson, UK) and Li-Cor 6400 (Li-Cor, Lincoln, NE) infrared gas analysers, respectively. Data were collected at air-level CO_2 concentrations using a flow rate of 200 cm^3 min^{-1} and chamber temperatures were maintained between 22 and 26 °C. After dark adaptation, irradiances were increased step-wise to saturating levels and steady-state CO_2 exchange rates were reached between increases.

Net O_2 evolution rates of leaf discs and silique wall pieces were measured in a leaf -disc O_2 electrode at 25 °C (Hansatech, Norfolk, UK). Saturating CO_2 conditions were established with 1M $NaHCO_3$ and tissues were dark-adapted in the chamber for at least 20 min before the initiation of data collection. Light was provided by a slide projector and irradiance was modulated with neutral density filters.

$^{14}CO_2$ PARTITIONING

Leaves and siliques were pulse-labelled with $^{14}CO_2$ as described by Lunn and Hatch (1995). Two leaf pieces of approximately 25 cm^2 were cut around the mid-rib of young fully-expanded leaves before placing the basal end in a water-filled trough of a perspex chamber. For siliques, the cut **pedicel** ends of four siliques were placed in the water-filled trough. Tissues were illuminated for 30 min at an irradiance of 1000 to 1200 µmol quanta m^{-2} s^{-1}, 400 to 420 µL L^{-1} CO_2 and 25 °C to reach steady-state photosynthetic rates before injection of $^{14}CO_2$ into the sealed chamber. After a 135 s pulse, leaves were removed and killed in boiling 80 % (v/v) ethanol for 1 min. Siliques were removed after 600 s and plunged into liquid nitrogen. Gentle crushing with a pestle allowed separation of silique wall and seed tissues before boiling in 80 % (v/v) ethanol. The rest of the extraction procedure and analysis was identical to Lunn and Hatch (1995).

CARBOHYDRATE AND LIGNIN ANALYSIS

Tissue samples were taken from three plants (replicates) just before sunrise (06:00) and after 12 h (18:00) during a partly sunny day in late spring. The day's accumulated PAR was 29.9 mol quanta m^{-2} as measured inside a glasshouse. Immediately after harvest, samples were frozen in liquid nitrogen and stored at -80 ^{o}C until analysis. Each leaf sample contained three 1.33 cm^2 leaf discs from the youngest, fully-expanded leaf on plants sown one month previously. Each silique sample contained two intact siliques of the same age.

Silique samples were separated into silique wall and seed fractions by gently crushing in liquid nitrogen. Each fraction was ground to a fine powder in liquid nitrogen and then transferred to a plastic centrifuge tube. After evaporation of the liquid nitrogen, carbohydrates were extracted in boiling 80% (v/v) ethanol as described by Lunn and Hatch (1995). Hexoses were measured spectrophotometrically in a 1mL assay mix containing 100 mM Tris-HCl / 5 mM $MgCl_2$, pH 8.1, 1 mM ATP, 0.5 mM NADP and 2 U Glc-6-P-dehydrogenase (EC 1.1.1.49) by the successive addition of 2 U hexokinase (EC 2.7.1.1) and 3.33 U phosphoglucoisomerase (EC 5.3.1.9). Seed extracts were treated with activated charcoal before assay to remove compounds that interfered with absorbance measurements. Sucrose and starch were assayed as per Lunn and Hatch (1995).

To localize seed carbohydrates, fresh seeds containing early-cotyledon embryos were dissected on ice into seed coat/endosperm and embryo fractions. Each fraction was ground to a powder in liquid nitrogen and then sucrose, hexose and starch were extracted and assayed as described above. In parallel to carbohydrate determinations, samples were used to determine the fresh and dry weights of each fraction and the water content was considered to be the difference between these weights. Tissues were oven-dried to constant weight at 90^{o}C. Both the carbohydrate and weight determinations were done in triplicate with approximately 20 tissues per replicate.

The aqueous-ethanol insoluble residues remaining after extraction of soluble carbohydrates and treatment with KOH (Lunn and Hatch, 1995) were assayed for cellulose and lignin. Residues were collected by centrifugation for 5 min at 12 000 *g* and then dried to constant weight at 90 ^{o}C. Non-cellulosic compounds were

solubilized with boiling acetic/nitric reagent and then cellulose was collected by centrifugation (Updegraff, 1969). Cellulose was hydrolyzed by boiling in 67 % (v/v) H_2SO_4 containing 0.13 % (w/v) anthrone for 16 min. A standard curve was generated using pre-dried microcrystalline cellulose (Avicel) (Merck, Darmstadt, Germany). For lignin assays, 20 to 70 mg oven-dried aqueous-ethanol insoluble residue underwent a two-stage acid hydrolysis procedure to solubilize other compounds (Sewalt et al., 1996). Acid-insoluble (Klason) lignin was collected by vacuum filtration and dried to constant weight at 90 °C before weighing.

MICROSCOPY

Developing 21 and 28 DAA seeds were vacuum infiltrated into a fixative solution containing 2 % (w / v) paraformaldehyde and 0.1 % (v / v) glutaraldehyde in 25 mM Na_2HPO_4 / NaH_2PO_4 buffer, pH 7.2 immediately after removal from the silique. After 1.5 h at 4 °C, the samples were washed with buffer and then taken through an ethanol dehydration series at 4 °C and then an infiltration series with LR White resin before polymerization at 45 °C for 1 to 1.5 h under a dry N_2 atmosphere. Embedded seeds were sectioned 1 µm thick using a Reichart Ultracut microtome, stained with toluidine blue O (0.025 % w / v in 1 % $NaBO_4$, pH 11), and visualized under bright-field.

ENZYME ASSAYS

Triplicate silique and leaf samples were taken at midday in late summer (whole-day accumulated PAR was 35.9 mol quanta m^{-2}) and were immediately frozen in liquid nitrogen before storage at -80°C until analysis. Siliques were gently crushed in liquid nitrogen to separate silique wall and seed tissue. Samples of silique wall containing approximately 40 µg chlorophyll or 15 seeds were extracted in 1.5 mL buffer. The extraction buffer contained 50 mM Hepes-KOH, pH 7.5, 10 mM $MgCl_2$, 1 mM EDTA, 1 mM EGTA, 2 mM DTT, 5 mM ε-aminocaproic acid, 1 mM PMSF, 1 mM benzamidine, 1 mM benzamide, 2% (w/v) insoluble PVP, 0.5% (w/v) BSA, 0.1% (v/v) Triton X-100, 2 µM leupeptin, and 2 µM antipain. A 100 µL sample of extract was added to 1 mL of cold methanol for chlorophyll determination (Porra et al., 1989). The remaining extract was centrifuged for 2 min at 12 000 *g* and a 0.5 mL sample of the supernatant was desalted by passage through a 4 mL

Sephadex G-25 (Pharmacia, Uppsala, Sweden) column pre-equilibrated with extraction buffer minus BSA, insoluble PVP and Triton X-100. All procedures were done at 4 °C. Enzymes were assayed immediately in duplicate.

For a separate experiment on seed components, seeds were dissected immediately after harvest at 4 °C and then frozen in liquid nitrogen and stored at -80 °C until analysis. Triplicate samples of 15 organs each were ground in 1.0 mL of extraction buffer and desalted as above.

Sucrose-phosphate synthase (EC 2.4.1.14). Total SPS activities were assayed by measuring the synthesis of Suc-6-P (and sucrose) from UDP-Glc and Fru-6-P (Huber and Huber, 1991). Each reaction contained 20 mM UDP-Glc, 5 mM Fru-6-P, 17.5 mM Glc-6-P and 50 µL extract in a total volume of 100 µL. The reaction was started by the addition of extract and incubated at 25 °C for 10 min. After stopping the reaction with 100 µL of 5 M KOH and 10 min heating at 100 °C to destroy unreacted hexoses and hexose phosphates, 1 mL of 0.14% (w/v) anthrone in 80% (v/v) H_2SO_4 was added before 40 min incubation at 40 °C. Suc-6-P (and sucrose) content was determined by relating the A_{628} to that of a standard curve (0-200 nmol sucrose). The recovery of sucrose was estimated by incubating 50 µL extract with 100 nmol sucrose under the above assay conditions.

Sucrose synthase (EC 2.4.1.13). UDP-dependent cleavage of sucrose into UDP-Glc and Fru was assayed (Copeland, 1990). Each reaction contained 20 mM Pipes-KOH, pH 6.5, 100 mM sucrose, 2 mM UDP and 20 µL extract in a total volume of 250 µL. Control reactions lacked UDP. Reactions were started by the addition of extract and incubated at 25 °C for 30 min. The reactions were stopped with 250 µL of 0.5M Tricine-KOH, pH 8.3 and boiling for 10 min. Fru was measured spectrophotometrically as described above.

Invertases (EC 3.2.1.26). Soluble acid and alkaline invertases were measured by incubation of 20 µL of extract with 100 mM sucrose in 100 mM acetic acid-NaOH, pH 5.0 (acid invertase) or 100 mM sodium acetate-acetic acid, pH 7.5 (alkaline invertase) in a total volume of 250 µL. Reactions were started by the addition of extract and incubated at 25 °C for 30 min. The reactions were stopped with 250 µL of 0.5M Tricine-KOH, pH 8.3 and boiling for 10 min. Control reactions

contained boiled extract. Glc was measured spectrophotometrically as described above.

RESULTS

PHOTOSYNTHESIS

As a first step in determining the important elements of silique carbon metabolism, the potential contribution from leaves was assessed by measuring leaf area after the emergence of the first flower. At weekly intervals, leaf area was measured non-destructively and leaf colour was used as an indicator of photosynthetic competence. Fully yellow leaves were classified as being senescent. By first flower, 40 percent of total leaf area was already senescent and all leaves were senescent by 35 DAFF (Fig. 2.1). By 35 DAFF, seed age on a plant would range from approximately 14 to 35 DAA due to canola's indeterminate growth habit. Embryos developed from mid- to late-cotyledon stages from 23 to 32 DAA, the period of maximum storage oil accumulation (Pomeroy et al., 1991).

The photosynthetic capacities of leaves and siliques were compared using CO_2 gas exchange analysis. Young fully-expanded leaves had a maximum net CO_2 assimilation rate of 32 μmol m^{-2} s^{-1} and were light-saturated over 800 μmol quanta m^{-2} s^{-1} (Fig. 2.2). In contrast, 28 DAA siliques had a maximum rate of 10 μmol m^{-2} s^{-1}. The silique light compensation point and the dark CO_2 evolution rate were several-fold higher than leaves. The photosynthetic capacity of silique wall was measured by removing the seeds and placing silique wall pieces into a leaf-disc O_2 electrode (Table 2.1). Under saturating conditions, silique wall evolved up to 5.2 μmol O_2 min^{-1} mg $chlorophyll^{-1}$, a rate equivalent to leaves, but much lower chlorophyll concentrations reduced photosynthesis per unit surface area.

Siliques were further compared to leaves by measuring the incorporation of $^{14}CO_2$ into the primary photosynthetic end products, sucrose and starch, after a short pulse under steady-state physiological conditions. Radioactivity in sucrose and aqueous-ethanol insoluble fractions was used to calculate the partitioning of photosynthate between sucrose and starch. Within the first hour of illumination both

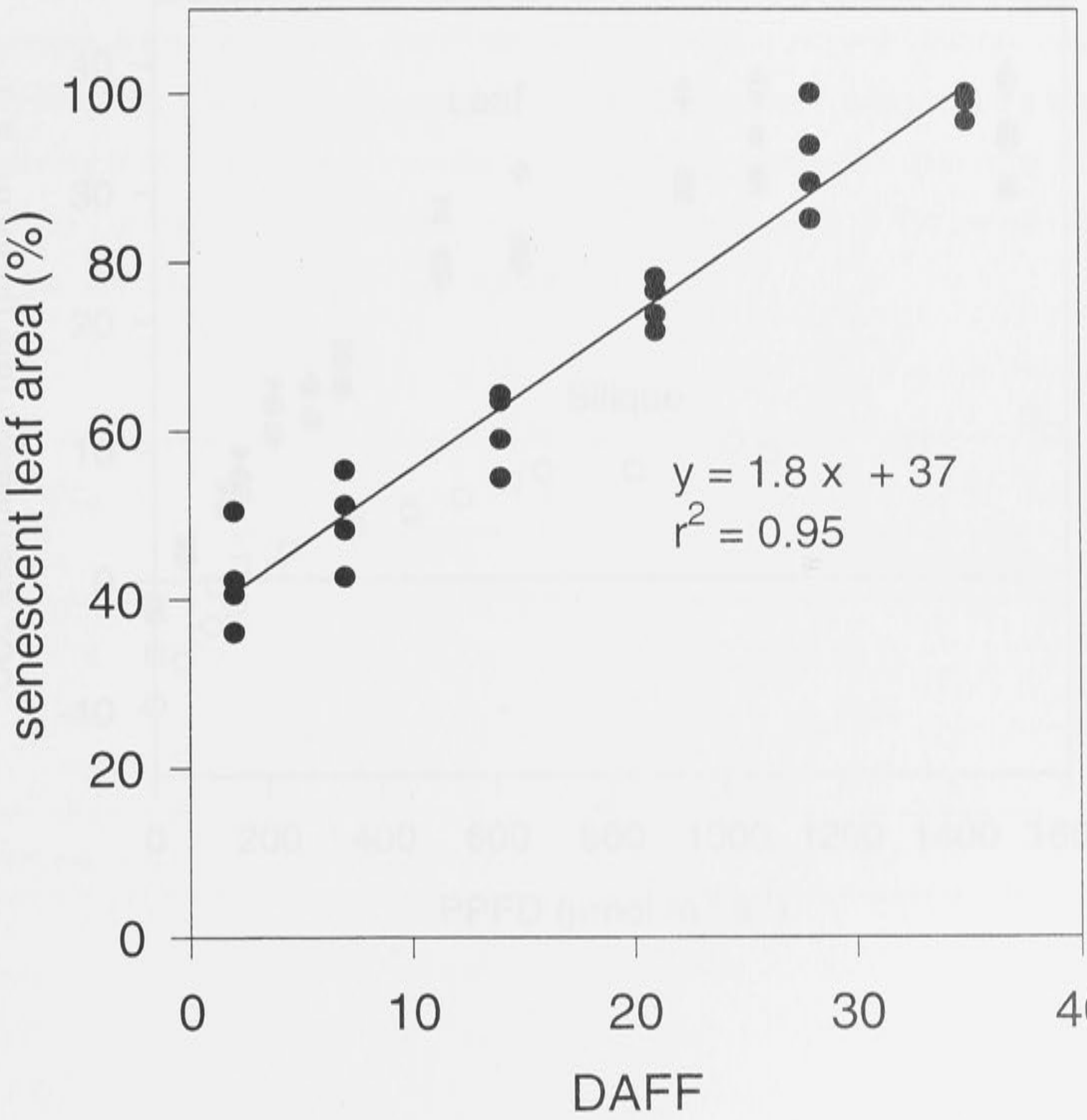

Figure 2.1. Increase of senscent leaf area after first flower. Fully yellow leaves were scored as senescent and their areas are expressed as a percentage of total area at first flower. Individual leaves did not increase in area after this time.

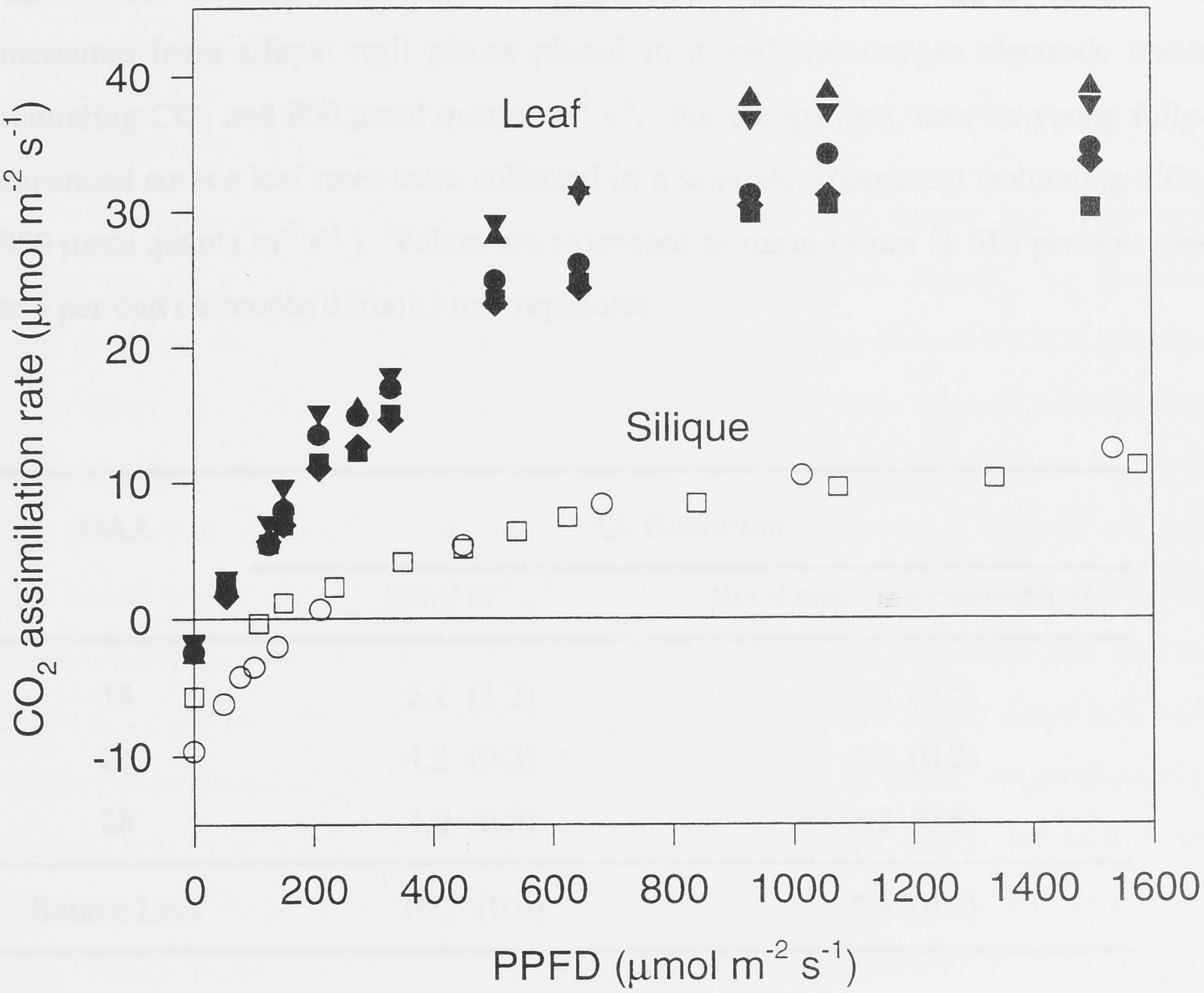

Figure 2.2. Photosynthetic capacity of leaves and siliques. The net CO_2 assimilation rates of young fully-expanded leaves (filled symbols) and 28 DAA siliques (open symbols) were measured at atmospheric CO_2 concentrations and varying irradiances using infrared gas analyzers. Each symbol shape represents measurement froma separate plant.

Table 2.1. Maximum silique wall photosynthetic capacity. O_2 evolution was measured from silique wall pieces placed in a leaf-disc oxygen electrode under saturating CO_2 and 800 µmol quanta m^{-2} s^{-1}. For comparison, data on young fully-expanded source leaf rates were collected in a separate experiment (saturating CO_2, 950 µmol quanta m^{-2} s^{-1}). Values are expressed as mean values (± SE) per unit area and per unit chlorophyll from 3 to 4 replicates .

DAA	O_2 Evolution	
	µmol m^{-2} s^{-1}	*µmol min^{-1} mg chlorophyll^{-1}*
14	5.1 (1.3)	3.6 (0.5)
21	4.3 (0.3)	4.2 (0.2)
28	4.0 (0.3)	5.2 (0.6)
Source Leaf	36.2 (0.6)	5.5 (0.1)

source leaves and siliques preferentially partitioned newly fixed carbon into sucrose (Table 2.2). Near the end of the photoperiod, leaves were producing more starch than sucrose while siliques continued to partition more photosynthate into sucrose. At both times, silique sucrose to starch partitioning ratios were 3 to 4-fold higher than leaves. Negligible radioactivity was found in seeds and in all other tissues hexoses contained less than 2.5 percent of total radioactivity.

CARBOHYDRATE CONTENTS

Carbohydrate accumulation in silique wall and seed tissues was examined during the progression from embryo early- to late-cotyledon stages. All samples were taken on a single day from plants sown on the same day (plants for leaf samples sown later). To guard against a position effect, only the main raceme and the first two branches were used for sampling. As well, samples for all experiments reported here were taken from plants aged 30 to 40 DAFF. The contents of hexose, sucrose and starch of developing siliques are presented in Fig. 2.3. In silique wall, the predominant carbohydrates were glucose and fructose (Fig. 2.3A). With age, hexose levels fell rapidly. Although present in a smaller quantity, starch also decreased with development while sucrose levels were essentially stable. In seeds, the predominant carbohydrate was starch (Fig. 2.3B). Along with sucrose, starch levels did not significantly change in the 21 to 35 DAA period. Hexoses did, however, drop significantly between 21 and 28 DAA. This period corresponds to the beginning of rapid embryo fresh weight gains (see Chapter 3). The data presented in Fig. 2.3 are drawn from samples taken at the beginning of the photoperiod (06:00). An equal number of samples were taken near the end of the photoperiod (18:00). There were no significant differences between the morning and evening samples in either silique wall or seed (data not shown). As a comparison, starch increased five-fold in photosynthetically-active leaves (Table 2.3).

To investigate carbohydrate distribution within young seeds, embryos were dissected from the seed coat and liquid endosperm before separate analysis for hexoses, sucrose and starch. On a dry weight basis, sucrose was evenly distributed between the seed coat/endosperm and the embryo while hexoses and starch were much more prevalent in the seed coat/endosperm (Table 2.4). Assuming that the

Table 2.2. Photosynthate partitioning in canola leaves and siliques. The relative rates of $^{14}CO_2$ incorporation into sucrose and starch were measured in leaves and siliques undergoing steady-state photosynthesis at an irradiance of 1000-1200 μmol quanta m^{-2} s^{-1}, 400-420 μL L^{-1} CO_2 and 25 °C. Measurements were made in duplicate 1h and 9h after the start of the photoperiod.

Tissue	Age	Photosynthate Partitioning (^{14}C sucrose to ^{14}C starch)	
		1 h	9 h
Leaf	Expanded	1.8	0.8
Silique	21 DAA	5.7	3.1
	35 DAA	6.0	2.5

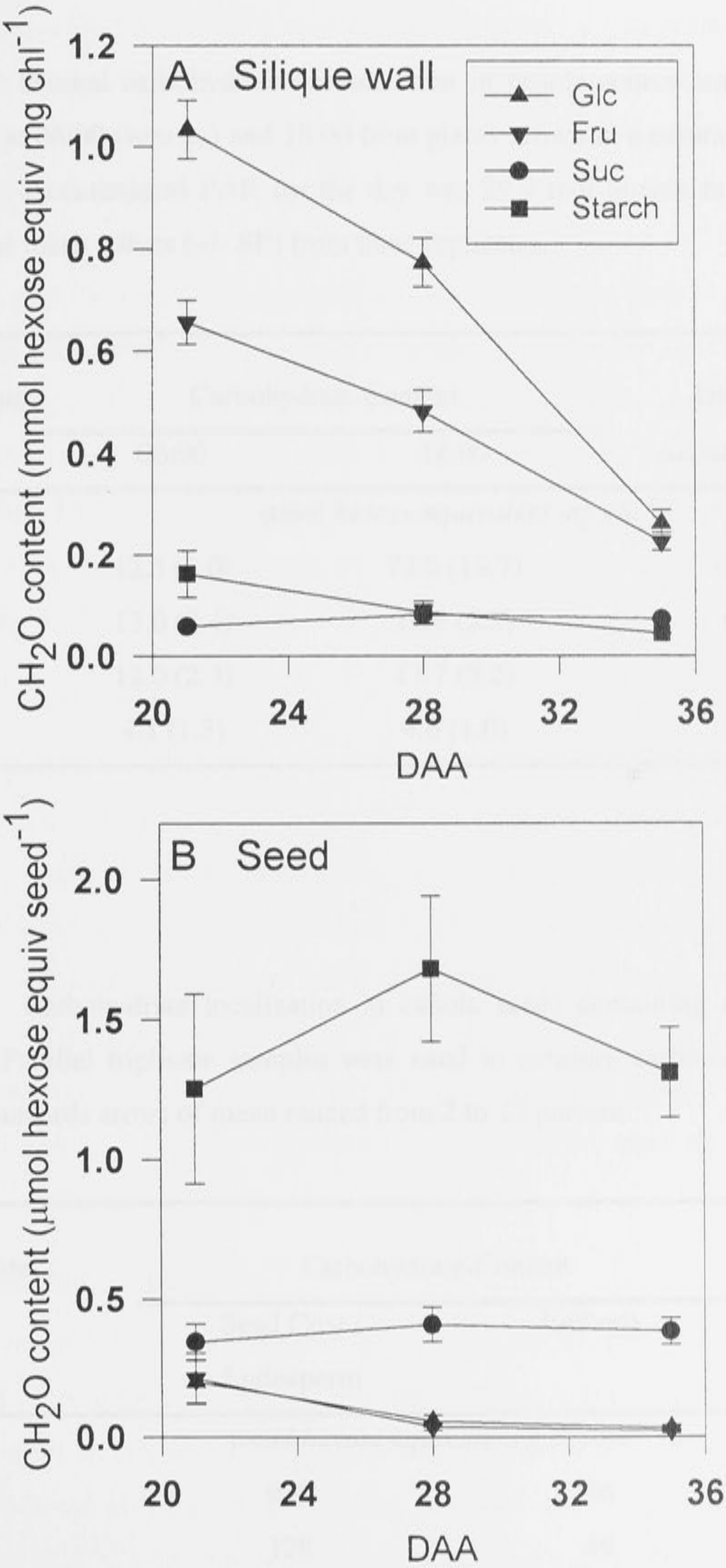

Figure 2.3. Carbohydrate content of developing silique wall (A) and seed (B). Samples were taken at sunrise on a single day. Mean values and standard errors of three replicates are plotted for each measured carbohydrate and age.

Table 2.3. Diurnal carbohydrate accumulation in canola source leaves. Samples were taken at 06:00 (sunrise) and 18:00 from plants grown in a naturally-illuminated glasshouse. Accumulated PAR for the day was 29.9 mol quanta m^{-2}. Values are expressed as mean values (+/- SE) from three replicates.

Carbohydrate	Carbohydrate Content		Diurnal
	06:00	18:00	Accumulation
	µmol hexose equivalent mg chl^{-1}		
Starch	12.5 (1.0)	73.2 (19.7)	60.7
Glc	13.0 (2.4)	19.8 (5.3)	6.8
Fru	12.0 (2.3)	17.7 (5.2)	5.7
Suc	4.1 (1.3)	4.6 (1.0)	0.5

Table 2.4. Carbohydrate localization in canola seeds containing early-cotyledon embryos. Parallel triplicate samples were used to measure carbohydrates and dry weight. Standards errors of mean ranged from 2 to 23 percent.

Carbohydrate	Carbohydrate Content	
	Seed Coat / Endosperm	Embryo
	µmol hexose equivalent g dry wt^{-1}	
Starch	939	266
Glc	128	49
Fru	145	62
Suc	312	318

sugars were evenly distributed within organs, there was a concentration difference between the seed coat/endosperm and the embryo for hexoses (68 vs. 18 mM) and sucrose (78 vs. 52 mM). It was difficult to separate very small embryos completely from the liquid endosperm therefore some of the hexose and starch in the embryo samples may have come from liquid endosperm adhesion. Asymmetric carbohydrate distribution may be more pronounced than indicated by the data in Table 2.4. In young seeds, starch seemed to be evenly distributed between the seed coat and liquid endosperm (Fig. 2.4C). Seed coat starch completely disappeared by 28 DAA (Fig. 2.4D) and the partial consumption of the liquid endosperm by the expanding embryo (compare Fig. 2.4A and B) would further reduce total seed starch content. At 28 DAA, endosperm cells proximal to the seed coat still contained abundant starch granules (Fig. 2.4D).

CELL WALL THICKENING

Silique wall secondary cell-wall thickening may be an additional sink for carbon during development. Secondary cell walls are comprised of cellulose, lignin, hemicellulose, and pectin (Aspinall, 1980). To estimate the importance of secondary cell wall thickening cellulose and lignin contents were determined. With aging, silique wall cellulose and Klason lignin (acid-insoluble) contents rose significantly (Table 2.5). To allow comparison to Fig. 2.3A, cellulose contents rose from 1.1 mmol hexose equivalents mg chl^{-1} at 21 DAA to 2.4 mmol hexose equivalents mg chl^{-1} at 35 DAA. The cellulose content alone is higher than combined hexose, sucrose and starch after 21 DAA.

SUCROSE METABOLIC ENZYMES

To investigate the pathways of carbohydrate metabolism, the activities of key enzymes of sucrose metabolism were measured in silique wall, seed and leaf tissues. Care was taken to prevent proteolysis during extraction by including a variety of protease inhibitors in the extraction buffer. As well, all extraction procedures were done quickly at 4 °C followed immediately by enzyme assay. Assay conditions were pre-optimized for each tissue to ensure that saturating substrate concentrations were used and that the rate of product formation was linear with respect to time and the amount of extract assayed. For SPS, sucrose recoveries after incubation with

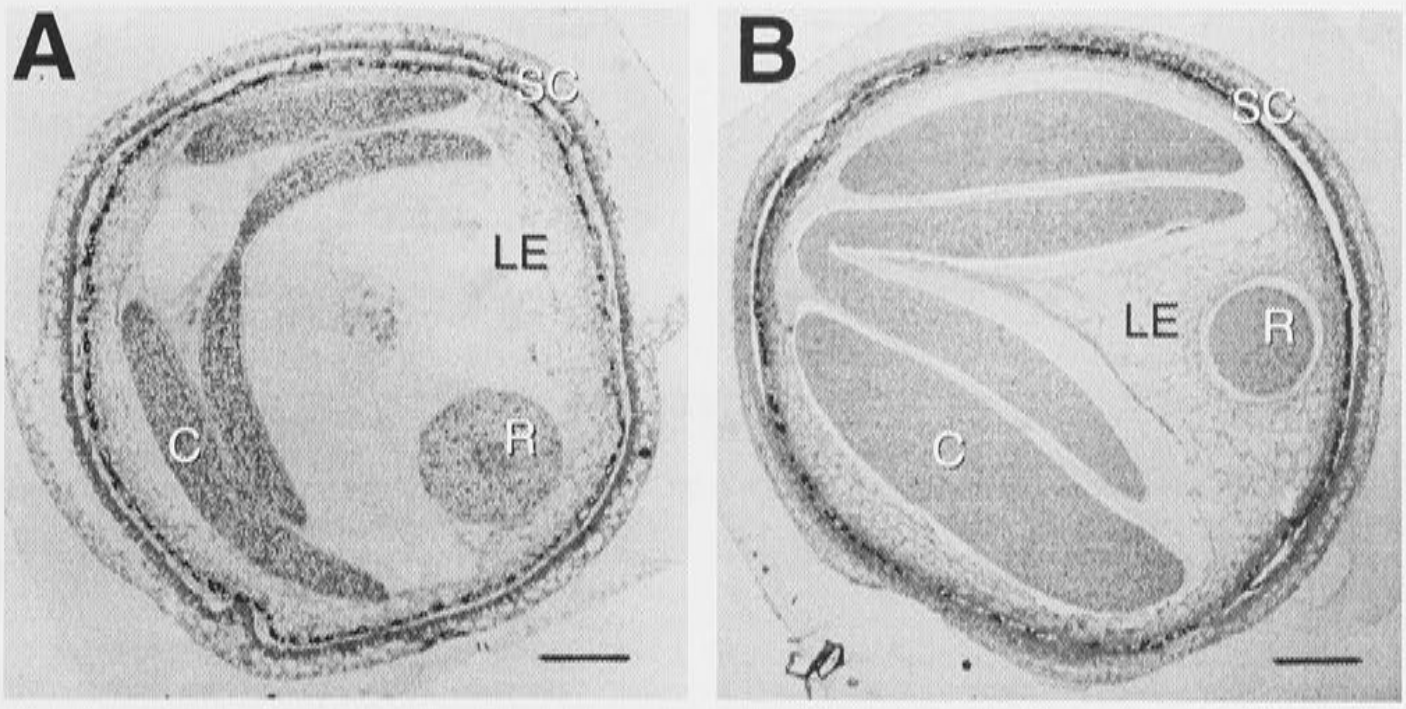

Figure 2.4. Morphology and starch distribution of developing 21 DAA (A, C) and 28 DAA (B, D) seeds. Sections were cut from LR White resin-embedded seeds, stained with toluidine blue O, and photographed under bright-field. The cotyledons (C), radicle (R), liquid endosperm (LE), seed coat (SC), outer integument (OI), sclerenchyma (S), pigment layer (P), and starch granules (SG) are marked. Bars, 250 μm (A, B), 25 μm (C, D).

Table 2.5. Cellulose and Klason lignin contents of developing canola silique wall. Samples were taken at sunrise. Values are expressed as mean values (+/- SE) from three replicates.

DAA	Cellulose	Klason Lignin
	$g\ m^{-2}$	$g\ m^{-2}$
21	10.1 (2.3)	6.9 (1.7)
28	18.5 (3.0)	12.8 (0.1)
35	21.1 (0.9)	15.2 (1.8)

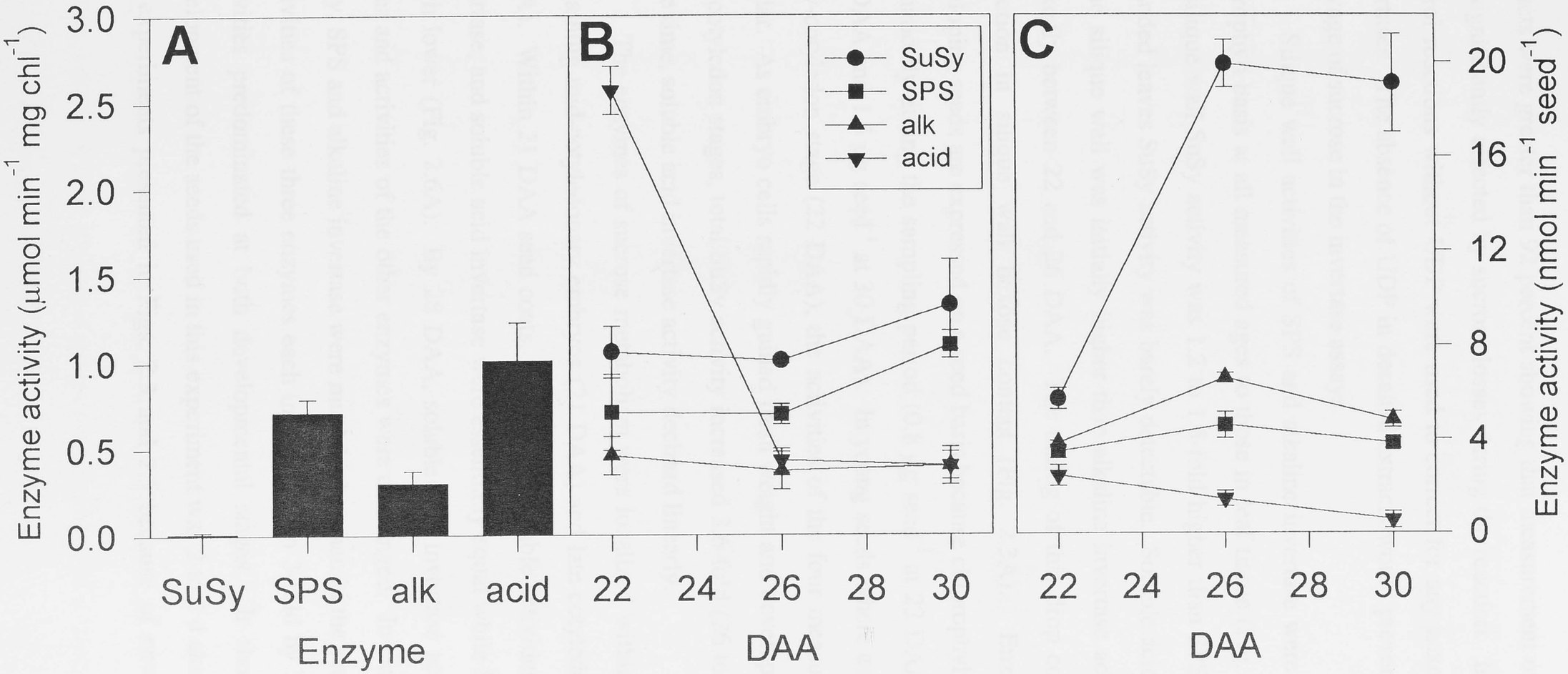

Figure 2.5. Total enzyme activities of source leaves (A), developing silique wall (B), and seed (C). Samples were taken at midday on a single day. Mean values and standard errors of three replicates are plotted for SuSy, SPS, alkaline invertase (alk), and soluble acid invertase (acid).

extracts were greater than 92 percent showing that measurement of SPS activity was not significantly affected by sucrose losses during the reaction. In the SuSy assays, control reactions without UDP were used to correct for any hexose production via invertases. The absence of UDP in desalted extracts would prevent SuSy-dependent cleavage of sucrose in the invertase assays.

Silique wall activities of SPS and alkaline invertase were very similar on a chlorophyll basis at all measured ages to those in leaf tissue (Fig. 2.5, A and B). In the silique wall SuSy activity was 1.2 to 1.5-fold higher than SPS whereas in fully-expanded leaves SuSy activity was barely detectable. Soluble acid invertase activity in the silique wall was initially higher than alkaline invertase activity but dropped markedly between 22 and 26 DAA. The timing of this drop corresponded to the reduction in silique wall hexose content (Fig. 2.3A). Enzyme activities in developing seeds are expressed on a seed basis because chlorophyll content increased dramatically during the sampling period (0.8 μg seed^{-1} at 22 DAA, 1.4 μg seed^{-1} at 26 DAA and 1.5 μg seed^{-1} at 30 DAA). In young seeds where embryos were at the early-cotyledon stage (22 DAA), the activities of the four measured enzymes were similar. As embryo cells rapidly gained fresh weight and developed to the mid- and late-cotyledon stages, total SuSy activity increased 3.6-fold (26 to 30 DAA). At the same time, soluble acid invertase activity declined linearly.

The enzymes of sucrose metabolism were localized within developing seeds containing mid-cotyledonary embryos (21 DAA) and late-cotyledonary embryos (28 DAA). Within 21 DAA seed coats, the total extractable activities of SuSy, alkaline invertase, and soluble acid invertase were essentially equal while SPS activities were much lower (Fig. 2.6A). By 28 DAA, soluble acid invertase activities were 71 % lower and activities of the other enzymes were unchanged. In embryos, activities of SuSy, SPS and alkaline invertase were much higher than in the seed coat (Fig. 2.6B). Activities of these three enzymes each increased 2 to 3-fold by 28 DAA and SuSy activities predominated at both developmental stages. It should be noted that development of the seeds used in this experiment was 2 to 3 d ahead of those used in the experiments presented in Figs. 2.3 and 2.5 because of environmental effects.

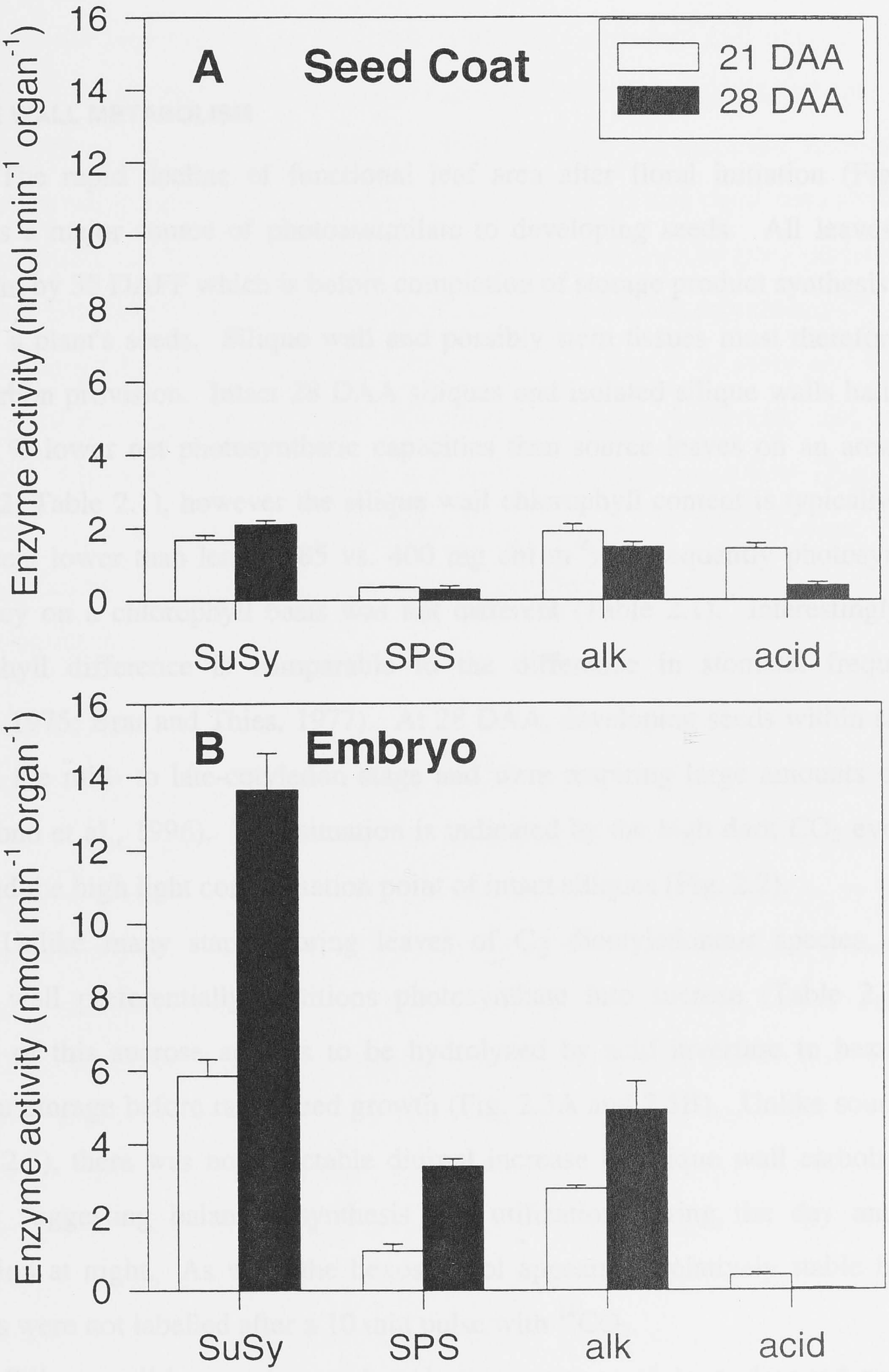

Figure 2.6. Total activities of seed coat (A) and embryo (B) sucrose metabolic enzymes. Seeds at two developmental stages (21, 28 DAA) were dissected into seed coat and embryo fractions before making separate extracts. Mean values and standard errors of three replicates are plotted for SuSy, SPS, alkaline invertase (alk), and soluble acid invertase (acid).

DISCUSSION

SILIQUE WALL METABOLISM

The rapid decline of functional leaf area after floral initiation (Fig. 2.1) removes a major source of photoassimilate to developing seeds. All leaves were senescent by 35 DAFF which is before completion of storage product synthesis in the bulk of a plant's seeds. Silique wall and possibly stem tissues must therefore take over carbon provision. Intact 28 DAA siliques and isolated silique walls had 70 % and 89 % lower net photosynthetic capacities than source leaves on an area basis (Fig. 2.2; Table 2.1), however the silique wall chlorophyll content is typically 75 to 80 percent lower than leaves (85 vs. 400 mg chl m^{-2}) consequently photosynthetic efficiency on a chlorophyll basis was not different (Table 2.1). Interestingly, this chlorophyll difference is comparable to the difference in stomatal frequencies (Major, 1975; Brar and Thies, 1977). At 28 DAA, developing seeds within siliques were at the mid- to late-cotyledon stage and were respiring large amounts of CO_2 (Eastmond et al., 1996). This situation is indicated by the high dark CO_2 evolution rates and the high light compensation point of intact siliques (Fig. 2.2).

Unlike many starch-storing leaves of C_3 dicotyledonous species, canola silique wall preferentially partitions photosynthate into sucrose (Table 2.2). A portion of this sucrose appears to be hydrolyzed by acid invertase to hexose for vacuolar storage before rapid seed growth (Fig. 2.3A and 2.5B). Unlike source leaf (Table 2.3), there was no detectable diurnal increase in silique wall carbohydrates thereby suggesting balanced synthesis and utilization during the day and little utilization at night. As well, the hexose pool appears to relatively stable because hexoses were not labelled after a 10 min pulse with $^{14}CO_2$.

Silique wall hexose storage is only temporary as contents dropped markedly at the onset of rapid seed growth (Fig. 2.3A). Although present in lesser amounts, starch also declined over this period. These trends suggest the remobilization of silique wall carbon to seeds. The parallel timing of silique wall carbon loss and rapid seed growth has been previously observed under different growth conditions (Norton and Harris, 1975; see Mendham and Salisbury, 1995). In addition, silique wall carbon reserves can be used for internal metabolic events as suggested by the

continued high SuSy activities 22 to 30 DAA (Fig. 2.5B). Silique wall cellulose and lignin contents increased 21 to 35 DAA indicating secondary cell wall thickening (Table 2.5). In addition, other carbon compounds such as hemicellulose and pectin will be involved in thickening (Aspinall, 1980). There are therefore simultaneous large carbon requirements for secondary cell wall synthesis and rapid seed growth. It is proposed that this carbon is drawn from a silique wall sucrose pool derived from photosynthesis, import (ie. younger siliques, stem) and hexose resynthesis (Fig. 2.7). This sucrose pool can be depleted by a combination of export to seeds and SuSy or alkaline invertase-cleavage to fuel secondary cell wall thickening and protein synthesis. Although silique wall sucrose contents were always low (Fig. 2.3A), continuous input and output is not reflected by this type of measurement. In the absence of leaves (Fig. 2.1), silique wall tissue must be a major supplier of carbon to developing seeds.

SEED METABOLISM

In this chapter, seed carbohydrate metabolism has been examined during early-, mid- and late-cotyledon stages corresponding to maximum fatty acid accumulation (Pomeroy et al., 1991). Imported sucrose is likely to be the predominant carbon source for seed growth. At 21 DAA, seed starch content was higher than sucrose or hexose (Fig. 2.3B). Embryos were at the mid-cotyledon stage by 28 DAA and had filled the seed by 35 DAA. Starch and hexose in seeds containing early-cotyledon embryos were localized to the seed coat or liquid endosperm (Table 2.4). In contrast, sucrose was evenly distributed between seed fractions. Seed starch is a temporary carbon reserve during early developmental stages and is depleted early in the filling phase (Norton and Harris, 1975; Munshi and Kochhar, 1994). In pea, there is a transitory starch accumulation in seed coat parenchyma cells until rapid embryo growth (Rochat and Boutin, 1992) and in canola there was a very striking disappearance of seed coat starch during rapid embryo growth (Fig. 2.4). It is tempting to speculate that this starch is remobilized to the growing embryos, however seed coat starch disappearance has also been correlated

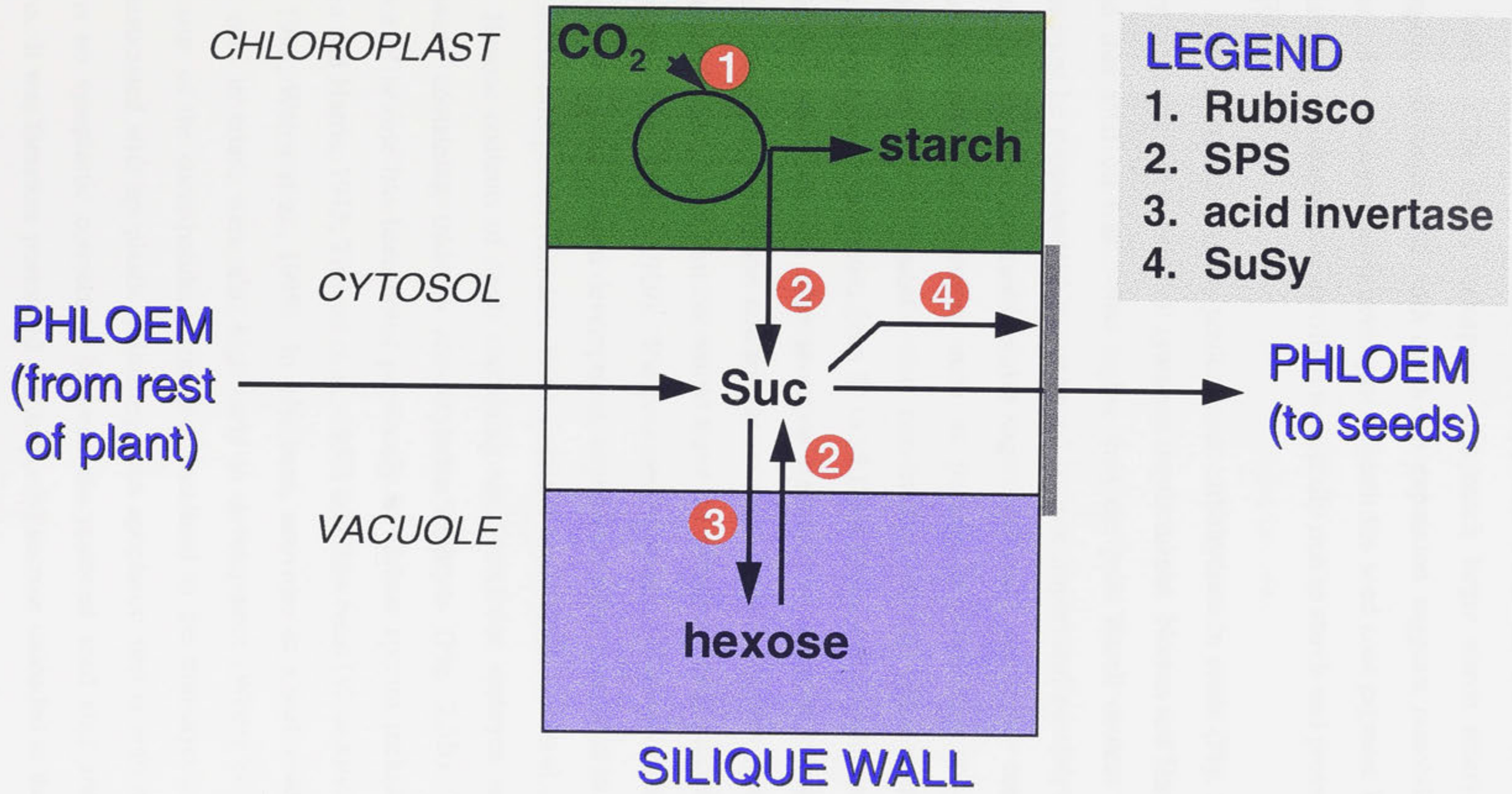

Figure 2.7. Proposed model of carbohydrate metabolism in developing silique walls during the seed filling period.

with mucilage (high molecular weight heteropolysaccharides; Werker, 1997) production in the seed coat epidermis (Hyde, 1970; Van Caeseele et al., 1981; Kuang et al., 1996). The liquid endosperm is a much larger starch reserve and its consumption in conjunction with cotyledon expansion suggests remobilization to embryos. The remnant starch noted just beneath the seed coat pigment layer (Fig. 2.4D) is likely the aleurone layer which is typically rich in starch and protein (Kuang et al., 1996).

Although starch was the predominant carbohydrate in seeds (Fig. 2.3B), the quantity is insufficient to fulfil oil synthesis requirements. Norton and Harris (1975) reported that total oil was 5-fold higher than the peak starch content. Clearly, reserves must be supplemented by continued sucrose import and possibly seed CO_2 fixation. In addition to measured soluble sugars and starch, seeds may contain other potential reserve carbon sources such as pectins, hemicellulose and sucrosyl-oligosaccharides. It is doubtful that non-fructan sucrosyl-oligosaccharides are present in appreciable quantities from 21 to 35 DAA because equimolar quantities of Glc and Fru were released after invertase treatment of aqueous phase samples. Invertase cleavage of common non-fructan sucrosyl-oligosaccharides would release either a single Glc or Fru unit but would leave the remaining oligosaccharide intact (for structures, see Keller, 1989). The presence of sucrosyl-oligosaccharides during the desiccation phase of seed development, beyond the range measured in this study, would not be unexpected (Hendrix, 1990; Leprince et al., 1990; Kuo et al., 1997)

Hexose contents of seeds containing early-cotyledon embryos were higher than seeds containing mid- to late-cotyledon embryos (Fig. 2.3B). This early presence of hexose has been noted previously in various species including canola (Norton and Harris, 1975; Tittonel et al., 1995) and faba bean (*Vicia faba* L.) (Heim et al., 1993; Weber et al., 1995). In faba bean, activities of a seed coat cell wall-bound acid invertase were also high early in development (Weber et al., 1995). Expression of the corresponding gene was localized to the thin-layer parenchyma cells associated with apoplastic unloading. An apoplastic step is required because there is no symplastic connection between the maternal seed coat and the filial embryo. It was therefore postulated that imported sucrose unloaded in the seed coat is hydrolyzed by acid invertase while being transferred to the endosperm (for review,

see Patrick and Offler, 1995). In maize, a cell wall-bound invertase is critical for full endosperm growth (Cheng et al., 1996). In dicotyledonous seeds, the young embryo could then take up hexose from the endosperm possibly by utilizing a hexose transporter in cotyledon epidermal cells (Weber et al., 1997a).

As canola embryos began the transition from cell division to cell expansion (21 to 28 DAA), seed hexose dropped (Fig. 2.3B). In faba bean, young embryos cultured without hexose stopped cell division and initiated expansion (Weber et al., 1996a). Similarly in pea, embryos cultured on high sucrose favoured cell expansion (Ambrose et al., 1987). As well, hexose seems to inhibit SuSy activity (Morell and Copeland, 1985; Heim et al., 1993; Quick and Schaffer, 1996; Weber et al., 1996b; Dejardin et al., 1997). On the disappearance of hexose from developing canola seeds (Fig. 2.3B), SuSy activities rapidly increased while the other enzymes measured did not change as dramatically (Fig. 2.5C). Comparing a number of species, SuSy was found to be high in active sinks but not in quiescent sinks (Sung et al., 1989). No similar correlation with sink type was found with six glycolytic enzymes and soluble invertase activities were low in both sink types.

SuSy activity has been positively correlated with storage product synthesis (Chourey and Nelson, 1976; Edwards and ap Rees, 1986; Doehlert, 1990; Heim et al., 1993; Weber et al., 1995; Zrenner et al., 1995; Ross et al., 1996; Dejardin et al., 1997). In each of these cases, a starch-storing sink was examined. Interestingly in canola, SuSy also mirrored storage product synthesis even though seeds are a predominantly oil-storing sink and was primarily localized to the embryo (Fig. 2.6). SuSy activity was much lower in early stages when starch was accumulating compared to activities after the switch to oil deposition. Using statistical cluster analysis, SuSy clustered with starch and ADP-Glc pyrophosphorylase in starch-storing maize endosperm (Doehlert, 1990). Instead of SuSy, oil clustered with hexokinase activity in oil-storing maize embryos (Doehlert, 1990). The implication is that invertase supplied carbon for oil synthesis because hexokinases are required to convert free hexose to hexose phosphate. Mature maize kernel contains 66 percent starch and 4 percent oil (Doehlert, 1990) whereas mature canola seed contains 54 percent oil and insignificant starch (Murphy and Cummins, 1989). It appears that SuSy activity reflects the synthesis of the predominant storage product regardless of

its form; starch in grains and oil in oilseeds. Compared to invertase, SuSy-mediated cleavage conserves ATP and its bidirectional capability may allow for finer metabolic control.

Estimates were made to assess the sucrose flux needed to support oil synthesis in canola seeds. From Murphy and Cummins (1989) it was calculated that embryos form 0.13 mg oil d^{-1} during rapid accumulation. Based on this deposition rate and the mature seed composition of fatty acid types (Murphy and Cummins, 1989), 410 nmol of total fatty acid and 140 nmol of glycerol 3-P would be needed daily. Assuming that the required 3.7 µmol acetyl-CoA, 3.3 µmol ATP and 6.6 µmol NADPH is entirely supplied by sucrose flux through the pentose phosphate pathway, glycolysis and the pyruvate dehydrogenase complex, 1.6 µmol of sucrose would be needed daily. An additional 0.03 µmol sucrose would satisfy glycerol 3-P requirements. Although oil synthesis is the predominant carbon sink some carbon will be used for cell wall and protein synthesis therefore calculated sucrose requirements are a minimum. From maximum extractable activities at 26 DAA (Fig. 2.5C), SuSy and alkaline invertase are in excess and therefore could metabolize the necessary carbon but soluble acid invertase activity is insufficient. The much higher embryo SuSy activity and its developmental timing suggests that it plays a major role in providing sucrose for oil synthesis.

Developing seeds had appreciable total SPS activities at all measured stages (Figs. 2.5C and 2.6). The barely detectable activities in seed coats suggest that SPS is not involved in starch remobilization. Sucrose synthesis via SPS could have two possible roles in canola embryos. First, SPS could catalyze sucrose formation from newly-fixed CO_2 as in source tissues (Stitt et al., 1987). Although Eastmond et al. (1996) reported that developing embryos are capable of *in vitro* photosynthesis, it was speculated that embryo Rubisco-dependent CO_2 fixation under the low light conditions within the silique *in vivo* would be of little significance (for detailed discussion, see Chapter 3). Second, SPS could resynthesize sucrose from hexose produced by cleavage of imported sucrose. A continuous cycle of synthesis and degradation in sink tissues has been previously described (Dancer et al., 1990; Wendler et al., 1990; Geigenberger and Stitt, 1991) and could regulate metabolite supply for sink growth. In such a cycle small changes in enzyme activity can

markedly alter the rate and direction of net flux (Wendler et al., 1990). In canola embryos synthesizing oil, the ratio of total cleavage and synthetic enzyme activities suggest that the bulk of imported sucrose is cleaved by SuSy and alkaline invertase to be used in respiration while a small proportion of the resulting hexose may be recycled by SuSy and SPS. In contrast to invertase, SuSy-mediated sucrose cleavage produces UDP-Glc and Fru and would require less energy to resynthesize sucrose in a futile cycle.

In summary (Fig. 2.8), developing canola seeds appear to store imported sucrose transiently as starch and hexose outside of the embryo before storage product synthesis. Acid invertase localized to the seed coat appears to mediate hexose production. A consequence of high hexose concentrations is the promotion of cell division (Weber et al., 1996a) and the inhibition of transfer cell development (Offler et al., 1997), SuSy activity (Quick and Schaffer, 1996), and storage product synthesis (Weber et al., 1996b). Once embryos have consumed the liquid endosperm and filled the seed's internal space, imported sucrose could possibly be actively transported intact to the embryo via epidermal transfer cells (Harrington et al., 1997a,b; Weber et al., 1997a) before cleavage by SuSy in storage parenchyma cells. The bulk of hexose would be converted to hexose-phosphate to feed into glycolysis. Flux to respiration may be modulated by a continuous cycle of sucrose cleavage and resynthesis.

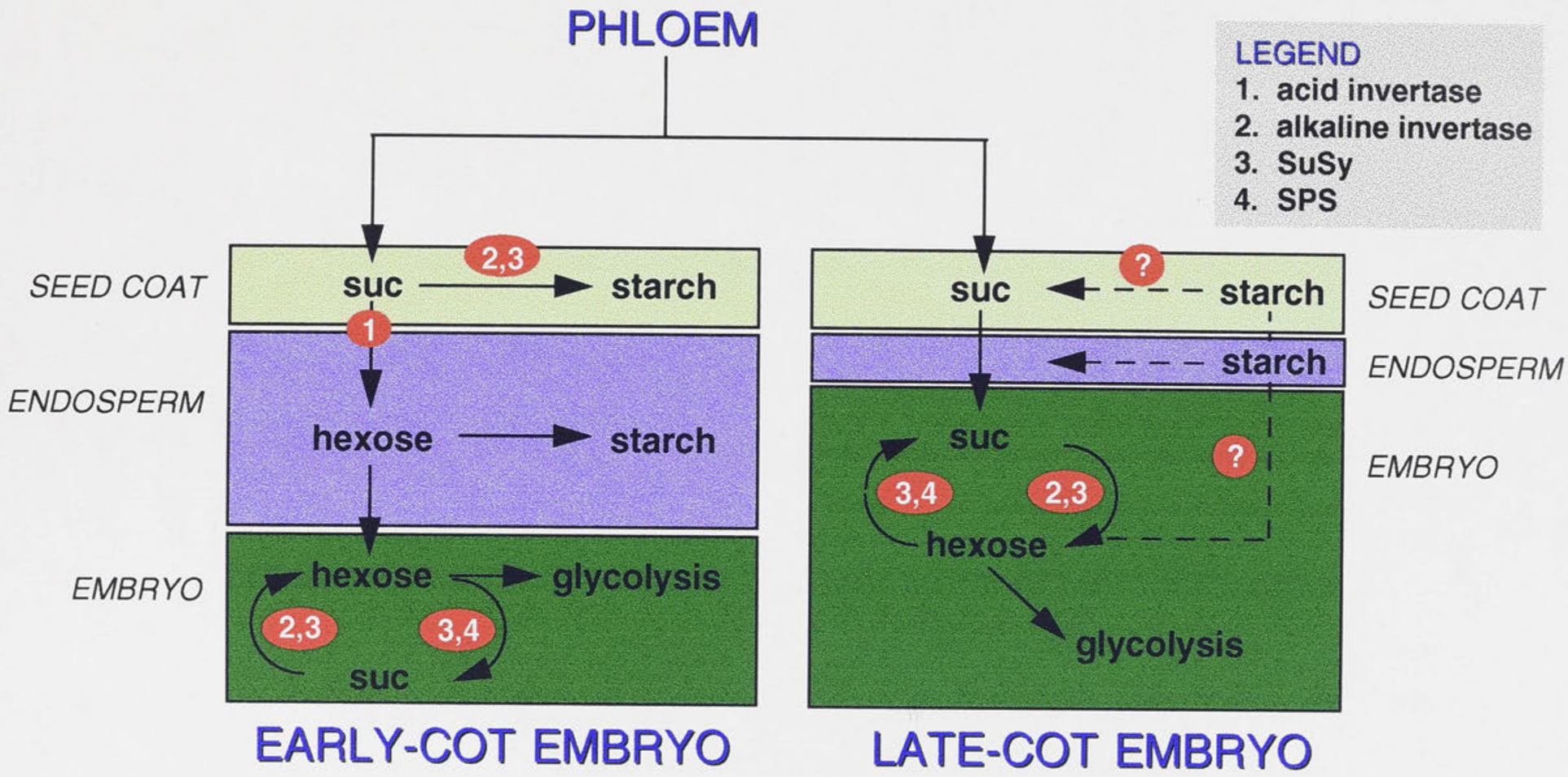

Figure 2.8. Proposed model of carbohydrate metabolism in developing seeds. Separate models are presented for seeds transiently storing carbohydrates (early-cot embryo) and for seeds remobilizing these reserves during the storage product synthesis phase (late-cot embryo).

CHAPTER 3: DEVELOPING SEEDS AND SILIQUE WALL MINIMIZE RESPIRATORY CO_2 LOSS

INTRODUCTION

Oil extracted from canola seeds is of high economic value but surprisingly little is known about the initial steps of carbon provision to filling seeds. The results presented in Chapter 2 identified the enzymes involved in the initial provision of metabolizable sugars which pass through respiratory pathways to produce the carbon substrates and energy required for seed growth and the synthesis of complex storage products. A consequence of respiration is the evolution of CO_2 which if allowed to escape to the atmosphere would represent a significant carbon loss. Seeds and the surrounding silique (pod) may have developed mechanisms to reduce this respiratory carbon loss.

The two major enzymes capable of CO_2 fixation in higher plants are Rubisco and PEP carboxylase (PEPC). Rubisco and associated Calvin cycle enzymes catalyze the conversion of ribulose-1, 5-bisphosphate and CO_2 into triose-P within the chloroplast. This carboxylation is light-dependent because the ATP and NADPH required in the Calvin cycle are produced after light absorption by chlorophyll pigments in the photosynthetic electron transport chain. In C_3 plants PEPC catalyses the carboxylation of glycolytic PEP and CO_2 into oxaloacetate, a TCA cycle intermediate.

In pea, it has been well established that Rubisco and PEPC in the pod wall endocarp refix seed-respired CO_2 thereby reducing carbon loss (Atkins et al., 1977; Flinn et al., 1977; Price and Hedley, 1980; Price and Hedley, 1988). The endocarp is composed of a few cell layers on the inner side of the pod wall and is separated from the rest of the pod wall by a sclerenchyma layer (Atkins et al., 1977; Price et al., 1988). Over 20 % of incident light reaches the pea endocarp (Atkins et al., 1977; Price et al., 1988; Donkin and Price, 1990) where absorption by abundant chlorophyll (Price et al., 1988; Donkin and Price, 1990) drives Rubisco-dependent CO_2 fixation thereby reducing the pod cavity CO_2 concentration (Flinn et al., 1977;

Flinn, 1985; Donkin and Price, 1989). CO_2 refixation by elevated endocarp PEPC seems to be equally as important (Atkins et al., 1977; Price and Hedley, 1980; Price and Hedley, 1988). A lack of similarly detailed studies in *Brassica* has led to speculation of an analogous situation (Mendham and Salisbury, 1995).

In addition to the silique wall, *Brassica* seeds may be able to refix their own respired CO_2. PEPC has been shown to catalyze CO_2 fixation in *B. rapa* seeds (Singal et al., 1987; Singal et al. 1995). Developing canola seeds are very green and chlorophyll content has been shown to peak during active filling (Rakow and McGregor, 1975; Crouch and Sussex, 1981; McGregor, 1995; Eastmond et al., 1996). Until recently, the potential contribution of seed photosynthesis in CO_2 refixation or in energy provision has not been directly addressed. Eastmond et al. (1996) have demonstrated that developing seeds have the capacity for light-dependent O_2 evolution and that Rubisco protein is present but speculated that net carbon gain *in vivo* would be unlikely.

Determining the function of seed chlorophyll is of particular industrial importance. In the world's major canola-growing regions, cool temperatures and frost during seed maturation can result in chlorophyll remaining in harvested seed (Mendham and Salisbury, 1995). During processing, chlorophyll is extracted with oil and expensive purification steps are required to prevent chlorophyll-induced catalyst blocking and oil oxidation (see Ward et al., 1995). This problem has led to suggestions of using genetic engineering to reduce seed chlorophyll (Plant Biotechnology Institute, 1996).

In this chapter, the CO_2 refixation capacities of canola seeds and inner silique wall were examined during seed filling. Contributions of Rubisco and PEPC in each tissue were assessed and an estimate made on the relative importance of each tissue. Determination of the physiological significance of seed chlorophyll was a particular emphasis.

MATERIALS AND METHODS

MATERIALS

Growth conditions of canola (cv. Westar) plants and materials were as described in Chapter 2. $NaH^{14}CO_3$ was obtained from Amersham.

SILIQUE DEVELOPMENT

To produce developmental curves of fresh weights and chlorophyll contents, plants were sampled on two occasions; 15 to 27 DAA (ie. top to bottom of raceme) at 31 DAFF and 27 to 39 DAA at 41 DAFF. Fresh weights and silique measurements were taken immediately after harvest with 4 to 5 replicates per tissue and age. Silique surface areas were calculated by treating a silique as a cylinder or as a box and the reported areas represent the average of these two calculations. All samples were ground in cold methanol to extract chlorophyll (Porra et al., 1989).

ENZYME ASSAYS

Total activities of leaf, silique wall and seed Rubisco and PEPC were measured on the same extracts as described in Chapter 2.

Rubisco (EC 4.1.1.39). A radiometric assay was used to measure Rubisco activity. Desalted extract (50 µL) was activated in 125 mM Tricine-KOH, pH 8.3, 14 mM $KHCO_3$, and 14 mM $MgCl_2$ at 25 °C for 10 minutes in a total volume of 112 µL before the addition of 120 µL reaction mix containing 52 mM Tricine-KOH, pH 8.3, 7 mM $KH^{14}CO_3$ (24 GBq mol^{-1}), 14 mM $MgCl_2$, and 35 mM DTT. Reactions were initiated with 20 µL of 10 mM RuBP and stopped after 60 s at 25 °C with 50 µL 1 M HCl. A 100 µL aliquot was spotted onto a glass fibre disk and then counted for ^{14}C in a scintillation counter. Each extract was assayed in duplicate with individual blanks (no RuBP).

PEPC (EC 4.1.1.31). Activities were measured in a continuous spectrophotometric assay at 25 °C. A background rate was established in 50 mM Tricine-KOH, pH 8.3, 1 mM $KHCO_3$, 5 mM $MgCl_2$, 5 mM Glc-6-P, 2 mM DTT, 0.2 mM NADH, 2.0 U malate dehydrogenase (EC 1.1.1.37) and 20 µL extract in a 1 mL total volume. The reaction was started by the addition of 10 µL 250 mM PEP.

Activities were calculated from the linear portion of the reaction rate after correction for the background rate. All samples were measured in duplicate.

SILIQUE WALL PROPERTIES

Light Transmission. The proportion of incident PPFD transmitted through adaxial silique wall was measured using a quantum sensor and a cool white fluorescent light source. For each replicate, light readings were taken in the presence and absence of silique wall from three points along the silique wall surface.

Silique Cavity CO_2 Concentration. A gas-tight syringe was used to sample 20 µL from the silique cavity. Gas samples were then injected into a 1.6 mL gas-tight cuvette attached to a mass spectrometer (MM6, VG Instruments, Winsford, UK). A teflon membrane separated the gas in the cuvette from the vacuum of the mass spectrometer and gas was continually inlet from the cuvette into the mass spectrometer source. The mass spectrometer was focused on mass 44 (CO_2) and its response to CO_2 was calibrated by injecting known amounts of CO_2. Gas samples were taken from plants which had been placed in the dark or light (800 to 1100 µmol quanta m^{-2} s^{-1}) for at least 1 h prior to sampling.

Sectioning and Staining. Hand sections of silique wall were stained in either 0.05 % (w / v) toluidine blue O (Sigma) or 1.6 % (w / v) phlorglucinol (Sigma). The phlorglucinol stock solution was prepared by dissolving 2 % (w / v) phlorglucinol in ethanol and the working solution was made by combining 80 % stock solution with 20 % concentrated HCl.

Chlorophyll Distribution. Chlorophyll fluorescence of silique wall transverse sections was quantified using a Nikon Optiphot microscope and Image1 software (Universal Imaging Corp., West Chester, PA). Before use, hand sections of silique wall were floated in 10 µM DCMU for at least 30 minutes to maximize the fluorescence signal. Fluorescence readings were taken across the section approximately one cell layer at a time. Sections were positioned in the light field using weak white light and then left in the dark for one minute prior to exposure to fluorescence excitation light. Fluorescence excitation and measurement was performed using a Nikon-compatible epifluorescence cube attachment (Chroma Technology Corp., Brattleboro, VT). The light from a mercury vapour lamp passed

through a 540 nm short wavelength cut-off filter to the sample while the emitted fluorescence passed through a 660 nm long wavelength cut-on filter to the video display. Photodestruction was minimised by brief exposures to the intense short-wavelength excitation light.

O_2 EXCHANGE

O_2 evolution rates of intact embryos were measured in liquid O_2 electrodes (Rank Brothers, Cambridge, UK). Samples of 10 embryos were placed in the cuvette with 50 mM Hepes-NaOH, pH 7.6 and 10 mM $NaHCO_3$ (Eastmond et al., 1996). Dark O_2 consumption rates were added to net O_2 evolution rates at 175 and 400 µmol quanta m^{-2} s^{-1} to estimate gross O_2 evolution.

To determine the gaseous permeability of seed coat, samples of 10 seeds or embryos were placed in the liquid O_2 electrodes. Nitrogen was used to make stepwise reductions of the O_2 concentration within the sample cuvette from air-saturated levels (253 µM at 25 °C) and linear O_2 consumption rates were measured at each step in darkness.

PULSE-MODULATED CHLOROPHYLL FLUORESCENCE

Samples of 10 seeds or embryos were placed in a cuvette with a continuous flow of compressed air passing across the tissues which was humidified by passage through a water bubbler. A 1 % CO_2 in air mixture was used to provide high CO_2 while a soda lime scrubber was used to remove CO_2 from a compressed air line. Tissues acclimatized to these atmospheres in the dark for 20 min before fluorescence measurement initiation using a PAM 101 Chlorophyll Fluorometer fitted with a PAM 103 flash trigger control, a Schott KL1500-T lamp and a polyfurcated fibre optic system (Heinz Walz, Effeltrich, Germany). Actinic light at 160 and 350 µmol quanta m^{-2} s^{-1} was provided by a slide projector and 1 s saturating flashes were applied at 1 min intervals. Photosynthetic electron transport rates were calculated by the equation:

$$J = \left(\frac{F_m' - F_s}{F_m'}\right) * PPFD * 0.85 * 0.25$$

where F_m' was the maximal fluorescence signal during a saturating light flash, F_s was the steady-state fluorescence signal, and PPFD was the incident actinic light. It was assumed that tissue light absorbance was 85 % (Seaton and Walker, 1992) and that 1 electron was transported for every 4 photons absorbed. A detailed discussion of fluorescence analysis can be found in Genty et al. (1989).

RESULTS

Fresh weights and chlorophyll contents were measured during silique development (Fig. 3.1). Silique fresh weight reached a maximum by 23 DAA with the majority being in the silique wall (Fig. 3.1A). Seeds, specifically embryos, began to gain mass after the silique wall and continued throughout the sampling period (Fig. 3.1B). Silique wall began losing chlorophyll around 30 DAA (Fig. 3.1C) while seed chlorophyll exponentially increased from 19 DAA and reached a peak by 31 DAA (Fig. 3.1D). The bulk of seed chlorophyll was localized to the embryo. The proportion of chlorophyll a and b pigments were calculated from the data presented in Fig. 3.1. There were no large changes in either silique wall or seed chlorophyll a/b ratios from 15 to 39 DAA, however silique wall had higher ratios than seed (2.9 ± 0.05 vs. 2.0 ± 0.04).

Total activities of Rubisco and PEPC, the two enzymes capable of CO_2 fixation, were assayed in leaf, silique wall and seed tissues. All extraction procedures included protease inhibitors and were performed quickly at 4 °C followed by immediate assay. Assay conditions were pre-optimized to ensure saturating substrate concentrations, peak activation times (Rubisco), and linear reaction rates over time. On a chlorophyll basis, silique wall Rubisco and PEPC activities were significantly higher than source leaf but the Rubisco-PEPC ratios were similar (Table 3.1). Silique wall Rubisco activities declined with development, particularly between 26 and 30 DAA, which lowered the Rubisco-PEPC ratio from 19.1 to 11.9. In developing seeds, Rubisco activities were much lower than silique wall or leaf whereas PEPC activities were several fold higher yielding Rubisco-PEPC ratios of 0.80 at 22 DAA and 1.29 at 30 DAA (Table 3.1).

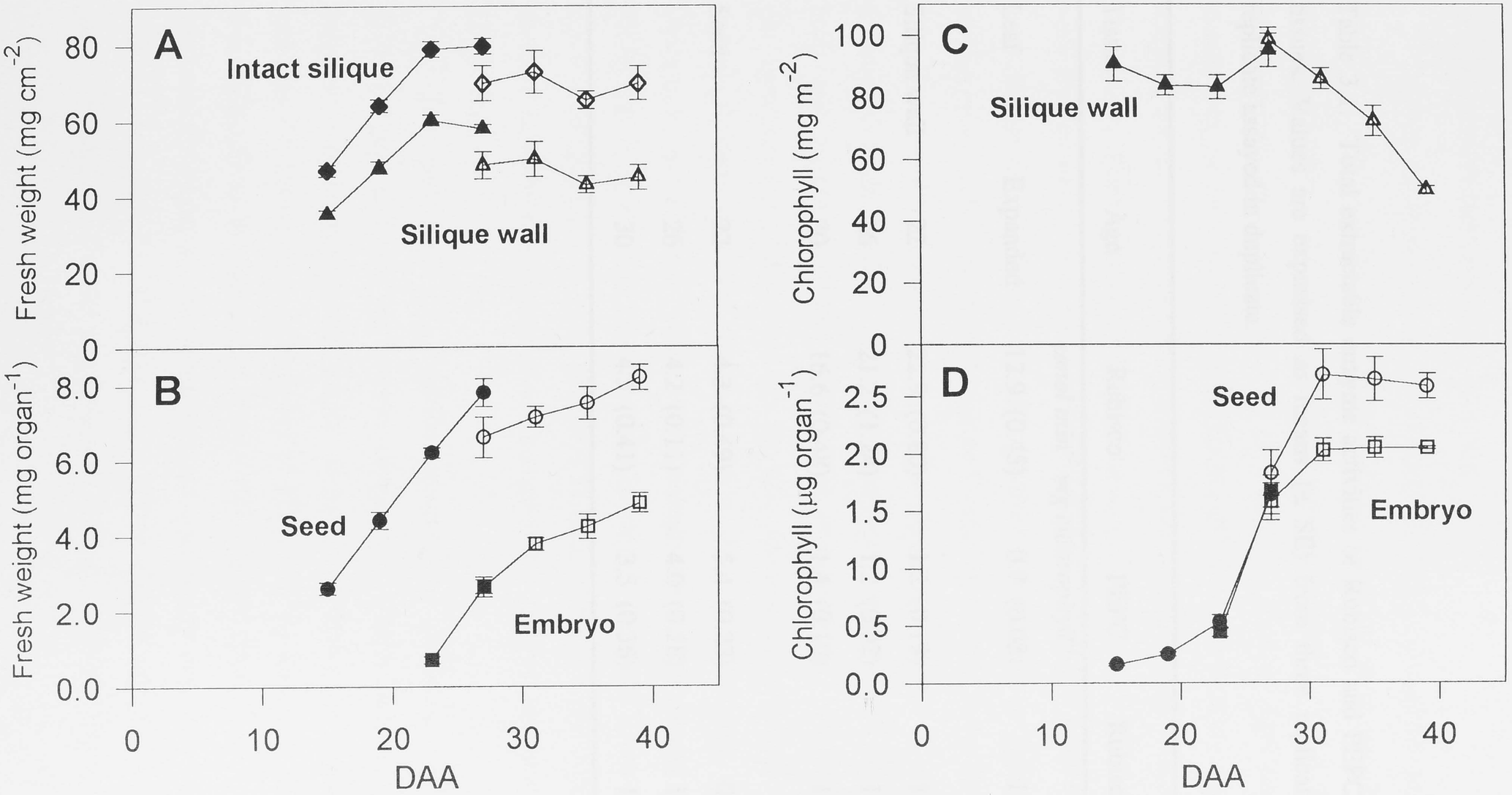

Figure 3.1. Fresh weight (A, B) and chlorophyll contents (C, D) of developing intact siliques (A), silique walls (A, C), seeds (B, D), and embryos (B, D). Mean values and standard errors from five replicates are plotted. Plants were sampled on two days; 15 to 27 DAA at 31 DAFF (filled symbols) and 27 to 39 DAA at 41 DAFF (open symbols).

Table 3.1. Total extractable enzyme activities of Rubisco and PEPC from canola tissues. Values are expressed as means (± SE) from three replicates with each replicate assayed in duplicate.

Tissue	Age	Rubisco	PEPC	Rubisco:PEPC
		μmol min^{-1} mg chlorophyll^{-1}		
Leaf	Expanded	12.9 (0.45)	0.7 (0.05)	18.4
Silique wall	22	22.9 (0.80)	1.2 (0.19)	19.1
	26	21.2 (1.24)	1.2 (0.02)	17.7
	30	16.6 (0.48)	1.4 (0.10)	11.9
Seed	22	4.3 (0.49)	5.4 (0.23)	0.80
	26	4.2 (0.11)	4.0 (0.18)	1.05
	30	4.5 (0.41)	3.5 (0.36)	1.29

SEED PHOTOSYNTHESIS AND CO_2 FIXATION

Given the abundance of seed chlorophyll (Fig. 3.1D) and measurable Rubisco activities (Table 3.1) the potential for Rubisco-dependent seed carbon fixation was examined. The enclosing silique wall transmitted 20 ± 0.5 % (n = 16) of PPFD to developing seeds from 22 to 34 DAA. Incident light to seeds would therefore be no more than 400 µmol quanta m^{-2} s^{-1} under field conditions and light reaching the chlorophyll-rich embryos would be reduced further because of seed coat attenuation. Embryo photosynthetic electron transport, as gross O_2 evolution, rates were derived from dark respiration rates and net O_2 evolution rates at 175 and 400 µmol quanta m^{-2} s^{-1} (Table 3.2). It is assumed that there is no light-stimulated O_2 consumption, such as photorespiration or O_2 photoreduction, under high CO_2 (Table 3.3). Photosynthetic electron transport capacity decreased from 21 to 27 DAA on a chlorophyll basis (Table 3.2), however there was no difference on a fresh weight basis and increased 2.5-fold on a whole embryo basis. The capacity to use photosynthetically-produced energy for CO_2 fixation was assessed by measuring embryo Rubisco activities. Rubisco activity per unit chlorophyll was maintained between 21 and 27 DAA (Table 3.2) as embryo chlorophyll content increased (Fig. 3.1D). If it is assumed that the Rubisco rate is maximal under the high CO_2 concentrations found *in vivo* (Table 3.3) then embryo Rubisco-dependent CO_2 fixation capacity was in excess of photosynthetic electron transport at both ages (Table 3.2).

The seed coat's CO_2 fixation capacity was also examined. Seeds were dissected into seed coat and embryo samples and assayed for Rubisco and PEPC activities at two developmental stages. In seeds containing small early-cotyledonary embryos (21 DAA), the vast majority of PEPC activity and some Rubisco activity was localized to the seed coat (Table 3.4). In 28 DAA seeds containing late-cotyledonary embryos, seed coat Rubisco was barely detectable and PEPC was slightly lower than 21 DAA seed coat. With the large embryo growth between 21 and 28 DAA (Fig. 3.1) the proportions of Rubisco and PEPC localized to embryos

Table 3.2. Estimation of photosynthetic electron transport and light-dependent CO_2 fixation capacities of canola embryos. Gross O_2 evolution rates were measured at 175 and 400 µmol quanta m^{-2} s^{-1} in a liquid electrode and Rubisco activities were determined using saturating conditions. Values are expressed as means (± SE) from 3 to 4 replicates.

DAA	Gross O_2 evolution		Rubisco
	175	400	
	µmol min^{-1} mg chlorophyll^{-1}		
21	2.6 (0.5)	3.0 (0.5)	4.9 (1.3)
27	1.5 (0.2)	1.9 (0.2)	4.7 (0.1)

Table 3.3. Silique cavity CO_2 concentration. Using a gas-tight syringe, a 20 µL sample was taken from siliques placed in the dark or light (800 to 1100 µmol quanta m^{-2} s^{-1}) and then injected into a mass spectrometer for analysis. Values are expressed as means (± SE) from 2 to 6 replicates.

	CO_2 Concentration (%)	
DAA	Dark	Light
26	1.6 (0.24)	0.8 (0.19)
30	2.1 (0.36)	1.4 (0.36)
34	1.8 (0.29)	2.5 (0.39)

Table 3.4. Localization of Rubisco, PEPC and chlorophyll within developing canola seeds. Values are expressed as means (± SE) from 3 replicates. Chl, Chlorophyll.

	21 DAA			28 DAA		
Organ	Rubisco	PEPC	Chl	Rubisco	PEPC	Chl
	nmol min^{-1} organ^{-1}		μg *organ^{-1}*	*nmol min^{-1} organ^{-1}*		μg *organ^{-1}*
Seed coat	2.6	5.6	0.6	0.5	4.6	0.6
	(0.06)	(0.41)	(0.07)	(0.37)	(0.22)	(0.10)
Embryo	4.1	0.9	1.6	14.3	4.5	3.8
	(0.34)	(0.06)	(0.43)	(1.22)	(0.19)	(0.13)
Seed	9.7	6.7	1.4	16.3	7.8	3.6
	(1.51)	(0.34)	(0.22)	(0.47)	(0.52)	(0.15)

also dramatically increased. Embryo Rubisco appears to be the largest contributor to seed CO_2 fixation capacity in this age range (Table 3.4).

During experimentation on seeds and embryos, it became apparent that the seed coat could be a barrier to gaseous diffusion. To test this possibility, intact seeds and isolated embryos were placed in the dark in liquid O_2 electrode cuvettes. The O_2 concentration of the liquid phase was progressively reduced from 250 μM (air-saturated at 25°C) and net O_2 consumption (respiration) rates of the tissues were measured. Embryo response to O_2 concentration was hyberbolic and was saturated at approximately 50 % of air levels (Fig. 3.2). In contrast, seed response to O_2 was linear and was not saturated at atmospheric O_2 levels thereby suggesting that diffusion across the seed coat to the embryo severely limited the respiration rate.

If the seed coat is a major barrier to gaseous diffusion, it is possible that seed photosynthesis proceeds independently of externally-supplied CO_2; that is CO_2 fixation is solely dependent on trapped embryo-respired CO_2. To test this hypothesis, photosynthetic electron transport rates calculated from pulse-modulated chlorophyll fluorescence data were compared for seeds and embryos placed in air containing 1 % or 0 % CO_2. This technique provides an estimate of the gross rate of electron transport to photosynthetic electron acceptors whereas O_2 evolution measurements only determine the net balance between photosynthetic O_2 production and respiratory O_2 consumption. In tissues dependent on the external atmosphere, such as leaves, there should be a large decrease in photosynthetic electron transport in the absence of CO_2 due to the reduced regeneration of NADP and ADP by the Calvin cycle. In contrast, electron transport and light-dependent CO_2 fixation in a closed photosynthetic system should be unaffected by the external atmosphere. Intact seeds appear to be self-sufficient for CO_2 because electron transport rates were the same in either 1 % or 0 % CO_2 (Table 3.5). Somewhat surprisingly, the removal of the seed coat diffusion barrier only resulted in a small but statistically significant drop in electron transport for embryos exposed to CO_2-free air ($p \leq 0.01$) (Table 3.5).

SILIQUE WALL CO_2 FIXATION

Apart from seed CO_2 fixation, the possibility that the silique wall can incorporate cavity CO_2 was investigated. Transverse sections of silique wall showed

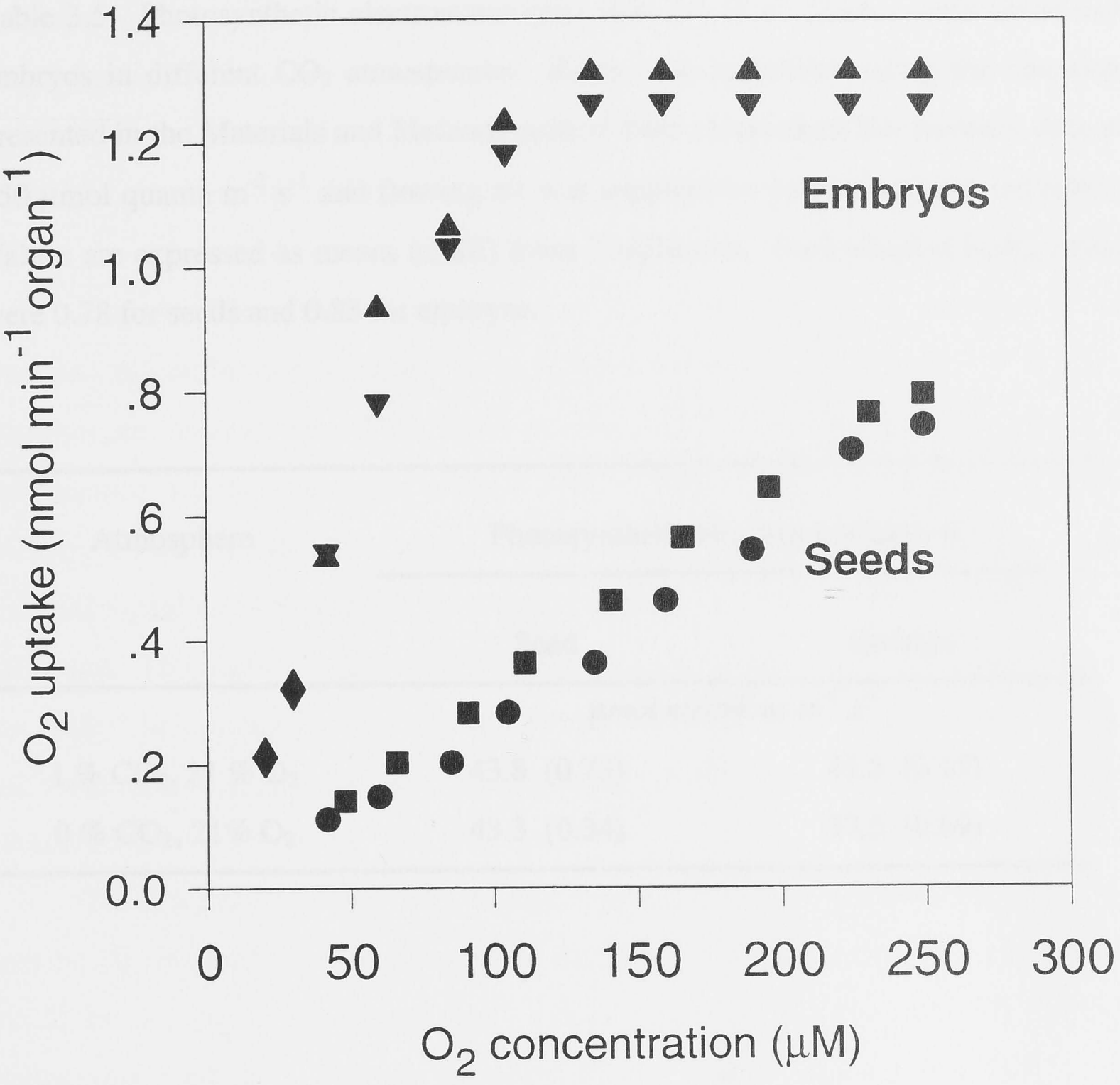

Figure 3.2. Gaseous permeability of 28 DAA intact canola seeds and isolated embryos. Tissues were placed in liquid-phase O_2 electrodes and O_2 uptake rates (respiration) were measured in the dark at different O_2 concentrations. The O_2 concentration inside the cuvette was reduced step-wise with a stream of nitrogen.

Table 3.5. Photosynthetic electron transport rates (J) of 27 DAA canola seeds and embryos in different CO_2 atmospheres. Rates were calculated using the equation presented in the Materials and Methods section from chlorophyll fluorescence data at 350 µmol quanta m^{-2} s^{-1} and flowing air was supplied by compressed gas cylinders. Values are expressed as means (± SE) from 3 replicates. Dark-adapted F_v:F_m ratios were 0.78 for seeds and 0.83 for embryos.

Atmosphere	Photosynthetic electron transport (J)	
	Seed	Embryo
	µmol electrons m^{-2} s^{-1}	
1 % CO_2, 21 % O_2	43.8 (0.73)	41.5 (0.15)
0 % CO_2, 21% O_2	43.3 (0.34)	37.5 (0.69)

a sclerenchyma cell layer near the inner surface (Fig. 3.3A) which stained intensely with toluidine blue O, a general stain, and phlorglucinol (Fig. 3.3B), a phenol alcohol-specific stain. The endocarp is composed of this sclerenchyma layer and a single cell layer on the interior surface. The sclerenchyma layer may act as a gaseous diffusion barrier causing a build-up of endocarp and seed respired CO_2 within the silique cavity in both the dark and light (Table 3.3). Light-dependent CO_2 fixation significantly lowered cavity CO_2 only at 26 DAA ($p = 0.03$), a time when silique wall chlorophyll is high (Fig. 3.1C) and seed respiration is low (Eastmond et al., 1996).

Brassica siliques are too small to dissect into layers therefore another method was used to analyze photosynthetic activity distribution within the endocarp. Using a fluorescence microscope fitted with a chlorophyll-specific filter, chlorophyll fluorescence across transverse silique wall sections was quantified (Fig. 3.4). DCMU, which blocks photosynthetic electron transport, was used to maintain maximal signal and precautions were taken to minimize photodestruction during data collection. The highest silique wall chlorophyll concentration was in the outer layers just under the epidermis. Chlorophyll concentration dropped in the interior layers but there was a small rise in endocarp chlorophyll. Endocarp chlorophyll was calculated to be 6.2 % of the total (Fig. 3.4).

To estimate endocarp CO_2 fixation capacity, it was assumed that Rubisco distribution is equivalent to chlorophyll therefore total endocarp Rubisco activity would be 6.2 % of the silique wall values reported in Table 3.1. Without a comparable method to quantify endocarp PEPC, it was assumed that PEPC was equally distributed across the silique wall and endocarp PEPC would be 16 % of the total silique wall activity (Table 3.1) based on thickness measurements (Srinivasan and Morgan, 1996). Having estimates of endocarp Rubisco and PEPC activities and also seed measurements (Table 3.1), it was possible to estimate the relative contributions of endocarp and seed CO_2 fixation (Table 3.6). It is assumed that PEPC and Rubisco are independently fixing CO_2 and are not linked as in C_4 photosynthesis. To make the comparison between tissues, enzyme activities were first converted to a common silique surface area basis. Table 3.6 shows that the relative seed to endocarp fixation capacities increased from 22 to 30 DAA because of

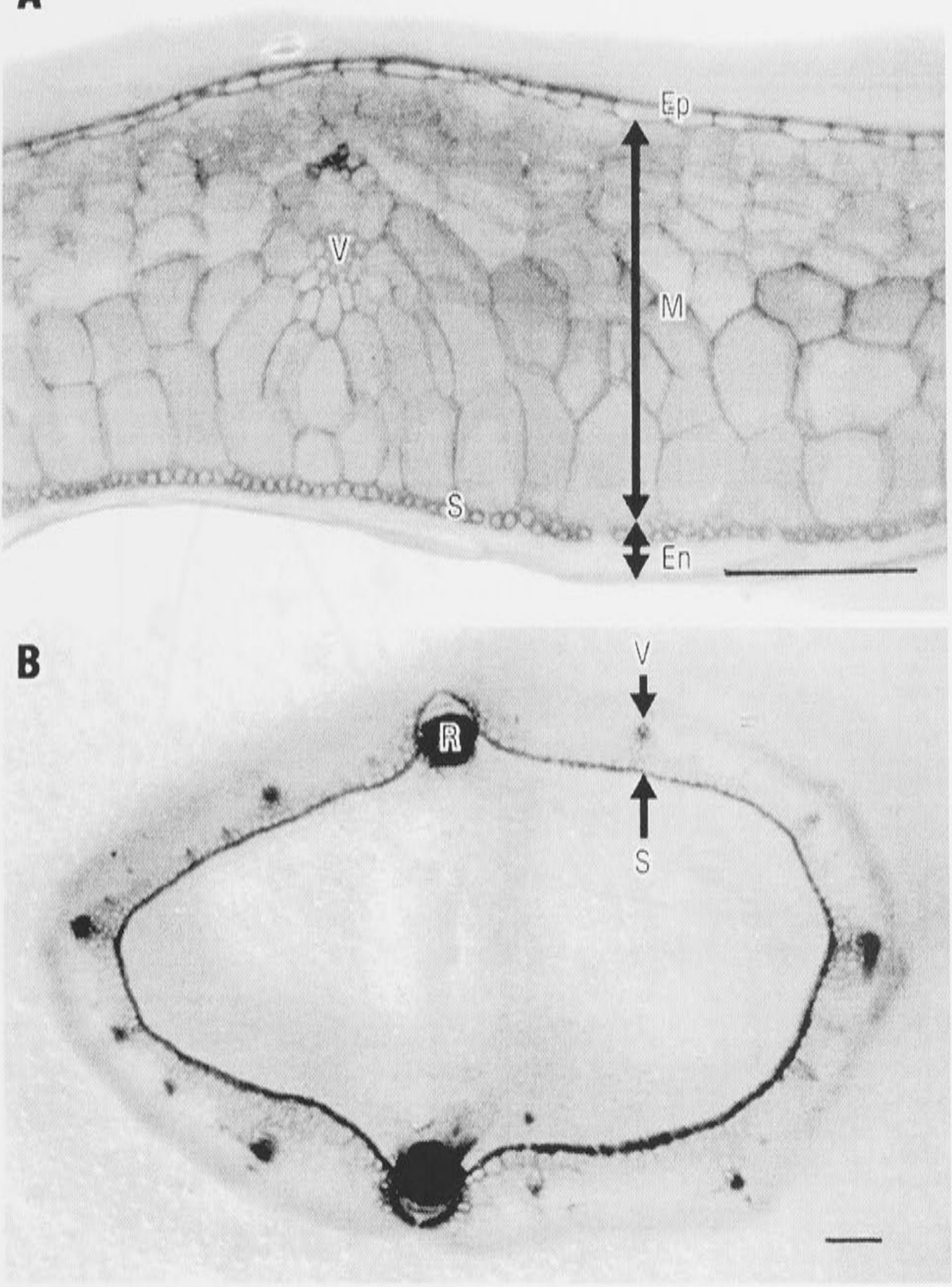

Figure 3.3. Anatomy of canola silique wall transverse hand sections. The section in panel A was stained with toluidine blue O and the section in panel B was stained with phlorglucinol before photographing. The epidermis (Ep), mesocarp (M), sclerenchyma (S), endocarp (En), vascular bundle (V), and replar bundle (R) are marked. Bars, 300 μm.

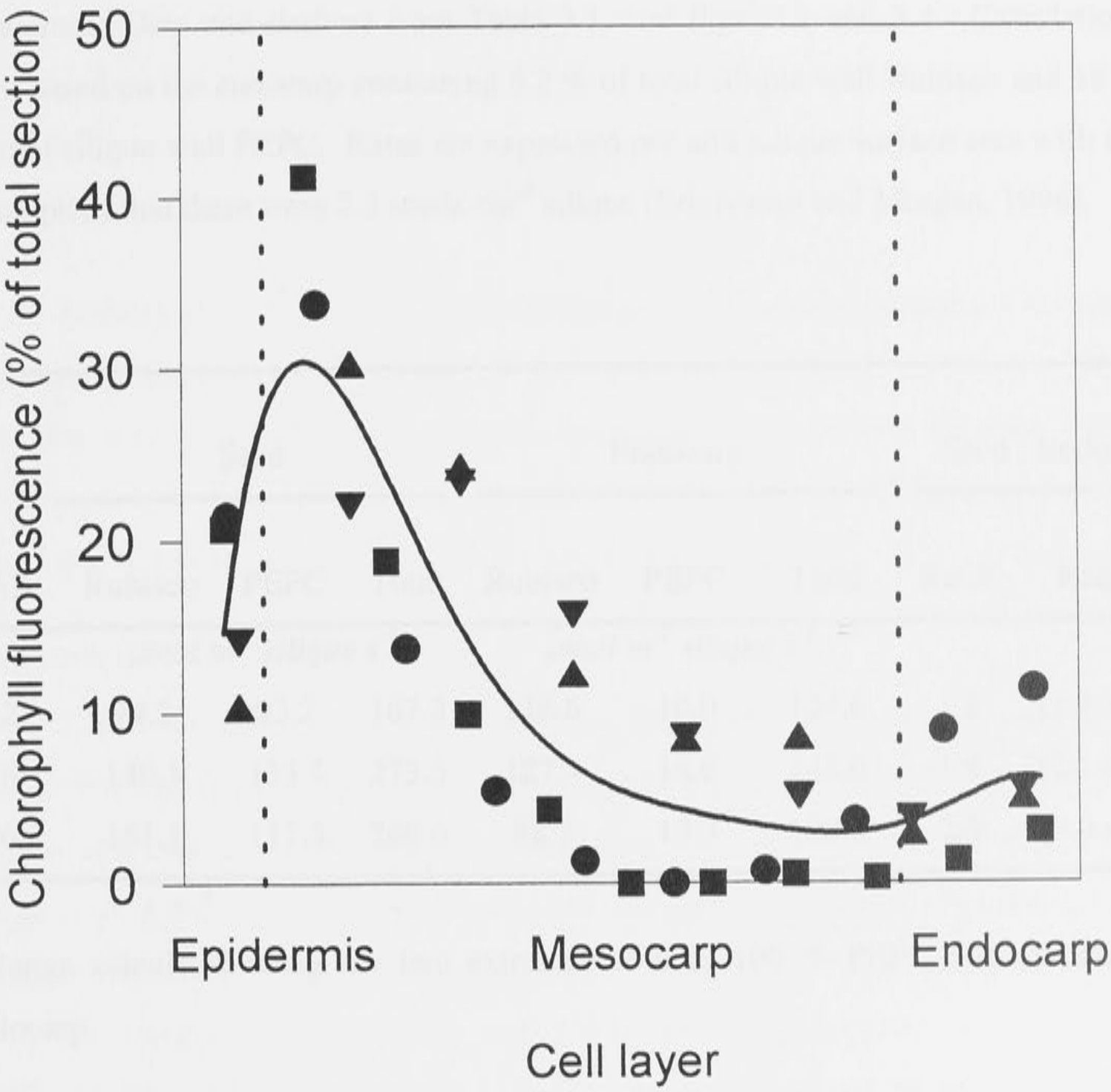

Figure 3.4. Chlorophyll distribution across 21 DAA canola silique wall transverse sections. Hand sections were floated in 10 μM DCMU for 30 min prior to signal quantification using a Nikon Optiphot microscope fitted with a chlorophyll fluorescence-specific filter and quantification software. Individual points from four separate determinations are plotted with a fitted regression curve ($r^2 = 0.73$).

Table 3.6. Estimation of relative canola seed and silique wall endocarp CO_2 fixation capacities. Data was derived from Table 3.1, and Figs. 3.1 and 3.4. Calculations were based on the endocarp containing 6.2 % of total silique wall Rubisco and 16 % of total silique wall PEPC. Rates are expressed per unit silique surface area with the assumption that there were 2.3 seeds cm^{-2} silique (Srinivasan and Morgan, 1996).

	Seed			Endocarp			Seed : Endocarp	
DAA	Rubisco	PEPC	Total	Rubisco	PEPC	Total	Ratio	Range[a]
	μmol m^{-2} silique s^{-1}			*μmol m^{-2} silique s^{-1}*				
22	74.2	93.2	167.3	118.6	16.0	134.6	1.2	(1.4 - 0.8)
26	140.1	133.4	273.5	127.4	18.6	146.0	1.9	(2.1 - 1.1)
30	151.1	117.5	268.6	88.7	19.3	108.0	2.5	(3.0 - 1.3)

[a] Range calculated using the two extremes of 0 to 100 % PEPC localization to endocarp.

a large increase in seed Rubisco activities and a smaller decrease in endocarp Rubisco activities. Given the imprecise estimate of endocarp PEPC localization, endocarp to seed fixation ratios were also calculated under two extremes; 0 and 100 % PEPC localization to the endocarp. Even with 100 % PEPC localization, seed fixation capacity exceeded the endocarp capacity after 22 DAA (Table 3.6).

DISCUSSION

Refixation of respired CO_2 in developing siliques could potentially conserve significant amounts of carbon needed for costly oil synthesis in embryos. This refixation may occur at two points; within the silique wall or within the seed. These two tissues were assessed for their CO_2 fixation capacities via Rubisco and PEPC during the oil filling period.

DEVELOPMENTAL PROFILES

Under a variety of growth conditions, the timing of maximum embryo oil content corresponded with maximum fresh weight (Rakow and McGregor, 1975; Murphy and Cummins, 1989; Hocking and Mason, 1993; Perry and Harwood, 1993; Singal et al., 1995). It is therefore concluded that maximum fatty acid synthesis rates correlate with fresh weight gains regardless of environment. The timing of growth, however, is temperature-dependent and will be variable (Mendham and Salisbury, 1995). In this study, rapid embryo fresh weight gains occurred between 23 and 30 DAA (Fig. 3.1B) therefore fatty acids would also be accumulated during this period. Early- to mid-cotyledon stage embryos were 10 % of total seed fresh weight at 23 DAA and exponentially grew to late-cotyledon stage by 31 DAA composing 50 to 60 % of seed weight. Pomeroy et al. (1991) reported that embryo fresh weight and fatty acid content exponentially increased in unison from mid- to late-cotyledon stages.

In addition to fresh weight and fatty acids, seed chlorophyll rapidly accumulated 20 to 30 DAA (Fig. 3.1D). The majority of chlorophyll was localized to the embryo. No data was collected after 39 DAA, however embryo cotyledons were yellow by 50 DAA suggesting rapid degreening 39 to 50 DAA. This narrow chlorophyll peak has been reported previously (Rakow and McGregor, 1975;

McGregor, 1995). Seed chlorophyll a/b ratios were lower than silique wall possibly indicating shade adaptation to 80 % light attenuation by the silique wall.

SEED PHOTOSYNTHESIS

The use of O_2 electrodes to measure light-dependent O_2 evolution is a convenient way to determine photosynthetic capacity. Eastmond et al. (1996) demonstrated that canola seeds and embryos are capable of evolving net O_2 with increasing irradiances and under saturating CO_2. The high light compensation point for embryos (250 to 300 µmol m^{-2} s^{-1}) is indicative of large respiration rates. Respiration per embryo increased with growth but remained essentially constant on a fresh weight basis. We have generated similar results under different growth conditions and using a different cultivar (data not shown). A limitation of O_2 evolution data is that although it measures photosynthetic electron transport, it can not determine the fate of the produced NADPH and ATP. This energy could potentially be used to drive Rubisco-dependent CO_2 fixation as in leaves or it could be directly used to drive other metabolic processes such as fatty acid synthesis.

To address this question, ratios between photosynthetic electron transport rates (gross O_2 evolution) and light-dependent CO_2 fixation capacity (Rubisco activity) were determined (Table 3.2). Given the elevated CO_2 concentrations within siliques (Table 3.3), photorespiration should be eliminated therefore respiration rates in the dark and in the light may be equivalent and gross O_2 evolution rates could be estimated by adding dark respiration O_2 rates to net O_2 evolution rates at physiological light levels. Another consequence of high CO_2 concentrations is that Rubisco activities would be maximal therefore *in vitro* total Rubisco activities likely represent *in vivo* rates. The fixation of 1 mol CO_2 by Rubisco in the Calvin cycle requires the evolution of 1 mol O_2 from photosynthetic electron transport to produce the necessary energy. In both early- and late-cotyledonary embryos the CO_2 fixation capacity was higher than the photosynthetic electron transport capacity (Table 3.2). It therefore seems that energy produced from light harvesting was destined for Rubisco-dependent CO_2 fixation, however contributions to fatty acid biosynthesis cannot be conclusively ruled out from these data. The photosynthetic electron transport capacity to produce NADPH has been estimated to be of the same order of

magnitude as the fatty acid synthesis requirements derived from the data of Murphy and Cummins (1989).

CO_2 FIXATION CAPACITIES

Total activities of Rubisco and PEPC were measured in developing seeds, silique wall and leaf (Table 3.1). In seeds, Rubisco was measurable and much lower than leaf and silique wall photosynthetic tissues. This difference is somewhat misleading because Rubisco activities of leaf and silique wall growing in atmospheric CO_2 concentrations would be less than 50 % of V_{max} (Mate et al., 1996), whereas seed activities *in vivo* would likely approach their maximums because of extremely elevated silique cavity CO_2 (Table 3.3). Seed PEPC activities were significantly higher than leaf and silique wall (Table 3.1) indicative of a large role of anapleurotic metabolism. In contrast to seeds, Rubisco-PEPC ratios in leaf and silique wall were very large (Table 3.1). High leaf and silique wall ratios and low seed ratios have been noted previously in *B. rapa* (Singal et al., 1987). Large and comparable ratios in *B. rapa* leaf and silique wall were also found in another study while in contrast the pea pod wall ratio was less than one (Khanna-Chopra and Sinha, 1976). This difference is interesting because pea pod wall is known to refix seed-derived respiratory CO_2 (Atkins et al., 1977; Flinn et al., 1977).

Similar to pea, canola silique wall has a sclerenchyma layer near the inner surface (Fig. 3.3A). This layer stained for phenol alcohols, the precursors for lignin or suberin, and was continuous around the silique (Fig. 3.3B) and presumably acts as a gaseous diffusion barrier which elevates cavity CO_2 concentrations (Table 3.3). In contrast to pea, the endocarp layer did not contain enriched levels of chlorophyll (Fig. 3.4). To estimate endocarp CO_2 fixation capacity, it was assumed that Rubisco and chlorophyll distributions were equivalent and that PEPC was equally distributed across the silique wall. From these estimates it appears that seeds themselves are primarily responsible for CO_2 refixation and become increasingly important during the oil filling phase (Table 3.6). Silique cavity CO_2 concentrations were not significantly reduced in the light after 26 DAA (Table 3.3) indicating a lack of significant light-dependent CO_2 fixation capacity in the endocarp or the outer seed

coat, the tissues between the silique wall sclerenchyma layer and the seed coat diffusion barriers.

Before rapid oil accumulation (21 DAA), seed CO_2 fixation capacity was primarily in the seed coat (Table 3.4). As the embryo grew to fill the seed's volume, its capacity exceeded the seed coat mainly because of increased Rubisco activity. Embryo PEPC activity also dramatically increased between 21 and 28 DAA, the oil filling phase. $^{14}CO_2$ pulse-chase experiments are needed to determine the fate of CO_2 fixed by embryo Rubisco and PEPC. It is unknown whether triose-P from the Calvin cycle would be used to synthesize sucrose and starch as in leaves or would enter glycolysis. CO_2 fixed by PEPC into oxaloacetate may replenish TCA cycle intermediates depleted by protein and chlorophyll synthesis or may be sequentially converted to malate, pyruvate, and acetyl-CoA for use in fatty acid synthesis (Fig. 1.7).

Embryo loss of respired CO_2 was presumably slowed by a poorly permeable seed coat. Intact seeds had an elevated apparent K_m for respiratory O_2 (Fig. 3.2) and photosynthetic electron transport, as measured by pulse-modulated chlorophyll fluorescence, was unaffected by external CO_2 concentration for seeds but not isolated embryos (Table 3.5). Electron transport rates of these 27 DAA embryos in CO_2-free air were, however, much higher than predicted even after 1 h without exogenous CO_2. The thickness of the expanded cotyledons at this developmental stage may generate a long path-length for CO_2 diffusion to the atmosphere. As chlorophyll, Rubisco, and PEPC are presumably distributed throughout the cotyledons, respired CO_2 could be refixed at any point along this diffusion path. The majority of Rubisco-dependent refixation would likely occur at the outer cell layers where light availability is maximal.

Besides providing energy for Rubisco-dependent refixation, embryo photosynthesis may play another important role. The seed coat retards O_2 diffusion from the atmosphere to embryos and appears to limit respiratory activity in the dark at atmospheric O_2 concentrations (Fig. 3.2). Growing embryos require increasing amounts of O_2 to support increasing respiration rates (Eastmond et al., 1996) therefore O_2 evolved by seed photosynthetic electron transport may be necessary for high embryo respiration and growth rates. This theory agrees with the observations

that soybean seed yield was dramatically reduced after growth in subambient oxygen atmospheres (Quebedeaux and Hardy, 1975; Sinclair et al., 1987). Furthermore, embryo uptake of ^{14}C-labelled assimilates was inhibited by low O_2 concentrations and less lipid and protein were formed possibly indicating a respiratory limitation (Quebedeaux and Giaquinta, 1978; Thorne 1982).

The thickness of late-cotyledonary embryos poses special considerations. For the purposes of this chapter, it has been simplistically assumed that enzyme activities and photosynthetic capacity are evenly distributed throughout embryos. Although casual observation suggests even chlorophyll distribution throughout developing cotyledons, it is quite conceivable that respiration, PEPC activity and storage product synthesis are localized within developing cotyledons while light harvesting and Rubisco activity would surely be greatest in the outer cotyledon cell layers. This concept must be considered when interpreting the results of this chapter until localization experiments have been conducted.

CO_2 refixation is likely limited by light. PEPC is independent of light and would have plentiful CO_2 substrate (Table 3.3). Rubisco would also have abundant CO_2 but light-dependent production of ATP and NADPH would be modulated by tissue light attenuation. Seeds would receive 20 % of incident light which could be up to 400 µmol quanta m^{-2} s^{-1} under Australian summer conditions, a level greater than the light compensation point for intact seeds (data not shown). With additional PEPC CO_2 fixation (Table 3.1), seeds could have a net carbon gain for much of the photoperiod. A key part of this refixation capacity is Rubisco-catalyzed CO_2 fixation in embryos (Table 3.4) which is driven by energy produced from chlorophyll light absorption. Seed photosynthesis may also be important for producing O_2 to fuel respiration. Any reduction in embryo chlorophyll content by genetic engineering to reduce industrial processing problems may therefore adversely affect seed growth and would need careful temporal targeting. Endocarp refixation would also contribute to total refixation (Table 3.6) and together these carbon recoveries supplement carbon imported into seeds from other plant parts. Even if seed and endocarp fixation does not exceed respiratory CO_2 losses it is important to note that any loss reduction would surely benefit seed growth. Preliminary estimates have indicated that refixation capacity is of the same order of magnitude as seed growth

rates, however further experiments are needed to evaluate the levels of CO_2 refixation relative to sucrose import.

CHAPTER 4 : TISSUE CULTURE AND TRANSFORMATION

INTRODUCTION

Genetic engineering is a powerful method to make defined changes in plant metabolism. A number of techniques have produced stably transformed plants and most of them rely on totipotency, the ability to form plants from single or a small group of cells. Transformation typically relies on selection pressure to distinguish rare transformed cells. To produce a shoot these transformed cells must also be competent for regeneration, another rare event. Efficient techniques are therefore those capable of both high transformation and high regeneration frequencies.

Agrobacterium-mediated transformation (De Block et al., 1984; Horsch et al., 1984) and particle bombardment (Klein et al., 1987) are the most common methods to deliver foreign DNA into plants. Like other dicotyledonous species, canola has been transformed by *Agrobacterium* (Fry et al., 1987; Pua et al., 1987; Charest et al., 1988; Radke et al, 1988; De Block et al., 1989; Moloney et al., 1989; Boulter et al., 1990; Damgaard and Rasmussen, 1991; Schröder et al., 1994) although other methods have been used (Guerche et al., 1987; Neuhaus et al., 1987; Chen and Beversdorf, 1994). Once feasibility has been established it is necessary to develop an efficient and routine procedure that is not labour-intensive and genotype-dependent. The choice and culturing of target tissue greatly influences transformation success.

Stem segments (Fry et al., 1987; Pua et al., 1987), thin cell layers (Charest et al., 1988), hypocotyls (Radke et al, 1988; De Block et al., 1989; Schröder et al., 1994), cotyledonary petioles (Moloney et al., 1989) and inflorescence stalks (Boulter et al., 1990) have all been used for *Agrobacterium tumefaciens* transformation of canola. Of these tissues, cotyledonary petioles appear to be the best choice, offering high-frequency reliable regeneration and being relatively easy to transform. Ono et al. (1994) reported that 98 out of 100 *B. napus* genotypes regenerated shoots from cotyledonary petioles. Moloney et al. (1989) reported up to 55 percent of cotyledonary petioles yielded transgenic shoots after *Agrobacterium* transformation.

The objectives of the work described in this chapter were to construct *Agrobacterium* transformation vectors, to introduce gene expression constructs into canola cotyledonary petioles and to regenerate transformed shoots. The gene constructs to be introduced were intended to perturb assimilate partitioning by supplementing regulatory enzymes in carbon and nitrogen transport compound biosynthetic pathways. The physiological and biochemical consequences of these defined changes will be assessed in Chapter 5.

MATERIALS AND METHODS

TRANSFORMATION VECTORS

Agrobacterium tumefaciens-mediated transformation vectors containing a selectable marker gene and a gene of interest were either obtained or were constructed. All DNA manipulations were done using standard procedures (Sambrook et al., 1989). Initial construct cloning was completed in *E. coli* followed by transfer to a binary plasmid for subsequent introduction into an *Agrobacterium* strain.

35S - GUS - 35S 3' / pGA492. A binary plasmid containing a CaMV 35S - β glucuronidase (GUS) - 35S 3' expression construct in the *Agrobacterium* strain AGL1 (Lazo et al., 1991) was provided by T.J.V. Higgins (CSIRO Plant Industry). The backbone of this binary plasmid is pGA492 (An, 1987) and has been named pMCP3 (Shade et al., 1994) after the cloning of several genes within the T-DNA region.

35S - spinach S158A - ocs / pBin19. A binary plasmid containing a spinach (*Spinacia oleracea* L.) SPS cDNA (GenBank S54379) was provided by U. Sonnewald (IPK, Gatersleben, Germany) (Fig. 4.1). The phosphorylation site at position 158 of SPS had been mutagenized from serine to alanine, thereby removing one mechanism of regulating enzyme activity (McMichael et al., 1993). This mutagenized cDNA was cloned in the sense direction into pBinAR (Hofgen and Willmitzer, 1990) as an EcoRV - SmaI fragment. The binary plasmid provided by Sonnewald was introduced into the hypervirulent *Agrobacterium* strain AGL1 by

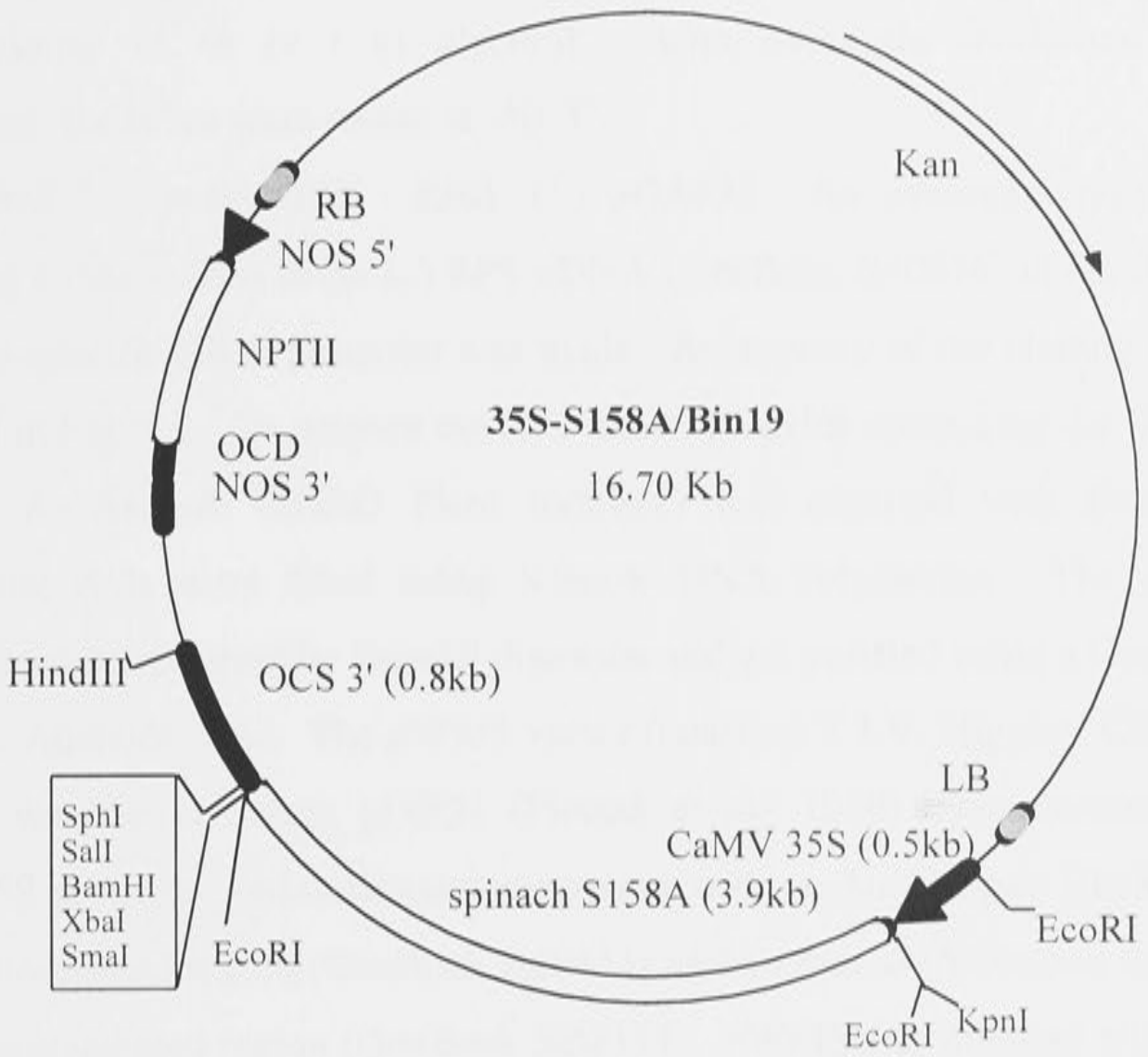

Figure 4.1. Plasmid map of a pBin19 *Agrobacterium* binary vector containing a CaMV 35S- spinach S158A- *ocs* and a *nos- nptII- nos* gene construct within the T-DNA region. Note that only key restriction sites are shown.

triparental mating. A single colony was inoculated into 10 mL MGL liquid medium with 60 μg mL^{-1} kanamycin monosulphate (Sigma, St. Louis, MO) and 20 μg mL^{-1} rifampicin (Sigma, St. Louis, MO) and grown to saturation at 28 °C. Aliquots of 1.5 mL were centrifuged in an Eppendorf tube and the pellet was resuspended in 0.5 mL LB containing 15 % (v / v) glycerol. After overnight incubation at room temperature, the tubes were stored at -80 °C.

RbcS 5' - maize SPS - RbcS 3' / pGA492. An overexpression construct containing a maize (*Zea mays* L.) SPS cDNA (GenBank S40876) under the control of a tissue-specific RbcS promoter was made. A summary of the cloning strategy is presented in Fig. 4.2. To prepare the SPS insert, pTZ19R containing the SPS cDNA (courtesy A. Ashton, CSIRO Plant Industry) was digested with EcoRI. The overhanging ends were filled using Klenow DNA polymerase. The insert was released from the plasmid by BamHI digestion and gel purified using a Geneclean kit (Bresatec, Adelaide, SA). The pWM5 vector (courtesy T.J.V. Higgins, CSIRO Plant Industry) was derived from pDH51 (Pietzak et al., 1986) by replacement of the CaMV 35S promoter and terminator sequences with an *Arabidopsis* RbcS promoter and 5' untranslated region (GenBank X13611) and a tobacco (*Nicotiana tabacum* L.) RbcS 3' untranslated region (GenBank X02353). pWM5 was digested with SalI and the overhanging ends were filled with Klenow DNA polymerase. It was then digested with BamHI and treated with alkaline phosphatase before ligation with the purified SPS fragment. Ligations were transformed into $CaCl_2$-competent *E. coli* NM522. Insertions were confirmed by diagnostic restriction digests of alkaline lysis miniprep DNA from ampicillin-resistant colonies.

To clone into a binary plasmid, the SPS / pWM5 construct was digested with EcoRI and the 5.5 kb RbcS 5' - SPS - RbcS 3' fragment was gel purified from the plasmid backbone. This fragment was ligated with EcoRI-digested and alkaline phosphatase-treated pGA492 (An, 1987). Insertions and their direction was assessed by diagnostic restriction digests. The resulting construct is illustrated in Fig. 4.3. This binary plasmid was introduced into *Agrobacterium* (AGL1) by triparental mating. A single colony was inoculated into 10 mL MGL with 6 μg mL^{-1} tetracycline (Sigma, St. Louis, MO) and 20 μg mL^{-1} rifampicin and grown to

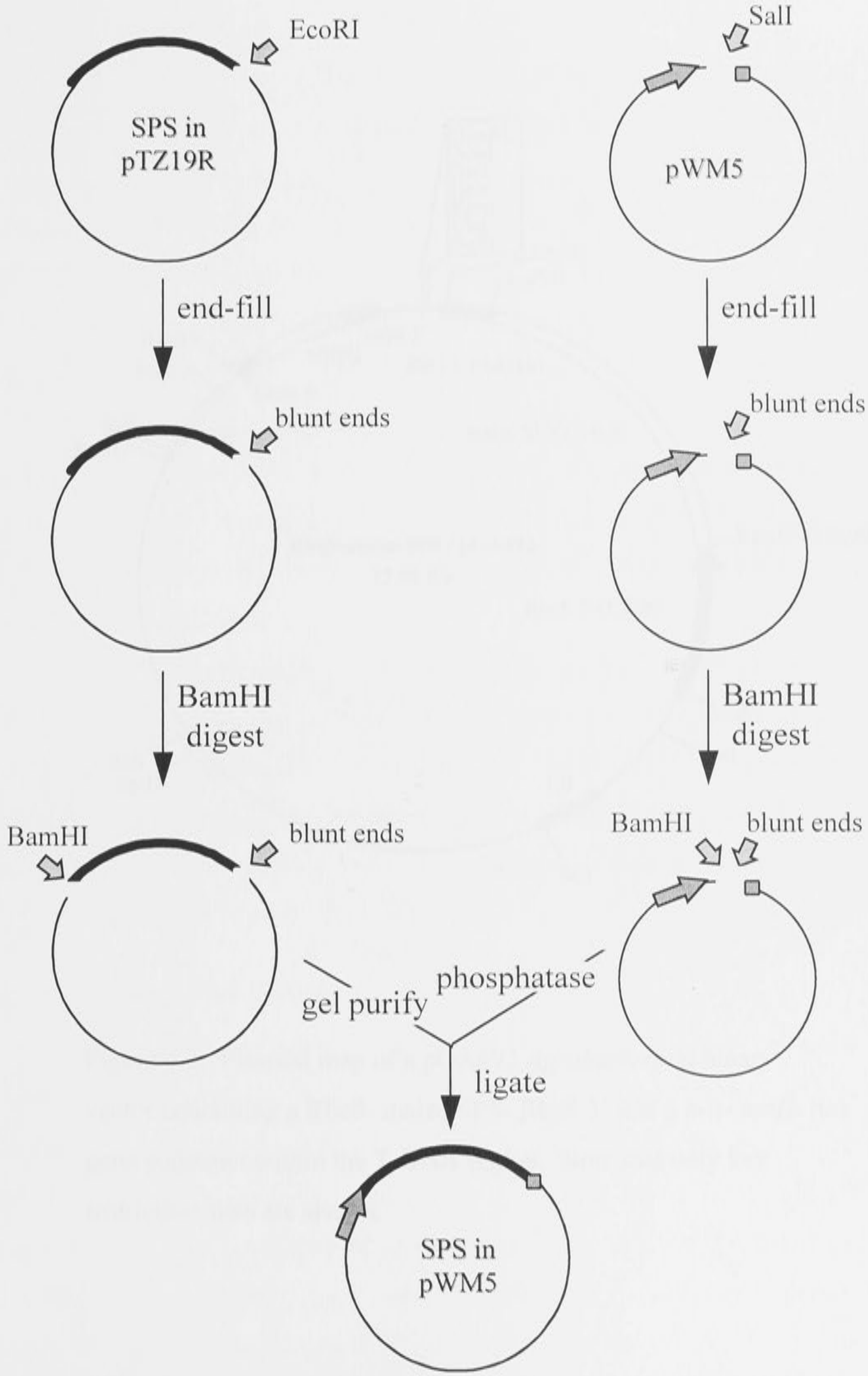

Figure 4.2. Cloning strategy for the construction of an *E. coli* plasmid containing a RbcS- maize SPS- RbcS 3' gene construct.

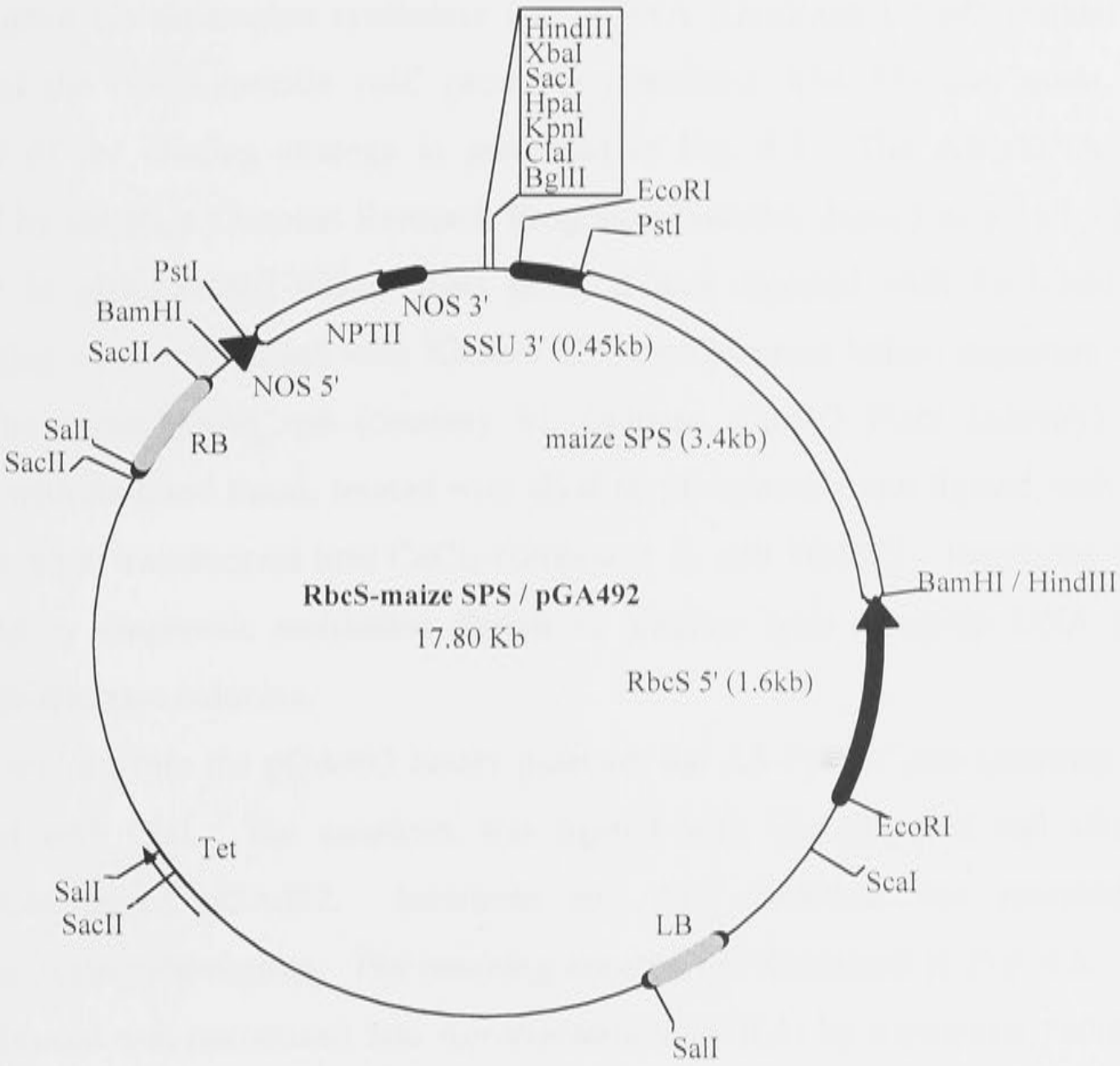

Figure 4.3. Plasmid map of a pGA492 *Agrobacterium* binary vector containing a RbcS- maize SPS- RbcS 3' and a *nos- nptII- nos* gene construct within the T-DNA region. Note that only key restriction sites are shown.

saturation at 28 °C. Glycerol stocks were prepared as described for 35S - spinach S158A - ocs / pBin19 and stored at -80 °C.

rolC - rice AS - nos / pGA492. An overexpression construct containing a rice (*Oryza sativa* L.) asparagine synthetase (AS) cDNA (GenBank U55873) under the control of the tissue-specific *rolC* promoter (GenBank X64255) was made. A summary of the cloning strategy is presented in Fig. 4.4. The AS cDNA was provided by the Rice Genome Research Program (Tsukuba, Japan) as a SalI - NotI fragment in pBluescriptII SK+. This plasmid was digested with SacI and the overhanging ends were filled with Klenow DNA polymerase before digestion with SalI. The vector pRolC.cas (courtesy M. Graham, CSIRO Plant Industry) was digested with SalI and SmaI, treated with alkaline phosphatase and ligated with AS. Ligations were transformed into $CaCl_2$-competent *E. coli* NM522. Insertions were confirmed by diagnostic restriction digests of alkaline lysis miniprep DNA from ampicillin-resistant colonies.

To clone into the pGA492 binary plasmid, the AS / pRolC.cas construct was linearized with ClaI. The construct was ligated with ClaI-digested and alkaline phosphatase-treated pGA492. Insertions and their direction was assessed by diagnostic restriction digests. The resulting construct is illustrated in Fig. 4.5. This binary plasmid was introduced into *Agrobacterium* (AGL1) by triparental mating as described for RbcS 5' - maize SPS - RbcS 3'.

TISSUE CULTURE OPTIMIZATION

The cotyledonary petiole culture procedure was based on Moloney et al. (1989). *B. napus* seeds cv. Westar were surface-sterilized in 70 % (v / v) ethanol for 30 s followed by 20 min in 1 % (v / v) sodium hypochlorite. The seeds were rinsed three times in sterile deionized water for 5 min each. Seeds were then placed on germination medium containing MS salts (Murashige and Skoog, 1962), B5 vitamins (Gamborg et al., 1968), 100 mg L^{-1} *myo*-inositol, 3 % (w / v) sucrose and 0.8 % (w / v) purified agar (Sigma, St. Louis, MO) at a density of 16 or 20 seeds per plate. The 100 x 20 mm plates were wrapped with Micropore surgical tape (3M Health Care, St. Paul, MN). Seeds were germinated at 24 °C in a 16 h photoperiod (30 - 40 µmol m^{-2} s^{-1}) provided by Philips PowerMiser Daylight TLD36W/54 fluorescent tubes.

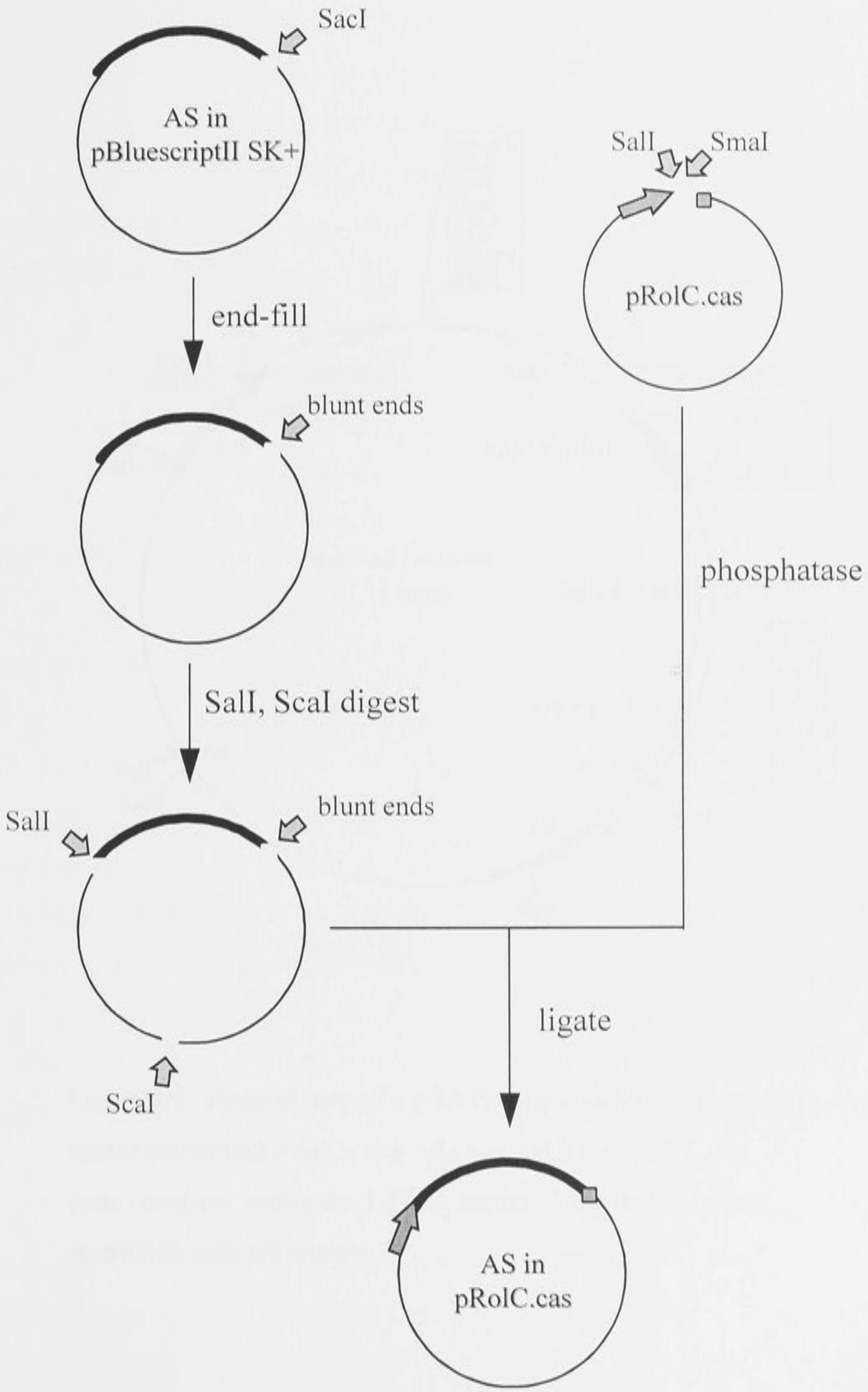

Figure 4.4. Cloning strategy for the construction of an *E. coli* plasmid containing a *rolC*- rice AS- *nos* gene construct.

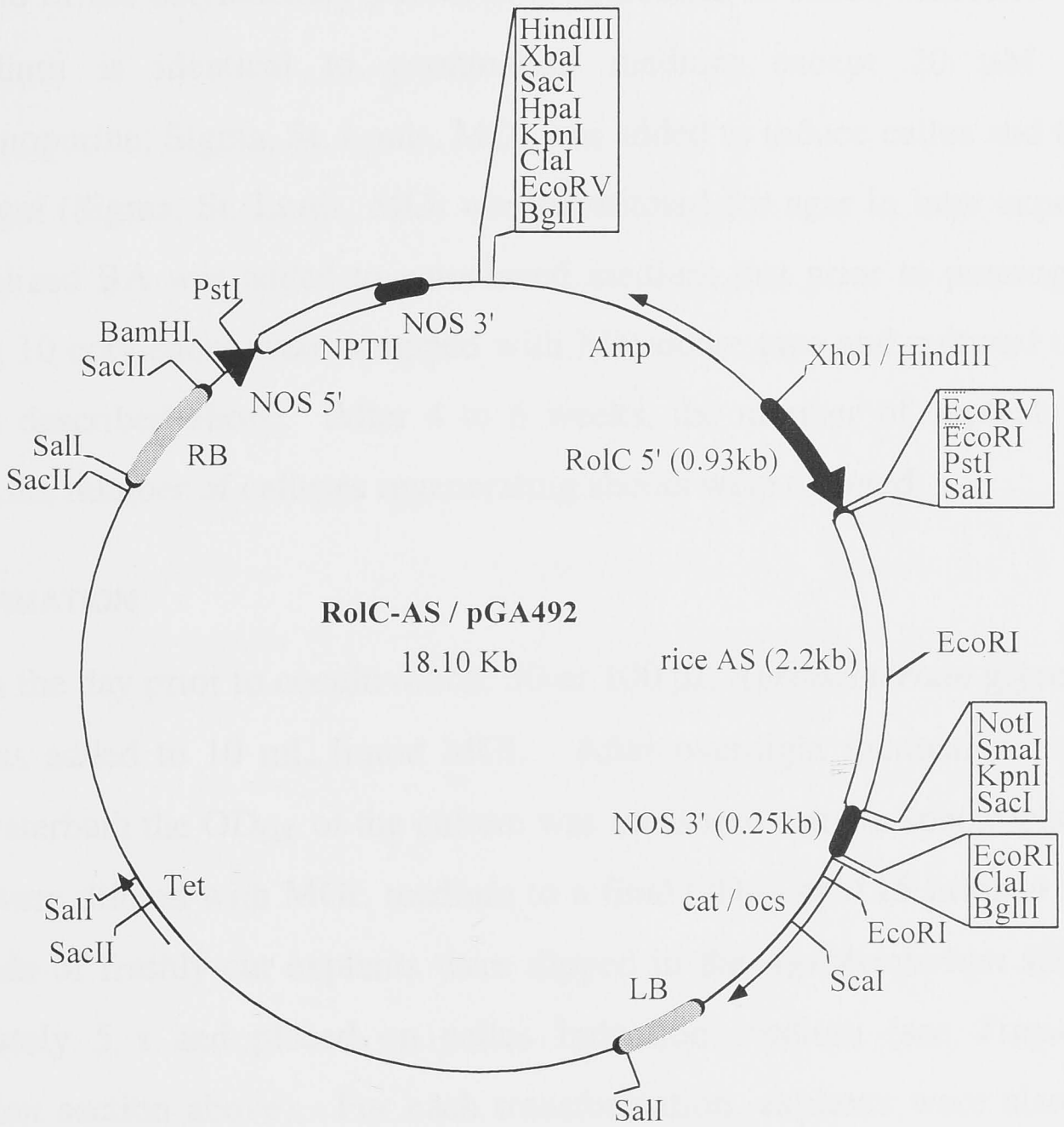

Figure 4.5. Plasmid map of a pGA492 *Agrobacterium* binary vector containing a *rolC*- rice AS- *nos* and a *nos- nptII- nos* gene construct within the T-DNA region. Note that only key restriction sites are shown.

Explants were prepared by cutting the cotyledonary petiole close to the hypocotyl without including any apical meristem cells. Four to five day-old seedlings had recently formed chlorophyll and the petioles were 1 to 3 mm in length. The cut end of the cotyledonary petiole was embedded in callus induction medium. This medium is identical to germination medium except 20 μM BA (6-benzylaminopurine; Sigma, St. Louis, MO) was added to induce callus and 0.3 % (w / v) Phytagel (Sigma, St. Louis, MO) was substituted for agar in later experiments. Filter-sterilized BA was added to autoclaved medium just prior to pouring. Plates containing 10 cotyledons were wrapped with Micropore tape and cultured under the conditions described above. After 4 to 6 weeks, the number of explants forming callus and the number of calluses regenerating shoots were counted.

TRANSFORMATION

On the day prior to cocultivation, 50 or 100 μL *Agrobacterium* glycerol stock culture was added to 10 mL liquid MGL. After overnight incubation in a 28 °C shaking waterbath the OD_{600} of the culture was measured using a spectrophotometer. Cultures were diluted with MGL medium to a final OD_{600} of 0.15 prior to use. The petiole ends of freshly-cut explants were dipped in the *Agrobacterium* solution for approximately 5 s and placed on callus induction medium (see *Tissue culture optimization* section above). For each transformation, explants were also cultured without exposure to *Agrobacterium*. After 3 d incubation at the light and temperature conditions described previously, selection was initiated by transferring cocultivated explants to callus induction medium supplemented with 15 or 20 mg L^{-1} kanamycin monosulphate and 200 mg L^{-1} Timentin (ticarcillin and clavulanic acid; SmithKline Beecham Australia, Dandenong, VIC). These antibiotics were added to cooled autoclaved medium just prior to pouring. Half of the explants not exposed to *Agrobacterium* were also transferred to selection medium as a selection control. As a regeneration control, the other uncocultivated explants remained on medium without antibiotics. Subculture to fresh selection medium was after 3 weeks and then biweekly until callus was necrotic.

PLANT REGENERATION FROM SELECTION MEDIUM

Shoots regenerating on selection medium were cut from the callus and placed on modified selection medium where sucrose was reduced to 1 % (w / v), kanamycin was increased to 50 mg L^{-1}, and BA was omitted. No callus was subcultured with shoots. Once a shoot had formed 2 to 3 leaves, it was dipped in 1 mg mL^{-1} IBA (indole-3-butyric acid) (Sigma, St. Louis, MO) for 15 s to stimulate root formation and then placed on modified selection medium in round 65 x 75 mm plastic jars with screw caps. At each biweekly subculture, non-rooting shoots were again treated with IBA. Sometimes the basal ends of shoots were recut at a stem node prior to IBA treatment.

Shoots that formed roots were transferred to pots containing a vermiculite : perlite mixture (1:1, v / v) in a naturally-illuminated glasshouse fitted with shadecloth. Pots were initially covered with plastic food wrap to maintain humidity. Once hardened and established, shoots were transferred to a compost and perlite mixture (1:1, v / v) in an unshaded glasshouse with temperatures set at 23 / 15 °C day / night. Seed was collected from mature plants.

T_0 SCREENING

Regenerated shoots were tested for activity of the introduced NPTII gene product using a dot blot assay modified from McDonnell et al. (1987). A 1.3 cm^2 leaf punch was taken from shoots either in culture or in soil and ground fresh in an 1.5 mL Eppendorf tube with granular washed quartz and 50 to 70 µL extraction buffer (62 mM Tris-HCl, pH 6.8, 10 % (v / v) glycerol, 10 mM DTT). After 5 min centrifugation, 30 µL of supernatant was added to 30 µL reaction mix (65 mM Tris, 12 mM $MgCl_2$, 200 mM NH_4Cl, pH 7.1, 10 µM ATP, 30 µM neomycin, 10 mM NaF, 10 µCi mL^{-1} [γ^{32}P]ATP). Samples were incubated at 37 °C for 1 h prior to spotting 40 µL onto cellulose phosphate paper (Whatman P81). The paper was pretreated with 20 mM ATP and 100 mM pyrophosphate. Once the spots were dry, the blot was washed at 60 °C for 20 min in 10 % (w / v) proteinase K and 1 % (w / v) SDS. The blot was then washed 1 to 2 times in 10 mM $NaPO_4$, pH 7.5 for 20 min at 60 °C. The blot was sealed in plastic and placed in a Phosphor Screen (Molecular Dynamics, Sunnyvale, CA) overnight before Phosphorimager scanning.

RESULTS

TISSUE CULTURE OPTIMIZATION

From published reports, *Agrobacterium* transformation of *B. napus* using cotyledonary petioles seemed to be the most efficient and the least labour-intensive method (Moloney et al., 1989). To adapt this system to this laboratory's conditions, plant regeneration frequencies were first tested because good regeneration is a prerequisite for successful transformation. The age of germinating Westar seedlings was thought to be a critical factor therefore explants were cultured 4 to 7 d after seed plating. Petioles younger than 3 d were too short to prepare explants. From 4 to 7 d the proportion of explants which produced callus rose exponentially (Fig. 4.6). There was, however, very little shoot regeneration. Only one callus from the 7 d treatment produced shoots. The seed used in this experiment germinated slowly. Using seeds with much quicker germination and development, regeneration was significantly higher from 5 day-old explants compared to 7 day-old ($p << 0.01$) (Fig. 4.7). In a separate experiment, 4 day-old explants regenerated higher numbers of shoots compared to 5 day-old explants (Fig. 4.8) although the difference was not significant ($p = 0.10$).

Explants were cultured from four seed sources; seeds provided by P. Salisbury (VIDA, Horsham, VIC) and D.J. Murphy (John Innes Centre, Norwich, UK) and seeds produced from these sources. Germination time varied amongst seed sources therefore explants were cultured when cotyledonary petioles were 1 to 3 mm in length rather than all at the same time. Explants from produced seeds were cultured 94 h after plating, Salisbury seed was cultured 100 h after plating and Murphy seed was cultured 139 h after plating. With this staging, regeneration frequencies were not significantly different between seed sources ($p = 0.82$) (Fig. 4.9).

As an alternative to BA for inducing callus and shoots, the cytokinin thidiazuron (TDZ) was tested from 0.1 to 10 µM. In addition, sterilizing BA by autoclaving or filtering was compared. Apart from explant age, there was no

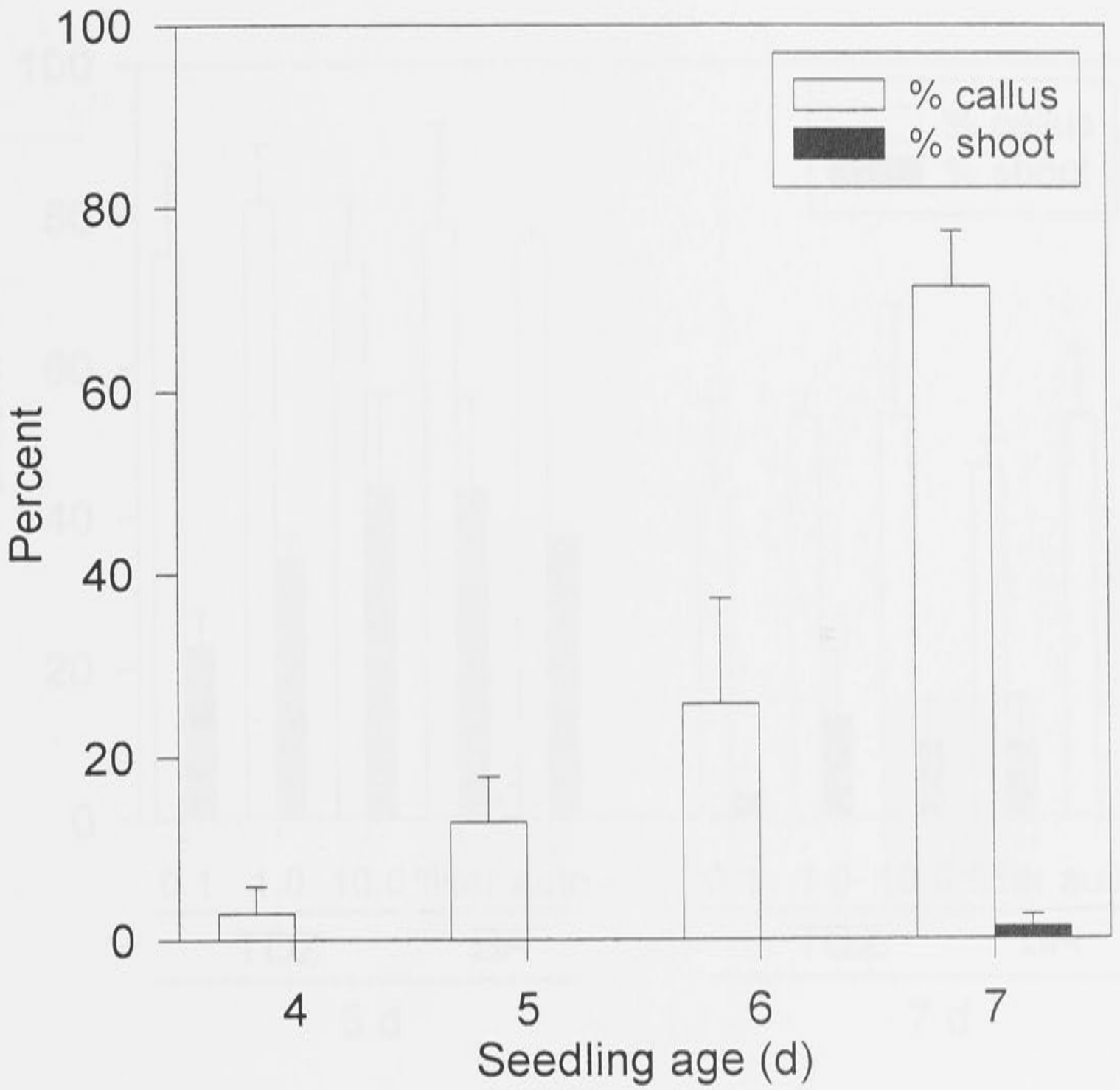

Figure 4.6. Effect of seedling age at time of culture initiation on callus production and shoot regeneration from canola cv. Westar cotyledonary petiole explants. Mean values (+/- SE) are plotted from 7 to 8 replicates per treatment. % callus = % explants that formed callus; % shoot = % explants that produced shoots.

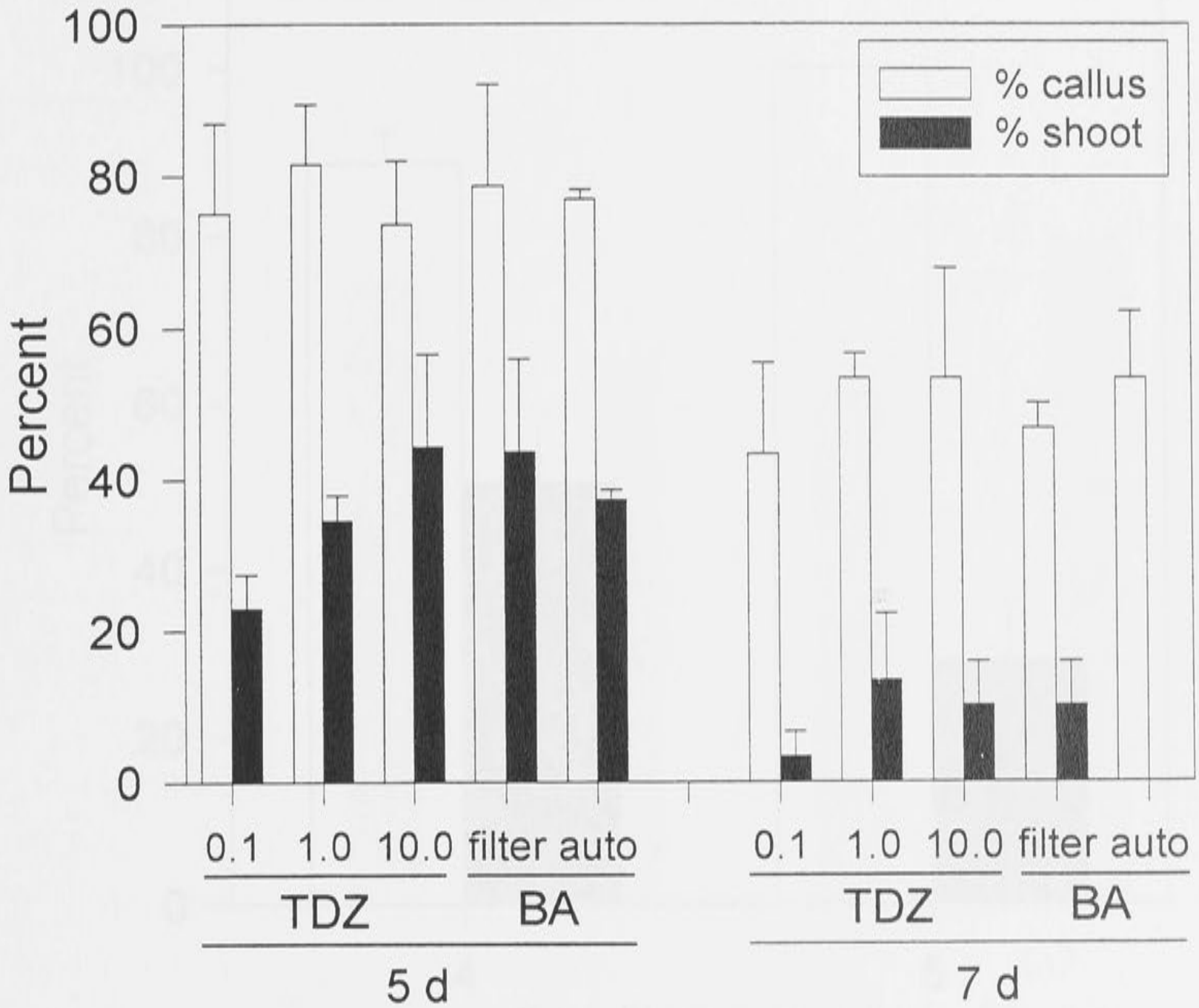

Figure 4.7. Effects of seedling age at the time of culture initiation and of callus inducing hormone on callus production and shoot regeneration from canola cotyledonary petiole explants. Mean values (+/- SE) are plotted from 3 to 4 replicates per treatment. % callus = % explants that formed callus; % shoot = % explants that produced shoots; filter = filter-sterilized BA; auto = autoclaved BA.

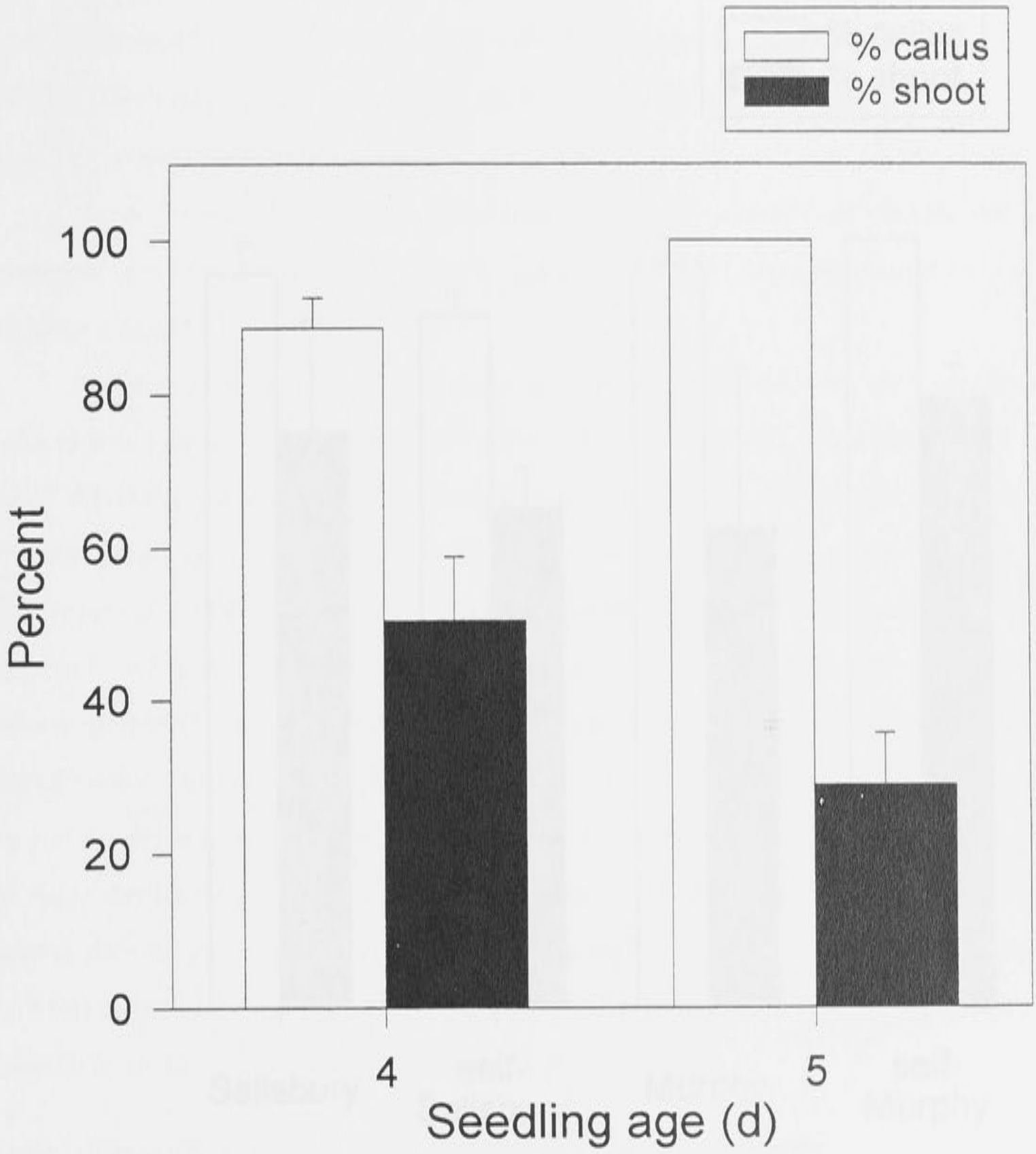

Figure 4.8. Effects of seedling age at the time of culture initiation on callus production and shoot regeneration from canola cotyledonary petiole explants. Mean values (+/- SE) are plotted from 4 to 5 replicates per treatment. % callus = % explants that formed callus; % shoot = % explants that produced shoots.

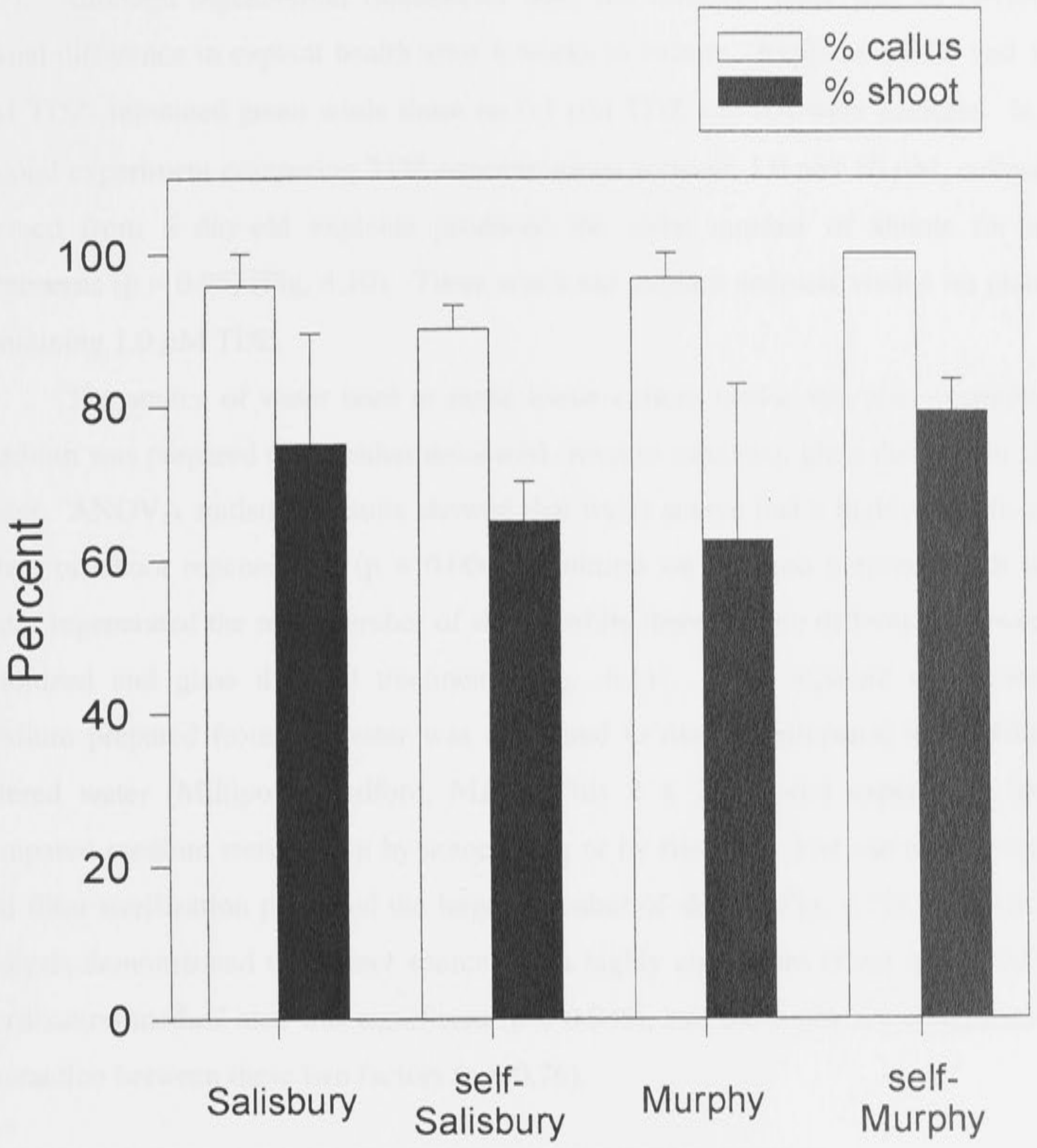

Figure 4.9. Effect of seed source on callus production and shoot regeneration from canola cotyledonary petiole explants. Mean values (+/- SE) are plotted from 3 to 5 replicates per treatment. % callus = % explants that formed callus; % shoot = % explants that produced shoots.

significant regeneration differences between any of the treatments (p = 0.17) (Fig. 4.7). Although regeneration frequencies were not different there was an obvious visual difference in explant health after 4 weeks in culture. Explants on 1.0 and 10 µM TDZ remained green while those on 0.1 µM TDZ and BA were necrotic. In a second experiment comparing TDZ concentrations between 1.0 and 10 µM, calluses formed from 5 day-old explants produced the same number of shoots for all treatments (p = 0.95) (Fig. 4.10). There was some explant necrosis visible on plates containing 1.0 µM TDZ.

The source of water used to make tissue culture media was also examined. Medium was prepared using either deionized (reverse osmosis), glass distilled or tap water. ANOVA statistical results showed that water source had a highly significant effect on shoot regeneration (p = 0.004). Cultures on medium prepared with tap water regenerated the most number of shoots while there was no difference between deionized and glass distilled treatments (Fig. 4.11). In a separate experiment, medium prepared from tap water was compared to medium prepared with MilliQ filtered water (Millipore, Bedford, MA). This 2 x 2 factorial experiment also compared medium sterilization by autoclaving or by filtering. The use of tap water and filter sterilization produced the largest number of shoots (Fig. 4.12). Statistical analysis demonstrated that water source had a highly significant effect (p = 0.003), sterilization method also was significant (p = 0.046), and there was not a significant interaction between these two factors (p = 0.76).

TRANSFORMATION AND REGENERATION FROM SELECTION MEDIUM

With the increase of plant regeneration frequencies to over 80 percent, the chances of recovering transgenic shoots was much higher. With the modifications to the tissue culture protocol shoots began to appear from explants cocultivated with *Agrobacterium*. The *Agrobacterium* cells contained a binary plasmid with a gene of interest and also the *nptII* kanamycin resistance gene under the control of *nos* promoter and terminator sequences (Figs. 4.1, 4.3 and 4.5). The addition of kanamycin to callus induction medium greatly reduced callus production. From a small site of initiation on the cut petiole end, callus gradually proliferated. In contrast to medium without kanamycin, callus was generally white, however some

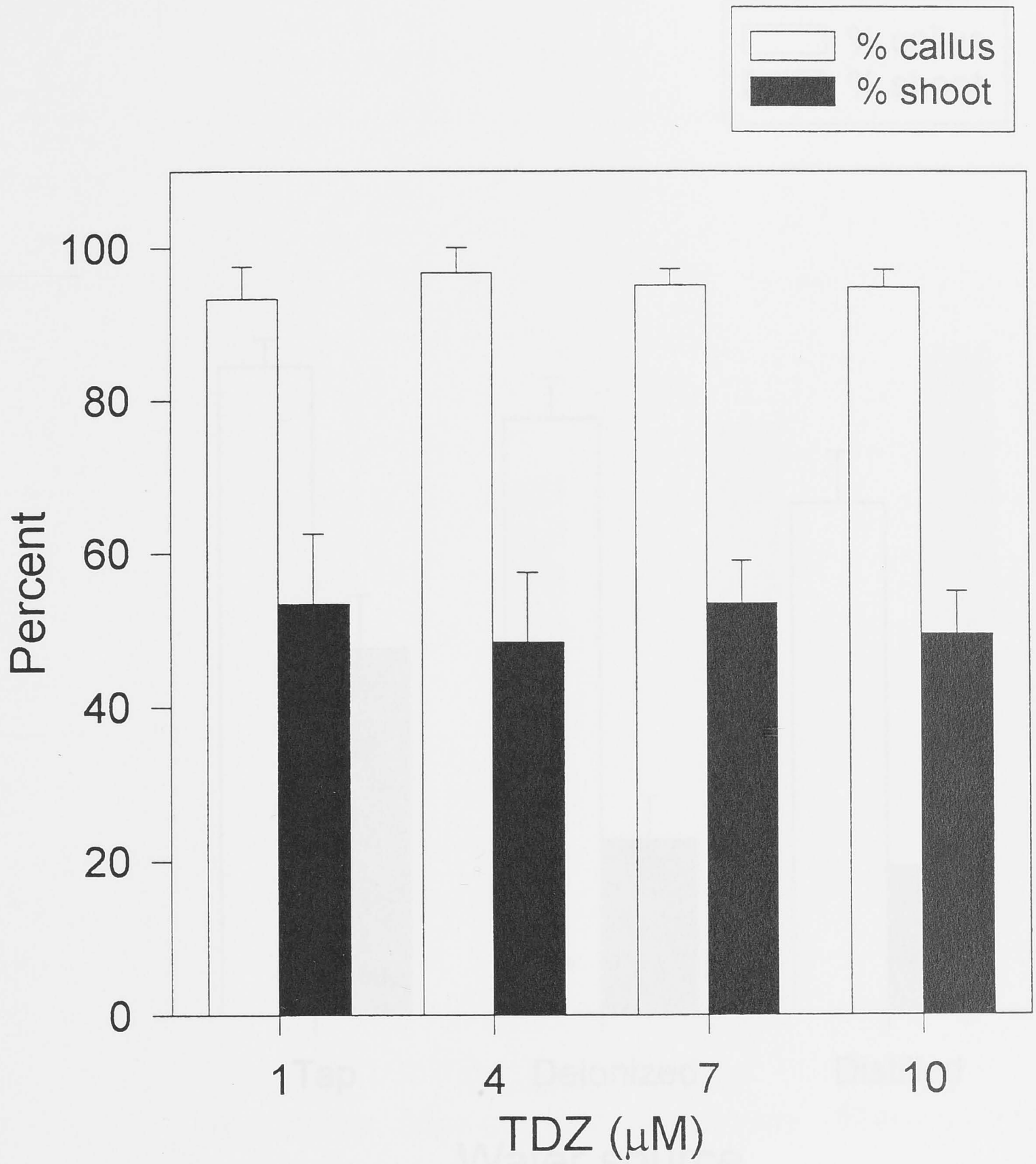

Figue 4.10. Effect of thidiazuron (TDZ) concentration on callus production and shoot regeneration from canola cv. Westar cotyledonary petiole explants. Mean values (+/- SE) are plotted from 6 replicates per treatment. % callus = % explants that formed callus; % shoot = % explants that produced shoots.

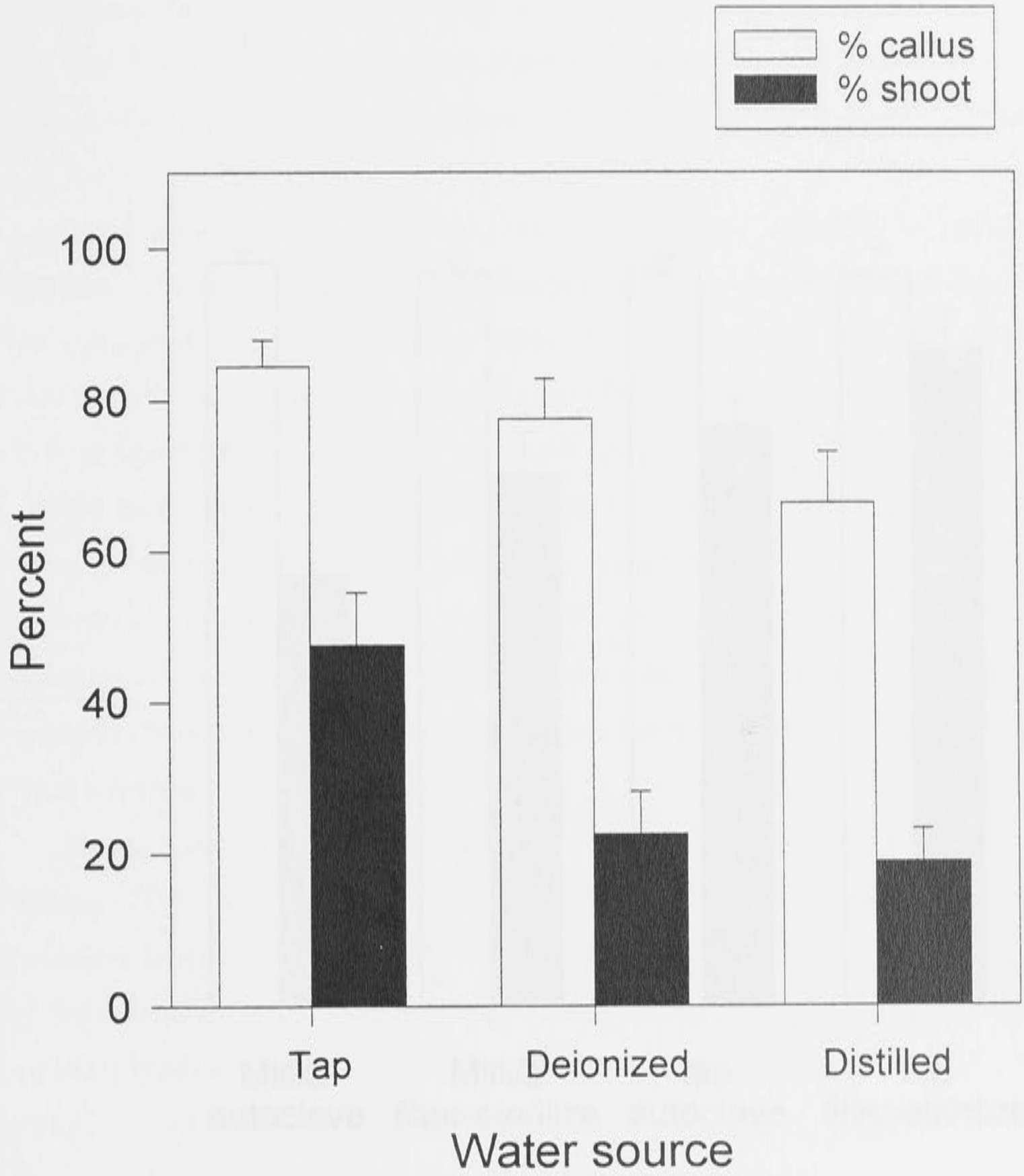

Figure 4.11. Effect of water source on callus production and shoot regeneration from canola cv. Westar cotyledonary petiole explants. Mean values (+/- SE) are plotted from 4 replicates per treatment. % callus = % explants that formed callus; % shoot = % explants that produced shoots.

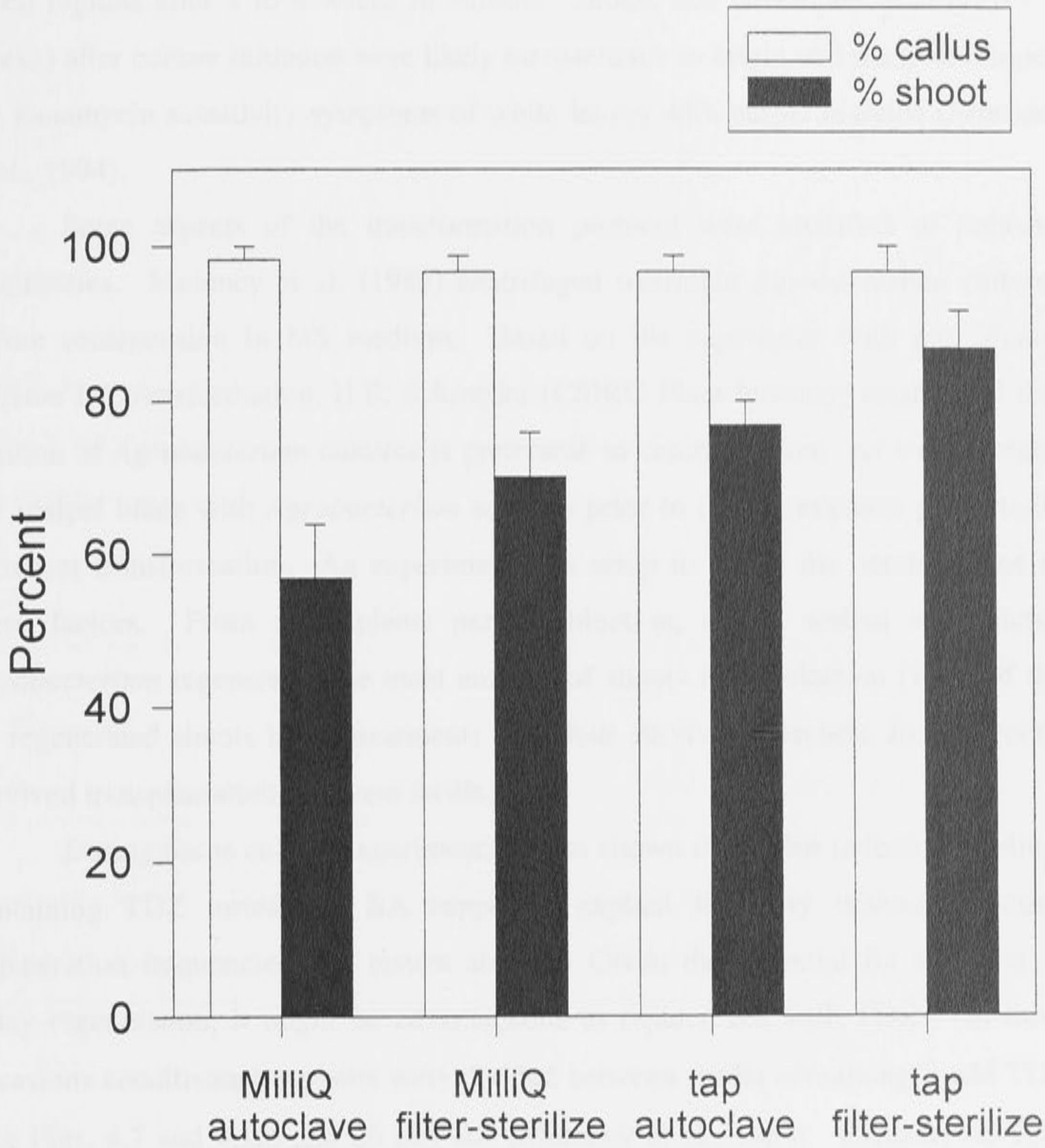

Figure 4.12. Effect of water source and sterilization method on callus production and shoot regeneration from canola cv. Westar cotyledonary petiole explants. Mean values (+/- SE) are plotted from 6 replicates per treatment. % callus = % explants that formed callus; % shoot = % explants that produced shoots.

portions of callus developed green pigmentation. Shoots regenerated from these green regions after 4 to 6 weeks in culture. Shoots that developed quickly (0 - 2 weeks) after culture initiation were likely meristematic in origin and many developed the kanamycin sensitivity symptoms of white leaves with purple margins (Schröder et al., 1994).

Some aspects of the transformation protocol were modified to improve frequencies. Moloney et al. (1989) centrifuged overnight *Agrobacterium* cultures before resuspension in MS medium. Based on his experience with pea (*Pisum sativum* L.) transformation, H.E. Schroeder (CSIRO Plant Industry) established that dilution of *Agrobacterium* cultures is preferable to centrifugation. As well, wetting the scalpel blade with *Agrobacterium* solution prior to cutting explants purportedly increases transformation. An experiment was setup to assess the combinations of these factors. From 50 explants per combination, a wet scalpel and diluted *Agrobacterium* regenerated the most number of shoots from selection (11). Of the 21 regenerated shoots in all treatments only four survived selection, formed roots, survived transplantation and were fertile.

During tissue culture experiments, it was shown that callus induction medium containing TDZ instead of BA supported explant longevity without affecting regeneration frequencies (see results above). Given the potential for selection to delay regeneration, it might be advantageous to replace BA with TDZ. On three occasions cocultivated explants were divided between media containing 2 µM TDZ (see Figs. 4.7 and 4.10) and 20 µM BA (Moloney et al., 1989). Explants on TDZ selection medium produced twice as many regenerated shoots as BA selection medium, however the number that survived to maturity was higher on BA selection medium (Table 4.1).

Table 4.2 summarizes all the transformation experiments with Westar. In parallel with cocultivated explants, two sets of controls were used. As a selection control, explants not exposed to *Agrobacterium* were plated on selection medium and subcultured to fresh medium at the same time as cocultivated explants. No shoots were ever produced from this control. As a regeneration control, explants not exposed to *Agrobacterium* were plated on callus induction medium. After 5 to 6 weeks, the numbers of explants forming callus and the number of calluses forming

Table 4.1: Effect of callus-inducing cytokinin on the regeneration of shoots from canola cotyledonary explants cocultivated with an *Agrobacterium* binary plasmid containing a *nptII* kanamycin resistance gene.

Hormone	No. Explants	No. Regenerants	No. T_1 Seed	No. NPTII Positive
BA (20 μM)	280	28 (10 %)	14 (5.0 %)	7 (2.5 %)
TDZ (2 μM)	220	46 (21 %)	9 (4.1 %)	4 (1.8 %)

Table 4.2: Summary of *Agrobacterium* cocultivation experiments to produce transgenic canola plants from cotyledonary petiole explants. See Materials and Methods for experimental details. nd, not determined; [a], first use of 4-5 day-old seedlings; [b], first use of Micropore tape; [c], first use of tap water, diluted *Agrobacterium*, and wet scalpel blade; [d], first use of Phytagel.

	Cocultivations					Negative Control					
Experiment Date	Construct	No. Explants	No. Regen	No. T1 Seed	No. NPTII +ve	No. Explants	No. Callus	% Callus	No. Shooting Callus	% Shooting Callus	
26-Oct-94	35S-SPS	80	0	0	0	60	17	28	0	0	
20-Dec-94	35S-SPS	60	0	0	0	50	nd	nd	10	20	
14-Feb-95	35S-SPS	70	0	0	0	nd	nd	nd	nd	nd	[a]
11-Mar-95	35S-SPS / 35S-GUS	120	0	0	0	50	nd	nd	33	66	[b]
28-Mar-95	35S-SPS / RbcS-GUS	100	0	0	0	45	40	89	23	51	
29-Mar-95	35S-SPS / RbcS-GUS	100	0	0	0	37	37	100	11	30	
6-May-95	35S-GUS	200	14	5	3	40	38	95	25	63	[c]
29-May-95	35S-S158	180	2	1	1	50	50	100	39	78	
12-Jun-95	RolC-AS	260	5	2	2	50	48	96	30	60	
4-Jul-95	35S-S158	180	22	2	1	60	56	93	45	75	[d]
19-Jul-95	RolC-AS	140	86	25	11	nd	nd	nd	nd	nd	
25-Sep-95	35S-S158	160	2	2	2	30	29	97	25	83	
3-Nov-95	35S-S158	220	28	10	6	37	37	100	24	65	
19-Dec-95	35S-S158	180	1	0	0	30	28	93	21	70	
16-Jan-96	35S-S158	200	0	0	0	40	39	98	35	88	
24-Apr-96	RbcS-SPS	210	315	18	7	30	29	97	22	73	
6-May-96	RbcS-SPS	210	120	8	1	30	30	100	16	53	
Totals		2670	595	73	34	639	478	91	359	56	

shoots were counted. As results became available from tissue culture optimization experiments, improvements were incorporated into the transformation protocol. With multiple improvements, regeneration from control plates reached a consistently high level by 6 May 1995 (Table 4.2). The first shoots to regenerate under kanamycin selection were also from explants cocultivated on this date. The regeneration frequency from selection was quite variable in the subsequent ten experiments. This variability did not seem to correlate with regeneration frequencies on control plates. Of 595 regenerated shoots (including multiple shoots from same callus), 489 (82 %) were discarded because they died on selection or showed kanamycin sensitivity symptoms, 5 (0.8 %) became contaminated with fungus, 20 (3.4 %) died in soil, 8 (1.3 %) were infertile and 73 (12 %) produced seed.

T_0 SCREENING

T_0 plants surviving on selection medium tested either positive or negative for NPTII enzyme activity (Table 4.2). A total of 168 regenerated shoots were tested for NPTII activity and 62 were tested on more than one occasion. Contradictory results were found for 15 of these plants. Fourteen plants initially tested positive but tested negative at a later date. Only one plant produced a positive result after initially testing negative. The unreliability of the dot blot assay resulted in all healthy-looking plants being maintained regardless of NPTII results.

DISCUSSION

The purpose of this research was to produce canola plants transformed with genes designed to elevate enzyme activities at key points in the biosynthetic pathways of carbon and nitrogen transport compounds. *Agrobacterium* vectors were constructed, regeneration from cotyledonary petiole target tissue was improved and shoots were produced after *Agrobacterium* cocultivation and selection.

TRANSFORMATION VECTORS

Carbon is transported to sink tissues as sucrose and SPS partly regulates its synthesis (see Chapter 1). The choice of the SPS cDNA was important to maximize

the chances of producing plants which overexpress SPS. Two strategies were used in this research. First, a spinach SPS cDNA was used which had a single amino acid change within the phosphorylation site (Ser-158 to Ala). SPS phosphorylation (post-translational modification) inactivates enzyme activity (Huber et al., 1989; Huber and Huber, 1992) and its prevention could enable SPS to remain active at all times. Second, a SPS cDNA from the monocotyledonous species maize was chosen because its sequence is divergent from dicotyledonous species and would reduce the chances of cosupression (Fig. 4.13). Overexpression of maize SPS in tomato (*Lycopersicon esculentum* Mill.) led to notable changes in leaf carbon partitioning and whole plant performance (Worrell et al., 1991; Galtier et al., 1993; Galtier et al., 1995; Micallef et al., 1995; Foyer and Galtier, 1996). SPS constructs were used with either a constitutive or tissue-specific promoter. RbcS promoters direct expression in photosynthetic cells where fixed carbon is synthesized into sucrose (Stitt et al., 1987).

Glutamine and asparagine are major transport forms of nitrogen (see Chapter 1). Manipulation of asparagine synthesis by overexpressing asparagine synthetase (AS) was chosen because glutamine feeds into many amino acid pathways whereas asparagine synthesis is a terminal pathway. An AS cDNA was used from the monocotyledonous species rice. Of the publicly-available plant AS sequences, rice AS is the most dissimilar to canola's close relative *B. oleracea* having 68 percent nucleotide identity within the coding region (Fig. 4.14). AS1 gene expression has been localized to vascular tissue in pea (Tsai, 1991) consequently the rice cDNA was cloned behind the phloem-specific *rolC* promoter from *Agrobacterium rhizogenes*. Constitutive overexpression of pea AS1 in tobacco led to 40-fold increases in leaf asparagine and decreases in its substrates, aspartate and glutamine (Brears et al., 1993).

TISSUE CULTURE AND TRANSFORMATION PROCEDURES

To introduce the gene constructs, *Agrobacterium tumefaciens*-mediated transformation of cotyledonary petioles was chosen. The method published by Moloney et al. (1989) yielded high numbers of transgenic shoots without stringent technical requirements. This simplicity should make the technique reproducible,

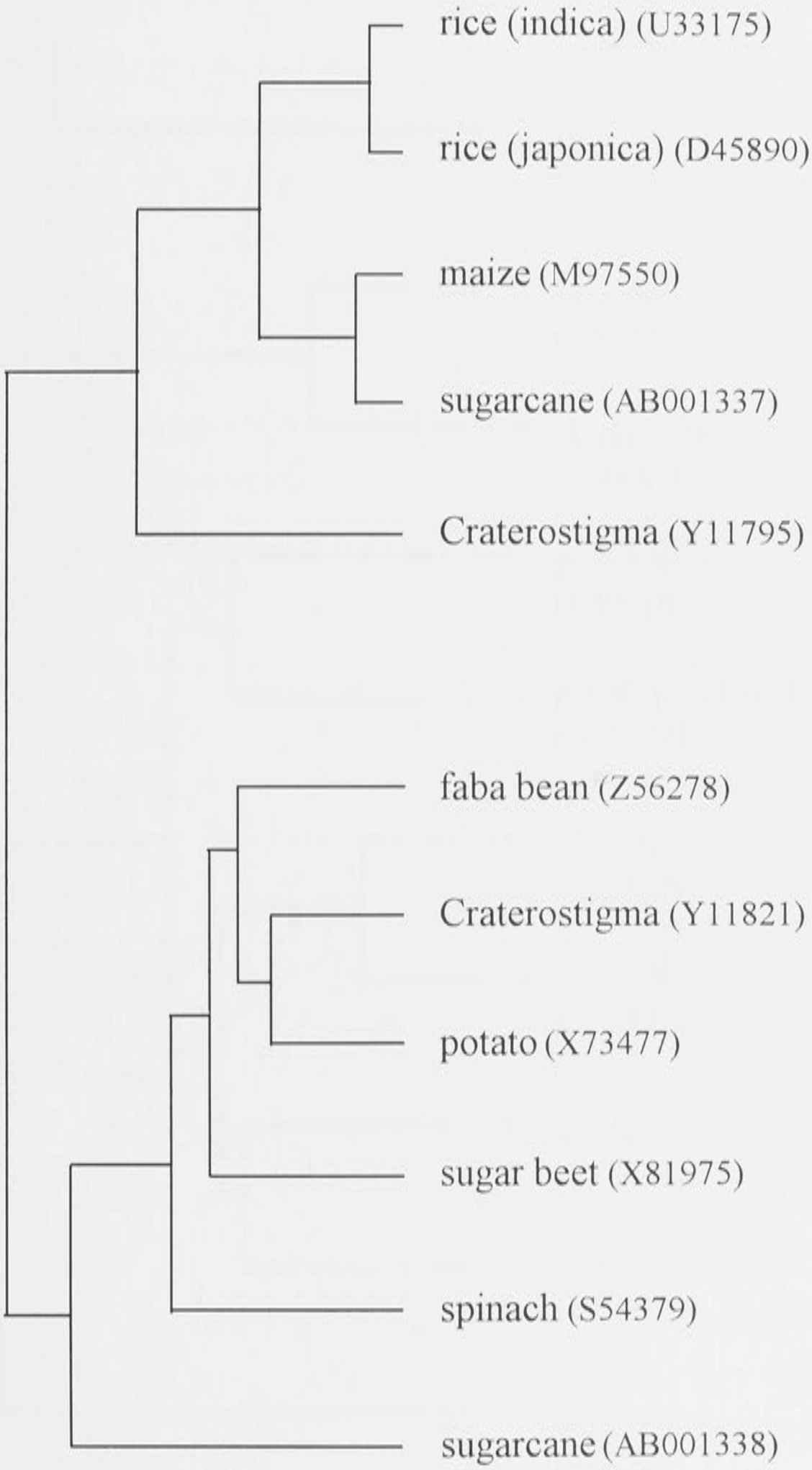

Figure 4.13. Dendrogram of plant sucrose-phosphate synthase (SPS) clones. Relationships of translated sequences were generated by the PILEUP command of Genetics Computer Group software (Madison, WI). Each species name is followed by its GenBank accession number.

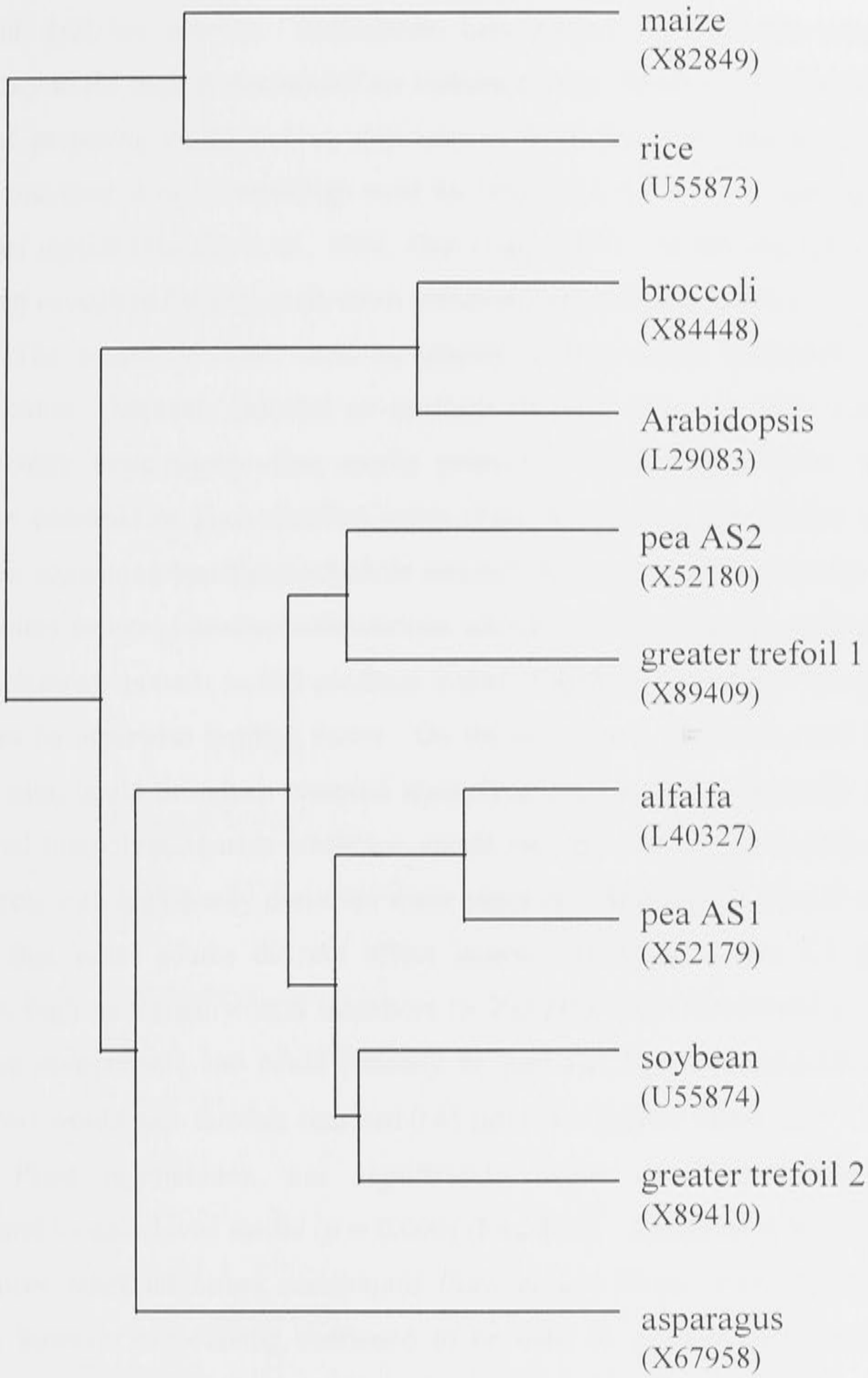

Figure 4.14. Dendrogram of full-length plant asparagine synthetase clones. Relationships of translated sequences were generated by the PILEUP command of Genetics Computer Group software (Madison, WI). Each species name is followed by its GenBank accession number.

however initial attempts to regenerate shoots from cotyledonary petioles failed (Fig. 4.6 and data not shown). Subsequent experiments improved the regeneration frequency to the high levels needed for transformation. Seedling development at the time of preparing explants is a very critical factor for regeneration. Under the conditions used, 4 to 5 d seedlings were the best (Figs. 4.7 and 4.8) and agrees with previous reports (Hachey et al., 1991; Ono et al., 1994). At this age, petioles were just long enough to cut separately from meristem cells at the hypocotyl.

The source of water used to prepare culture media profoundly affected regeneration. Explants cultured on medium prepared with tap water regenerated significantly more shoots than media prepared with MilliQ filtered, deionized (reverse osmosis) or glass distilled water (Figs. 4.11 and 4.12). Either tap water contains something beneficial which is retained by the various purification systems or the other sources introduce a deleterious substance. The abundance of macro- and micro-elements present in MS medium makes it difficult to believe that tap water contains an otherwise limiting factor. On the other hand, apparatus used for water purification could introduce bacterial lipopolysaccharides if not regularly cleansed. Bacterial lipopolysaccharide inhibition would only be evident in locations, such as Canberra, with high-purity domestic water supplies. Although Davies et al. (1989) found that water source did not affect lucerne (*Medicago sativa* L.) protoplast culture, high molecular weight inhibitors (> 200 kDa) were discovered in stocks of medium components and could possibly be bacterial lipopolysaccharides. These inhibitors would pass through standard 0.45 μm tissue culture filters.

Plant regeneration was significantly higher on filter-sterilized media compared to autoclaved media ($p = 0.046$) (Fig. 4.12). Autoclaving therefore likely introduces other inhibitory compounds (Sawyer and Hsiao, 1992; Schenk et al., 1991), however autoclaving continued to be used to sterilize media because the magnitude of the filter sterilization benefit did not warrant the added expense.

TDZ is a potent cytokinin that has been used successfully in a number of culture systems (Malik and Saxena, 1992; Huetteman and Preece, 1993; Murthy et al., 1996a,b; Tosca et al., 1996). It was therefore tested as an alternative to BA for canola cotyledonary petioles. An equivalent number of calluses produced shoots on TDZ- and BA-containing media (Fig. 4.7). The observation that explants cultured on

TDZ media seemed to survive longer is a trait important for transformation because selection lengthens regeneration time. TDZ use in selection medium did not appear to be beneficial because more escapes were produced without an increase in shoots reaching maturity (Table 4.1). BA was consequently used in all subsequent experiments.

Further changes were made to the Moloney et al. (1989) procedure. First, deep-dish plates (100 x 20 mm) were used and were wrapped with Micropore tape. This permeable tape allows for better gas exchange and combined with the larger plate volume decreases humidity (De Block et al., 1989). Second, Phytagel was used as the medium gelling agent instead of purified agar in later experiments. Increased culture performance on Phytagel-based media compared to agar-based media has been documented (Tremblay and Tremblay, 1991; Van Ark et al., 1991; Yadav et al., 1996). Third, in spite of unconvincing data *Agrobacterium* cultures were diluted without centrifugation and explants were cut with a scalpel blade wetted with *Agrobacterium*.

T_0 REGENERATION AND SCREENING

The improved shoot regeneration frequencies undoubtedly increased the probability of regenerating transformed shoots. After culture parameter modification, shoots regenerated from explants cocultivated with *Agrobacterium*. As documented in Table 4.2, the number of explants forming on selection medium was highly variable even though control plates had relatively consistent regeneration. It is possible that the window for successful transformation is narrower than the regeneration window. From 14 Feb 1995, seedling age at the time of cocultivation varied from 94 to 121 h but transformation success did not seem to correlate with absolute time. The optimal time will surely vary with season because seeds will germinate and develop at different rates. Petiole length is a more precise indicator for staging than seedling age.

The vast majority of shoots regenerated from selection were escapes (Table 4.2). Instead of showing the kanamycin sensitivity symptoms of white leaves with purple pigmentation (Schröder et al., 1994), most shoots died after a number of subculture rounds. Similar to other reports (Fry et al., 1987; Pua et al., 1987,

Schröder et al., 1994), the large number of escapes suggests ineffective kanamycin selection. The *nptII* resistance gene was under the control of the *nos* promoter in all constructs (Figs. 4.1, 4.3 and 4.5) which does not give particularly strong expression (Sanders et al., 1987). As well, selection medium initially contained 15 or 20 μg mL^{-1} kanamycin, a low concentration, but was increased to 50 μg mL^{-1} kanamycin once shoots had formed. This higher selection pressure was ineffective on shoots that already had 2 to 3 true leaves when transferred. Raising the initial selection pressure seems to be logical advice even though 15 or 20 μg mL^{-1} kanamycin was high enough to prevent regeneration from uncocultivated explants on selection medium. In addition, stringent biweekly subcultures to fresh selection medium are necessary because delaying subculture or using media prepared days earlier can allow shoots to regenerate due to kanamycin breakdown near the end of a subculturing round. Once shoots formed it was difficult to kill escapes.

An effective screen of T_0 plants would decrease the labour needed to maintain escapes. A quick and easy NPTII dot blot assay was used but the integrity of the results was suspicious. In contrast to other species used in this laboratory, canola extracts did not give a strong signal. Using protease inhibitors, larger tissue samples and changing washing conditions did not alleviate the problem (data not shown). A substance contained in canola extracts was not responsible for poor signals because the signal in a NPTII-positive *Flaveria bidentis* extract was not diminished when canola extract was mixed with it (data not shown). A number of canola regenerants that were tested on multiple occasions produced conflicting results. Curiously, all but one of these plants tested NPTII-positive initially and then later tested NPTII-negative. It is unknown whether these contradictory results are due to loss of *nptII* expression, patchy expression or simply because of assay problems. As a consequence, shoots that remained healthy in culture and in soil were taken to maturity regardless of NPTII results. A total of 73 shoots reached maturity of which 34 tested NPTII-positive at least once. Seed was collected from these mature plants.

CONCLUSION

Transgenic canola plants were produced after *Agrobacterium tumefaciens*-mediated transformation of cotyledonary petiole explants. The adaptation of a published protocol was not straight-forward and required modification. Alteration of tissue culture conditions greatly improved shoot regeneration frequencies and allowed the recovery of shoots from selection medium. The most critical factors were using 4 day-old seedlings for explants and using tap water to prepare media. A large number of escapes were regenerated from cocultivated explants on kanamycin selection medium. Future work should consider increasing the kanamycin concentration during callus induction or using an alternate selectable marker gene. A NPTII dot blot assay was an imperfect method to cull escapes because results were not always consistent. With the large number of escapes, screening by more time-consuming methods, such as Southern analysis, was deemed to be an unacceptable use of limited time. As well, screening T_0 plants for activity of the genes of interest would likely have been inconclusive because seedling growth was adversely affected by the culturing process thereby making reliable detection of enzyme activities significantly different from wild-type levels unrealistic. Instead, screening was conducted by germinating T_1 seed on kanamycin-containing medium (see Chapter 5). Although transformation frequencies fell well short of those reported by Moloney et al. (1989), they are comparable with other labs (C. Jones, John Innes Centre and D. Schulze, Pioneer Hi-Bred, personal communications). The protocol does not require extensive technical expertise or labour and is relatively genotype-independent (Ono et al., 1994). Only minor modifications should be needed to adapt it to Australian genotypes.

CHAPTER 5: ANALYSIS OF TRANSGENIC PLANTS

INTRODUCTION

The molecular alteration of enzymes involved in the biosynthesis of carbon and nitrogen transport compounds offers a powerful method of understanding the biochemical regulation of source-to-sink relations. As well, there is potential for the economic benefits of increased crop performance if the alterations are properly targeted. In tomato, overexpression of SPS resulted in increased photosynthetic capacity, increased sucrose partitioning in source tissues and an increased number of fruits (Worell et al., 1991, Galtier et al., 1993, Micallef et al., 1995, Galtier et al., 1995). In tobacco, overexpression of AS shifted the leaf amino acid composition towards asparagine, a transportable amino acid that conserves carbon (Brears et al., 1993). The parallel approaches of individually altering carbon and nitrogen assimilate supply can be combined in the long-term to study the interactions of these inter-related processes.

The objectives of this chapter were to confirm transformation in the plants produced after *Agrobacterium* cocultivation with SPS and AS overexpression gene constructs (see Chapter 4) and to conduct a preliminary biochemical and physiological assessment of effects in T_1 progeny. Once key traits have been identified, attention can be focussed for a more thorough and rigorous analysis of the regulation of source-to-sink assimilate provision.

MATERIALS AND METHODS

SEED GERMINATION ON KANAMYCIN

Approximately 20 seeds per T_0 line (ie. T_1 seed) were surface-sterilized and germinated on MS selection medium (see Chapter 4) containing 3 % (w / v) sucrose and 75 mg L^{-1} kanamycin sulphate (Sigma, St. Louis, MO). After two weeks,

seedlings showing any purpling or bleaching were scored as susceptible to kanamycin and seedlings without these symptoms were scored as resistant.

PLANT MATERIALS AND NPTII DOT BLOT

A few transgenic lines were selected for growth analysis. Ten seeds from each selected line were planted in a compost and perlite soil mix (1:1, v / v) and grown in a naturally-illuminated glasshouse with daily liquid nutrient and temperatures set at 23 °C / 15 °C day / night. Established seedlings were given an identification number and a 1.33 cm^2 leaf disc was sampled from each plant and tested for expression of *nptII*. The dot blot procedure described in Chapter 4 was modified to be more representative of the original protocol (McDonnell et al., 1987) by increasing DTT to 50 mM in the extraction buffer and $MgCl_2$ to 42 mM in the reaction mix. After Phosphorimager scanning of the blots, relative dot strengths were quantified using ImageQuant software (Molecular Dynamics, Sunnyvale, CA).

DNA EXTRACTION AND SOUTHERN BLOTTING

DNA extraction. Genomic DNA was isolated from leaf samples taken from T_0 plants and stored at -80 °C. Samples were ground in liquid nitrogen and the powder was transferred to 18 mL cell lysis solution containing 10 mM Tris-HCl, pH 8.0, 1 mM EDTA and 1 % (w / v) SDS. Samples were incubated at 65 °C for 1 h then cooled to room temperature before the addition of 90 µL RNase A. After a 15 min incubation at 37 °C, proteins were precipitated by adding 6 mL 6 M NH_4-acetate, vortexing vigorously and centrifuging at 3 000*g* for 10 min. As a further purification, 12 mL phenol:chloroform (1:1, v / v) was added to the supernatant, the solution was vigorously vortexed and then centrifuged. The aqueous phase was transferred to a fresh tube containing 18 mL ice-cold isopropanol. The precipitated DNA was pelleted by a 5 min centrifugation at 3 000*g*. After removal of the supernatant, the DNA pellet was washed with 18 mL 70 % (v / v) ethanol. After centrifugation and supernatant removal, the pellet was dried in a vacuum desiccator for 5 min. DNA was resuspended in 200 µL TE by incubation in a 65 °C water bath for 5 min. DNA concentrations were determined by measuring the absorbance at 260 nm and using the conversion factor of 50 µg DNA mL^{-1}.

Southern blotting. Where available, 10 µg DNA was digested with EcoRI (NEB, Beverly, MA) overnight at 37 °C. The resulting fragments were separated using 1 % agarose gel electrophoresis and the DNA was then capillary transferred to a GeneScreen Plus membrane (DuPont NEN, Boston, MA) using the alkali transfer method (Sambrook et al., 1989). Membranes were pre-hybridized for at least 10 h at 65 °C in a solution containing 50 mM Hepes, 3 x SSC, 1 % (w / v) SDS, 0.2 % (w / v) Ficoll, , 0.2 % (w / v) BSA, 0.2 % (w / v) PVP and 18 mg L^{-1} sheared herring sperm DNA. The hybridization solution was the same except 10 % (w / v) dextran sulphate and a ^{32}P-labelled DNA probe was added (see below). After hybridization for at least 6 h at 65 °C, membranes were washed once in 2 x SSC at room temperature for 2 min, once in 2 x SSC at 65 °C for 20 min, once in 1 x SSC at 65 °C for 20 min, and once in 0.5 x SSC, 0.1 % (w / v) SDS at 65 °C for 20 min (gene copy number blot only). Washed membranes were placed in a Phosphor Screen for 1 to 4 d before Phosphorimager scanning.

Probe preparation. Gel-purified DNA fragments were used to prepare ^{32}P-labelled probes for hybridizations. A full-length 3.9 kb spinach SPS cDNA (GenBank S54379) was used to screen S158A-cocultivated transformants and a full-length 2.2 kb rice AS cDNA (GenBank U55873) was used to screen AS-cocultivated transformants. To determine gene copy number, both S158A- and AS-cocultivated transformants were probed with a 387 bp NcoI / PstI *nptII* fragment (GenBank V00618). These fragments were used as templates in random priming labelling reactions using a Ready-To-Go dCTP labelling kit (AMRAD Pharmacia, Sydney, NSW) and 50 µCi α^{32}P-dCTP (Amersham, Sydney, NSW). After a 1 h incubation at 37 °C, DNA-incorporated radiolabel was separated from unincorporated radiolabel using a Sephadex G-50 spin column. Probes were denatured for 2 to 3 min at 100 °C before addition to hybridization solutions.

RNA EXTRACTION AND NORTHERN BLOTTING

RNA extraction. Total RNA was isolated from expanding leaves (1 g fresh weight) taken from *rolC*-AS T_1 plants and quickly frozen in liquid nitrogen. Standard precautions were taken to prevent RNA degradation. Samples were ground to a fine powder in liquid nitrogen and then homogenized in 2 volumes NTES (0.1 M

NaCl, 10 mM Tris, pH 8.0, 1 mM EDTA, 1.0 % (w / v) SDS) and 3 volumes phenol:chloroform (1:1, v / v). The homogenate was centrifuged at 10 000*g* for 10 min. The aqueous phase was transferred to a fresh tube and mixed with 0.1 volume of 20 % (w / v) Na-acetate, pH 5.5, before adding 2 volumes ice-cold ethanol. Nucleic acids were allowed to precipitate for at least 30 min at 4 °C before centrifugation at 10 000*g* for 10 min. The supernatant was poured off and the pellet was resuspended with 2 mL sterile dH_2O before adding an equal volume of 4 M LiCl. After mixing, the tubes were left at 4 °C overnight to fully precipitate the RNA. After centrifugation at 10 000*g* for 10 min and removal of the supernatant, pellets were dissolved with 0.5 mL sterile dH_2O and RNA was reprecipitated with 2 volumes of ethanol for at least 1 h at 4 °C. The RNA was again collected by centrifugation and the pellet was washed with 80 % (v / v) ethanol before a final resuspension in sterile dH_2O. RNA concentrations were determined by measuring the absorbance at 260 nm and using the conversion factor of 40 µg RNA mL^{-1}.

Northern blotting. RNA fragments (10 µg per lane) were separated using denaturing formaldehyde-agarose gel electrophoresis (Sambrook et al., 1989). As positive controls, RNA isolated from light-grown and etiolated rice seedlings were included (courtesy Graham Scofield, CSIRO Plant Industry). Separated RNA was blotted to a GeneScreen Plus membrane, pre-hybridized and hybridized as described above for *Southern blotting*. The only difference was that 50 mM NaOH was substituted for 0.4 M NaOH during the alkaline capillary transfer. The membrane was probed with the full-length AS cDNA described above for *Probe preparation*. After hybridization, the membrane was washed once in 2 x SSC at room temperature for 2 min and then through a series of single washes containing 0.1 % (w / v) SDS at 65 °C for 20 min; 2 x SSC, 1 x SSC, 0.5 x SSC, 0.1 x SSC. The blot was exposed to a Phosphor Screen for 1 d before Phosphorimager scanning and ImageQuant quantification.

SPS ASSAYS

Leaf, silique wall and seed tissues from 35S- S158A T_1 lines were assayed for SPS activities and compared with untransformed plants. Samples from young fully-expanded leaves were taken mid-morning 35 d after planting and quickly

frozen in liquid nitrogen before storage at -80 °C. A second complete set of leaf samples was taken 12 d later. Although all seeds were planted on the same day, plants flowered at different times. Assuming that developmental stage affects SPS V_{max} more than environmental effects, silique samples were taken over a 10 day period when plants were 28 to 40 DAFF. Regardless of sample date, 26 DAA siliques were quickly harvested in the mid-morning and were immediately frozen in liquid nitrogen.

For assays, all tissues were ground in extraction buffer (see Chapter 2) but BSA and Triton X-100 were omitted to allow protein determination. Leaf extracts were desalted by passage through a Sephadex column and assayed in duplicate as described in Chapter 2. Extract protein concentrations were determined from a Bradford assay kit using γ-globulin as a standard (Bio-Rad, Hercules, CA).

As a result of high absorbances in blank samples using the anthrone SPS assay and low sucrose production rates, silique wall and seed samples were assayed using a radiometric procedure. Silique samples were gently crushed under liquid nitrogen to separate silique wall from seed tissues. From a single sample, two silique wall and two seed extracts were prepared. Extracts were not desalted and 50 µL of extract was immediately used in reactions containing 22.5 mM [^{14}C]Fru-6-P pre-equilibrated with phosphoglucoisomerase (EC 5.3.1.9) and 20 mM UDP-Glc in a total volume of 100 µL. The reactions were stopped after 10 min at 25 °C by boiling for 5 min. Pre-boiled extract was used as a control reaction. Sugars in the reactions were dephosphorylated by treating with 3.5 U alkaline phosphatase (Boehringer) overnight at 40 °C. A 20 µL aliquot of each reaction and 10 µL of a marker mixture containing 2 % (w / v) Suc, 1.5 % (w / v) Glc, and 1.5 % (w / v) Fru were spotted onto paper chromatograms (Whatman 3MM) and were run for 25 h in ethyl acetate:pyridine:dH_2O (8:2:1, v / v) to separate sucrose from hexoses. The sucrose location was determined by dipping the strips containing the marker mixture in 1 % (v / v) H_3PO_4 in acetone followed by 0.5 % (v / v) *p*-anisidine and 0.5 % (v / v) aniline in chloroform. The strips were then developed at 100 °C. The region corresponding to the sucrose peak was cut out from the reaction strips and placed in 1 to 2 mL dH_2O to solubilize the sucrose. Scintillation fluid was added and ^{14}C was counted in a liquid scintillation counter.

CARBOHYDRATE CONTENTS

Silique wall and seed tissues from 35S- S158A T_1 lines were assayed for carbohydrate contents and compared with untransformed plants. Intact 26 DAA siliques were harvested at dusk, on the same or the next day as the SPS samples described above, and immediately frozen in liquid nitrogen before storage at -80 °C until analysis. Two silique wall and two seed extracts were prepared from each sample. The boiling ethanol extraction and spectrophotometric sugar and starch assay procedures were as described in Chapter 2.

SEED YIELD AND WEIGHT

The seed produced from 35S- S158A T_1 lines was harvested 143 to 144 d after planting (81-105 DAFF). Immature seed-bearing racemes that appeared late because of the daily nutrient regime were not included in the analysis. Harvested seeds were allowed to dry to final moisture contents in the laboratory for one week before total seed weight per plant and triplicate samples of 100 seeds were weighed from each line.

RESULTS

A large number of plants were regenerated from selection media after *Agrobacterium* cocultivation with overexpression gene constructs designed to perturb the synthesis of carbon and nitrogen transport compounds (**see Table 4.2**). Before the extent of these perturbations could be assessed it was necessary to confirm transgene incorporation in the regenerated shoots. Seeds produced from each primary transformant (T_1 seed) were germinated on medium containing 75 mg L^{-1} kanamycin, a concentration previously determined to produce purpling and bleaching susceptibility symptoms in the first true leaves of 88 % of untransformed seedlings. Individual progeny were scored as kanamycin-resistant or -susceptible and a population average was calculated for each T_1 line. A number of lines had high resistance averages, indicative of expression of the introduced *nptII* kanamycin resistance gene, and were chosen for further analysis (Fig. 5.1, **gray bars**).

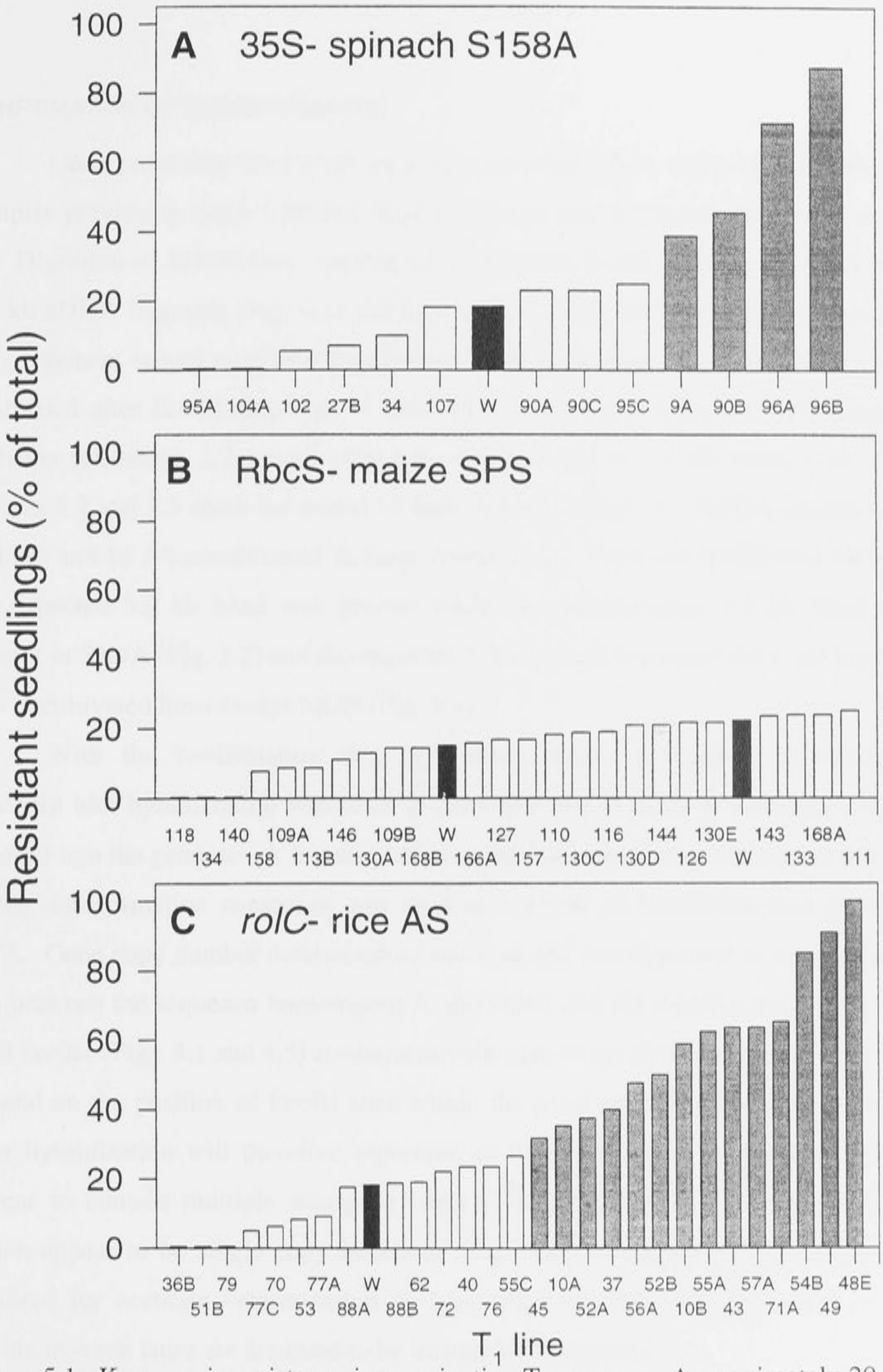

Figure 5.1. Kanamycin resistance in germinating T_1 progeny. Approximately 20 T_1 seeds from each primary transformant were germinated on MS medium containing 75 mg L^{-1} kanamycin sulphate and seedlings were scored for sensitivity symptoms after two weeks. Plotted values represent mean numbers of resistant seedlings within each T_1 segregating population. Resistance in untransformed seedlings is represented by black bars (W) and T_1 lines chosen for further analysis are represented by dark gray bars. SK- prefixes have been omitted from all labels.

CONFIRMATION OF TRANSFORMATION

Once promising lines were identified, genomic DNA was isolated from leaf samples previously taken from the original primary transformants and stored at -80 ^{o}C. Digestion of 35S-S158A - cocultivated lines with EcoRI releases the full-length 3.9 kb cDNA fragment (Fig. 4.1) and hybridization with the ^{32}P-labelled full-length SPS fragment would confirm the presence of the transgene. Confirmation can be confirmed after EcoRI digestion of *rolC*-AS - cocultivated lines and hybridization with the full-length 2.2 kb AS cDNA by the presence of 1.3 kb bands (Fig. 4.5). Figures 5.2 and 5.3 show the results of these hybridization for 3 S158A-cocultivated T_0 lines and 14 AS-cocultivated T_0 lines, respectively. For both SK90B and SK96A, the expected 3.9 kb band was present while an approximately 4.4 kb band was present in SK9A (Fig. 5.2) and the expected 1.3 kb bands were present in all lanes of AS- cocultivated lines except SK45 (Fig. 5.3).

With the confirmation that regenerants were successfully transformed, Southern blot hybridization was used to determine the number of transgene copies inserted into the genome. A fragment of the *nptII* kanamycin resistance gene present in the transformation constructs was used as a probe of EcoRI-digested genomic DNA. Gene copy number determination relied on the fact that there is not an EcoRI site between the sequence homologous to the probe and the *Agrobacterium* T-DNA right border (Figs. 4.1 and 4.5) consequently the size of the hybridizing fragment will depend on the position of EcoRI sites within the plant genome. Each band visible after hybridization will therefore represent an individual copy. Most tested lines appear to contain multiple transgene copies, except SK9A and possibly SK57A which appear to be single copy insertions (Fig. 5.4). Complete DNA digestion is required for accurate determination of gene copy number and the fainter bands visible in some lanes are assumed to be incompletely digested.

TRANSGENE EXPRESSION AND ACTIVITY

Several transformants having high numbers of progeny expressing the *nptII* transgene (Fig. 5.1) were chosen for growth analysis. Ten T_1 seeds from each chosen

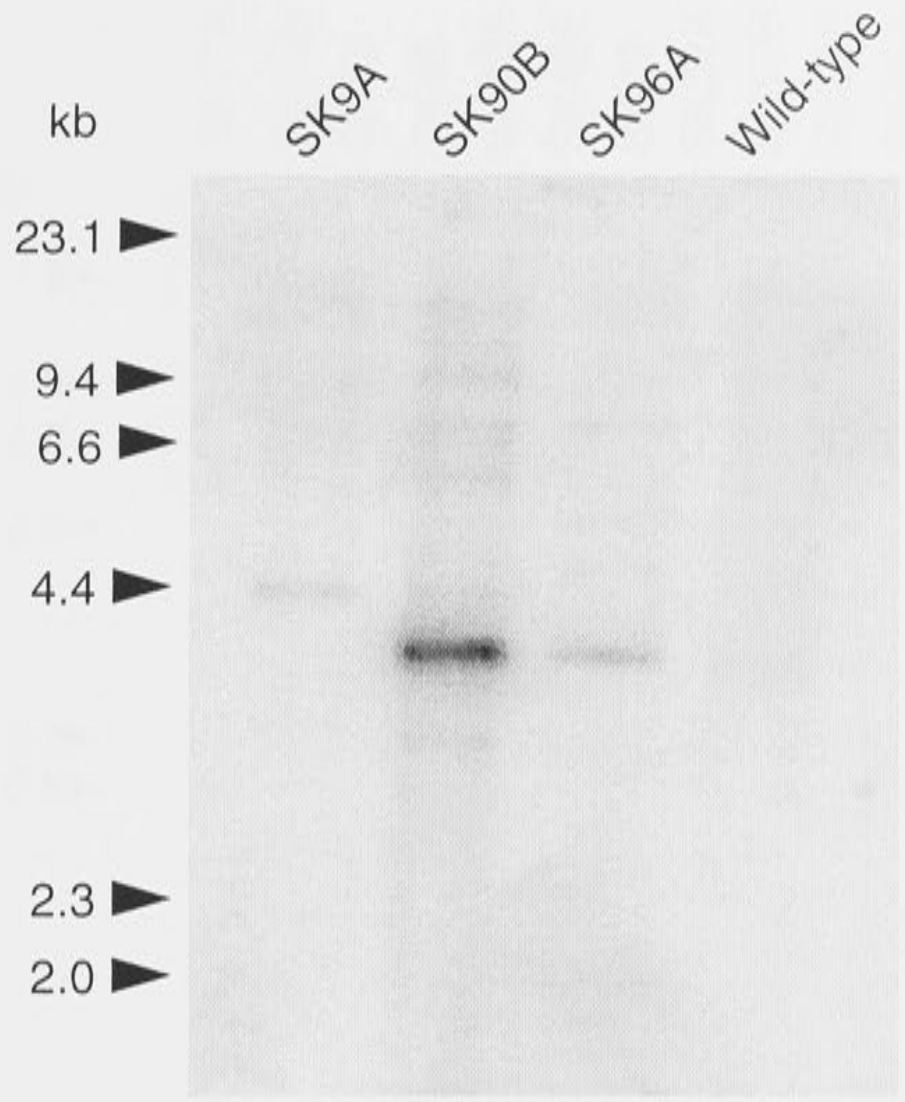

Figure 5.2. Detection of the S158 transgene in primary transformants. Leaf genomic DNA (10 µg) was digested with EcoRI to release the full-length coding sequence (3.9 kb), electrophoresed in 1 % agarose, and transferred to a GeneScreen Plus membrane. Hybridization was with the full-length spinach SPS cDNA at 65 °C.

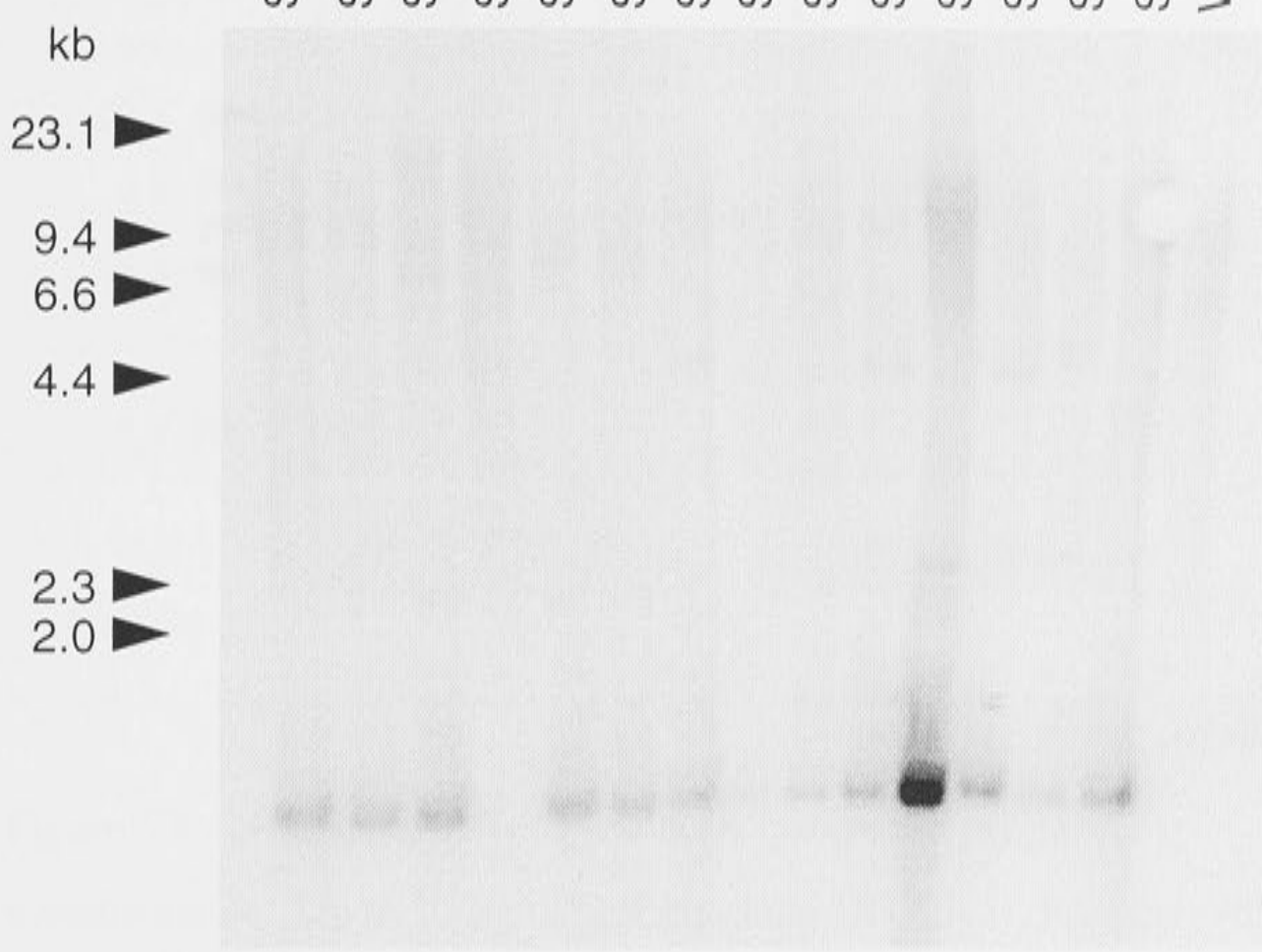

Figure 5.3. Detection of the AS transgene in primary transformants. Leaf genomic DNA (10 µg) was digested with EcoRI to release the coding and *nos* terminator sequences into two equally sized fragments (1.3 kb), electrophoresed in 1 % agarose, and transferred to a GeneScreen Plus membrane. Hybridization was with the full-length 2.2 kb rice AS cDNA at 65 °C.

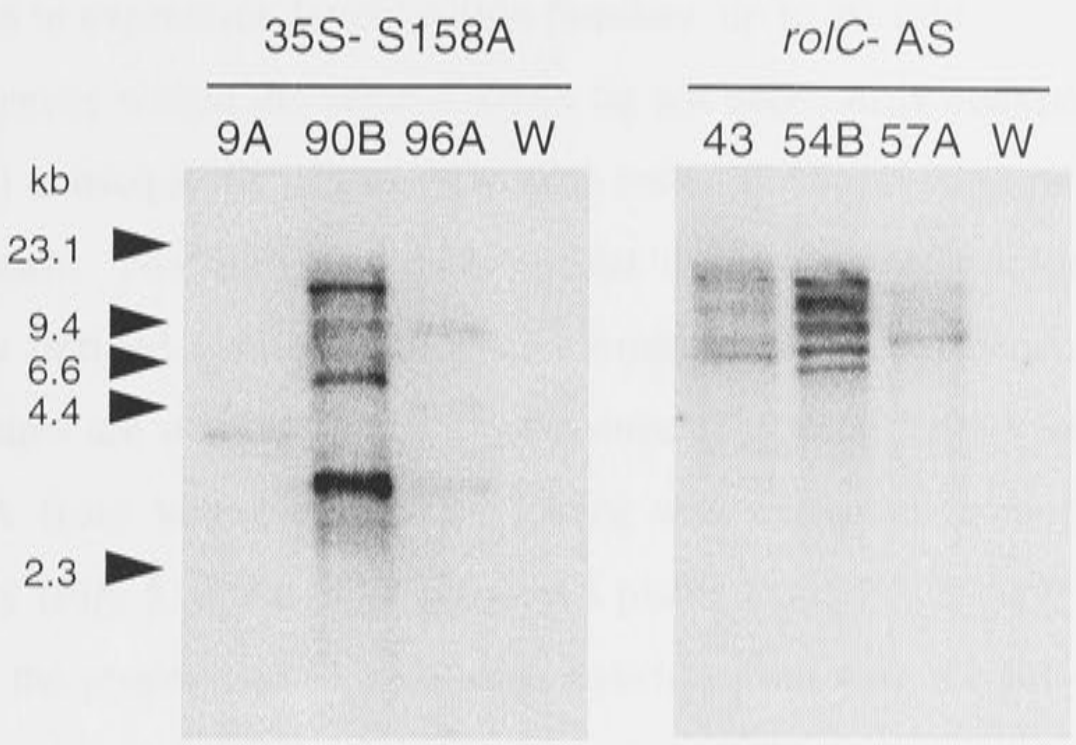

Figure 5.4. Determination of gene copy number in primary transformants. Up to 10 µg of leaf genomic DNA was digested with EcoRI, electrophoresed in 1 % agarose, and transferred to a GeneScreen Plus membrane. Hybridization was with a 387 bp *nptII* fragment at 65 °C and the blot was washed at high stringency (0.5 x SSC). DNA loadings were variable because of limited DNA quantities. W, wild-type.

line were planted in soil and all emerging seedlings were assayed for NPTII activity (Fig. 5.5). From this small sample size, it was not possible to calculate segregation ratios, however the high numbers of progeny expressing *nptII* within each family is consistent with independent multiple copy insertions (Fig. 5.4). There is clearly a wide variation in expression levels within families, up to 20-fold.

Transgenes within the same T-DNA do not necessarily coexpress (Peach and Velten, 1991) consequently plants were also tested for expression or activity of the genes of interest. Northern blot analysis was used to detect transgene expression from progeny derived from *rolC*-AS transformants (Fig. 5.6) because the enzyme assay procedures are unreliable and troublesome (Joy et al., 1983; Joy and Ireland, 1990). RNA from young expanding leaves was extracted from plants showing NPTII activity (Fig. 5.5B) and 3 of these 13 plants (nos. 22, 25, 39) had detectable transcripts of the proper size (2.2 kb) after hybridization with the full-length rice AS cDNA while no cross-hybridization to endogenous AS was detectable in any of the 6 wild-type samples (nos. 50 - 56). Transcript levels were, however, quite low compared to rice RNA from young seedlings (5 - 8 % of light-grown rice). Three plants which showed NPTII activity were not included in the northern analysis because the plants were too small (SK48E-16, SK49-23, SK57A-44).

For S158A transformants, total extractable SPS activity was assayed for all plants tested for NPTII activity (Fig. 5.5A) and one additional plant, designated SK9A-0, which was accidentally omitted from the NPTII assay. In young fully-expanded leaves, no SPS maximal activity differences on a protein basis between transformed and wild-type plants were apparent (Fig. 5.7A). Expression of the rates on a chlorophyll or surface area bases suggested that SK90B-7, 9 and SK96A-13, 14 were 29, 26, 46 and 66 % lower than wild-type while SK9A-6 and SK96B-16 activities were over 2-fold higher (Fig. 5.7B). In 26 DAA silique wall, each plant within SK9A and also SK96B-20 had higher SPS activities than wild-type; up to 3.6-fold (Fig. 5.8A). SK90B-8, SK96A-12, and SK96B-15 all had lower SPS activities than wild-type; 92, 92, and 51 % reductions. Expression of the rates on a chlorophyll basis did not change the relative levels. In 26 DAA seeds, some plants within each T_1 line had increased SPS activities (8.6-fold for SK96B-17) and no plants had

A 35S- S158A

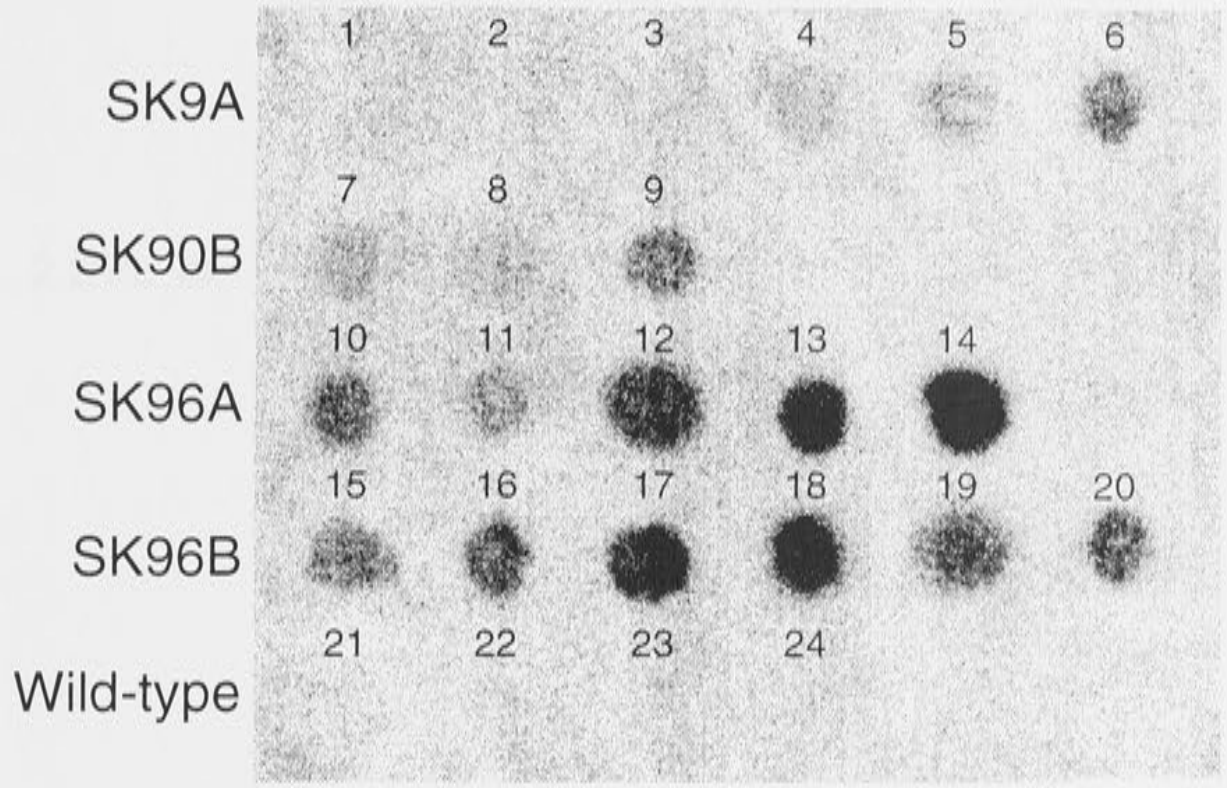

B *rolC*- AS

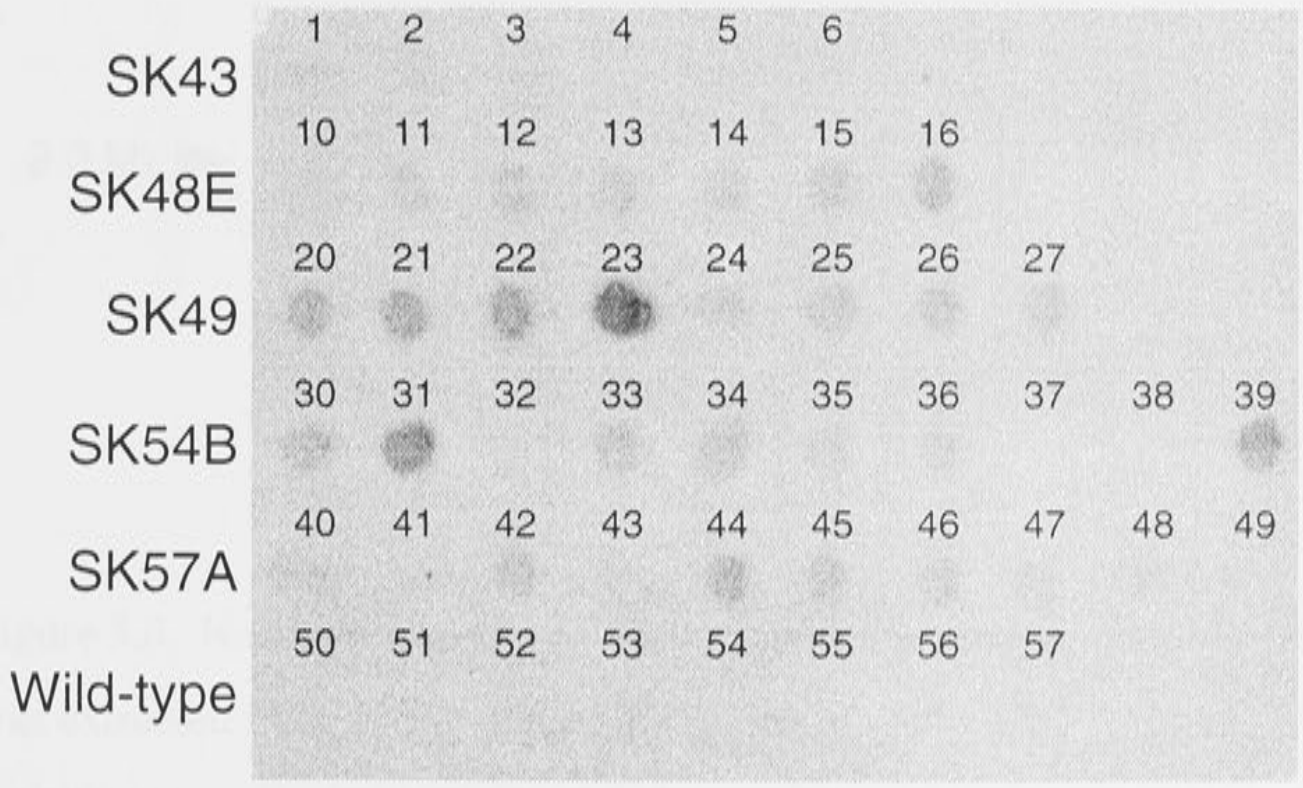

Figure 5.5. NPTII activities in the T_1 progeny of 35S- S158A (A) and *rolC*- AS (B) transformants. Leaf discs (1.33 cm^2) from each seedling emerging after the planting of 10 seeds per T_1 line was assayed using a NPTII dot blot procedure (McDonnell et al., 1987).

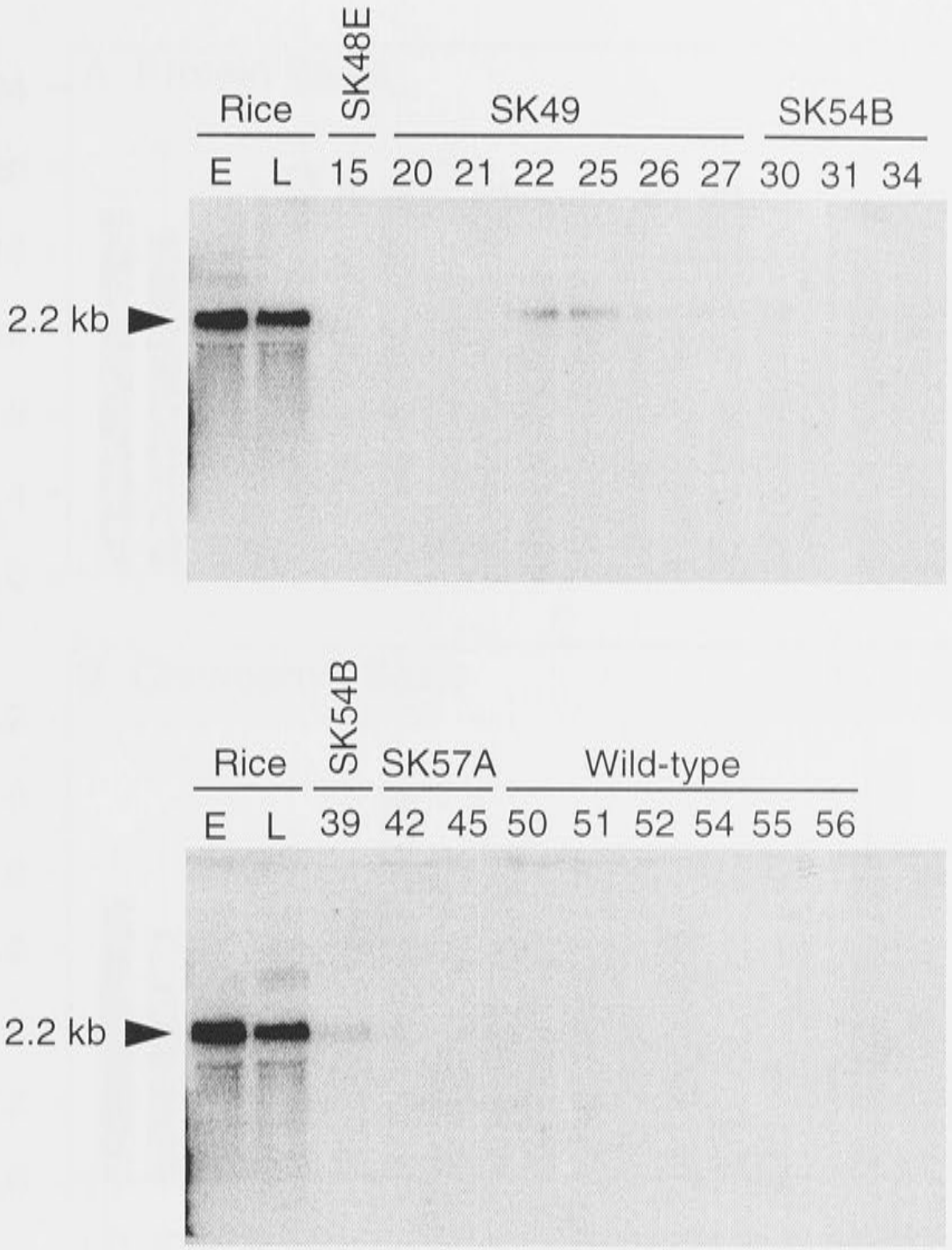

Figure 5.6. Northern analysis of AS transgene expression. Total RNA was extracted from young expanding leaves of *rolC*- AS T_1 progeny and 10 µg was loaded per lane and electrophoresed in denaturing agarose / formaldehyde gels before blotting to a GeneScreen Plus membrane. As positive controls, 10 µg RNA from etiolated (E) and light-grown (L) rice seedlings were included. Hybridization was with the 2.2 kb full-length rice AS cDNA at 65 °C followed by high stringency washing (0.1 x SSC).

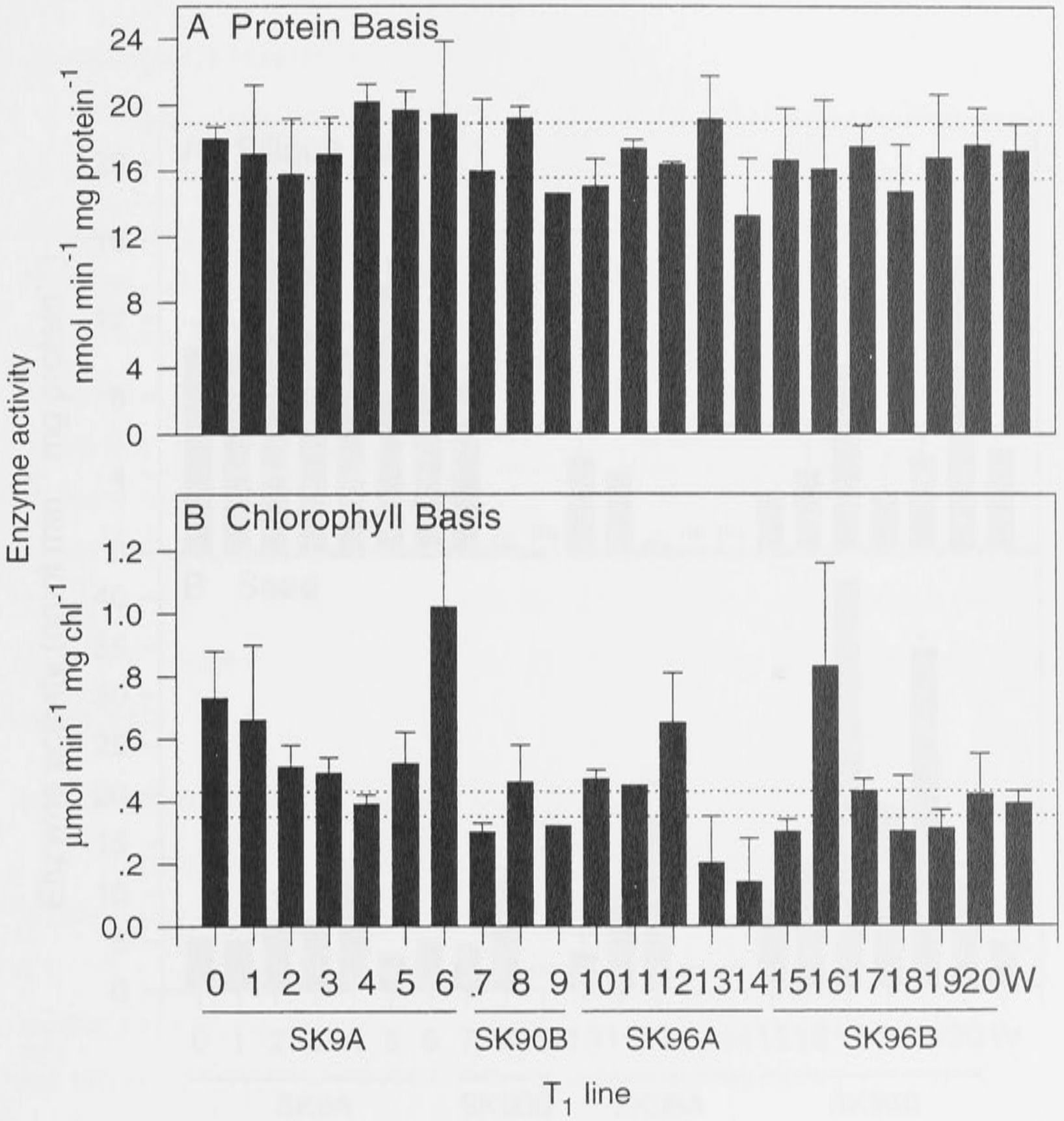

Figure 5.7. Total extractable SPS activities in T_1 progeny of 35S- S158A progeny. Mean values and standard errors from duplicate extracts are plotted for young fully-expanded leaves on a protein (A) and a chlorophyll basis (B). W, wild-type.

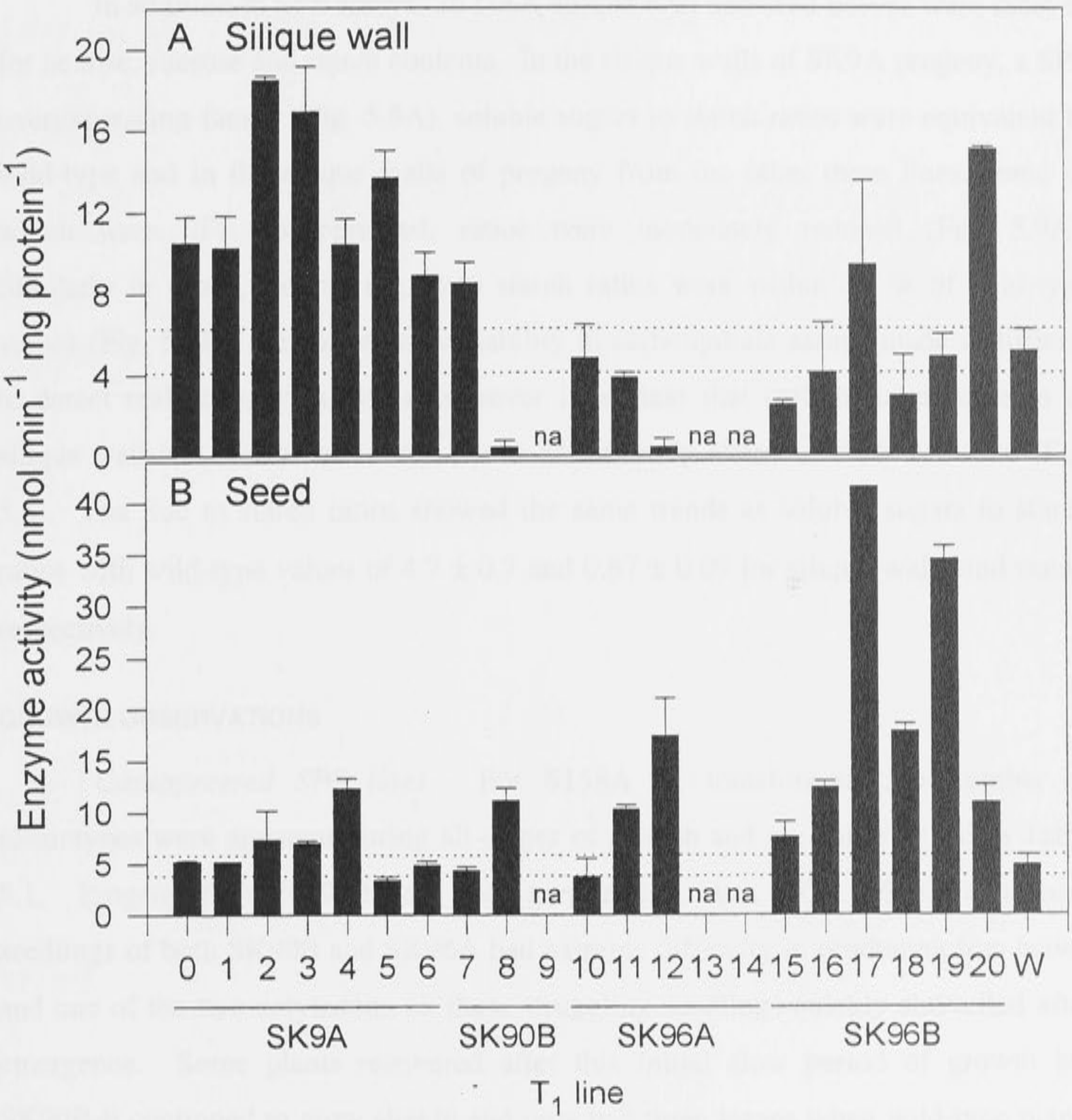

Figure 5.8. Total extractable SPS activities in T_1 progeny of 35S- S158A progeny. Mean values and standard errors from duplicate extracts are plotted for 26 DAA silique wall (A) and 26 DAA seed (B). W, wild-type; na, not available.

reduced SPS activities (Fig. 5.8B). Relative activities between plants were consistent when expressed per unit chlorophyll or per seed.

CARBOHYDRATE CONTENTS

In addition to SPS assays, 26 DAA silique wall and seed tissues were assayed for hexose, sucrose and starch contents. In the silique walls of SK9A progeny, a SPS overexpressing family (Fig. 5.8A), soluble sugars to starch ratios were equivalent to wild-type and in the silique walls of progeny from the other three lines, some of which were SPS cosuppressed, ratios were moderately reduced (Fig. 5.9A). Similarly in seeds, soluble sugars to starch ratios were within 50 % of wild-type values (Fig. 5.9B). The inherent variability in carbohydrate assays made it difficult to detect real changes in ratios, however it is clear that carbohydrate contents of silique wall and seed tissues were not as dramatically altered as SPS activities (Fig. 5.8). The Suc to starch ratios showed the same trends as soluble sugars to starch ratios with wild-type values of 4.7 ± 0.7 and 0.87 ± 0.09 for silique walls and seeds, respectively.

GROWTH OBSERVATIONS

Cosuppressed SPS lines. For S158A T_1 transformants, a number of phenotypes were apparent during all stages of growth and are summarized in Table 5.1. Progeny from SK90B had poor germination rates (30 - 46 %) and some seedlings of both SK90B and SK96A had extreme difficulty in producing true leaves and one of the two cotyledons on these struggling seedlings quickly shrivelled after emergence. Some plants recovered after this initial slow period of growth but SK90B-9 continued to grow slowly and only had three leaves when wild-type plants and its sibling (SK90B-8) started to flower (Fig. 5.10A). SK90B-9 and another sibling, SK90B-7, flowered later than most plants; 119 d and 62 d after planting (Table 5.2). Once SK90B-9 reached the flowering stage, no petals emerged and many buds aborted hence no siliques were formed. Atypically, this plant had large number of small leaves along its racemes (Fig. 5.10B). Closer examination of floral buds revealed a striking morphology. The unopened buds appeared very swollen compared to wild-type (Fig. 5.11A) because a second bud was contained within each one (Fig. 5.11B). To contain these buds, the four sepals were broader and shorter

Table 5.1. Observed phenotypes in T_1 progeny of 35S- S158A transgenic canola.

T_1 LINE	PHENOTYPE	AFFECTED PLANTS
SK9A	none	
SK90B	low germination rates	
	slow emergence and growth	9
	delayed flowering	7, 9
	altered floral morphology	9
	abortion	9
SK96A	slow emergence	
	wilted leaves	13, 14
	unexpanded leaves	13, 14
	poor root production	13, 14
	abortion	13, 14
	short siliques	11
SK96B	extra green leaves	17
	thin stems	17
	early flowering	16
	altered floral morphology	17, 18
	short siliques	17, 18, 19, 20

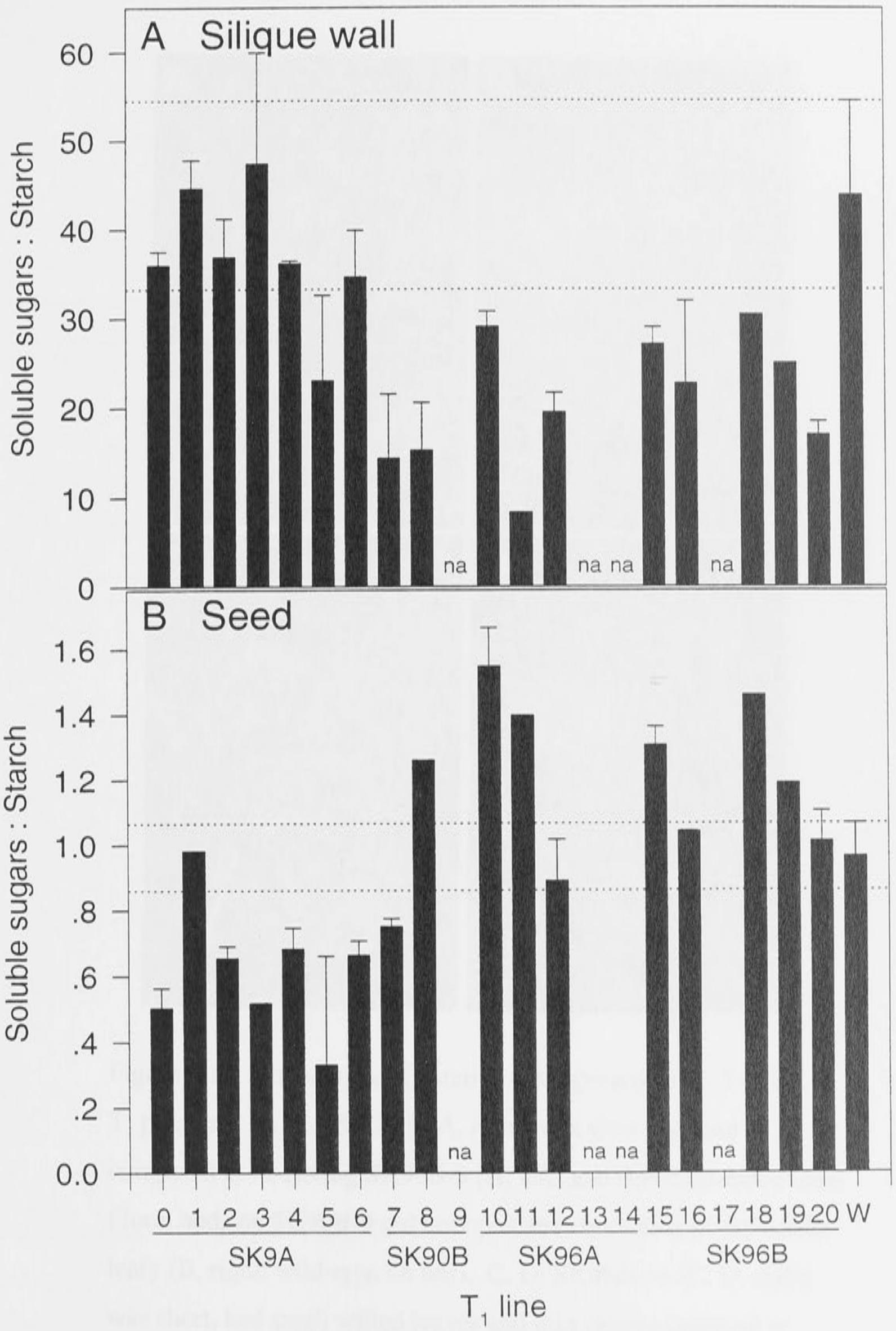

Figure 5.9. Ratios of soluble sugars to starch in T_1 progeny of 35S- S158A progeny. Mean values and standard errors from duplicate extracts are plotted for 26 DAA silique wall (A) and seed (B). W, wild-type; na, not available.

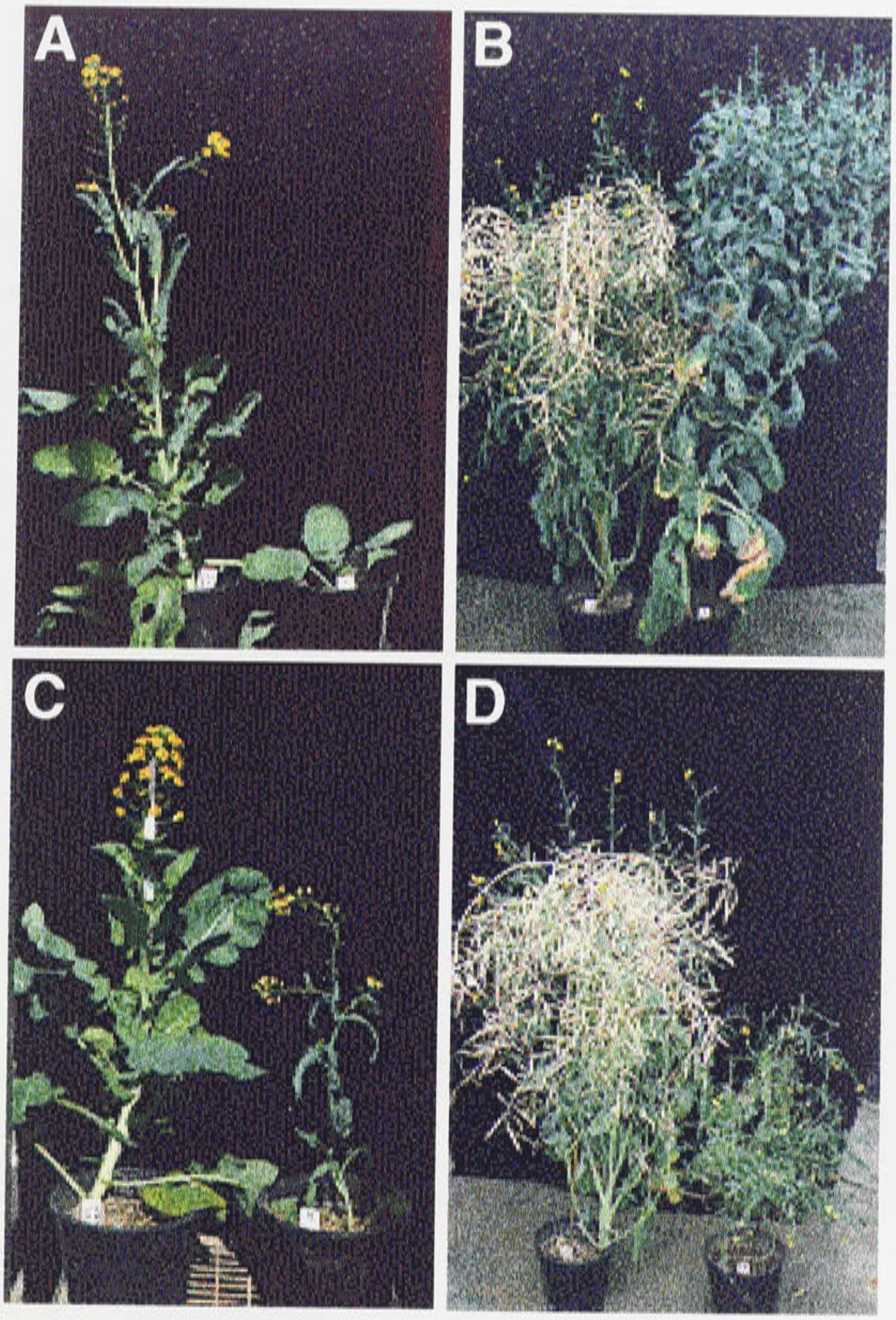

Figure 5.10. Phenotypes of putative cosuppressed 35S- S158A T_1 progeny. A, B: SK90B-9 (A, right) was slow growing compared to its sibling SK90B-8 (A, left) and flowered much later. Floral buds on SK90B-9 did not open and racemes were unusually leafy (B, right; wild-type on left). C, D: SK96A-14 (C, D, right) was short, had small wilted leaves and thin stems compared to wild-type (C, D, left). SK96A-14 flowered at the same time as wild-type plants but did not set seed.

Table 5.2. Number of days to first flower in T_1 progeny of 35S- S158A transgenic canola. Values considered to be outside of the normal range are highlighted.

T_1 LINE	PLANT NO.	DAYS TO FIRST FLOWER	T_1 LINE	PLANT NO.	DAYS TO FIRST FLOWER
SK9A	0	48	SK96A	10	48
	1	49		11	45
	2	49		12	54
	3	49		13	45
	4	52		14	52
	5	55	SK96B	15	45
	6	51		16	38
SK90B	7	62		17	43
	8	50		18	44
	9	119		19	55
				20	56
Wild-type				21	50
				22	48
				23	53

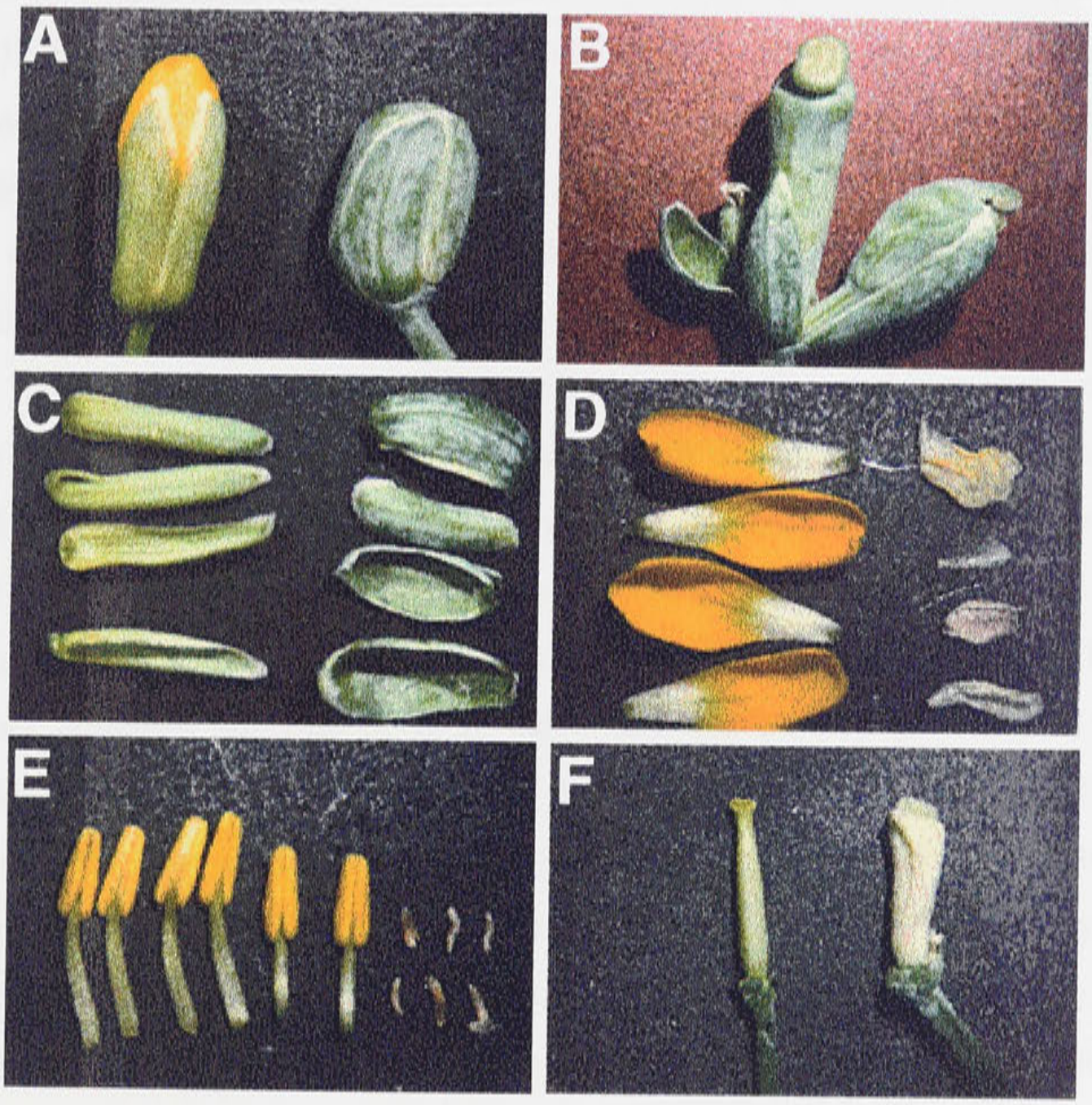

Figure 5.11. Characterization of mutant floral morphology in SK90B-9, a putative cosuppressed T_1 plant from a 35S- S158A transformant. A: unopened floral bud, B: opened mutant bud showing second axillary bud, C: sepals, D: petals, E: stamens, F: carpels. In all panels, wild-type organs are on the left and SK90B-9 organs are on the right.

than wild-type sepals (Fig. 5.11C). In the mutant, petals and stamens were shrivelled while the carpels were extremely thickened (Fig. 5.11D-F).

In SK96A, two of the five T_1 progeny (nos. 13 and 14) were severely wilted at all stages of growth (Fig. 5.10C). Leaves on these plants did not expand (Fig. 5.12A) and in combination with reduced root production presumably caused the poor biomass accumulation and short stature. In addition, stems and branches were very spindly and the plants were not self-supporting (Fig. 5.10D). These plants flowered at the same time as wild-type plants (Table 5.2) but many siliques aborted and no more than six seeds were produced on each plant.

Overexpressing SPS lines. No phenotypes were detected in progeny of SK9A during any growth period even though silique wall tissues were overexpressing SPS (Fig. 5.8A). In SK96B, all segregants appeared essentially normal during vegetative growth. The leaves of SK96B-17 appeared to be greener than other plants and the leaf surface was dimpled and the margins curled downwards (Fig. 5.12B), however the data collected for Fig. 5.7A revealed that the chlorophyll content was not significantly different from other plants. At flowering, this plant and SK96B-18 had swollen floral buds similar to the cosuppressed SK90B-9 plant described above. In contrast to SK90B-9, SK96B-17 flowers appeared to pollinate and many carpels started to extend into a silique, however many aborted shortly thereafter (Fig. 5.12C). The siliques that did continue through development were quite short and consequently contained few seeds per silique, a phenotype shared by its siblings SK96B-18, 19 and 20. The stems and racemes of SK96B-17 were markedly thinner than other plants. Another phenotype documented within this family was early flowering (SK96B-16, Table 5.2).

rolC- AS. For AS T_1 transformants, several phenotypes were detected and some were common to several families. Progeny within SK49 and SK57A had increased numbers of leaves during reproductive growth resulting from the production of branches from axillary meristems near the base of the plant (Fig. 5.12D). Individual leaves of SK54B-31 appeared to be much larger than wild-type leaves. Other phenotypes within AS transformants were thickened stems (SK49-20, 21, 22, 26, and 27), horizontal stem growth (SK49-25, SK54B-39), floral bud abortion (SK54B-39) and increased numbers of racemes (SK57A-45, 11 vs. 5).

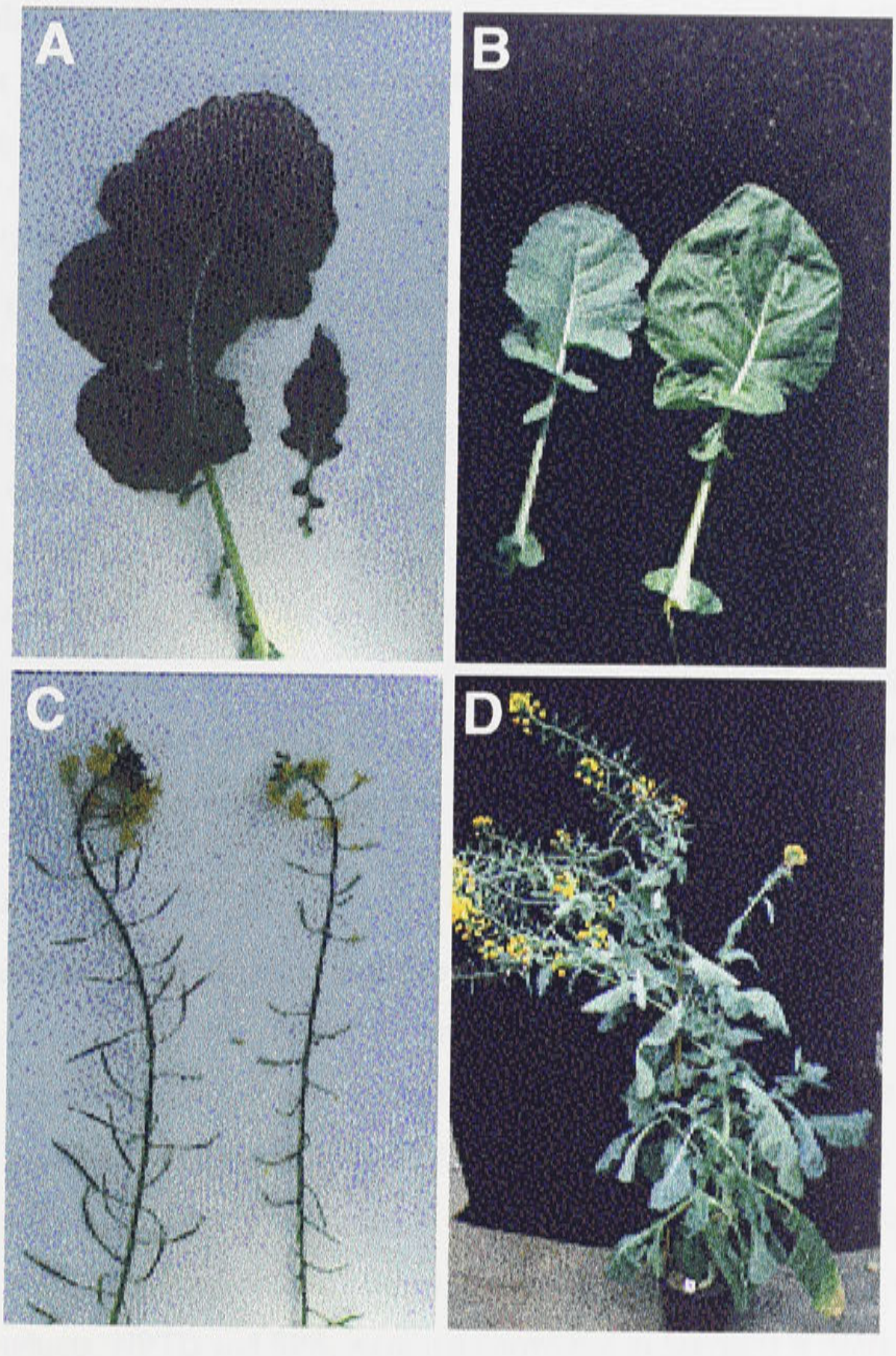

Figure 5.12 Phenotypes of T_1 progeny. A: Largest leaves of wild-type (left) and 35S- S158A SK96A-14 (right). B: Apparent increased chlorophyll content in leaf of 35S- S158A SK96B-17 (right) compared to wild-type (left). Note that leaf sizes cannot be compared. C: Silique abortion in SK96B-17 (right; wild-type on left). D: Increased leaf area from lower axillary meristems in *rolC*- AS SK49-22.

Observation of phenotypes within AS transformants was hindered by crowded growth conditions causing poor light interception from low-angled winter sun. Future work will need to separate environmental effects from true effects of transformation.

PLANT PERFORMANCE

The T_1 progeny of S158A transformants were grown to maturity and yield parameters were determined to quantify plant performance integrated over the entire life cycle. The range of seed produced per plant was highly variable between plants (Fig. 5.13). With the exception of SK9A-1, 2, and 3, all transformants had less seed than wild-type plants. Due to the floral abnormalities described in the previous section, SK90B-9, SK96A-13, 14 and SK96B-17 produced very few or no seeds. Short siliques was the only phenotype observed for SK96B-19 during growth, however its yield was also severely reduced. Weight per 100 seeds, an indicator of seed density and size, was consistent across all plants (Table 5.3).

CORRELATIONS

Correlation analysis was used to determine any relationships between measured parameters for the T_1 S158A transformants (Table 5.4). Of particular interest was the strong positive correlation between the silique wall soluble sugars to starch ratios and seed yield ($r = 0.70$) and the negative correlation between seed SPS V_{max} and yield ($r = -0.58$). As well, silique wall SPS V_{max} and seed soluble sugars to starch ratios were negatively correlated ($r = -0.66$). Interestingly, activities of the two transgene products, NPTII and SPS, were not correlated in leaves ($r = -0.01$).

DISCUSSION

With over 70 plants regenerating from selection medium after *Agrobacterium* cocultivation and producing T_1 seed, it was necessary to reduce the number of analyzed lines to a manageable size. Screening primary transformants for altered phenotypes was not attempted because it was felt that environmental and tissue culture effects would mask any transgene effects. Instead, T_1 seed was germinated

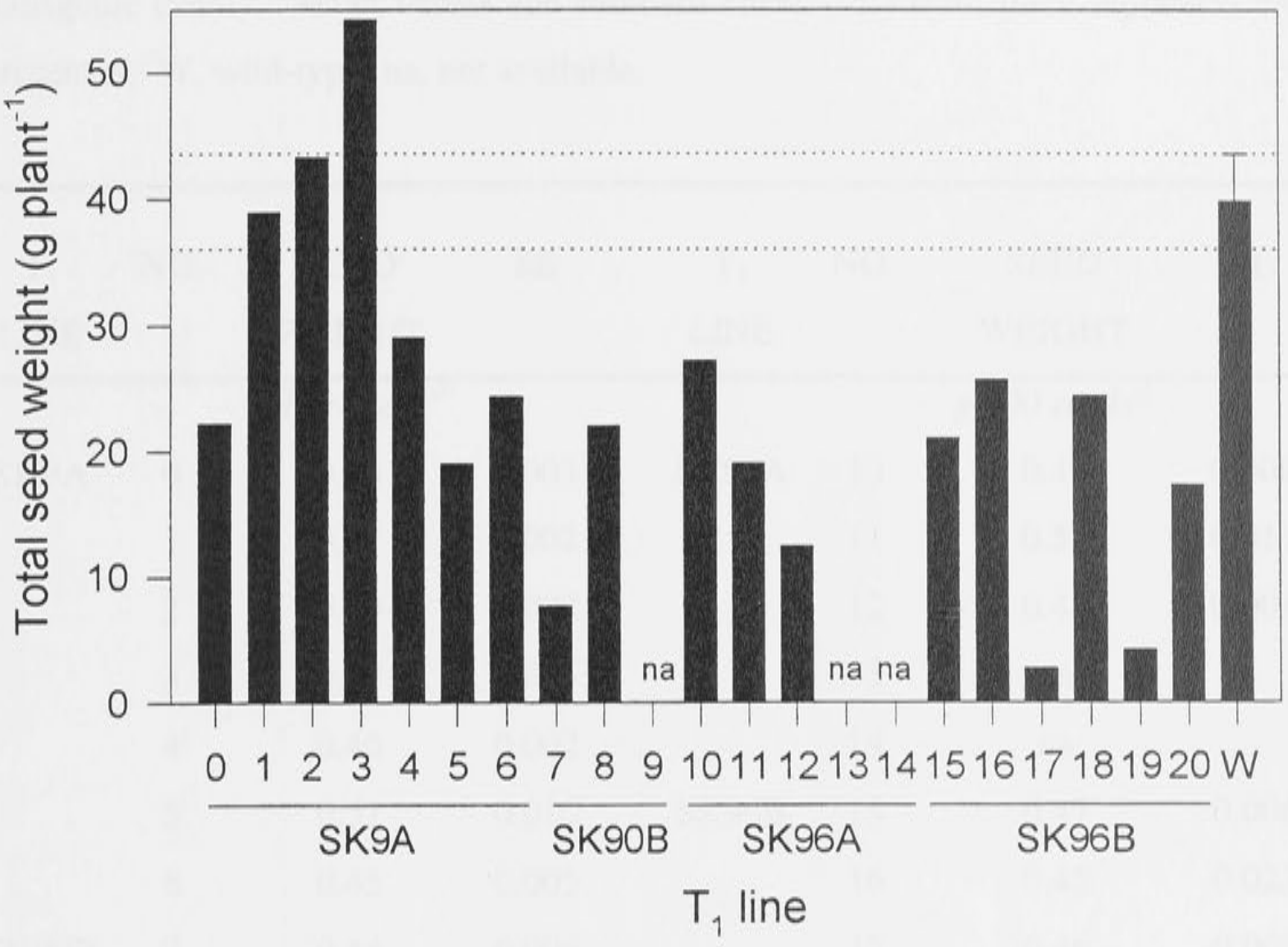

Figure 5.13. Seed yield in T_1 progeny of 35S- S158A transformants. Mature seeds were harvested from each plant and weighed. Wild-type yields (W) are derived from three separate plants. na, not available.

Table 5.3. Weight per 100 seeds harvested from T_1 progeny of 35S- S158A transgenic canola. Mean values and standard errors (SE) from three replicates are presented. W, wild-type; na, not available.

T_1 LINE	NO.	SEED WEIGHT	SE	T_1 LINE	NO.	SEED WEIGHT	SE
		g 100 seeds^{-1}				*g 100 seeds^{-1}*	
SK9A	0	0.44	0.003	SK96A	10	0.49	0.009
	1	0.47	0.002		11	0.53	0.013
	2	0.50	0.007		12	0.48	0.008
	3	0.47	0.004		13	na	
	4	0.46	0.002		14	na	
	5	0.51	0.010	SK96B	15	0.47	0.006
	6	0.45	0.005		16	0.45	0.022
SK90B	7	0.44	0.006		17	0.46	0.007
	8	0.43	0.005		18	0.49	0.011
	9	na			19	0.38	0.015
					20	0.53	0.007
				W	21	0.42	0.001
					22	0.52	0.007
					23	0.46	0.002

Table 5.4. Correlations between measured traits in T1 progeny of 35S- S158A transgenic canola. Coefficients greater than 0.50 are highlighted.

	Leaf NPTII	Leaf SPS	Wall SPS	Seed SPS	Wall Sugar:starch	Seed Sugar:starch	First Flower	Yield	Seed 100wt
Leaf NPTII	1.00								
Leaf SPS	-0.01	1.00							
Wall SPS	-0.39	0.29	1.00						
Seed SPS	0.73	0.12	-0.17	1.00					
Wall Sugars:starch	-0.37	-0.38	0.31	-0.23	1.00				
Seed Sugars:starch	0.44	-0.36	-0.66	0.31	-0.15	1.00			
First Flower	-0.07	-0.16	0.23	-0.18	-0.07	-0.35	1.00		
Yield	-0.70	-0.23	0.30	-0.58	0.70	-0.19	-0.33	1.00	
Seed 100wt	-0.08	0.12	0.31	-0.33	-0.12	0.03	-0.11	0.13	1.00

on selection medium and seedlings were scored for their ability to tolerate kanamycin. This tolerance would necessitate expression of the introduced *nptII* resistance gene and although it is realized that *nptII* expression is not a prerequisite for expression of the other introduced transgenes (ie. S158A, AS) (Peach and Velten, 1991), the seed germination test was a very simple and quick method of choosing promising lines. From the results, four families from 35S- S158A cocultivations and 14 *rolC*- AS families had resistance averages greater than wild-type seedlings and were chosen for further analysis (Fig. 5.1). Strangely, no lines from RbcS- maize SPS cocultivations showed greater resistance levels than wild-type seedlings. Attempts to reisolate the binary plasmid from the *Agrobacterium* RbcS- maize SPS glycerol stock cultures failed presumably indicating the loss of the plasmid during final preparation.

CONFIRMATION OF TRANSFORMATION

After identifying promising families, incorporation of the S158A and AS transgenes was confirmed in the primary transformants (Figs. 5.2 and 5.3). Of the chosen lines, SK45 was the only line in which a transgene could not be detected by Southern blot analysis and interestingly its T_1 seedlings had the lowest average resistance to kanamycin (Figs. 5.1 and 5.3). Many high molecular bands were visible on hybridized Southern blots and likely represent incompletely digested DNA or cross-hybridization to endogenous sequences because of the low stringency blot washing (1 x SSC). Of more concern is the predominant 4.4 kb band, higher than the expected 3.9 kb band, in the SK9A lane of the S158A Southern blot (Fig. 5.2). This band could be the result of partial digestion if the EcoRI site between at the 5' end of S158A coding sequence was not digested and the EcoRI sites at the 5' end of the 0.5 kb 35S promoter and at the 3' end of the 3.9 kb S158A coding sequence were properly digested (see Fig. 4.1). T_0 genomic DNA was in very limited supply but as much DNA as possible was used to determine gene copy number in some of the chosen lines. The majority of lines contained multiple T-DNA copies at independent insertion sites (Fig. 5.4) reflecting the inherent bias of the seed germination screening procedure to select multiple copy transformants. For a single insertion, a 3:1

phenotypic segregation ratio would be expected in the T_1 generation after self-pollination.

GROWTH AND PERFORMANCE OF T_1 LINES

35S- S158A Seedling Growth. Growth of T_1 plants from four S158A transgenic lines revealed a number of phenotypes. Segregants of SK90B and SK96A were slow growing during emergence and SK90B-9 continued to grow slowly at later stages. Even though leaf maximal SPS activities within these plants were no different to others on a protein basis, reduced protein contents in SK90B-9 and SK96A-14 resulted in lower activities on area and on chlorophyll bases. If SPS was also suppressed in germinating seedlings then the slow growth phenotype could be explained by reductions in sucrose synthesis after gluconeogenic degradation of seed storage products and therefore reductions in the supply of remobilized carbon to growing meristems (Geigenberger and Stitt, 1991). The reduced protein contents suggest a carbon shortage to the respiratory pathways which provide substrates for amino acid synthesis.

Vegetative Growth. During vegetative growth, the suppression of SPS was manifested in separate ways within SK90B and SK96A. SK90B-9 leaves appeared normal but the growth rate was simply slower and it took twice as long for this plant to reach the flowering stage (Fig. 5.10A and Table 5.2). For SK96A-13 and 14, leaf initiation seemed to occur at similar rates to wild-type plants but these leaves did not expand and were constantly wilted (Fig. 5.12A). Flowering time was not affected in these two plants (Table 5.2). A suppression in the capacity to synthesize Suc in source leaves may affect the amount of assimilate which is transported to sink tissues and Suc supply to apical meristems has been implicated in the modulation of flowering time (Friend et al., 1984). The observation that flowering time was delayed in the putative cosuppressed SK90B-9 plant and promoted in the putative overexpressing SK96B-16 agrees with this hypothesis (Table 5.2) and is consistent with the effects of elevated SPS activities on flowering in tomato (Micallef et al., 1995).

Pollination. Poor pollination was apparent in a number of T_1 plants. In the most severe example, pollen-bearing stamens were completely shrivelled and ovule-

containing carpels were extremely enlarged in all SK90B-9 flowers (Fig. 5.11). It is unknown if the stigmas would be receptive to pollen from other plants. The complete lack of pollination obviously explains the absence of siliques and seeds on this plant (Fig. 5.13). SK96A-13 and 14 and SK96B-17 also had extreme reproductive difficulties but abortion in these plants occurred after pollinated carpels extended to less than 2 cm (Fig. 5.12C). Moderate swelling of floral buds was evident in SK96B-17 and 18.

Floral abortion in three of the four independently-transformed S158A lines suggests that this phenotype is caused by SPS-mediated alterations in sucrose metabolism rather than secondary effects of the transformation process. In addition, *rolC*- AS transgenic plants did not display the same difficulties. The limited data available on floral carbohydrate metabolism has concentrated on sucrose cleavage (Hawker et al., 1976; Miller and Ranwala, 1994; Aloni et al., 1996, 1997; Xu et al., 1996; Collier, 1997) and cannot explain the observed phenotype. It is intriguing to speculate that the constitutive expression of S158A in petals and stamens, which have large respiratory requirements, arrested the ability to utilize imported carbon by diverting cleaved hexoses into SPS-mediated Suc resynthesis at the expense of glycolysis. Alternatively, the combination of a futile Suc synthesis / degradation cycle and SPS cosuppression in these tissues may keep hexose to sucrose ratios high preventing cell expansion analogous to the situation in developing embryos (Ambrose et al., 1987; Weber et al., 1996a). A third possibility is that sucrose is an essential signal in floral transduction pathways (for reviews, see Sheen, 1990; Koch, 1996).

Silique Growth. In contrast to leaves, T_1 plants showed major differences in maximal SPS activities. Measurement of 26 DAA silique wall SPS activities revealed that segregants of SK9A all had higher V_{max} activities (3.6-fold in SK9A-2) than wild-type plants (Fig. 5.8A). This increased capacity for sucrose synthesis did not correlate with carbohydrate ratios (Table 5.4). In the two apparent cosuppressed lines, SK90B and SK96A, silique wall SPS activities were reduced by 92 % in two of the five plants able to produce siliques (nos. 8 and 12; Fig. 5.8A) and the corresponding reductions in soluble sugars lowered the soluble sugars to starch ratio by 60 % (Fig. 5.9A). Smaller changes in carbohydrates compared to SPS activity have been previously documented in tomato (Worrell et al., 1991; Galtier et al.,

1993, 1995) and highlights the important point that SPS activities *in vivo* will not reach maximum capacity because its substrate concentrations will not be saturating.

In the absence of saturating substrates, post-translational modification of SPS activation state modulates its activity and previous efforts to overexpress SPS in tobacco and potato failed because the excess SPS protein was not activated (Sonnewald et al., 1994). To avoid this problem in the present work, the introduced transgene contained a single amino acid change designed to prevent phosphorylation deactivation, however the DNA sequence of the spinach clone was apparently too similar to the endogenous canola SPS sequence thereby causing cosuppression at the transcriptional level in the leaves and silique wall of some T_1 progeny. The degree of identity between these genes is unknown because full-length SPS sequences from either canola or *Arabidopsis*, a close relative, have not been reported. In seeds and silique wall of some progeny, SPS was successfully overexpressed up to 8.6-fold. A possible explanation for this difference is that each tissue could be expressing different SPS isoforms and the sequences of the endogenous forms present in silique walls and seeds may be sufficiently heterologous to the introduced spinach cDNA, originally cloned from leaves, to avoid cosuppression. Indeed, it has been recently reported that there are multiple SPS isoforms in potato (Reimholz et al., 1997). Furthermore, two cDNA clones have been isolated from *Craterostigma plantagineum* Hochst and also sugarcane and analysis of the sequences indicates that one clone of each species clusters with sequences from monocotyledonous species and the other clone clusters with sequences from dicotyledonous species (Fig. 4.13). Alternatively, cosuppression may be minimized in silique wall and seed tissues because the endogenous SPS is only active in a minority of specific cells and constitutive expression of S158A in the other cells leads to a net increase in SPS activity for the entire organ. The localization of chlorophyll to a few outer silique wall cell layers (Fig. 3.4) and the normal association of SPS with photosynthesis supports this argument. In seeds, SPS activity is predominantly in the embryo (Fig. 2.6) and the heterogeneity of metabolism within embryos means that endogenous SPS is likely to be further compartmentalized. *In vivo* SPS activity in cells where it

is not normally active would be dependent on the presence of its UDP-Glc and Fru-6-P substrates.

Seed growth. While T_1 progeny of SK9A were overexpressing SPS in silique wall, overexpression in 26 DAA seeds was most pronounced in progeny of SK96B (8.6-fold increase in SK96B-17; Fig. 5.8B). Some plants within each of the other three lines overexpressed SPS 2.1- to 3.6-fold. In contrast to leaf and silique wall, no plants had lower maximal activities than wild-type plants. Seed SPS activities were not correlated to accumulated carbohydrates but were negatively correlated to seed yield (Table 5.4). This correlation may be indicative of a shift in the net direction of the proposed embryo futile cycle (see Chapter 2) towards Suc synthesis rather than cleavage thereby affecting hexose supply to glycolysis. There was not, however, an obvious accumulation of Suc or Fru (Fig. 5.9). Future work should closely examine this question and include measurements of the central metabolite UDP-Glc. Regardless of mechanism, seed yield was severely reduced in the SPS overexpressing plants SK96B-17 and 19 (Fig. 5.13). All progeny in the four T_1 families produced seeds of the same weight indicating that seed number is more easily affected than seed weight by SPS perturbation (Table 5.3).

rolC- AS. Only a minimal examination of *rolC*- AS T_1 plants was conducted because of time constraints. Three plants had detectable transcripts of the rice AS transgene (Fig. 5.6) and strangely the stems of two of these plants were observed to grow predominantly horizontally rather than vertically (SK49-25, SK54B-39). The transcript levels in leaves was less than 10 % of the levels in young rice seedlings and this difference may reflect the inclusion of stem tissue in the rice samples because expression of the pea AS1 gene has been localized to vascular tissue (Tsai, 1991). This localization was the basis for choosing the vascular tissue-specific promoter, *rolC*, to drive rice AS transgene expression in these experiments. The apparent thickened stems observed in the progeny of SK49 needs to be correlated with transgene expression and accumulation of nitrogenous or carbon compounds.

Northern analysis also revealed that AS mRNA levels in etiolated rice seedlings were 2-fold higher than in light-grown seedlings (Fig. 5.6). This accumulation agrees with previous reports that AS expression is repressed by light in pea and maize (Tsai and Coruzzi, 1990, 1991; Tsai, 1991; Dembinski et al., 1996)

and is enhanced during carbohydrate deprivation in maize root tips (Chevalier et al., 1996). The more efficient use of carbon by asparagine rather than the predominant transport compound glutamine (Lea and Miflin, 1980; Siegiechowicz, 1988) may offer increased performance during stress periods (for review, see Rabe, 1990) therefore this concept should be considered when the transgenic AS plants produced in this research are fully characterized.

CONCLUSION

In this chapter, plants regenerated from tissue culture after *Agrobacterium* cocultivation were confirmed to be transgenic and many expressed the introduced *nptII* kanamycin resistance gene. As well, expression of the rice AS cDNA transgene was confirmed in the leaves of three T_1 plants from two families. For plants transformed with the spinach S158A mutant SPS cDNA, SPS V_{max} activities in leaves were the same as wild-type levels on a protein basis, however SPS activities in three T_1 plants from two families appeared to be cosuppressed and one T_1 plant appeared to overexpress leaf SPS when the data was expressed per unit chlorophyll or per unit area. The cosuppressed plants had severe flower fertility problems and the overexpressing plant flowered early thereby suggesting an important role for sucrose in the flowering process. In 26 DAA silique wall and seeds, up to 3.6- and 8.6-fold increases in SPS V_{max} were documented possibly indicating less susceptibility to cosuppression of endogenous SPS isoforms in these tissues. Seed SPS activities were negatively correlated to seed yield which supports the hypothesis of a continuous Suc synthesis / degradation cycle regulating carbohydrate supply to respiratory pathways in developing embryos (see Chapter 2). Sugar to starch ratios of 26 DAA silique wall and seed tissues were equivalent or moderately different to wild-type ratios and only the seed soluble sugars to starch ratio was correlated to SPS activity. The silique wall soluble sugars to starch ratio was positively correlated to seed yield which further highlights the importance of silique wall to assimilate partitioning.

CHAPTER 6: GENERAL DISCUSSION

OVERVIEW

SILIQUE WALL AS A SOURCE

The thesis has focussed on the biochemical basis of assimilate supply to developing canola seeds. During the phase of storage oil synthesis in embryos, carbon assimilate sources were identified and examined. With the rapid loss of photosynthetic leaf area shortly after first flower (Fig. 2.1), the silique wall plays a major role in carbon assimilation and its photosynthetic capacity per unit chlorophyll was equivalent to source leaves but less per unit area (Table 2.1 and Fig. 2.2). A major difference to leaves was the discovery that silique walls preferentially partition photosynthate into Suc over starch and accumulate vacuolar hexose (Table 2.2, Fig. 2.7). Remobilization of these carbohydrate reserves is not entirely to filling seeds because there are large simultaneous carbon requirements for silique wall secondary cell wall thickening (Table 2.5). The importance of silique wall carbohydrates to seed filling was highlighted by a positive correlation between the soluble sugars to starch ratio and seed yield in transgenic plants with varying capacities to synthesize Suc (Table 5.4).

SEED CARBOHYDRATES AS A SOURCE

Transient reserves within seeds were found to be a second source of carbohydrates to expanding embryos. Before the onset of rapid embryo fresh weight gain, and therefore storage product synthesis, starch and smaller amounts of hexoses were localized to the seed coat and liquid endosperm (Table 2.4 and Fig. 2.4). Similar to the silique wall, the growing embryo may not be the only sink for these reserves because seed coat mucilage production (Van Caeseele et al., 1981; Kuang et al., 1996) and increasing sclerenchyma lignification (Fig. 2.4) apparently occur simultaneously.

SEED CO_2 FIXATION AS A SOURCE

The potential of refixed CO_2 to act as a third source of carbon was examined in silique wall and seed tissues. Developing seeds had a higher CO_2 fixation capacity than the silique wall endocarp during the oil filling period (Table 3.6) and embryo Rubisco was the major component of this capacity (Table 3.4). The morphology of the reproductive structures is a critical component because the cotyledon thickness, the seed coat and the silique wall sclerenchyma layer presumably all restrict gaseous diffusion consequently there was a massive increase in silique cavity CO_2 concentrations (Table 3.3) that would elevate Rubisco's activity *in vivo*. PEPC-mediated CO_2 fixation in developing seeds is also a significant component and may either replenish TCA cycle intermediates or be converted within leucoplasts to acetyl-CoA, the precursor to fatty acids.

Rubisco-mediated CO_2 fixation is normally dependent of energy produced by photosynthetic electron transport and it has been previously assumed that the quantity of light reaching the chlorophyll-rich embryos would be insufficient to drive significant energy production. Under Australian conditions, seeds would receive up to 400 µmol quanta m^{-2} s^{-1} and allowing for a further 55 % attenuation by the seed coat, embryos had very respectable electron transport rates at 175 µmol quanta m^{-2} s^{-1} (Table 3.2). These rates were less than Rubisco V_{max} therefore it is possible that the produced energy is utilized for CO_2 fixation, however NADPH production rates were of the same order of magnitude as fatty acid synthesis requirements and energy partitioning between these two alternatives was not assessed.

EMBRYO SINK METABOLISM

Regardless of carbon source, the ultimate sink of economic interest in canola is the oil-rich cotyledons. Imported sucrose is proposed to be cleaved by seed coat acid invertase during early developmental stages (Fig. 2.8), a time when the combined hexose content is approximately twice as high as sucrose (Fig. 2.3). By analogy to other dicotyledonous species, this ratio may maintain embryo cell division rates (Weber et al., 1996a) and inhibit SuSy activity (for review, see Quick and Schaffer, 1996). In parallel with rapid embryo growth, acid invertase activities and hexose contents declined (Figs. 2.3, 2.6 and 3.1) and the resulting high sucrose to hexose ratio may be involved in the

transition to cell expansion and the relief of SuSy inhibition. Embryo SuSy maximum activities rose over 2-fold during this period (Fig. 2.6) suggesting that it is the predominant enzyme of sucrose metabolism during the storage product synthesis phase, in common with starch-storing species (see Chapter 1). Interestingly, significant SPS activities were measured in developing embryos and it is proposed that a continuous Suc synthesis / degradation cycle modulates carbon supply to glycolysis, analogous to other sinks (Fig. 2.8 and Dancer et al., 1990; Wendler et al., 1990; Geigenberger and Stitt, 1991).

MOLECULAR ALTERATION OF ASSIMILATE SUPPLY

The molecular alteration of enzyme activities is an excellent way to elucidate the regulatory mechanisms involved in source to sink relations but the development of gene constructs, the transformation and regeneration of plant tissues, and the screening for suitable lines can unfortunately take several years. In this thesis, a modified *Agrobacterium*-mediated transformation protocol was utilized to transfer gene constructs, designed to increase sucrose and asparagine supply, into cotyledonary petiole explants. Tissue culture regeneration frequencies had to be increased by modifying several culture parameters including explant age (Figs. 4.7 and 4.8) and medium water source (Figs. 4.11 and 4.12) before plantlets were regenerated from selection medium. Many T_1 progeny had detectable phenotypes (Table 5.1) and S158A transgenics had either increased or decreased SPS activities compared to untransformed plants in leaf, silique wall and seed tissues (Figs. 5.7 and 5.8) while expression of the rice AS transgene was detected in some T_1 progeny derived from AS transformants (Fig. 5.6). This initial screening successfully identified several promising lines with which a detailed and rigorous growth analysis can be conducted. Although several phenotypes were common to independently-transformed lines, the biggest challenge in future work will be to separate environmental and pleiotropic effects from direct transgene effects. This is particularly important here where effects on assimilate supply can have large implications for the growth and morphology of transformed lines.

SOME REMAINING ISSUES

SOURCE TISSUES

The research reported in this thesis has formed a foundation for the understanding of source to seed carbon provision in canola. As described above, several notable and novel features have been documented here but there are still many unanswered questions. One of canola's unique developmental features is rapid leaf senescence shortly after the initiation of flowering and one's first impression is that this loss of carbon assimilation capacity would be detrimental to plant performance. The large amounts of dry matter needed to quickly form the reproductive structures and the corresponding thickening of the main stem (Fig. 1.1A) must be in excess of leaf photosynthetic capacity and senescence-mediated assimilate remobilization at the leaf's expense may be the only way to get plant development to a stage where siliques are self-supporting. Remobilization of nitrogen from leaf proteolysis may be more important than carbon provision because it was observed that plants retained leaf area longer when grown with daily nutrient watering possibly suggesting that, in the absence of sufficient soil nitrogen, seed nitrogen needs are met by accelerated leaf senescence (Rood et al., 1984a). It will be interesting to screen the *rolC*- AS transgenic plants to determine if a shift of transported organic nitrogen to the more conservative asparagine form has any effect on the timing of leaf senescence initiation.

Seemingly surplus amounts of dry matter are invested in the racemes and main stem during the flowering period. This unharvested material is responsible for canola's low production efficiency; harvest indices (seed to total shoot biomass) are typically around 20 % (Thurling, 1974; Rood et al., 1984a; Kasa and Kondra, 1986). Excessive numbers of flowers are formed and many abort, particularly those appearing near the end of the flowering period, possibly reflecting an inadequate assimilate supply (Habekotté, 1993). This sensitivity was illustrated by the pollination problems documented in cosuppressed S158A transgenics (see Chapter 5). The rationale for choosing to overexpress SPS was to examine the potential to increase Suc production in source tissues and, after export to the phloem, to increase Suc supply to sink tissues. In tomato plants overexpressing SPS, fruit yield increased without affecting total biomass

production thereby raising the harvest index (Micallef et al., 1995). One T_1 canola plant, which overexpressed SPS 3-fold in silique wall, had a 36 % increase in seed yield (Figs. 5.8A and 5.13). A positive correlation between silique wall carbohydrate ratios and seed yield also support the hypothesis that carbon supply from silique walls is an important yield determinant. Future experiments should examine the harvest indices and abortion frequencies in overexpressing plants to examine the theory that Suc supply affects yield, indicative of a source limitation.

There are two further issues that have not been addressed in this thesis. First, the influence of stems on assimilate provision, either by primary fixation or remobilization, is unknown. No research has adequately examined this phenomenon in canola, however it is known that stems do contain chlorophyll and stomata (Major, 1975; Brar and Thies, 1977) and it has been suggested that *B. rapa* stems do not remobilize significant reserves to filling seeds (Rood et al., 1984a). Second, clear data is needed to substantiate the claim that siliques do not export carbon and solely supply the seeds contained within (Major et al., 1978),

ALTERNATIVE SINKS

The focus of this thesis has been on developing seed sinks, due to their economic importance, but there are also a number of other competing sinks. As outlined in the previous section, stems and racemes consume large amounts of dry matter, apparently without later remobilization. Obviously, a plant that is over 1.5 m tall needs a strong stem to remain upright and much of this dry matter is probably in the form of lignin. It would, however, be interesting to stain stem transverse sections with iodine to detect the presence of starch in the large pithy stem core at various developmental stages. If significant amounts of non-structural carbohydrates are present then a potential strategy to increase seed yield would be to use antisense engineering to specifically reduce carbohydrates in stems.

As noted in Chapter 2, silique wall secondary cell wall thickening has a very large carbon demand. Although the sclerenchyma layer (Fig. 3.3) apparently acts as a gaseous diffusion barrier to impede the loss of respired CO_2 to the atmosphere, lignin and cellulose contents continued to rise after its formation (Table 2.2) and phlorglucinol staining of silique wall transverse sections revealed that mesocarp cells progressively

thickened towards the epidermis with development. It may be useful to increase seed-available carbohydrates by the molecular reduction of flux to cell wall thickening, however a suitable cell type-specific promoter is not presently available. Even if this strategy was technically feasible, the strength provided by thickening likely enables siliques to maintain their horizontal orientation, which is efficient for light interception, while the increasing weight of seeds would be exerting downward pressure.

Similarly in the seed coat, the synthesis of mucilage, fibre and phenolic-rich pigments (Fig. 2.4) require carbon and it may be attractive to engineer flux diversions towards oil- and protein-storing embryos, however these polymers may serve critical physiological functions. First, the seed coat sclerenchyma or mucilage layers are likely to be responsible for the gaseous diffusion barrier proposed to increase the efficiency of embryo CO_2 fixation (see Chapter 3). Second, lignin and tannins cross-link with polysaccharides to give the seed coat strength and therefore physical protection of the embryo (Werker, 1997). Third, phenolics also protect the embryo against pathogen attack and premature germination (Werker, 1997). Mature canola seeds are typically black, from the seed coat pigments, but some plant breeders are currently developing yellow-seeded lines which contain less fibre and the seed meal contains increased amounts of digestible energy (K. Bett, personal communication). If an absent sclerenchyma layer is responsible for the reduced fibre content then the relative importance of the seed coat diffusion barrier and hence CO_2 refixation to yield could be assessed. Presumably the seed coat pigment layer is missing from yellow seeds and the increased digestibility could either result from less phenolic binding to proteins or from the reduction of pigment and fibre sinks leading to increased carbohydrate content. This latter option would imply that storage oil pathways cannot utilize excess carbon. It will also be interesting to determine if yellow seeds are more susceptible to pathogens than phenolic-rich black seeds.

SEED METABOLISM

The enzymes involved in the utilization of seed-imported Suc have been characterized (see Chapter 2). Invertase-mediated cleavage is important during the initial cell division stages while SuSy-mediated cleavage predominates during the cell expansion (storage product synthesis) phase. The manipulation of invertase activity in young seeds may be of some value because cotyledon cell number is a critical

determinant of final size and hence yield (see Weber et al., 1996a and references therein). Although acid invertase activity was localized to canola seed coats (Fig. 2.6), the measurements predominantly reflect activity of the soluble form and not the insoluble form associated with the apoplastic carbohydrate transfer from the seed coat to the liquid endosperm (Weber et al., 1995; Cheng et al., 1996). The inclusion of detergent and chelating agents in the extraction buffer used in this research may have solubilized some insoluble acid invertase, however repeated extractions in nonsaline buffer followed by the release of the bound form in saline buffer are required to distinquish soluble acid invertase from the full activity of the insoluble form (for review, see Quick and Schaffer, 1996).

Once developing embryos have grown large enough to come in contact with the seed coat, Suc is proposed to be actively transferred without cleavage to cotyledons (Patrick and Offler, 1995; Harrington et al., 1997a, b; Patrick, 1997; Weber et al., 1997a) where SuSy-mediated cleavage provides substrate for glycolysis (Fig. 2.6). Interestingly, significant activities of the Suc synthesis enzyme SPS were measured in developing embryos. From previous work in other sink tissues, it has been proposed that a continuous Suc synthesis / degradation cycle modulates hexose supply (Dancer et al., 1990; Wendler et al., 1990; Geigenberger and Stitt, 1991), however this proposal assumes that SuSy and SPS activities are present in the same cells. There are likely to be heterogenous populations of cells within developing cotyledons with cells in some regions synthesizing storage products while cells in other regions are still dividing, however *in situ* localization of SPS and SuSy transcripts were co-localized in developing faba bean cotyledons (Weber et al., 1996b). Similar studies in canola of the *in situ* or immunolocalization of SPS, SuSy and invertases would be valuable.

The concept of cellular heterogeneity also impacts on the utilization of photosynthetically-produced energy. Embryo photosynthesis is likely to be confined to the few outer layers of developing cotyledons where light availability is highest while fatty acid synthesis may be occurring in cells several layers beneath the outer surface. Even within single cells, individual plastids may not be photosynthesizing and also producing storage fatty acids. Although it has been estimated that embryo photosynthetic electron transport rates are of the same order of magnitude as fatty acid requirements (see

Chapter 3), this compartmentation argues against the direct provision of photosynthetically-produced reducing power to fatty acid synthesis and argues for Rubisco-mediated CO_2 fixation. Experimental data has, however, documented reductant flow to alternative sinks in developing soybean and *Arabidopsis* seeds (Wilms et al., 1997) and high uncoupled photosynthetic electron transport rates in isolated canola embryo plastids (Eastmond et al., 1996). There is also a curious light-dependence of fatty acid synthesis in developing oilseeds (Browse and Slack, 1985; Fuhrmann et al., 1994; Eastmond et al., 1997). Substrate could be produced independently of light by PEPC-mediated CO_2 fixation into malate and the subsequent decarboxylation of malate within leucoplasts produces enough NADPH to supply fatty acid requirements in castor (Dennis and Blakeley, 1993). Even though canola seeds have significant PEPC activities, pyruvate appears to be a superior substrate compared to malate for fatty acid synthesis (Kang and Rawsthorne, 1994). The fates of photosynthetically-produced energy and CO_2-derived carbon remain to be definitively resolved.

PERSPECTIVE

The research presented in this thesis has provided important data on source to sink relations in canola. The great time required to produce transgenic plants necessitates the prudent choice of genetic engineering targets consequently the identification of the key enzymes and processes involved in source tissue carbon assimilation and its subsequent utilization in seed sink tissues is invaluable. In addition, this research has challenged the commonly-held beliefs that silique wall CO_2 refixation is as important in canola as it apparently is in pea and that seed chlorophyll and photosynthesis are artifacts and serve no significant physiological function. As well, transgenic T_1 plants have been produced containing gene constructs designed to perturb the supply of carbon and nitrogen assimilates to sinks and preliminary analysis has identified a number of intriguing phenotypes. The common theme of this research was the integration of cellular metabolism with whole-plant growth and performance; a perspective requiring the bridging of the gaps between individual genes and enzymes and empirical crop physiological research. Canola is a species of great potential and a heightened knowledge of its physiology can be exploited for economic advantage.

LITERATURE CITED

Addo-Quaye AA, Scarisbrick DH, Daniels RW (1986) Assimilation and distribution of ^{14}C photosynthate in oilseed rape (*Brassica napus* L.). Field Crops Res **13**:205-215

Aloni B, Karni L, Zaidman Z, Schaffer AA (1996) Changes of carbohydrates in pepper (*Capsicum annuum* L.) flowers in relation to their abscission under different shading regimes. Ann Bot **78**:163-168

Aloni B, Karni L, Zaidman Z, Schaffer AA (1997) The relationship between sucrose supply, sucrose-cleaving enzymes and flower abortion in pepper. Ann Bot **79**:601-605

Ambrose MJ, Wang TL, Cook SK, Hedley CL (1987) An analysis of seed development in *Pisum sativum* L. IV. Cotyledon cell population *in vitro* and *in vivo*. J Exp Bot **38**:1909-1920

Amor Y, Haigler CH, Johnson S, Wainscott M, Delmer DP (1995) A membrane-associated form of sucrose synthase and its potential role in synthesis of cellulose and callose in plants. Proc Natl Acad Sci USA **92**:9353-9357

An G (1987) Binary T_i vectors for plant transformation and promoter analysis. Methods Enzymol **153**:292-305

Andrews M (1986) The partitioning of nitrate assimilation between root and shoot of higher plants. Plant Cell Environ **9**:511-519

Aspinall GO (1980) Chemistry of cell wall polysaccharides. *In* J Preiss, ed, The Biochemistry of Plants, Vol 3, Carbohydrates: Structure and Function. Academic Press, New York, pp 473-500

Atkins CA, Flinn AM (1978) Carbon dioxide fixation in the carbon economy of developing seeds of *Lupinus albus* (L.). Plant Physiol **62**:486-490

Atkins CA, Kuo J, Pate JS, Flinn AM, Steele TW (1977) Photosynthetic pod wall of pea (*Pisum sativum* L.). Distribution of carbon dioxide-fixing enzymes in relation to pod structure. Plant Physiol **60**:779-786

Baulcombe DC (1996) RNA as a target and an initiator of post-transcriptional gene silencing in transgenic plants. Plant Mol Biol **32**:79-88

Bell JM (1995) Meal and by-product utilization in animal nutrition. *In* DS Kimber, DI McGregor, eds, Brassica Oilseeds: Production and Utilization. CAB International, Wallingford, UK, pp 301-337

Blakeley SD, Dennis DT (1993) Molecular approaches to the manipulation of carbon allocation in plants. Can J Bot **71**:765-778

Boulter ME, Croy E, Simpson P, Shields R, Croy RRD, Shirsat AH (1990) Transformation of *Brassica napus* L. (oilseed rape) using *Agrobacterium tumefaciens* and *Agrobacterium rhizogenes* - a comparison. Plant Sci **70**:91-99

Brar G, Thies W (1977) Contribution of leaves, siliques and seeds to dry matter accumulation in ripening seeds of rapeseed, *Brassica napus* L. Z Pflanzenphysiol Bd **82**:1-13

Brears T, Liu C, Knight TJ, Coruzzi GM (1993) Ectopic overexpression of asparagine synthetase in transgenic tobacco. Plant Physiol **103**:1285-1290

Burrel MM, Mooney PJ, Blundy M, Carter D, Wilson F, Green J, Blundy KS, ap Rees T (1994) Genetic manipulation of 6-phosphofructokinase in potato tubers. Planta **194**:95-101

Campbell DC, Kondra ZP (1978) Relationships among growth patterns, yield components and yield of rapeseed. Can J Plant Sci **58**:87-93

Charest PJ, Holbrook LA, Gabard J, Iyer VN, Miki BL (1988) *Agrobacterium*-mediated transformation of thin cell layer explants from *Brassica napus* L. Theor Appl Genet **75**:438-445

Chen JL, Beversdorf WD (1994) A combined use of microprojectile bombardment and DNA imbibition enhances transformation frequency of canola (*Brassica napus* L.). Theor Appl Genet **88**:187-192

Cheng W-H, Taliercio EW, Chourey PS (1996) The *miniature1* seed locus of maize encodes a cell wall invertase required for normal development of endosperm and maternal cells in the pedicel. Plant Cell **8**:971-983

Chevalier C, Bourgeois E, Just D, Raymond P (1996) Metabolic regulation of asparagine synthetase gene expression in maize (*Zea mays* L.) root tips. Plant J **9**:1-11

Chourey PS, Nelson OE (1976) The enzymatic deficiency conditioned by the *shrunken-1* mutations in maize. Biochem Genet **14**:1041-1055

Clarke JM, Simpson GM (1978) Growth analysis of *Brassica napus* cv. Tower. Can J Plant Sci **58**:587-595

Collier DE (1997) Changes in respiration, protein and carbohydrates of tulip tepals and *Alstroemeria* petals during development. J Plant Physiol **150**:446-451

Copeland L (1990) Enzymes of sucrose metabolism. Methods Plant Biochem **3**:73-85

Coruzzi, GM (1991) Molecular approaches to the study of amino acid biosynthesis in plants. Plant Sci **74**:145-155

Crookston RK, O'Toole J, Ozburn JL (1974) Characterization of the bean pod as a photosynthetic organ. Crop Sci **14**:708-712

Crouch ML, Sussex IM (1981) Development and storage-protein synthesis in *Brassica napus* L. embryos *in vivo* and *in vitro*. Planta **153**:64-74

Damgaard O, Rasmussen O (1991) Direct regeneration of transformed shoots in *Brassica napus* from hypocotyl infections with *Agrobacterium rhizogenes*. Plant Mol Biol **17**:1-8

Dancer JE, Hatzfeld WD, Stitt M (1990) Cytosolic cycles regulate the accumulation of sucrose in heterotrophic cell-suspension cultures of *Chenopodium rubrum*. Planta **182**:223-231

Davies PA, Larkin PJ, Tanner GJ (1989) Enhanced protoplast division by media ultrafiltration. Plant Sci **60**:237-244

De Block M, De Brouwer D, Tenning P (1989) Transformation of *Brassica napus* and *Brassica oleracea* using *Agrobacterium tumefaciens* and the expression of the *bar* and *neo* genes in the transgenic plants. Plant Physiol **91**:694-701

De Block M, Herrera-Estrella L, Van Montagu M, Schell J, Zambryski P (1984) Expression of foreign genes in regenerated plants and in their progeny. EMBO J **3**:1681-1689

Dembinski E, Wisniewska I, Zebrowski J, Raczynska-Bojanowska K (1996) Negative regulation of asparagine synthetase in the leaves of maize seedlings by light, benzyladenine and glucose. Physiol Plant **96**:66-70

Dejardin A, Rochat C, Maugenest S, Boutin J-P (1997) Purification, characterization and physiological role of sucrose synthase in the pea seed coat (*Pisum sativum* L.). Planta **201**:128-137

Dekker JH, Sharkey TD (1992) Regulation of photosynthesis in triazine-resistant and -susceptible *Brassica napus*. Plant Physiol **98**:1069-1073

Dembinski E, Wisniewska I, Zebrowski J, Raczynska-Bojanowska K (1996) Negative regulation of asparagine synthetase in the leaves of maize seedlings by light, benzyladenine and glucose. Physiol Plant **96**:66-70

Dennis DT, Blakeley SD (1993) Carbon and cofactor partitioning in oilseeds. *In* PR Shewry, K Stobart, eds, Seed Storage Compounds: Biosynthesis, Interactions, and Manipulation. Clarendon Press, Oxford, pp 262-275

Dennis DT, Miernyk JA (1982) Compartmentation of nonphotosynthetic carbohydrate metabolism. Annu Rev Plant Physiol **33**:27-50

Dickinson S, Altabella T, Chrispeels M (1991) Slow growth phenotype of transgenic tomato expressing apoplastic invertase. Plant Physiol **95**:420-425

Doehlert DC (1990) Distribution of enzyme activities within the developing maize (*Zea mays*) kernel in relation to starch, oil and protein accumulation. Physiol Plant **78**:560-567

Donkin ME, Price DN (1989) A comparison of pod space CO_2 concentrations in green, yellow, and purple podded varieties of *Pisum sativum* L. J Plant Physiol **135**:295-300

Donkin ME, Price DN (1990) Optical properties of the pod wall of the pea (*Pisum sativum* L.): I. General aspects. J Plant Physiol **137**:29-35

Dua A, Talwar G, Singh R (1994) Changes in structure and function of photosynthetic apparatus of *Brassica* pods during seed maturation. Indian J Biochem Biophys **31**:171-176

Eastmond P, Kang F, Rawsthorne S (1997) The effect of light on fatty acid and starch synthesis by plastids isolated from developing embryos and leaves of *Brassica napus* L. Plant Physiol *in press*

Eastmond P, Kolácná L, Rawsthorne S (1996) Photosynthesis by developing embryos of oilseed rape (*Brassica napus* L.). J Exp Bot **47**:1763-1769

Edwards G, Walker D (1983) C_3, C_4: Mechanisms, and Cellular and Environmental Regulation, of Photosynthesis. Blackwell Scientific, Oxford, pp 1-542

Edwards J, ap Rees T (1986) Sucrose partitioning in developing embryos of round and wrinkled varieties of *Pisum sativum*. Phytochemistry **25**:2027-2032

Flinn AM (1985) Carbon dioxide fixation in developing seeds. *In* PD Hebblethwaite, MC Heath, TCK Dawkins, eds, The Pea Crop: A Basis for Improvement. Butterworths, London, pp 349-357

Flinn AM, Atkins CA, Pate JS (1977) Significance of photosynthetic and respiratory exchanges in the carbon economy of the developing pea fruit. Plant Physiol **60**:412-418

Fowler DB, Downey RK (1970) Lipid and morphological changes in developing rapeseed, *Brassica napus*. Can J Plant Sci **50**:233-247

Foyer CH, Galtier N (1996) Source-sink interaction and communication in leaves. *In* E Zamski, AA Schaffer, eds, Photoassimilate Distribution in Plants and Crops. Marcel Dekker, New York, pp311-340

Freyman S, Charnetski WA, Crookston RK (1973) Role of leaves in the formation of seed in rape. Can J Plant Sci **53**:693-694

Friend DJC, Bodson M, Bernier G (1984) Promotion of flowering in *Brassica campestris* L. cv. Ceres by sucrose. Plant Physiol **75**:1085-1089

Frommer WB, Sonnewald U (1995) Molecular analysis of carbon partitioning in solanaceous species. J Exp Bot **46**:587-607

Fry J, Barnason A, Horsch RB (1987) Transformation of *Brassica napus* with *Agrobacterium tumefaciens* based vectors. Plant Cell Rep **6**:321-325

Fuhrmann J, Johnen T, Heise K-P (1994) Compartmentation of fatty acid metabolism in zygotic rape embryos. J Plant Physiol **143**:565-569

Furbank RT, Taylor WC (1995) Regulation of photosynthesis in C_3 and C_4 plants: A molecular approach. Plant Cell **7**:797-807

Galtier N, Foyer CH, Huber J, Voelker TA, Huber SC (1993) Effects of elevated sucrose-phosphate synthase activity on photosynthesis, assimilate partitioning, and growth in tomato (*Lycopersicon esculentum* var UC82B). Plant Physiol **101**:535-543

Galtier N, Foyer CH, Murchie E, Alred R, Quick P, Voelker TA, Thepenier C, Lasceve G, Betsche T (1995) Effects of light and atmospheric carbon dioxide enrichment on photosynthesis and carbon partitioning in the leaves of tomato (*Lycopersicon esculentum* L.) plants over-expressing sucrose phosphate synthase. J Exp Bot **46**:1335-1344

Gamborg OL, Miller RA, Ojima K (1968) Nutrient requirements of suspension cultures of soybean root cells. Exp Cell Res **50**:151-158

Geigenberger P, Lerchl J, Stitt M, Sonnewald U (1996) Phloem-specific expression of pyrophosphatase inhibits long-distance transport of carbohydrates and amino acids in tobacco plants. Plant Cell Environ **19**:43-55

Geigenberger P, Stitt M (1991) A "futile" cycle of sucrose synthesis and degradation is involved in regulating partitioning between sucrose, starch and respiration in cotyledons of germinating *Ricinus communis* L. seedlings when phloem transport is inhibited. Planta **185**:81-90

Geiger DR, Servaites JC (1994) Dynamics of self-regulation of photosynthetic carbon metabolism. Plant Physiol Biochem **32**:173-183

Genty B, Briantais J-M, Baker NR (1989) The relationship between the quantum yield of photosynthetic electron transport and quenching of chlorophyll fluorescence. Biochim Biophys Acta **990**:87-92

Gottlob-McHugh SG, Sangwan RS, Blakeley SD, Vanlerberghe GC, Ko K, Turpin DH, Plaxton WC, Miki BL, Dennis DT (1992) Normal growth of transgenic tobacco plants in the absence of cytosolic pyruvate kinase. Plant Physiol **100**:820-825

Guerche P, Charbonnier M, Jouanin L, Tourneur C, Paszkowski J, Pelletier G (1987) Direct gene transfer by electroporation in *Brassica napus*. Plant Sci **52**:111-116

Habekotté B (1993) Quantitative analysis of pod formation, seed set and seed filling in winter oilseed rape (*Brassica napus* L.) under field conditions. Field Crops Res **35**:21-33

Hachey JE, Sharma KK, Moloney MM (1991) Efficient shoot regeneration of *Brassica campestris* using cotyledon explants cultured *in vitro*. Plant Cell Rep **9**:549-554

Hajirezaei M, Sonnewald U, Viola R, Carlisle S, Dennis D, Stitt M (1994) Transgenic potato plants with strongly decreased expression of pyrophosphate:fructose-6-phosphate phosphotransferase show no visible phenotype and only minor changes in metabolic fluxes in their tubers. Planta **192**:16-30

Harrington GN, Franceschi VR, Offler CE, Patrick JW, Tegeder M, Frommer WB, Harper JF, Hitz WD (1997a) Cell specific expression of three genes involved in plasma membrane sucrose transport in developing *Vicia faba* seed. Protoplasma **197**:160-173

Harrington GN, Nussbaumer Y, Wang X-D, Tegeder M, Franceschi VR, Frommer WB, Patrick JW, Offler CE (1997b) Spatial and temporal expression of sucrose transport-related genes in developing cotyledons of *Vicia faba* L. Protoplasma *in press*

Harvey DM, Hedley CL, Keely R (1976) Photosynthetic and respiratory studies during pod and seed development in *Pisum sativum* L. Ann Bot **40**:993-1001

Hawker JS, Walker RR, Ruffner HP (1976) Invertase and sucrose synthase in flowers. Phytochemistry **15**:1441-1443

Hedley CL, Harvey DM, Keely RJ (1975) Role of PEP carboxylase during seed development in *Pisum sativum*. Nature **258**:352-354

Heim U, Weber H, Bäumlein H, Wobus U (1993) A sucrose-synthase gene of *Vicia faba* L.: Expression pattern in developing seeds in relation to starch synthesis and metabolic regulation. Planta **191**:394-401

Heineke D, Sonnewald U, Büssis D, Günter G, Leidreiter K, Wilke I, Raschke K, Willmitzer L, Heldt HW (1992) Apoplastic expression of yeast-derived invertase in potato. Plant Physiol **100**:301-308

Hendrix DL (1990) Carbohydrates and carbohydrate enzymes in developing cotton ovules. Physiol Plant **78**:85-92

Ho LC (1988) Metabolism and compartmentation of imported sugars in sink organs in relation to sink strength. Annu Rev Plant Physiol Plant Mol Biol **39**:355-378

Hocking PJ, Mason L (1993) Accumulation, distribution and redistribution of dry matter and mineral nutrients in fruits of canola (oilseed rape), and the effects of nitrogen fertilizer and windrowing. Aust J Agric Res **44**:1377-1388

Hoff T, Truong H-N, Caboche M (1994) The use of mutants and transgenic plants to study nitrate assimilation. Plant Cell Environ **17**:489-506

Hofgen R, Willmitzer L (1990) Biochemical and genetic analysis of different patatin isoforms expressed in various organs of potato (*Solanum tuberosum*). Plant Sci **66**:221-230

Horsch RB, Fraley RT, Rogers SG, Sanders PR, Lloyd A, Hoffman N (1984) Inheritance of functional foreign genes in plants. Science **223**:496-498

Hozyo Y, Kato S, Kobayashi H (1972) Photosynthetic activity of the pods of rape plants (*Brassica napus* L.) and the contribution of the pods to the ripening of rapeseeds. Proc Crop Sci Soc Japan **41**:420-425

Huber JLA, Huber SC (1992) Site-specific serine phosphorylation of spinach leaf sucrose-phosphate synthase. Biochem J **283**:877-882

Huber JLA, Huber SC, Nielsen TH (1989) Protein phosphorylation as a mechanism for regulation of spinach leaf sucrose-phosphate synthase activity. Arch Biochem Biophys **270**:681-690

Huber SC, Huber JL (1991) Regulation of maize leaf sucrose-phosphate synthase by protein phosphorylation. Plant Cell Physiol **32**:319-326

Huber SC, Huber JL (1996) Role and regulation of sucrose-phosphate synthase in higher plants. Annu Rev Plant Physiol Plant Mol Biol **47**:431-444

Huber SC, Huber JL, Liao PC, Gage DA, McMichael RW, Chourey PS, Hannah LC, Koch K (1996) Phosphorylation of serine-15 of maize leaf sucrose synthase - occurrence *in vivo* and possible regulatory significance. Plant Physiol **112**:793-802

Huetteman CA, Preece JE (1993) Thidiazuron: a potent cytokinin for woody plant tissue culture. Plant Cell Tissue Organ Cult **33**:105-119

Hurry VM, Strand Å, Tobiæson M, Gardeström P, Öquist G (1995) Cold hardening of spring and winter wheat and rape results in differential effects on growth, carbon metabolism and carbohydrate content. Plant Physiol **109**:697-706

Hyde BB (1970) Mucilage-producing cells in the seed coat of *Plantago ovata*: developmental fine structure. Amer J Bot **57**:1197-1206

Jellito T, Sonnewald U, Willmitzer L, Hajirezaei MR, Stitt M (1992) Inorganic pyrophosphate content and metabolites in leaves and tubers of potato and tobacco plants expressing *E. coli* pyrophosphatase in their cytosol: biochemical evidence that sucrose metabolism has been manipulated. Planta **188**:238-244

Jones TL, Ort DR (1997) Circadian regulation of sucrose phosphate synthase activity in tomato by protein phosphatase activity. Plant Physiol **113**:1167-1175

Joy KW, Ireland RJ (1990) Enzymes of asparagine metabolism. Methods Plant Biochem **3**:287-296

Joy KW, Ireland RJ, Lea PJ (1983) Asparagine synthesis in pea leaves, and the occurrence of an asparagine synthetase inhibitor. Plant Physiol **73**:165-168

Juan AS, Vasconcelos AC (1994) Overexpression of cytosolic fructose-1,6-bisphosphatase in transgenic tobacco plants (abstract No. 636). Plant Physiol **105**:S-118

Kang F, Rawsthorne S (1994) Starch and fatty acid synthesis in plastids from developing embryos of oilseed rape (*Brassica napus* L.). Plant J **6**:795-805

Kasa GR, Kondra ZP (1986) Growth analysis of spring-type oilseed rape. Field Crops Res **14**:361-370

Keller F (1989) Biochemistry and physiology of non-fructan sucrosyl-oligosaccharides and sugar alcohols in higher plants. J Plant Physiol **134**:141-147

Khanna-Chopra R, Sinha SK (1976) Importance of fruit wall in seed yield of pea (*Pisum sativum* L.) and mustard (*Brassica campestris* L.). Indian J Exp Biol **14**:159-162

Kimber DS, McGregor DI (1995) The species and their origin, cultivation and world production. *In* DS Kimber, DI McGregor, eds, Brassica Oilseeds: Production and Utilization. CAB International, Wallingford, UK, pp 1-7

Klein TM, Wolf ED, Wu R, Sanford JC (1987) High-velocity microprojectiles for delivering nucleic acids into living cells. Nature **327**:70-73

Koch KE (1996) Carbohydrate-modulated gene expression in plants. Annu Rev Plant Physiol Plant Mol Biol **47**:509-540

Korbitz W (1995) Utilization of oil as a biodiesel fuel. *In* DS Kimber, DI McGregor, eds, Brassica Oilseeds: Production and Utilization. CAB International, Wallingford, UK, pp 353-371

Koßmann J, Müller-Röber B, Riesmeier JW, Willmitzer L (1996) Potential for modifying source-sink interactions through the genetic manipulation of carbohydrate metabolism. *In* E Zamski, AA Schaffer, eds, Photoassimilate Distribution in Plants and Crops. Marcel Dekker Inc, New York, pp 369-387

Kriedemann P (1966) The photosynthetic activity of the wheat ear. Ann Bot **30**:349-363

Kuang A, Xiao Y, Musgrave ME (1996) Cytochemical localization of reserves during seed development in *Arabidopsis thaliana* under spaceflight conditions. Ann Bot **78**:343-351

Kühn C, Quick WP, Schulz A, Riesmeier JW, Sonnewald U, Frommer WB (1996) Companion cell-specific inhibition of the potato sucrose transporter SUT1. Plant Cell Environ **19**:1115-1123

Kuo TM, Lowell CA, Smith PT (1997) Changes in soluble carbohydrates and enzymic activities in maturing soybean seed tissues. Plant Sci **125**:1-11

Lam H-M, Coschigano K, Schultz C, Melo-Oliveira R, Tjaden G, Oliveira I, Ngai N, Hsieh M-H, Coruzzi G (1995) Use of *Arabidopsis* mutants and genes to study amide amino acid biosynthesis. Plant Cell **7**:887-898

Lam H-M, Coschigano KT, Oliveira IC, Melo-Oliveira R, Coruzzi GM (1996) The molecular-genetics of nitrogen assimilation into amino acids in higher plants. Annu Rev Plant Physiol Plant Mol Biol **47**:569-593

Lazo GR, Stein PA, Ludwig RA (1991) A DNA transformation-competent *Arabidopsis* genomic library in *Agrobacterium*. Bio/Technology **9**:963-967

Lea PJ, Forde BG (1994) The use of mutants and transgenic plants to study amino acid metabolism. Plant Cell Environ **17**:541-556

Lea PJ, Miflin BJ (1980) Transport and metabolism of asparagine and other nitrogen compounds within the plant. *In* BJ Miflin, ed, The Biochemistry of Plants Vol 5. Academic Press, New York, pp 569-607

Lemoine R, Kühn C, Thiele N, Delrot S, Frommer WB (1996) Antisense inhibition of the sucrose transporter in potato: Effects on amount and activity. Plant Cell Environ **19**:1124-1131

Leprince O, Bronchart R, Deltour R (1990) Changes in starch and soluble sugars in relation to the acquisition of desiccation tolerance during maturation of *Brassica campestris* seed. Plant Cell Environ **13**:539-546

Lerchl J, Geigenberger P, Stitt M, Sonnewald U (1995) Impaired photoassimilate partitioning caused by phloem-specific removal of pyrophosphate can be complemented by a phloem-specific cytosolic yeast-derived invertase in transgenic plants. Plant Cell **7**:259-270

Lewis GJ, Thurling N (1994) Growth, development, and yield of three oilseed *Brassica* species in a water-limited environment. Aust J Exp Agric **34**:93-103

Lohaus G (1995) Vom source zum sink: Phloemtransport verschiedener kohlenstoff- und stickstoffverbindungen. Ph.D. thesis. Georg August Universität zu Göttingen, Göttingen

Lovell PH, Lovell PJ (1970) Fixation of CO_2 and export of photosynthate by the carpel in *Pisum sativum*. Physiol Plant **23**:316-322

Lunn JE, Hatch MD (1995) Primary partitioning and storage of photosynthate in sucrose and starch in leaves of C_4 plants. Planta **197**:385-391

Major DJ (1975) Stomatal frequency and distribution in rape. Can J Plant Sci **55**:1077-1078

Major DJ, Bole JB, Charnetski WA (1978) Distribution of photosynthates after $^{14}CO_2$ assimilation by stems, leaves, and pods of rape plants. Can J Plant Sci **58**:783-787

Malik KA, Saxena PK (1992) Thidiazuron induces high-frequency shoot regeneration in intact seedlings of pea (*Pisum sativum*), chickpea (*Cicer arietinum*) and lentil (*Lens culinaris*). Aust J Plant Physiol **19**:731-740

Mate CJ, von Caemmerer S, Evans JR, Hudson GS, Andrews TJ (1996) The relationship between CO_2-assimilation rate, Rubisco carbamylation and Rubsico activase content in activase-deficient transgenic tobacco suggests a simple model of activase action. Planta **198**:604-613

McDonald BE (1995) Oil properties of importance in human nutrition. *In* DS Kimber, DI McGregor, eds, Brassica Oilseeds: Production and Utilization. CAB International, Wallingford, UK, pp 291-299

McDonnell RE, Clark RD, Smith WA, Hinchee MA (1987) A simplified method for the detection of neomycin phosphotransferase II activity in transformed plant tissues. Plant Mol Biol Rep **5**:380-386

McGregor DI (1995) Chlorophyll clearing in developing canola seed. *In* DJ Murphy, ed, Proc 9th Intl Rapeseed Congress. GCIRC, Paris, pp 506-508

McMichael RW, Klein RR, Salvucci ME, Huber SC (1993) Identification of the major regulatory phosphorylation site in sucrose-phosphate synthase. Arch Biochem Biophys **307**:248-252

McMichael RW, Kochansky J, Klein RR, Huber SC (1995) Characterization of the substrate specificity of sucrose-phosphate synthase protein kinase. Arch Biochem Biophys **321**:71-75

Mendham NJ, Salisbury PA (1995) Physiology: crop development, growth and yield. *In* DS Kimber, DI McGregor, eds, Brassica Oilseeds: Production and Utilization. CAB International, Wallingford, UK, pp 11-64

Micallef BJ, Haskins KA, Vanderveer PJ, Roh K-S, Shewmaker CK, Sharkey TD (1995) Altered photosynthesis, flowering, and fruiting in transgenic tomato plants that have an increased capacity for sucrose synthesis. Planta **196**:327-334

Miller WB, Ranwala AP (1994) Characterization and localization of three soluble invertase forms from *Lilium longiflorum* flower buds. Physiol Plant **92**:247-253

Moloney MM, Walker JM, Sharma KK (1989) High efficiency transformation of *Brassica napus* using *Agrobacterium* vectors. Plant Cell Rep **8**:238-242

Morell M, Copeland L (1985) Sucrose synthase of soybean nodules. Plant Physiol **78**:149-154

Morrison MJ, Stewart DW, McVetty PBE (1992) Maximum area, expansion rate and duration of summer rape leaves. Can J Plant Sci **72**:117-126

Müller-Röber BT, Sonnewald U, Willmitzer L (1992) Inhibition of the ADP-glucose pyrophosphorylase in transgenic potatoes leads to sugar-storing tubers and influences tuber formation and expression of tuber storage protein genes. EMBO J **11**:1229-1238

Munshi SK, Kochhar A (1994) Carbohydrate metabolism in the siliqua relating to oil-filling in mustard seeds. J Agron Crop Sci **172**:126-136

Murashige T, Skoog F (1962) A revised medium for rapid growth and bioassays with tobacco tissue cultures. Physiol Plant **15**:473-479

Murphy DJ, Cummins I (1989) Biosynthesis of seed storage products during embryogenesis in rapeseed, *Brassica napus*. J Plant Physiol **135**:63-69

Murthy BNS, Singh RP, Saxena PK (1996a) Induction of high-frequency somatic embryogenesis in geranium (*Pelargonium* x *hortorum* Bailey cv. Ringo Rose) cotyledonary cultures. Plant Cell Rep **15**:423-426

Murthy BNS, Victor J, Singh RP, Fletcher RA, Saxena PK (1996b) *In vitro* regeneration of chickpea (*Cicer arietinum* L.): stimulation of direct organogenesis and somatic embryogenesis by thidiazuron. Plant Growth Reg **19**:233-240

Neuhaus G, Spangenberg G, Mittelsten Scheid O, Schweiger H-G (1987) Transgenic rapeseed plants obtained by the microinjection of DNA into microspore-derived embryoids. Theor Appl Genet **75**:30-36

Newman T, de Bruijin FJ, Green P, Keegstra K, Kende H, McIntosh L, Ohlrogge J, Raikhel N, Somerville S, Thomashow M, Retzel E, Somerville C (1994) Genes galore: A summary of methods for accessing results from large-scale partial sequencing of anonymous *Arabidopsis* cDNA clones. Plant Physiol **106**:1241-1255

Norton G, Harris JF (1975) Compositional changes in developing rape seed (*Brassica napus* L.). Planta **123**:163-174

Offler CE, Liet E, Sutton EG (1997) Transfer cell induction in cotyledons of *Vicia faba* L. Protoplasma *in press*

Ohlrogge JB, Jaworski JG (1997) Regulation of fatty acid synthesis. Annu Rev Plant Physiol Plant Mol Biol **48**:109-136

Oliveira IC, Lam H-M, Coschigano K, Melo-Oliveira R, Coruzzi G (1997) Molecular-genetic dissection of ammonium assimilation in *Arabidopsis thaliana*. Plant Physiol Biochem **35**:185-198

Ono Y, Takahata Y, Kaizuma N (1994) Effect of genotype on shoot regeneration from cotyledonary explants of rapeseed (*Brassica napus* L.). Plant Cell Rep **14**:13-17

Patrick JW (1997) Phloem unloading: sieve element unloading and post-sieve element transport. Annu Rev Plant Physiol Plant Mol Biol **48**:191-222

Patrick JW, Offler CE (1995) Post-sieve element transport of sucrose in developing seeds. Aust J Plant Physiol **22**:681-702

Paul M, Sonnewald U, Hajirezaei M, Dennis D, Stitt M (1995) Transgenic tobacco plants with strongly decreased expression of pyrophosphate: fructose-6-phosphate 1-phosphotransferase do not differ significantly from wild type in photosynthate partitioning, plant growth or their ability to cope with limiting phosphate, limiting nitrogen and suboptimal temperatures. Planta **196**:277-283

Paul MJ, Lawlor DW, Driscoll SP (1990) The effect of temperature on photosynthesis and carbon fluxes in sunflower and rape. J Exp Bot **41**:547-555

Peach C, Velten J (1991) Transgene expression variability (position effect) of CAT and GUS reporter genes driven by linked divergent T-DNA promoters. Plant Mol Biol **17**:49-60

Pechan PA, Morgan DG (1985) Defoliation and its effects on pod and seed development in oil seed rape (*Brassica napus* L.). J Exp Bot **36**:458-468

Perry HJ, Harwood JL (1993) Changes in the lipid content of developing seeds of *Brassica napus*. Phytochemistry **32**:1411-1415

Pietzak M, Shillito RD, Hohn T, Potrykus I (1986) Expression in plants of two bacterial antibiotic resistance genes after protoplast transformation with a new plant expression vector. Nucl Acids Res **14**:5857-5868

Plant Biotechnology Institute Bi-Annual Report (1996) National Research Council Canada, Saskatoon

Plaxton WC (1996) The organization and regulation of plant glycolysis. Annu Rev Plant Physiol Plant Mol Biol **47**:185-214

Pomeroy MK, Kramer JKG, Hunt DJ, Keller WA (1991) Fatty acid changes during development of zygotic and microspore-derived embryos of *Brassica napus*. Physiol Plant **81**:447-454

Porra RJ, Thompson WA, Kriedemann PE (1989) Determination of accurate extinction coefficients and simultaneous equations for assaying chlorophylls *a* and *b* extracted with four different solvents: verification of the concentration of chlorophyll standards by atomic absorption spectroscopy. Biochim Biophys Acta **975**:384-394

Price DN, Hedley CL (1980) Developmental and varietal comparisons of pod carboxylase levels in *Pisum sativum* L. Ann Bot **45**:283-294

Price DN, Hedley CL (1988) The effect of the *gp* gene of fruit development in *Pisum sativum* L. II. photosynthetic implications. New Phytol **110**:271-277

Price DN, Smith CM, Hedley CL (1988) The effect of the *gp* gene of fruit development in *Pisum sativum* L. I. structural and physical aspects. New Phytol **110**:261-269

Pua E-C, Mehra-Palta A, Nagy F, Chua N-H (1987) Transgenic plants of *Brassica napus* L. Bio/Technology **5**:815-817

Quebedeaux B, Chollet R (1975) Growth and development of soybean (*Glycine max* L. Merr.) pods. Plant Physiol **55**:745-748

Quebedeaux B, Giaquinta RT (1978) Oxygen effects on metabolite distribution of $^{14}CO_2$-derived assimilates in developing soybean seeds (abstract No. 40). Plant Physiol **61**:S-8

Quebedeaux B, Hardy RWF (1975) Reproductive growth and dry matter production of *Glycine max* (L.) Merr. in response to oxygen concentration. Plant Physiol **55**:102-107

Quick WP, Schaffer AA (1996) Sucrose metabolism in sources and sinks. *In* E Zamski, AA Schaffer, eds, Photoassimilate Distribution in Plants and Crops. Marcel Dekker Inc, New York, pp 115-156

Rabe E (1990) Stress physiology: the functional significance of the accumulation of nitrogen-containing compounds. J Hort Sci **65**:231-243

Radke SE, Andrews BM, Moloney MM, Crouch ML, Kridl JC, Knauf VC (1988) Transformation of *Brassica napus* L. using *Agrobacterium tumefaciens*: developmentally regulated expression of a reintroduced napin gene. Theor Appl Genet **75**:685-694

Rakow G, McGregor DI (1975) Oil, fatty acid and chlorophyll accumulation in developing seeds of two "linolenic acid lines" of low erucic acid rapeseed. Can J Plant Sci **55**:197-203

Reimholz R, Geiger M, Haake V, Deiting U, Krause KP, Sonnewald U, Stitt M (1997) Potato plants contain multiple forms of sucrose phosphate synthase, which differ in their tissue distributions, their levels during development, and their responses to low temperature. Plant Cell Environ **20**:291-305

Riesmeier JW, Willmitzer L, Frommer WB (1994) Evidence for an essential role of the sucrose transporter in phloem loading and assimilate partitioning. EMBO J **13**:1-7

Rochat C, Boutin J-P (1992) Temporary storage compounds and sucrose-starch metabolism in seed coats during pea seed development (*Pisum sativum*). Physiol Plant **85**:567-572

Rood SB, Major DJ (1984) Influence of plant density, nitrogen, water supply and pod or leaf removal on growth of oilseed rape. Field Crops Res **8**:323-331

Rood SB, Major DJ, Carefoot JM, Bole JB (1984a) Seasonal distribution of nitrogen in oilseed rape. Field Crops Res **8**:333-340

Rood SB, Major DJ, Charnetski WA (1984b) Seasonal changes in $^{14}CO_2$ assimilation and ^{14}C translocation in oilseed rape. Field Crops Res **8**:341-348

Ross HA, McRae D, Davies HV (1996) Sucrolytic enzyme activities in cotyledons of the faba bean. Developmental changes and purification of alkaline invertase. Plant Physiol **111**:329-338

Sambrook J, Fritsch EF, Maniatis T (1989) Molecular cloning: A laboratory manual. Ed 2. Cold Spring Harbor Laboratory Press, Cold Spring Harbor, NY

Sanders PR, Winter JA, Barnason AR, Rogers SG, Fraley RT (1987) Comparison of cauliflower mosaic virus 35S and nopaline synthase promoters in transgenic plants. Nucl Acids Res **15**:1543-1558

Sangwan RS, Singh N, Plaxton WC (1992) Phosphoenolpyruvate carboxylase activity and concentration in the endosperm of developing and germinating castor oil seeds. Plant Physiol **99**:445-449

Sasaki T, Song J, Koga-Ban Y, Matsui E, Fang F, Higo H, Nagasaki H, Hori M, Miya M, Murayama-Kayano E, Takiguchi T, Takasuga A, Niki T, Ishimaru K, Ikeda H, Yamanoto Y, Mukai Y, Ohta I, Miyadera N, Havukkala I, Minobe Y (1994) Toward cataloguing all rice genes: large-scale sequencing of randomly chosen rice cDNAs from a callus cDNA library. Plant J **6**:615-624

Sawyer H, Hsiao K-C (1992) Effects of autoclave-induced carbohydrate hydrolysis on the growth of *Beta vulgaris* cells in suspension. Plant Cell Organ Tiss Cult **31**:81-86

Schenk N, Hsiao K-C, Bornman CH (1991) Avoidance of precipitation and carbohydrate breakdown in autoclaved plant tissue culture media. Plant Cell Rep **10**:115-119

Schröder M, Dixelius C, Rahlen L, Glimelius K (1994) Transformation of *Brassica napus* by using the *aadA* gene as selectable marker and inheritance studies of the marker genes. Physiol Plant **92**:37-46

Scott P, Kruger NJ (1995) Influence of elevated fructose 2,6-bisphosphate levels on starch mobilization in transgenic tobacco leaves in the dark. Plant Physiol **108**:1569-1577

Scott P, Lange AJ, Pilkis SJ, Kruger NJ (1995) Carbon metabolism in leaves of transgenic tobacco (*Nicotiana tabacum* L.) containing elevated fructose 2,6-bisphosphate levels. Plant J **7**:461-469

Seaton GR, Walker DA (1992) Validating chlorophyll fluorescence measures of efficiency: observations on fluorimetric estimation of photosynthetic rate. Proc Royal Soc London B **249**:41-47

Sewalt VJH, Glasser WG, Fontenot JP, Allen VG (1996) Lignin impact on fibre degradation: 1-quinone methide intermediates formed from lignin during *in vitro* fermentation of corn stover. J Sci Food Agric **71**:195-203

Shade RE, Schroeder HE, Pueyo JJ, Tabe LM, Murdock LL, Higgins TJV, Chrispeels MJ (1994) Transgenic pea seeds expressing the α-amylase inhibitor of the common bean are resistant to bruchid beetles. Bio/Technology **12**:793-796

Sheen J (1990) Metabolite repression of transcription in higher plants. Plant Cell **2**:1027-1038

Sheoran IS, Sawhney V, Babbar S, Singh R (1991) *In vivo* fixation of CO_2 by attached pods of *Brassica campestris* L. Ann Bot **67**:425-428

Shewmaker CK, Boyer CD, Wiesenborn DP, Thompson DB, Boersig MR,

Oakes JW, Stalker DM (1994) Expression of *Escherichia coli* glycogen synthase in the tubers of transgenic potatoes (*Solanum tuberosum*) results in a highly branched starch. Plant Physiol **104**:1159-1166

Siegiechowicz KA, Joy KW, Ireland RJ (1988) The metabolism of asparagine in plants. Phytochemistry **27**:663-671.

Sinclair TR, Ward JP, Randall CA (1987) Soybean seed growth in response to long-term exposures to differing oxygen partial pressures. Plant Physiol **83**:467-468

Singal HR, Laura JS, Singh R (1992) Ontogenic changes in photosynthetic carbon reduction cycle metabolites and enzymes of sucrose metabolism in *Brassica campestris* pods. Photosynthetica **26**:463-468

Singal HR, Sheoran IS, Singh R (1986a) In vivo enzyme activities and products of $^{14}CO_2$ assimilation in flag and ear parts of wheat (*Triticum aestivum* L.). Photosyn Res **8**:113-122

Singal HR, Sheoran IS, Singh R (1986b) Products of photosynthetic $^{14}CO_2$ fixation and related enzyme activities in fruiting structures of chick-pea. Physiol Plant **66**:457-462

Singal HR, Sheoran IS, Singh R (1987) Photosynthetic carbon fixation characteristics of fruiting structures of *Brassica campestris* L. Plant Physiol **83**:1043-1047

Singal HR, Talwar G, Dua A, Singh R (1995) Pod photosynthesis and seed dark CO_2 fixation support oil synthesis in developing *Brassica* seeds. J Biosci **20**:49-58

Sinha SK, Sane PV (1976) Relative photosynthetic rate in leaves and fruit wall of pea. Indian J Exp Biol **14**:592-594

Smith AM, Denyer K (1992) Starch synthesis in developing pea embryos. New Phytol **122**:21-33

Smith AM, Martin C (1993) Starch biosynthesis and the potential for its manipulation. *In* D Grierson, ed, Biosynthesis and Manipulation of Plant Products. Blackie Academic, Glasgow, pp 1-54

Smith RG, Gauthier DA, Dennis DT, Turpin DH (1992) Malate- and pyruvate-dependent fatty acid synthesis in leucoplasts from developing castor endosperm. Plant Physiol **98**:1233-1238

Sonnewald U (1992) Expression of *E. coli* inorganic pyrophosphatase in transgenic plants alters photoassimilate partitioning. Plant J **2**:571-581

Sonnewald U, Brauer M, von Schaewen A, Stitt M, Willmitzer L (1991) Transgenic tobacco plants expressing yeast-derived invertase in either the cytosol, vacuole or apoplast: a powerful tool for studying sucrose metabolism and sink-source interactions. Plant J **1**:95-106

Sonnewald U, Lerchl J, Zrenner R, Frommer W (1994) Manipulation of sink-source relations in transgenic plants. Plant Cell Environ **17**:649-658

Sonntag NOV (1995) Industrial utilization of long-chain fatty acids and their derivatives. *In* DS Kimber, DI McGregor, eds, Brassica Oilseeds: Production and Utilization. CAB International, Wallingford, UK, pp 339-352

Srinivasan A, Morgan DG (1996) Growth and development of the pod wall in spring rape (*Brassica napus*) as related to the presence of seeds and exogenous phytohormones. J Agric Sci **127**:487-500

Stam M, Mol JN, Kooter JM (1997) The silence of genes in transgenic plants. Ann Bot **79**:3-12

Stark DM, Timmerman KP, Barry GF, Preiss J, Kishore GM (1992) Regulation of the amount of starch in plant tissues by ADP glucose pyrophosphorylase. Science **258**:287-292

Stitt M (1993) Control of photosynthetic carbon fixation and partitioning: how can use of genetically manipulated plants improve the nature and quality of information about regulation? Phil Trans R Soc Lond B **342**:225-233

Stitt M (1995a) Regulation of metabolism in transgenic plants. Annu Rev Plant Physiol Plant Mol Biol **46**:341-368

Stitt M (1995b) The use of transgenic plants to study the regulation of plant carbohydrate metabolism. Aust J Plant Physiol **22**:635-646

Stitt M, Huber S, Kerr P (1987) The control of photosynthetic sucrose formation. *In* MD Hatch, NK Boardman, eds, The Biochemistry of Plants, Vol 10, Academic Press, London, pp 327-409

Sundby C, Chow WS, Anderson JM (1993) Effects on photosystem II function, photoinhibition, and plant performance of the spontaneous mutation of serine-264 in the photosystem II reaction center D1 protein in triazine-resistant *Brassica napus* L. Plant Physiol **103**:105-113

Sung S-JS, Xu D-P, Black CC (1989) Identification of actively filling sucrose sinks. Plant Physiol **89**:1117-1121

Tayo TO, Morgan DG (1979) Factors influencing flower and pod development in oil-seed rape (*Brassica napus* L.). J Agric Sci **92**:363-373

Thorne JH (1982) Temperature and oxygen effects on ^{14}C-photosynthate unloading and accumulation in developing soybean seeds. Plant Physiol **69**:48-53

Thorne JH (1985) Phloem unloading of C and N assimilates in developing seeds. Annu Rev Plant Physiol **36**:317-343

Thurling N (1974) Morphophysiological determinants of yield in rapeseed (*Brassica campestris* and *Brassica napus*). I. Growth and morphological characters. Aust J Agric Res **25**:697-710

Tittonel ED, Kuchtova P, Cinti S, Palmieri S (1995) Effet de la fertilisation azotée sur l'activité PEP carboxylase dans le contrôle de l'accumulation de l'huile et des proteines pendant le developpement des graines de colza. *In* DJ Murphy, ed, Proc 9th Intl Rapeseed Congress. GCIRC, Paris, pp 550-552

Tosca A, Pandolfi R, Vasconi S (1996) Organogenesis in *Camellia* x *williamsii*: cytokinin requirement and susceptibility to antibiotics. Plant Cell Rep **15**:541-544

Tremblay L, Tremblay FM (1991) Effects of gelling agents, ammonium nitrate, and light on the development of *Picea mariana* (Mill) B.S.P. (black spruce) and *Picea rubens* Sang. (red spruce) somatic embryos. Plant Sci **77**:233-242

Tsai F-Y (1991) Molecular biological studies of the light-repressed and organ specific expression of plant asparagine synthetase genes. PhD thesis. Rockefeller University, New York

Tsai F-Y, Coruzzi GM (1990) Dark-induced and organ-specific expression of two asparagine synthetase genes in *Pisum sativum*. EMBO J **9**:323-332

Tsai F-Y, Coruzzi GM (1991) Light represses transcription of asparagine synthetase genes in photosynthetic and nonphotosynthetic organs of plants. Mol Cell Biol **11**:4966-4972

U N (1935) Genome analysis in *Brassica* with special reference to the experimental formation of *B. napus* and peculiar mode of fertilization. Jap J Bot **7**:389-452

Updegraff DM (1969) Semimicro determination of cellulose in biological materials. Anal Biochem **32**:420-424

Van Ark HF, Zaal MACM, Creemers-Molenaar J, Van der Walk P (1991) Improvement of the tissue culture response of seed-derived callus culture of *Poa pratensis* L.: effect of gelling agent and abscisic acid. Plant Cell Tissue Organ Cult **27**:275-280

Van Caeseele L, Mills JT, Sumner M, Gillespie R (1981) Cytology of mucilage production in the seed coat of Candle canola (*Brassica campestris*). Can J Bot **59**:292-300

von Schaewen A, Stitt M, Schmidt R, Sonnewald U, Willmitzer L (1990) Expression of a yeast-derived invertase in the cell wall of tobacco and *Arabidopsis* plants leads to accumulation of carbohydrate and inhibition of photosynthesis and strongly influences growth and phenotype of transgenic tobacco plants. EMBO J **9**:3033-3044

Ward K, Scarth R, Daun JK, Vessey JK (1995) Chlorophyll degradation in summer oilseed rape and summer turnip rape during seed ripening. Can J Plant Sci **75**:413-420

Wardlaw IF (1990) The control of carbon partitioning in plants. New Phytol **116**:341-381

Weber H, Borisjuk L, Heim U, Buchner P, Wobus U (1995) Seed coat-associated invertases of fava bean control both unloading and storage functions: Cloning of cDNAs and cell type-specific expression. Plant Cell **7**:1835-1846

Weber H, Borisjuk L, Heim U, Sauer N, Wobus U (1997a) A role for sugar transporters during seed development: molecular characterization of a hexose and a sucrose carrier in fava bean seeds. Plant Cell **9**:895-908

Weber H, Borisjuk L, Wobus U (1996a) Controlling seed development and seed size in *Vicia faba*: a role for seed coat-associated invertases and carbohydrate state. Plant J **10**:823-834

Weber H, Borisjuk L, Wobus U (1997b) Sugar import and metabolism during seed development. Trends Plant Sci **2**:169-174

Weber H, Buchner P, Borisjuk L, Wobus U (1996b) Sucrose metabolism during cotyledon development of *Vicia faba* L. is controlled by the concerted action of both sucrose-phosphate synthase and sucrose synthase: Expression patterns, metabolic regulation and implications for seed development. Plant J **9**:841-850

Weibull J, Melin G (1990) Free amino acid content of phloem sap from *Brassica* plants in relation to performance of *Lipaphis erysimi* (Hemiptera: Aphididae). Ann Appl Biol **116**:417-423

Wendler R, Veith R, Dancer J, Stitt M, Komor E (1990) Sucrose storage in cell suspension cultures of *Saccharum* sp. (sugarcane) is regulated by a cycle of synthesis and degradation. Planta **183**:31-39

Werker E (1997) Seed Anatomy. Gebrüder Borntraeger, Berlin

Wilms J, Kraml M, Dennis DT, Layzell DB (1997) Reductant use in developing soybean and *Arabidopsis* fruits in relation to oil synthesis (abstract No. 311). Plant Physiol **114**:S-80

Wolswinkel P (1992) Transport of nutrients into developing seeds: a review of physiological mechanisms. Seed Sci Res **2**:59-73

Worrell AC, Bruneau J-M, Summerfelt K, Boersig M, Voelker TA (1991) Expression of a maize sucrose phosphate synthase in tomato alters leaf carbohydrate partitioning. Plant Cell **3**:1121-1130

Wullshleger SD, Oosterhuis DM (1990) Photosynthetic and respiratory activity of fruiting forms within the cotton canopy. Plant Physiol **94**:463-469

Yadav RC, Saleh MT, Grumet R (1996) High frequency shoot regeneration from leaf explants of muskmelon. Plant Cell Tissue Organ Cult **45**:207-214

Zrenner R, Krause K-P, Apel P, Sonnewald, U (1996) Reduction of the cytosolic fructose-1,6-bisphosphatase in transgenic potato plants limits photosynthetic sucrose biosynthesis with no impact on plant growth and tuber yield. Plant J **9**:671-681

Zrenner R, Salanoubat M, Willmitzer L, Sonnewald U (1995) Evidence of the crucial role of sucrose synthase for sink strength using transgenic potato plants (*Solanum tuberosum* L.). Plant J **7**:97-107

Zrenner R, Willmitzer L, Sonnewald U (1993) Analysis of the expression of potato uridinediphosphate-glucose pyrophosphorylase and its inhibition by antisense RNA. Planta **190**:247-252

REFERENCES ADDED TO REVISED COPY

Stitt M, Sonnewald U (1995) Regulation of metabolism in transgenic plants. Annu Rev Plant Physiol Plant Mol Biol **46**:341-368

Xu J, Avigne WT, McCarty DR, Koch KE (1996) A similar dichotomy of sugar modulation and developmental expression affects both paths of sucrose metabolism: Evidence from a maize invertase gene family. Plant Cell **8**:1209-1220